Estimating Ship Transit Times in Ice-Covered Waters for Strategic Route Analysis and Search and Rescue Response Planning

by

Mark A. Stoddard

Submitted in partial fulfilment of the requirements
for the degree of Doctor of Philosophy

at

Dalhousie University
Halifax, Nova Scotia
March 2024

Dedication Page

This thesis is dedicated to the growing number of polar ship operators around the globe who just want to safely get from A to B as expeditiously as possible and for people in distress in polar waters who would benefit from improved rescue planning

TABLE OF CONTENTS

LIST OF TABLES

LIST OF FIGURES

ABSTRACT

Maritime traffic in the Arctic region is increasing as northern communities grow, tourism accelerates, and large resource development projects enter operation. Consequently, the number of vessels exposed to the navigational challenges and risks in the polar region will continue to rise. The situation is further complicated by fast-changing sea ice conditions due in part to climate change. This thesis explores the state of the art in sea ice risk assessment and transit time estimation in ice-covered waters, and presents a strategic route planning methodology that integrates several concepts from these two active areas of research. This methodology is used to enable the computation of innovative visual representations of marine-based search and rescue response time throughout the year in the Canadian Arctic. This is achieved by combining statistical methods, advanced geospatial data analysis, and network analysis techniques to overcome several computational challenges specific to route generation and transit time estimation in ice-covered waters. The results indicate that there is a statistical relationship between reported vessel speed from Automatic Information System (AIS) and the operational risk from sea ice determined at the time of reporting using the Polar Operational Limit Assessment Risk Indexing System (POLARIS). This relationship is used to specify the expected ship speed in different sea ice risk categories, which is then used to compute the fastest route and expected transit time between geographically separated locations in ice-covered waters. The model can generate the fastest route at different times of year and for different ship ice classes. This is achieved by exploiting the relationship that exists between vessel speed and the outcome of the POLARIS assessment. The methods and results presented in this thesis are shown to support a variety of strategic route analysis applications and provide the necessary computational toolset to apply advanced area-based management approaches to maritime search and rescue response planning.

LIST OF ABBREVIATIONS

ABM	Area Based Management
ABS	American Bureau of Shipping
AIRSS	Arctic Ice Regime Shipping System
AIS	Automatic Identification System
AMSA	Arctic Maritime Shipping Assessment
AOI	Area of Interest
API	Applications Programmers Interface
ARIA	Accessibility and Remoteness Index for Australia
ATAM	Arctic Transport Accessibility Model
CAC	Canadian Arctic Class
CCG	Canadian Coast Guard
CFAV	Canadian Forces Auxiliary Vessel
CIS	Canadian Ice Service
ETA	Estimated Time of Arrival
ETT	Expected Transit Time
FS	Finnish-Swedish Ice Classification
GCM	Global Climate Models / General Circulation Models
GDSIDB	Global Digital Sea Ice Data Bank
GPS	Global Positioning System
IACS	International Association of Classification Societies
I-ETA	Ice Risk-Adjusted Estimated Transit Time
IMO	International Maritime Organization

IN	Ice Numeral
IRI	Incident Response Isochrone
IRSA	Incident Response Service Area
KRISO	Korean Research Institute of Ship and Ocean Engineering
LRIT	Long Range Identification and Tracking
MARPOL	International Convention for the Prevention of Pollution from Ships
ML	Machine Learning
MRTC	Maximum Response Time Cut-Off
MSA	Maritime Situational Awareness
NPR	North Pole Route
NRC	National Research Council of Canada
NSDIC	National Snow and Ice Data Centre
NSR	Northern Sea Route
NWP	Northwest Passage
NWT	Northwest Territories
OW	Open Water
PC	Polar Class
POLARIS	Polar Operational Limitation Assessment Risk Indexing System
PWOM	Polar Waters Operations Manual
RI	Remoteness Index
RIO	POLARIS Risk Index Outcome
RQ	Research Question
RV	POLARIS Risk Value
SAAS	Service Area Analysis Scenario

S-AIS	Satellite Automatic Identification System
SAR	Search And Rescue
SISAR	Search and Rescue Program Information Management System
SOLAS	Safety of Life at Sea
SoVI	Social Vulnerability Index
USNIC	United States National Ice Centre
VHF	Very High Frequency (communications)
VOO	Vessel of Opportunity
WMO	World Maritime Organization

GLOSSARY

MSA	Accurate and timely knowledge of anything within the maritime domain that could impact the security, safety, economy, or environment
ETT	The estimated transit time for a ship to complete a planned route from origin to destination in ice-covered waters
I-ETA	The estimated transit time for a ship to complete the optimal (fastest) route from origin to destination in ice-covered waters
IRI	Incident Response Isochrone is an isoline formed by connecting locations that can be reached from an incident location by a marine-based SAR vessel at the specified maximum response time cut-off
IRSA	Incident Response Service Area is a polygon containing all locations that can be reached from an incident location by a marine-based SAR vessel within a specified maximum response time cut-off
MRTC	The maximum response time cut off (hours) used to construct the incident response service area and isochrone
POLARIS	Arctic navigational risk assessment methodology
RIO	Output of the POLARIS assessment that represents the navigational risk for a ship operating in sea ice
S-AIS	Reception of Automatic Identification System transmissions from space-based collection systems

ACKNOWLEDGEMENTS

I would like to extend my sincere thanks to my supervisor, Professor Ronald Pelot, for his unwavering support throughout my lengthy PhD program. I am deeply grateful to Dr. Laurent Etienne for introducing me to many of the geospatial analysis tools and techniques that would later serve as a launching point for my research. Many thanks to Dr. Floris Goerlandt for the insightful comments and suggestions he provided on an early version of this thesis and several related manuscripts. My deepest appreciation also goes to my entire committee for their resolute support over the years.

Lastly, I would like to thank my wife, Eva, for her patience over the past 10 years while I completed my PhD program; my beautiful daughter, Emilia, for constantly reminding me to take breaks to play; my parents, Paul and Janet, for their love and support; and my brother, Adam, for forcing me to question everything and to always challenge the status quo.

CHAPTER 1: Introduction

1.1 Background and Motivation

Maritime traffic in the Arctic region continues to increase as northern communities grow, tourism increases, and large resource development projects enter operation ((Muller, Knol-Kauffman, Jeuring, & Palerme, 2023), (Higginbotham & Grosu, 2014)). As activity increases, the number of vessels exposed to the navigational risks in the polar region will continue to rise. In response, the International Maritime Organization (IMO) introduced the 'International Code for Ships Operating in Polar Waters' (Polar Code), which entered effect in 2017. The Polar Code was developed to aid arctic marine transportation by specifically addressing the unique aspects of passage planning that relate to safety of navigation and environmental protection in the polar regions, that were beyond the scope of existing international and national shipping codes and regulations (International Maritime Organization, 2016). The Polar Code has also equipped ship operators with new tools to support passage planning and voyage risk assessment.

Passage planning in the polar regions involves navigational practices typically accepted as standard, with additional considerations based on the expectation of the presence of sea ice (Snider, 2012). The presence of sea ice, and the risk it presents to ship operations, has been widely studied, and continues to receive a great deal of attention in the literature (Arctic Council, 2009), (Bilge, et al., 2022), (Fedi, et al., 2018), (Crawford, Stroeve, Smith, & Jahn, 2021). The management of sea ice risk in navigation can be viewed as a simple risk problem where the risk is well understood and there is hardly any ambiguity in its interpretation (Renn & Sellke, 2011). When navigating in polar waters, if the risk from sea ice is high ships will operate with extreme caution to ensure ship safety and to minimize damage to the ships hull. Several sea ice risk assessment frameworks have been developed to assist mariners in assessing the navigational risk associated with ship operations in sea ice ((Maritime Safety Committee, 2014a), (Transport Canada, 1998)). These methods were originally designed to support tactical decision making on the bridge of a ship when operating in sea ice, relying on operator knowledge of their ship's vulnerability to observed sea ice conditions to provide an assessment of navigational risk. The results of these

assessments are non-controversial, and the uncertainties are low. The management of sea ice risk assumes a rational actor paradigm ((Renn, Jaeger, Rosa, & Webler, 2000), (Monroe & Maher, 1995)), where ship operators seek to maximize individual utility when navigating in ice-covered waters. In the context of sea ice risk, maximum individual utility is achieved by selecting actions that promise to minimize the likelihood of unfavorable outcomes due to ship interactions with sea ice. Unfavorable outcomes could include excessive damage to the ship's hull, prolonged delays in reaching the ship's destination, or worst-case, loss of life at sea.

The increasing availability of high-quality wide-area sea ice analysis from leading national authorities on sea ice, such as the Canadian Ice Service (CIS) and United States National Ice Centre (USNIC), has created a new opportunity to apply these tactical navigation decision tools and techniques to support the strategic assessment of navigational risk over wide areas ((Melia, Haines, & Hawkins, 2016), (Smith & Stephenson, 2013), (Somanathan, Flynn, & Szymanski, 2006), (Wang, Ding, Yang, & Dou, 2022) (Stoddard M. , Etienne, Fournier, Pelot, & Beveridge, 2016)).

The ability to quantitatively measure and assess the navigational risk from sea ice over wide areas is a key enabler of strategic decision making, supporting optimal route planning ((Aksenov, et al., 2017), (Fedi, et al., 2018), (Melia, Haines, & Hawkins, 2016), (Smith & Stephenson, 2013)), and the planning and provision of Search and Rescue (SAR) and emergency response services ((Stoddard & Pelot, 2020), (Arctic Council, 2009), (Boylan, 2021)). Navigational risk is considered a fundamental measure in strategic route planning, and is often computed to support a variety of decision applications in the arctic maritime domain ((Goerlandt, Montewka, Zhang, & Kujala, 2017), (Kim, Jeong, Woo, & Han, 2018), (Lehtola, Montewka, Goerlandt, Guinness, & Lensu, 2019), (Tremblett, Garvin, & Oldford, 2021).

Maritime activity occurring in the remote polar region presents a greater risk than maritime activity occurring in less remote areas. The reasoning is that the prolonged transit times to remote regions of the Arctic due to sea ice will significantly impact SAR response times, salvage operations, or environmental response operations, increasing the consequences of

an incident. The geographic distance from a ship's current location to the nearest community, port, critical infrastructure, good or service, or other vessel could be small, but when navigational risk and safe shipping speeds are considered, it may be un-navigable or take an unreasonable amount of time to complete the transit. In this sense, remoteness directly contributes to the risks to ships and the risks from ships operating in the Arctic. Delayed SAR response puts mariners at risk (risk to ship), while delayed environmental response times may exacerbate the negative consequences of an incident on the local environment (risk from ship).

By combining sea ice risk assessment and new methods for transit time estimation, with network analysis techniques, it is possible to begin to connect geographically separated locations in the Arctic by marine-based transportation and determine the expected transit time between locations throughout the year. The results provide a greater understanding of marine-based transportation in ice-covered waters and have potential for broad application in the multi-disciplinary research field of Area-Based Management (ABM).

1.2 State of the Art

1.2.1 State of the Art in Arctic Navigation Risk Assessment

As maritime traffic in the Arctic increases, more vessels are exposed to navigational risks in the polar region. The vulnerability of a vessel to these navigational risks depends heavily on the type and class of ship, crew training and experience, and access to high quality information to support decision making. In the Arctic, environmental factors strongly influence maritime activity, including but not limited to, extreme weather, ice conditions, and daylight (DNV-GL, 2014). The arctic environment is not uniform; there are large seasonal variations in sea ice conditions, daylight, and weather, and these factors vary greatly throughout the Arctic (Lloyds of London, 2014). Efforts to better characterize the arctic environment have driven major advancements in sensors and systems supporting arctic maritime situational awareness and the observation and monitoring of maritime traffic throughout the Arctic.

Vessel position reporting systems, such as Automatic Identification System (AIS) allow an observer to determine the types of ships that are navigating in polar waters, as well as their position and speed at any time during their voyage ((Eriksen, Hoye, Narheim, & Jenslokken, 2006), (Cairns, 2005)). These systems are now integral to the safety and security of global maritime transportation. Remote sensing systems also offer an attractive tool for providing relevant and timely data from which a variety of shipping data analysis products can be created, including the characterization of ocean waves (Heiberg, Reistad, & A., 2006), coastlines (Olsen & Wahl, 2000), ocean currents ((Runge, et al., 2004), (Collard, et al., 2008), (Kang, Lee, Yang, & Yoon, 2008)), and sea ice ((Hirose, et al., 2008), (Chamberlain, Yue, Parsons, & Mulvie, 2008)). Remote sensing can often provide the necessary observations to quantify many of the environmental risk factors associated with arctic navigation, resulting in a significant increase in the use of quantitative risk assessment to analyze marine transportation in arctic waters.

(Khan, Khan, Veitch, & Yang, 2018) provide a detailed review of the quantitative risk assessment in arctic waters, specifying many of the key risk factors affecting safe navigation. Severe weather and ice conditions were identified as the primary environmental risk factors affecting safe navigation. The combination of remote sensing and vessel tracking data provides new opportunities for sense-making of observed maritime activity, especially in complex navigating environments like the Canadian Arctic. Sense-making involves turning observed circumstances into a situation that can be comprehended, and provide a basis for subsequent action to be taken (Weick & Sutcliffe, 2005). While a multitude of risk factors have been shown to impact safe navigation, the risk from sea ice in the Canadian Arctic deserves special attention (Marchenko, Borch, Markov, & Andreassen, 2015).

Transport Canada has long provided mariners with a quantitative method to help make sense of observed sea ice conditions and to characterize the relative risk that sea ice conditions pose to the structure of different ships, referred to as the Arctic Ice Regime Shipping System (AIRSS) (Transport Canada, 1998). AIRSS is a widely used maritime framework to assess navigation safety in each ice regime as a function of ice conditions and the structural and engineering capabilities of a particular vessel class (Smith &

Stephenson, 2013). The system uses a basic algorithm to determine a quantitative result called the Ice Numeral (IN). A positive IN indicates that a vessel can proceed through the observed sea ice operating conditions; a negative number indicates that a vessel should not proceed under the given operating conditions (Snider, 2012).

Many researchers have incorporated AIRSS into modeling and simulation studies to examine shipping in the Canadian Arctic. The efforts of (Howell & Yackel, 2004) provided an early demonstration of how AIRSS and historical CIS digital ice charts could be combined to assess navigational variability over three well-defined Western Arctic transit routes from 1969 to 2002. Transit routes were sampled at a 5km spacing and assigned an IN from a pre-computed IN raster grid of the operating area. The results were used to visualize the spatial variability of the IN for a Canadian Arctic Class 3 (CAC3) ship throughout their study Area of Interest (AOI), and along each Western Arctic transit routes. Each route was also examined based on the INs encountered during transit. A route containing a negative IN indicated that a section of the route was not suitable for operations. In (Wilson, Falkingham, Melling, & De Abreu, 2004), the authors further examined the area of interest presented in (Howell & Yackel, 2004) using several Global Climate Models (GCMs) to forecast future ice conditions. Their conclusion was that the future sea-ice conditions in the Canadian Arctic remain highly variable, and there could still be seasons of occasional heavy ice conditions that will present a significant navigational challenge to ships in the Western Arctic.

The work of (Somanathan, Flynn, & Szymanski, 2006) incorporated AIRSS into a transit simulation to compare the relative economics of shipping through the Northwest Passage (NWP) and shipping through the Panama Canal. Using historical sea ice analysis for the Canadian Arctic, the authors prepared probabilistic ice regimes that could be used in AIRSS. The computed IN and ship ice classification were then used to calculate transit speeds through the NWP for different ship ice classes in their simulation. The major conclusion of their study was that for the ice conditions observed in the Canadian Arctic for the period of 1999 through 2003, the NWP would not be economically favored over the traditional route through the Panama Canal. The results were specific to a ship with a CAC3 ice classification, where transit time was the main economic consideration.

(Etienne & Pelot, 2013) presented a simulation tool that can be used to determine feasible paths throughout the Canadian Arctic based on historical sea ice conditions. The feasibility of a shipping path was determined using AIRSS, where historical sea ice analysis and ship classification are used to calculate the IN and resulting "Go" or "No Go" ship limits along a given route. In (Smith & Stephenson, 2013), the authors provide a similar analysis of shipping route feasibility using AIRSS. Instead of focusing on the use of historical sea ice analysis, the authors considered several leading GCMs to construct future ice regimes for use in AIRSS. AIRSS was used to determine the feasibility of different trans-arctic routes for Polar Class (PC) 6 and open-water (OW) vessels. A feasible polar route consisted of a least-cost path (minimum total voyage time) from a start point to an end point, avoiding areas where the IN would obstruct a particular vessel class (IN < 0). A major conclusion of their paper was that by mid-century, September sea-ice conditions will have changed sufficiently in the NWP, such that trans-arctic shipping to/from North America could commonly capitalize on the approximately 30% geographic distance savings that this route offers over the Northern Sea Route (NSR), which follows the Russian coastline.

As previously mentioned, IMO's Polar Code promotes the use of the Polar Operational Limit Assessment Risk Indexing System (POLARIS) to determine sea ice risk (Maritime Safety Committee, 2014b). POLARIS has been produced by the shipping industry International Association of Classification Societies (IACS) to provide a quantitative framework to assess navigational safety in an ice regime, using observed or historical ice conditions and a vessel's ship ice classification (Maritime Safety Committee 2014b). An ice regime is defined as an area with a consistent distribution of any mix of ice types, including open water. Ice analysts working for national ice centers have access to a variety of high-resolution data sources to estimate the partial ice concentrations of various ice types in an ice regime and encode the information according to a WMO standard (Intergovernmental Oceanographic Commission of UNESCO, 2004). The concentration of each ice type within an ice regime is reported in tenths. For each ice type, there is an associated ice type score defined for each ship ice classification. The ice type score is referred to as a Risk Value (RV), and a collection of RVs (Risk Values) that correspond to an ice regime is referred to as a Risk Index Outcome (RIO). Using POLARIS, the RIO

result is determined by summing the RVs for each ice type present in the ice regime encountered, multiplied by the respective concentration (in tenths):

$$RIO = C_1RV_1 + C_2RV_2 + \cdots + C_nRV_n \qquad \text{Equation 1}$$

where $C_1, C_2, \ldots, C_n$ are the concentrations of the ice types present in an ice regime and $RV_1, RV_2, \ldots, RV_n$ are the risk values corresponding to each ice type, specific to a particular ship ice class. The resulting RIO value is then evaluated using a set of decision rules to determine the appropriate operational limitation due to the presence of sea ice in an area of operation.

POLARIS has already proven to be a useful tool for not only tactical decision-making onboard ships, but also for the strategic appraisal of navigational risk over wide areas in the Canadian Arctic and other polar and ice-covered regions (Stoddard M. A., Etienne, Pelot, Fournier, & Beveridge, 2018), (Fedi, et al., 2018), (Tremblett, Garvin, & Oldford, 2021), and (Wang, Ding, Yang, & Dou, 2022). While POLARIS has proven to be a useful tool for assessing sea ice risk, it provides little insight into the impact of calculated sea ice risk on expected transit times in ice-covered waters.

1.2.2 State of the Art in Transit Time Estimation in Ice-Covered Waters

Sea ice conditions have a strong influence on ship routing and the expected transit time between maritime locations (Howell & Yackel, 2004). To improve navigation safety in polar waters, most ships are subject to entry and exit date requirements for different maritime areas (commonly referred to as control zones), that are based on a ship's ice class (Transport Canada, 1998). A ship ice class is determined by organizations and national authorities, which develop and apply technical standards for the design, construction, and survey of ships. Many different ship classification societies exist around the world that establish and maintain technical standards for the construction and inspection of polar vessels. Examples of ship classification societies include the American Bureau of Shipping (ABS), Llyod's Register, Bureau Verita, and the International Association of Classification Societies (IACS).

In addition to simple shipping entry and exit date requirements, decision tools like the POLARIS assessment discussed in Section 1.2.1, provide a convenient tool to quickly assess sea ice conditions and the navigational risk to a polar class ship they present. While particularly useful for assessing the ice risk throughout an area of operation, the POLARIS methodology only provides general recommendations for safe ship speeds in elevated risk operations (RIO values between 0 and -10). To date, there have been no empirical studies that have produced results that can be used to specify ship speeds over the full range of POLARIS RIO results.

1.2.2.1 Ship Speeds in Ice

Estimating ship speed in varying sea ice conditions is critical to improving the estimation of travel time, fuel consumption, and emissions in ice-covered waters ((Fedi, et al., 2018), (Howell & Yackel, 2004), (McCallum, 1996)). Much research has been devoted to this topic, focusing on the development of quantitative methods to explain the complex relationship between ice features and ship design characteristics. The primary use of these methods is shipping route generation and optimization in ice-covered waters for the detailed study of arctic maritime traffic.

(McCallum, 1996) proposed the use of polynomial fitting between minimum and maximum expected ship speeds for several Canadian Arctic Class (CAC) ships in different ice risk regimes. Sea ice risk was determined using the Transport Canada Arctic Ice Regime Shipping System (AIRSS) (Transport Canada, 1998). A scaling procedure was used to produce speed curves for different ice class ships in different AIRSS ice risk regimes. However, these curves were only produced for ships below a Canadian Arctic Class (CAC) ship ice class rating, and with a maximum speed of 11 knots. The curves were also only produced for positive Ice Numerals (IN). (Somanathan, Flynn, & Szymanski, 2006) further discusses the use of AIRSS to predict ship speed decreases in different ice risk regimes. The authors evaluated the relative economics of shipping through the Northwest Passage and shipping through the Panama Canal. The authors used historical sea ice analysis to prepare probabilistic ice regimes along shipping routes in the Arctic. Ice conditions were simulated throughout the year and the impact of ice on ship operations was estimated by

the AIRSS Ice Numeral (IN). The authors then specified a relationship between IN and ship ice class to calculate a speed through ice.

(Kotovirta, Jalonen, Axell, Riska, & Berglund, 2009) examined the use of computer-based optimization to determine optimal routes in ice-covered waters. Their model combined the gridded outputs from an ice prediction model, with a ship performance model tailored to Baltic Sea ice conditions to determine ship speed in different ice conditions. The ship speed in various ice thickness was determined using a mathematical relationship between ship net thrust and ice thickness/resistance. AIS data was used for statistical validation of the transit times calculated by their method. The authors note that the quality of optimal routes depends on the quality and resolution of the ice condition data.

((Stephenson, Smith, & Agnew, 2011), (Smith & Stephenson, 2013), (Melia, Haines, & Hawkins, 2016), and (Aksenov, et al., 2017)) all discuss the use of coupled atmosphere-ocean GCM to project future sea ice thickness and concentration to study the future navigability of trans-arctic polar routes. Ship speed and transit time were calculated using the Arctic Transport Accessibility Model (ATAM), which combines high resolution projections of sea ice conditions from a GCM with the AIRSS algorithm to determine navigability and ship speed over wide areas. Ship travel times were specified using the IN versus Ship Speed relationship published in (McCallum, 1996).

(Loptien & Axell, 2014) examined the relationship between AIS ship speed data and sea ice forecasts in the Baltic Sea. By analyzing over 14,000 AIS vessel speed reports, and comparing with Baltic Sea ice charts, the authors were able to produce a mixed-effects model to predict vessel speed from forecasted ice properties (ice concentration, ice thickness, and ridge density). The authors observed decreases in ship speed, without consideration for ship ice class, when sea ice concentration and ice thickness increased from 0 cm to 30 cm. Interestingly, no further systematic speed drops occurred for ice thicknesses above 30 cm were reported. Their analysis shows that a large part of observed ship speed variation can be well explained by the corresponding forecasted sea ice properties, for average ice thicknesses less than 30cm.

(Montewka, Goerlandt, Kujala, & Lensu, 2015) reviewed the use of semi-empirical methods that estimate ship resistance and ship speed in sea ice. The authors noted that most prior work in this area characterized the ice conditions only by the average level ice thickness. In response, the authors developed a Bayesian network that could represent the probabilistic relationship between the ship's speed and many surrounding ice features. Given a set of ice features, the model could be used to compute the probability for a ship to attain a certain speed. Ice features were determined using the state-of-the-art HELMI ice model, allowing the authors to consider the joint effect of various ice features on ship performance.

(Kim, Jeong, Woo, & Han, 2018) present a physics-based method to calculate attainable speed in ice, defined as the speed that is possible to achieve in certain ice types and properties if the ship power level is fixed. Their method combines measures of resistance, self-propulsion (thruster performance), and resistance overload to calculate the attainable speed of a vessel in different ice thicknesses. Tank trials were conducted at the Korean Research Institute of Ship and Ocean Engineering (KRISO) to validate results from their calculation, showing good agreement between computed and measured results during tank testing.

(Simila & Lensu, 2018) discuss estimating the speed of ice-going ships by integrating Synthetic Aperture Radar (SAR) imagery and ship data from AIS. Their study focused on associating the reported vessel location and speed from AIS with features in synthetic aperture radar imagery. A random forest regression model was constructed to estimate ship speed from the features of synthetic aperture radar images. Their method translates SAR images collected over ice cover to expected ship speed maps which can be used for follow-on analysis, such as route planning and optimization. The authors were able to generate useful speed maps from a limited training set, although several uncertainties involved in the use of AIS data were noted. These uncertainties included; (1) changes in speed not due to ice condition, (2) uniformity of ice-going capabilities of observed ships, and (3) the use of frequently navigated channels with different ice properties.

(Dolny, 2018) provides a methodology for defining safe speeds for light ice-strengthened vessels operating in ice. The report provides an overview of several existing approaches for determining operational limitations of ships in various ice conditions. The author's methodology is founded on modern principles of modeling ship and ice interactions, combining collision mechanics, ice strength modeling, and structural strength modeling to determine safe ship speeds in ice. The model allows a user to explore damage estimates and develop safe speed envelopes based on deterministic impact scenarios for specific ship type. The authors note that no suitable model validation data set exists for light ice class or non-ice strengthened hulls in ice conditions. Therefore, extensive validation efforts were outside the scope of the project.

(Lehtola, Montewka, Goerlandt, Guinness, & Lensu, 2019) discuss the use of semi-empirical (simulation) models, and data-driven models to estimate vessel transit speed in different ice regimes. These models estimate a vessel's attainable speed based on the characteristics of the ice field and the ship. A ship operating outside of the ice field in open water is expected to transit at its design speed, where it achieves maximum efficiency. However, a ship operator may choose to operate at slower speeds in polar open water conditions to minimize the risk of high-speed collision with free floating ice.

(Montewka, Goerlandt, Lensu, & Guinness, 2019) provide an empirical study of attainable ship speed or the average ship speed in given ice conditions, with additional consideration for the probability of besetting in ice. The authors proposed a hybrid model, that combines the results from engineering and data driven models to determine attainable ship speed and probability of besetting in ice. The hybrid model is valid for the ice going bulk carrier 1A Super ice class operating in Baltic Sea ice conditions. The goal of the hybrid model is to help better explain the complexity of ship-ice interaction, and the uncertainty it introduces into route planning for ship operations in ice-covered waters. The authors conclude that the hybrid model provides knowledge of the fastest route through ice and can identify areas along the route that will be difficult for a vessel to proceed during independent operations. The authors highlight that the identification of difficult areas along a route is particularly important for planning and delivery of ice breaking services.

(Tremblett, Garvin, & Oldford, 2021) provided an example of a data-driven approach to estimate ship speeds in lake ice using POLARIS. Using shore-based AIS data collected in the North American Great Lakes region between 2010 and 2019, they examine the distribution of observed vessel speeds in different RIO risk category. The RIO for each ship was determined by using ships position as reported by AIS and associating the ship observation with the daily sea ice conditions as reported by the Canadian Ice Service (CIS). Using probability density functions of ship speed in each RIO category, the authors showed a clear trend of speed reduction with decreasing RIO values, both for mild and severe ice conditions. The authors note that for their study they had to assume that there was an approximate ice thickness equivalence between lake ice and ice types used in POLARIS. This assumption was required because POLARIS does not currently provide Risk Values specifically for seasonal lake ice.

Lastly, (Goerlandt, Montewka, Zhang, & Kujala, 2017) and (Liu, Musharraf, Li, & Kujala, 2022) discuss the particular case of expected ship speeds for escort and convoy operations in ice-covered waters. Both studies focus on the analysis of AIS data collected in the Baltic Sea during the winter months. (Liu, Musharraf, Li, & Kujala, 2022) provide results for expected escort and convoy operation speeds for different average sea ice thickness and concentration. The authors reported that as average sea ice thickness increases, transit speed is reduced. The mean value for a merchant vessel under escort was reported as 5.5 knots, increasing to 10 knots when escort was no longer required. Similarly, (Goerlandt, Montewka, Zhang, & Kujala, 2017) also utilized AIS data to analyze ship escort and convoy operations. Their analysis aimed to provide new insights into ship escort and convoy operations by combining AIS data and environmental data to contextualize reports of vessel speed in ice-covered waters. Escort and convoy speeds reported by AIS are provided for different sea ice thicknesses. The authors reported that a transit speed of 10 knots is reasonable for escort operations, however, in sea ice thicknesses greater than 0.6 meters, a convoy transit speed of 5 knots would be recommended for operational planning purposes.

1.2.2.2 Expected Transit Time in Ice-Covered Waters

The simplest method used to estimate transit time is a basic distance divided by speed calculation, where total distance is known, and the speed is fixed. This approach to transit time estimation is widely used in the maritime environment because ships are designed to operate at a particular speed to maximize fuel efficiency and minimize emissions. Ships may be forced to deviate from the maximum economic speed for several reasons, such as adverse weather, but it is expected that these deviations would only affect a small fraction of the total journey and are therefore not explicitly accounted for in the estimate of expected transit time of a given route.

Unfortunately, this basic speed calculation does not easily lend itself to estimating transit time when varied ice conditions are expected along a route, and their impact on ship speed is unknown. Ship impacts with thick first year and multi-year sea ice are one of the main causes of vessel damage in polar waters (Kubat & Timco, 2003). It has been previously reported that ships will significantly reduce average speed when operating in areas of high total ice concentration to reduce the severity of damage from ice impact ((Goerlandt, Montewka, Zhang, & Kujala, 2017), (Fu, Zhang, Montewka, Yan, & Zio, 2016)). To minimize this risk of damage from ship impacts with ice, one approach is to break a voyage up into two primary route segments, (1) route segment to ice edge, and (2) route segment after crossing the ice edge (Snider, 2012). In this case, a ship would use its maximum economic speed up to the ice edge, and then a reduced the average speed used for the route segment after crossing the ice edge.

Simple route segmentation does not work as well for routes that span vast areas of highly variable sea ice conditions. As access to timely and high-quality sea ice analysis increases, it is becoming increasingly important for ship operators to incorporate this information into their route planning and analysis processes, particularly for calculations of estimated time of arrival.

1.2.2.3 Route Planning and Transit Time Estimation in Ice Covered Waters

Navigation risk assessment tools, such as POLARIS, are widely used to assess sea ice risk and determine its impact of safe ship operations (Fedi, et al., 2018). The POLARIS

assessment can be applied over wide areas using national sea ice analysis charts from the United States National Ice Centre (USNIC) and Canadian Ice Service (CIS) to determine the accessibility of maritime locations in the Arctic. Accessibility is a crucial element in SAR incident response operations, especially when considering the more remote maritime locations in the Canadian Arctic. POLARIS is a useful tool to determine the navigability in an intended area of operations, but it does not provide extensive guidance on the selection of safe ship speeds in different RIO categories, as previously discussed in Section 1.2.2.1

Due to the spatial variability of sea ice conditions, and the navigational complexity of the Canadian Arctic archipelago, standard approaches to calculate travel distance and time, such as Euclidean and Manhattan distance are not feasible or even practical. One approach is to determine transit distance and time using network analysis methods, relying on the computation of total network distance and travel time along predefined arcs in an undirected graph (Siljander, Venalainen, Goerlandt, & Pellikka, 2015). Several network analysis algorithms exist to compute the shortest / fastest path between a source node and destination node in a graph, such as Dijkstra's shortest path algorithm (Dijkstra, 1959).

(Smith & Stephenson, 2013) demonstrated the use of network analysis methods to study new trans-arctic shipping routes through the polar region. Their method successfully combined the Transport Canada AIRSS navigability assessment and sea ice data from different coupled atmosphere-ocean GCM, to generate trans-arctic shipping routes using a terrain sensitive least-cost path algorithm. The optimal route was the route that accumulated the lowest possible travel time between origin and destination along the network arcs. The total transit time is the linear sum of the travel time of each arc in the graph that was traversed (Smith & Stephenson, 2013). (Wang, Zhang, & Qian, 2018) provide a complementary example of combining AIRSS with GCM outputs, to generate routes in the Arctic using a modified A* network optimization algorithm. More recently, (Wei, Yan, Qi, Ding, & Wang, 2020) generated arctic shipping routes using a two-step process; (1) calculate the technical accessibility of a grid cell by an ice class ship, and (2) find the fastest route. Technical accessibility of a grid cell was determined using AIRSS with forecasted ice properties (thickness and concentration) from the output of a GCM. The cell-based

least-cost path algorithm in a geographical information system was then used to determine the optimal path from origin to destination.

All the route planning and transit time estimation methods previously discussed require an estimate of expected ship speed in different sea ice conditions and associated risk levels. A good estimate of ship speed in different POLARIS RIO categories is critical to computing accurate estimates of travel time and related metrics such as fuel consumption and emissions. Much research has been devoted to improving our understanding of the complex relationship between ice conditions, ship design, and operating characteristics. Early researchers, such as (McCallum, 1996) , (Somanathan, Flynn, & Szymanski, 2006) , and (Kotovirta, Jalonen, Axell, Riska, & Berglund, 2009) focused heavily on the development and use of mathematical relationships between ship design and ice thickness/resistance to determine expected ship speed. More recently, (Li, Goerlandt, Kujala, Lehtiranta, & Lensu, 2018) selected several state-of-the-art methods to predict ship resistance and performance in sea ice and conducted an evaluation of these methods using full-scale measurement data collected by two ships. The author's results show that the selected methods provide acceptable prediction of ship speed with certain underestimation.

Several researchers have adopted a data-driven approach, focusing on the analysis of AIS data collected in polar regions with daily sea ice analysis, to gain new insight into expected ship speed. (Loptien & Axell, 2014) examined the relationship between AIS reported speed over ground and sea ice forecasts in the Baltic Sea to produce a mixed-effects model to predict vessel speed from forecasted ice properties, such as ice concentration, ice thickness, and ridge density. (Lensu & Goerlandt, 2019) and (Goerlandt, Montewka, Zhang, & Kujala, 2017) provided two more recent examples of combining AIS and sea ice data for the Baltic Sea area, to obtain insights in their relationship with operational ship speeds in ice, for distinct types of ship operations. Lastly, (Tremblett, Garvin, & Oldford, 2021) used shore-based AIS data collected in the North American Great Lakes region between 2010 and 2019 to examine the distribution of observed vessel speeds in different RIO risk categories, derived from CIS sea ice charts produced for the Great Lakes Region.

Lastly, (Tran, Browne, Musharraf, & Veitch, 2023) present the results of a comprehensive literature review on pathfinding and optimization for vessels in ice. A review of 32 research

articles was performed, and systematically summarized. The results showed that main objectives for route planning in ice-covered water are to minimize travel distance, travel time, and fuel consumption. A wide range of approaches were used to optimize these objectives in order to produce least cost routes. Based on their literature review, the author's recommended that future research in the area of route planning in ice-covered waters should explore the inclusion of more operational constraints and introduce uncertainty in pathfinding. It was also recommended that all developers of new algorithms for pathfinding in ice should consider validation techniques to enhance the reliability and practicality of proposed optimal routing tools.

1.2.2.4 Strategic Ship Routing and Analysis in the Arctic

Global climate change, particularly its impact on sea ice conditions in the polar regions, continues to drive interest in the evolving economic feasibility of arctic navigation and commercial shipping, see e.g. (Melia, Haines, & Hawkins, 2016), (Aksenov, et al., 2017), (Boylan, 2021), and (Cau, et al., 2022)). The reported decline in arctic sea ice is projected to continue, and by mid-century the feasibility of trans-arctic navigation and commercial shipping by more polar ship classes will increase. While shipping in the Arctic may be becoming increasingly feasible, uncertain future sea ice conditions will continue to present a significant planning challenge to ship navigators. As the Arctic continues to open it will be increasingly important to have good methods to support strategic route analysis in ice-covered waters ((Crawford, Stroeve, Smith, & Jahn, 2021), (Wei, Yan, Qi, Ding, & Wang, 2020)).

Sea ice conditions exhibit a high degree of spatiotemporal variability and can create significant disruption to ship movement. National sea ice analysis authorities, such as the CIS and USNIC have been analyzing ice in polar waters for more than 60 years and have compiled sea ice statistics for different regions in the Arctic. Historical Information on the ice is gathered from an archive of weekly, bi-weekly, or monthly sea ice analysis charts to compute the sea ice climate normals for polar waters (Canadian Ice Service, 2021). Ice climate normals are used to describe the historical sea ice freeze-up / break-up dates and typical ice conditions (ice concentration and predominant ice type). While useful for

building a general understanding of expected sea ice conditions along a route, ice climate normals do not provide much insight into the navigational risk along a planned route due to complex interaction of ships and ice.

Operating ships in sea ice requires specialized knowledge and skill beyond that of many mariners (Snider, 2012). Knowledge of the environment, ice, available infrastructure, polar ship design and equipment, and ship handling in ice are all essential when planning routes in the Arctic. In January 2017, the International Maritime Organization (IMO) entered into force the Polar Code, which provides a legal framework to govern maritime operations in the Arctic and Antarctic waters. The Polar Code is the product of years of negotiations at the IMO to improve shipping safety in polar regions. The objective of the Polar Code is to address the unique hazards confronted by ships operating in the Arctic and Antarctic through the introduction of a variety of safety and pollution prevention measures, including those related to design and equipment, operations, crew training, and the protection of the marine environment (Fraser, 2020).

A key component of the Polar Code is the mandatory requirement for all ships intending to operate in the Arctic and Antarctic to carry a ship specific Polar Water Operational Manual (PWOM). The PWOM defines specific procedures for mitigating risks to and from ships operating in polar waters by ensuring that a vessel operates safely within ship design limits. To help mitigate the risk to a ship from sea ice, the PWOM requires ship operators to specify a practical methodology for assessing ship operational limits in ice. The IMO currently promotes the Polar Operational Limit Assessment Risk Indexing System (POLARIS), developed by the International Association of Classification Societies (IACS) (Fedi, et al., 2018).

(Stoddard M. , Etienne, Fournier, Pelot, & Beveridge, 2016) presented a method to compute different statistical aggregations of POLARIS RIO results using a historical archive of CIS sea ice analysis charts. Their results were intended to support a variety of strategic decision-making applications in the Canadian Arctic. One limitation noted by the authors was that their results are specific to the Canadian Arctic because of their reliance on CIS sea ice analysis charts, which are only produced for the Canadian Arctic. To overcome national

ice center product coverage area and temporal resolution limitations, researchers are increasingly using model data from sea ice forecasting models and coupled atmosphere-ocean general circulation models (GCM), to determine sea ice thickness and concentration (Fedi, et al., 2018). These sources typically provide researchers with a daily estimate of the average sea ice thickness (m) and corresponding sea ice concentration (%) at a specified spatial resolution (Bilge, et al., 2022).

(Smith & Stephenson, 2013) analyzed seven climate model projections of sea ice conditions, assuming two different climate change scenarios, to assess future changes in commercial shipping pathways from the Atlantic Ocean to the Pacific Ocean. Their analysis successfully combined the Transport Canada AIRSS navigability assessment, and data from different coupled atmosphere-ocean GCM, to generate trans-arctic shipping routes with expected transit time. Their routes, and estimated transit time results, reflect conditions for the peak late-summer shipping season only (September), and are driven solely by the projected reductions in sea ice thickness and concentration.

(Aksenov, et al., 2017) examined the feasibility of transporting cargo from Europe to Asia via trans-arctic shipping routes. The authors examined the navigability of common arctic sea routes, including the NWP, NSR, and North Pole Route (NPR) using high-resolution projections of ocean and sea ice conditions. Arctic sea route accessibility and transit times by different ice class ships were determined using the Arctic Transport Accessibility Model (ATAM) (Stephenson, Smith, & Agnew, 2011). The ATAM model assumes sea ice conditions are the primary factor impacting safe ship speeds and ship transit time in polar waters and relies on the use of the AIRSS Ice Numeral (IN) to assess a ships ability to safely navigate in different ice regimes (Transport Canada, 1998). A ship safe speed for different IN was used to estimate the trans-arctic total transit time through varying ice conditions.

(Melia, Haines, & Hawkins, 2016) utilized simulations from several global climate models (GCMs) to examine the future arctic shipping prospects for two polar vessel classes; (1) Open Water (not-ice strengthened), and (2) Polar Class PC6 (capable of operating in medium first year ice). Shipping routes were calculated using a speed of 16 knots in open

water and a six-degree-of-freedom numerical model to determine slower speeds in ice that account for different polar class vessel capabilities in sea ice (Tan, Su, Riska, & Moan, 2013). The results of their work indicate that traditional trans-arctic routes (NSR, NWP, and NPR) will become faster throughout the 21st century, but interannual variability will remain a significant factor in route availability and selection.

(Fedi, Faury, & Etienne, 2020) discuss the use of the European Union's Copernicus database to produce ice condition statistics (thickness and concentration) over a 28-year climatological period. To compute the POLARIS RIO using ice condition statistics from the Copernicus database researchers must first apply a set of rules to convert average ice thickness to its equivalent ice stage of development. Once this mapping is complete, it is possible to calculate the RIO value by multiplying the appropriate risk value that corresponds to the stage of development by the ice concentration. A limitation of this approach is that it does not consider partial concentrations of more than one ice type in an ice regime.

Lastly, (Wei, Yan, Qi, Ding, & Wang, 2020) generated arctic shipping routes using a two-step process, (1) calculate the technical accessibility of a grid cell by an ice classed ship, and (2) find the fastest route. Technical accessibility of a grid cell was determined using AIRSS with forecasted ice properties (thickness and concentration) from a GCM. A cell-based, least-cost path algorithm in a GIS was then used to determine the optimal path from origin to destination. More recently, (Lee, Roh, & Kim, 2021) proposed a cell-free seed-based genetic algorithm to obtain safe and economic shipping routes through the Arctic Ocean, using POLARIS and the prediction of sea ice properties (thickness and concentration) from a GCM.

1.3 Objectives and Structure of the Thesis

This thesis was written within the discipline of industrial engineering, and takes a strategic-level view when analyzing arctic navigational risk and transit time estimation. It draws on the engineering science of risk, navigation, and network optimization literature. The thesis takes a microscopic view of arctic navigation risk, focusing on the hazard of ship and sea ice interaction, and its impact on strategic ship routing and SAR response planning. Where

other engineering disciplines may focus on measuring sea ice pressures, or loads when determining expected ship speed and transit time in ice-covered waters, this thesis focuses on directly measuring ship speed in different sea ice conditions and statistically relating these measurements to sea ice risk and expected transit time in ice-covered water.

We assume that we are in a rational actor paradigm, where decisions are made that maximize reward (Renn, Jaeger, Rosa, & Webler, 2000). More specifically, we assume that navigational decisions are made that minimize the risk from ship and ice interaction. The quantitative modeling completed in this thesis considers the risk from ship and ice interaction as a simple risk, but acknowledge that some dimensions of sea ice risk are uncertain. The limited data and information on consequences from ship and ice interaction all contribute to a degree of unresolved uncertainty when determining sea ice risk.

Considerable progress has been made in recent years in managing most safety risks in the Arctic, largely through the introduction of new Polar Code (World Maritime Organization, 2016). Regardless, the consequence of an incident occurring in a remote ice-covered area in the Canadian Arctic remains very high. Ship and ice interaction is particularly hazardous, and is a major factor contributing to arctic maritime risk and navigation decision making in ice-covered water.

This thesis aims to improve strategic route planning and marine-based SAR response planning in the Arctic by introducing a new quantitative method to estimate transit time in ice-covered waters that can be combined with network analysis to enable the computer-generation of (1) the fastest path between two locations in the Arctic, (2) SAR incident response service areas, and (3) SAR incident response isochrones.

Using this method, we can compute, assess and visualize strategic routes through complex polar navigating environments, such as the Canadian archipelago, and examine marine-based SAR response in the Arctic. This method focuses on the use of the POLARIS assessment with USNIC sea ice analysis charts for the strategic assessment of sea ice risk and navigation decision making. The results presented in this thesis using this method are focused on independent ship operations, and only considers the impact of sea ice risk on transit time and optimal route selection. There are provisions for the use of the POLARIS assessment to support navigation risk assessment during icebreaker escort operations, but

this will not be discussed in detail in this thesis. The end-users include arctic ship operators and voyage planners, SAR coordinators and response planners, and those involved in Area-Based Management (ABM) of shipping risk in the Arctic. ABM consists of a suite of tools for the spatial organization and control of ocean space in achieving defined policy and planning goals, such as sustainability conservation, safety, and public order at sea (Chircop, Goerlandt, Pelot, & Aporta, 2024). This thesis focuses on ABM in the context of Canadian Arctic Search and Rescue (SAR), with emphasis on SAR response planning and evaluation.

This thesis has three high-level research objectives, as follows:

> **Research Objective 1:** Develop a spatiotemporal computation to estimate marine-based transit time in ice-covered waters that considers the time of year, expected ice conditions, ship ice classification, and sea ice risk.
>
> **Research Objective 2:** Propose a graph-theoretic approach to strategic route planning in ice-covered waters.
>
> **Research Objective 3:** Evaluate marine-based SAR response using network optimization and spatial analysis techniques.

The first research objective led to the formulation of RQs 1, 2, and 3, and were addressed in PI and PII, and PIII. The second research objective resulted in RQ 4 and was addressed in PIV. The third research objective resulted in RQs 5 and 6 and were addressed in PV and PVI. The research questions are listed below:

> **Research Question 1:** How can POLARIS be used to compute and visualize ice navigation risk throughout the Canadian Arctic? (PI&PII)
>
> **Research Question 2:** Is there a statistical relationship between ship speeds reported from the Canadian Arctic and the POLARIS Risk Index Outcome (RIO)? (PIII)
>
> **Research Question 3:** How can the expected transit time in ice-covered water be estimated for strategic decision applications, such as optimal route selection and marine-based SAR response time estimation? (PIII)

Research Question 4: How can an optimal path in ice-covered waters be computer-generated to support strategic route analysis? (PIV)

Research Question 5: How can network analysis methods and geospatial data processing techniques be used to support the analysis of marine-based SAR planning and incident response? (PV & PVI)

Figure 1 illustrates the relationships between the objectives, research questions, and the associated publications.

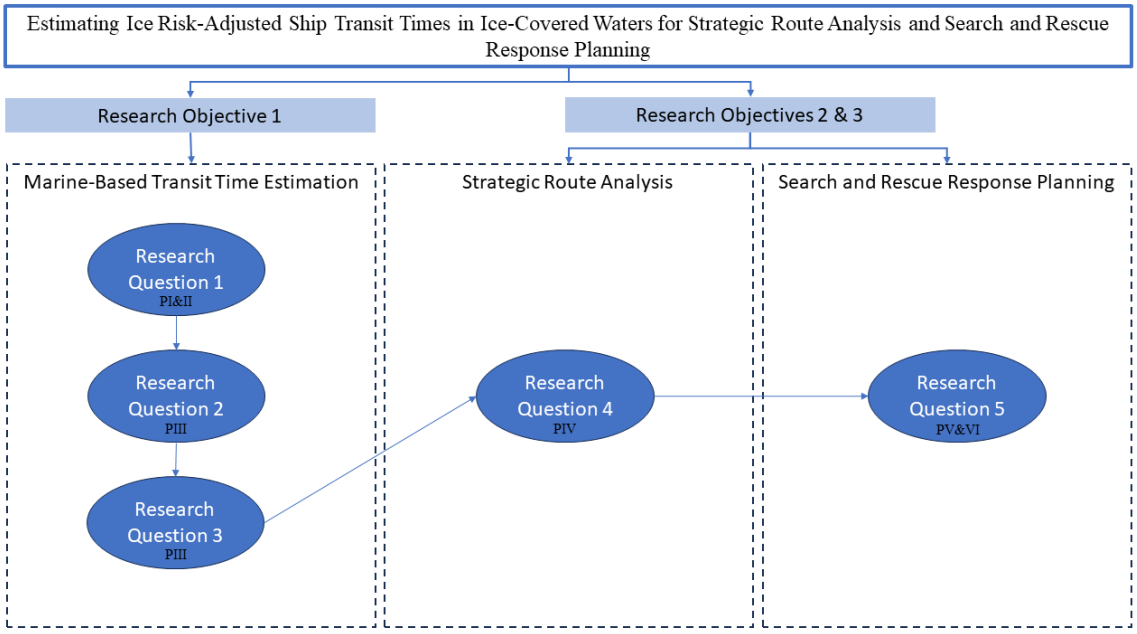

Figure 1. The overall structure of the thesis

CHAPTER 2: Research Methods

2.1 Assessing Arctic Navigational Risk using Sea Ice Analysis Charts and POLARIS (RO1 / RQ1 / PI&II)

The first method proposed in this thesis utilizes a historical archive of circumpolar sea ice analysis charts produced by the USNIC to produce several different statistical aggregations of historical POLARIS RIO results observed over the climatological period from 1991 to 2020. In total, 1,295 USNIC sea ice analysis charts were gridded using a Voronoi tessellation with an approximate Voronoi cell resolution of 12.5 km x 12.5 km. The tessellation applied to each chart produced 4,212,296 georeferenced cells, with each cell containing the sea ice analysis attributes from the processed ice analysis chart. The gridded USNIC sea ice analysis charts were then grouped into bi-weekly analysis periods, enabling the computation of different bi-weekly statistical aggregations of POLARIS RIO results. Figure 2 provides an overview of the processing flow to compute different statistical aggregations of the historical POLARIS RIO results.

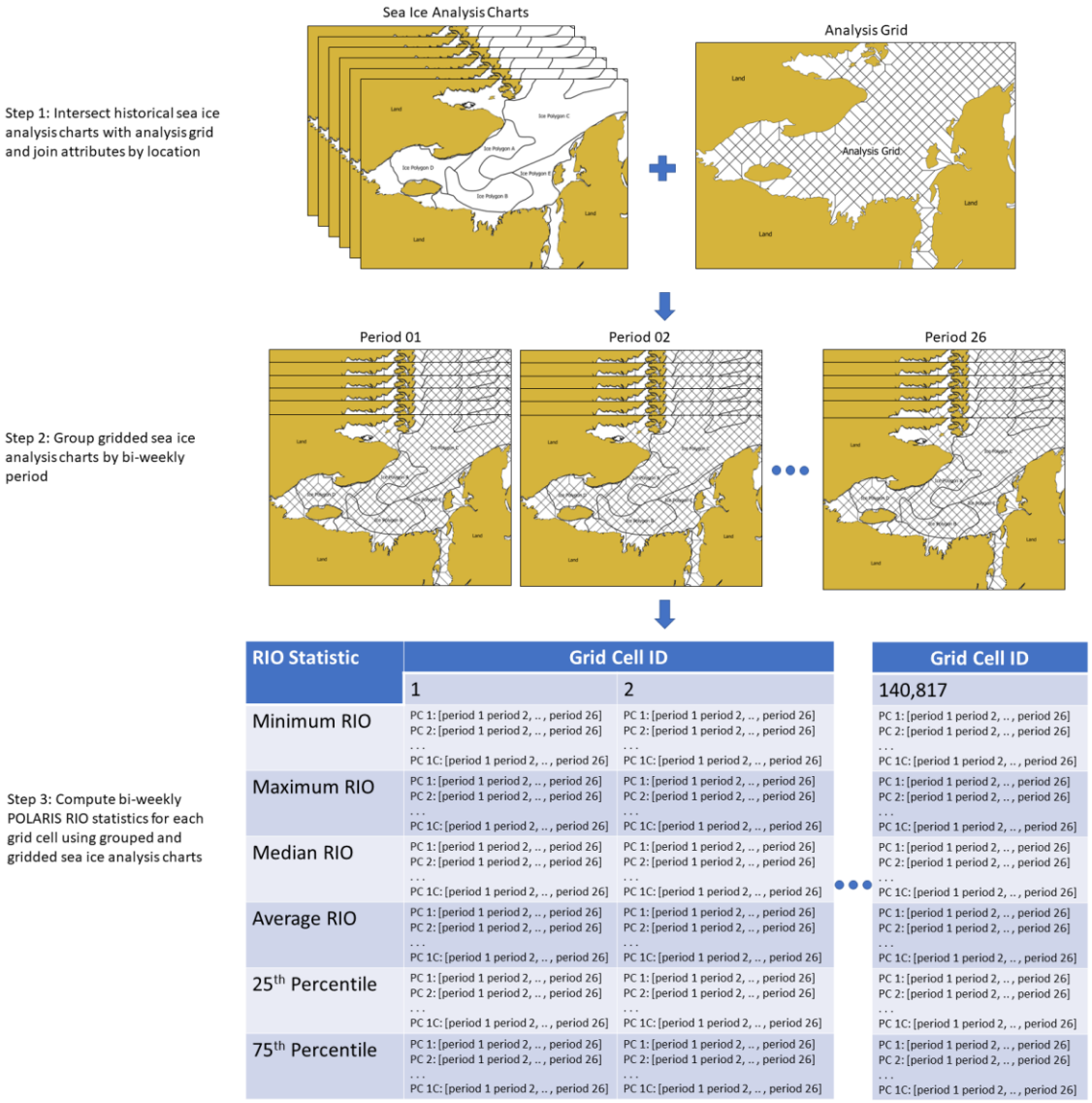

RIO Statistic	Grid Cell ID			Grid Cell ID
	1	2		140,817
Minimum RIO	PC 1: [period 1 period 2, .. , period 26] PC 2: [period 1 period 2, .. , period 26] . . . PC 1C: [period 1 period 2, .. , period 26]	PC 1: [period 1 period 2, .. , period 26] PC 2: [period 1 period 2, .. , period 26] . . . PC 1C: [period 1 period 2, .. , period 26]		PC 1: [period 1 period 2, .. , period 26] PC 2: [period 1 period 2, .. , period 26] . . . PC 1C: [period 1 period 2, .. , period 26]
Maximum RIO	PC 1: [period 1 period 2, .. , period 26] PC 2: [period 1 period 2, .. , period 26] . . . PC 1C: [period 1 period 2, .. , period 26]	PC 1: [period 1 period 2, .. , period 26] PC 2: [period 1 period 2, .. , period 26] . . . PC 1C: [period 1 period 2, .. , period 26]		PC 1: [period 1 period 2, .. , period 26] PC 2: [period 1 period 2, .. , period 26] . . . PC 1C: [period 1 period 2, .. , period 26]
Median RIO	PC 1: [period 1 period 2, .. , period 26] PC 2: [period 1 period 2, .. , period 26] . . . PC 1C: [period 1 period 2, .. , period 26]	PC 1: [period 1 period 2, .. , period 26] PC 2: [period 1 period 2, .. , period 26] . . . PC 1C: [period 1 period 2, .. , period 26]		PC 1: [period 1 period 2, .. , period 26] PC 2: [period 1 period 2, .. , period 26] . . . PC 1C: [period 1 period 2, .. , period 26]
Average RIO	PC 1: [period 1 period 2, .. , period 26] PC 2: [period 1 period 2, .. , period 26] . . . PC 1C: [period 1 period 2, .. , period 26]	PC 1: [period 1 period 2, .. , period 26] PC 2: [period 1 period 2, .. , period 26] . . . PC 1C: [period 1 period 2, .. , period 26]		PC 1: [period 1 period 2, .. , period 26] PC 2: [period 1 period 2, .. , period 26] . . . PC 1C: [period 1 period 2, .. , period 26]
25th Percentile	PC 1: [period 1 period 2, .. , period 26] PC 2: [period 1 period 2, .. , period 26] . . . PC 1C: [period 1 period 2, .. , period 26]	PC 1: [period 1 period 2, .. , period 26] PC 2: [period 1 period 2, .. , period 26] . . . PC 1C: [period 1 period 2, .. , period 26]		PC 1: [period 1 period 2, .. , period 26] PC 2: [period 1 period 2, .. , period 26] . . . PC 1C: [period 1 period 2, .. , period 26]
75th Percentile	PC 1: [period 1 period 2, .. , period 26] PC 2: [period 1 period 2, .. , period 26] . . . PC 1C: [period 1 period 2, .. , period 26]	PC 1: [period 1 period 2, .. , period 26] PC 2: [period 1 period 2, .. , period 26] . . . PC 1C: [period 1 period 2, .. , period 26]		PC 1: [period 1 period 2, .. , period 26] PC 2: [period 1 period 2, .. , period 26] . . . PC 1C: [period 1 period 2, .. , period 26]

Figure 2: Processing flow to compute the statistical aggregations of RIO value using historical archive of USNIC sea ice analysis charts (PIV)

For strategic navigation planning it is often necessary to plan routes based on the ice conditions expected to be encountered during a future voyage. PI and PII have demonstrated how different statistical aggregations of historical POLARIS RIO results can be used to support strategic navigation planning in polar waters. PII presented six statistical aggregations of historical RIO results observed throughout the Canadian Arctic between 2007 and 2014, including; (1) minimum RIO (worst case), (2) 25th percentile RIO, (3) average RIO, (4) median RIO, (5) 75th percentile, and (6) maximum RIO (best case).

More recently, PIV applied a similar gridding method to USNIC bi-weekly circumpolar sea ice analysis charts to compute the same six statistical aggregations of POLARIS RIO results observed over the climatological period from 1991 to 2020. Each statistical aggregation was computed on a bi-weekly basis, resulting in a final output of 26 gridded bi-weekly POLARIS risk maps. Figure 3 shows how the features of the bi-weekly POLARIS scenario risk map are spatially joined with the analysis grid to produce a gridded bi-weekly POLARIS scenario risk map. Once gridded, the results are grouped into 26 bi-weekly analysis periods to enable the computation of the six statistical aggregations in each grid cell.

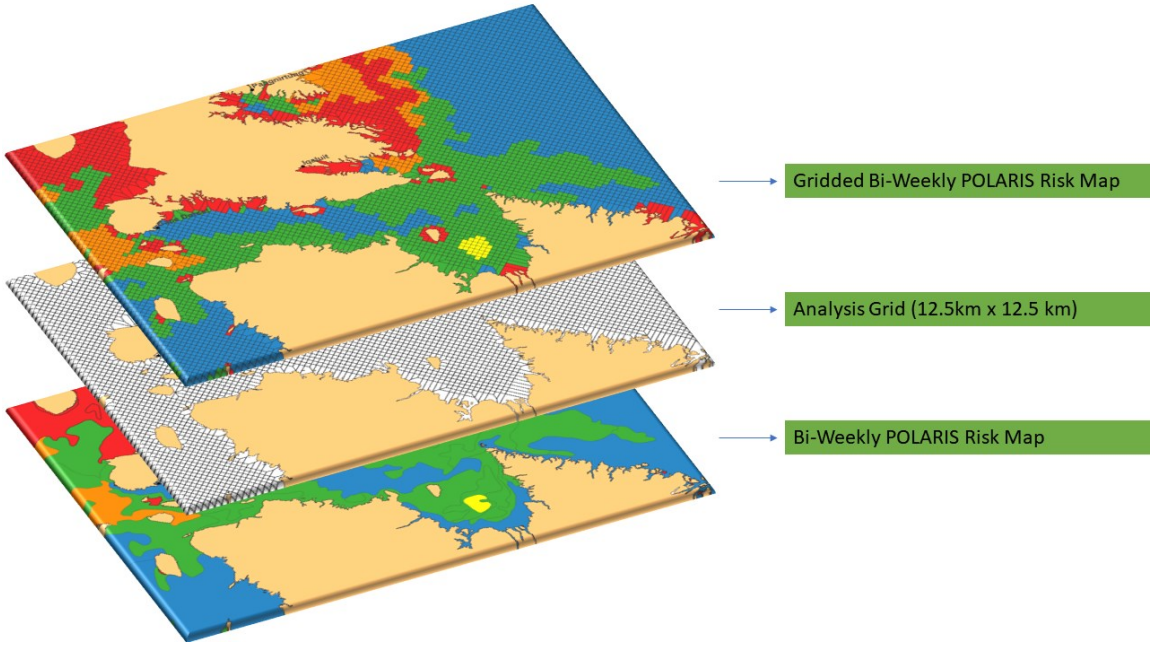

Figure 3: Geospatial processing of map layers to generate the gridded bi-weekly POLARIS scenario risk map (top layer)

2.2 Ship Speeds in Ice using AIS and POLARIS (RO1 / RQ2 / PIII)

2.2.1 AIS Reporting and Ship Ice Classification

AIS transponders are designed to provide position, speed, identification, and other information about the ship to other ships, coastal authorities automatically. Since 2004, SOLAS regulation V/19 -" Carriage requirements for shipborne navigational systems and equipment" has required all ships of 300 gross tonnage to carry AIS (International Maritime

Organization, 2004). The early days of AIS vessel tracking were dependent on establishing a network of shore-based AIS receivers to receive the AIS VHF transmissions of passing ships fitted with AIS transponders. The advent of satellite-based AIS (S-AIS) receivers, and rapid commercialization of space-based reception, has led to an explosion of global vessel tracking and related research that relies on S-AIS (Spire Maritime, 2023).

The S-AIS data set used for this study was collected by the ExactEarth Ltd. AIS satellite constellation. The data set covers 2018 and 2019 and contains approximately 22 million AIS position reports from 184 ships. The geographic extent of the AIS data set is 40N to 90N and 45W to 130W and is shown in Figure 4. Each AIS position report provides information on the vessel identity, type, time, position, speed, and navigation status. Currently, the International Telecommunication Union (ITU) AIS message specification does not include ship ice class, which is a necessary AIS message attribute to compute sea ice risk using POLARIS (International Telecommunication Union, 2014).

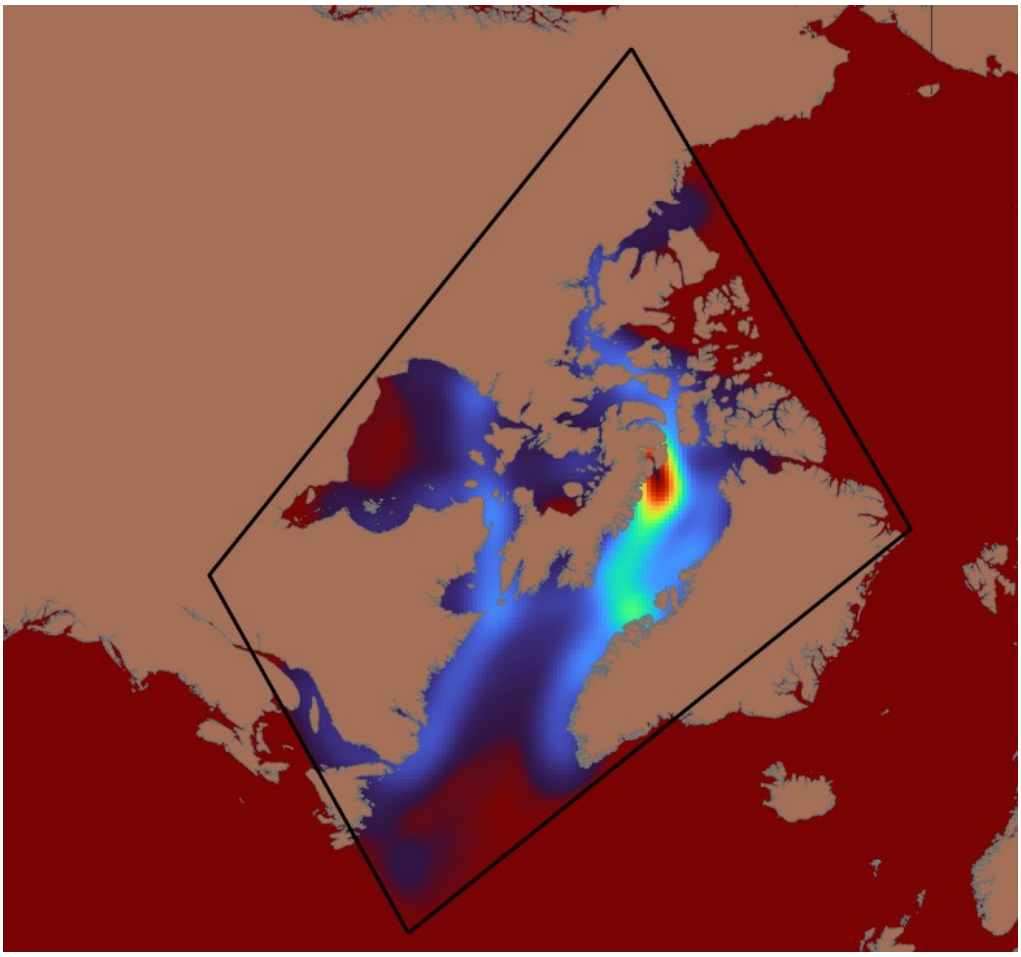

Figure 4: 2018-2019 Geographic extent of the S-AIS data set and message density (PIII)

To add the ice class attribute to the S-AIS data set we joined our AIS data with a database record of Finnish-Swedish (FS) ice class ships from Lloyd's Register[1]. The FS ice class ship database contained ship ice class information for 12,720 ships. These two data sets were joined by matching the IMO number from each S-AIS report with the IMO number associated with each of the FS ice class ship records in the Lloyd's Register database. S-AIS reports that could not be matched were removed from the S-AIS data set to facilitate follow-on analysis.

2.2.2 Joining S-AIS Messages with POLARIS RIO Results

QGIS Desktop 3.24.3 was used to perform the geospatial processing steps required to join the attributes of our S-AIS data set with the attributes of the intersecting USNIC sea ice

[1] https://www.lr.org/en/about-us/who-we-are/lr-ships-in-class/

analysis polygons (QGIS, 2023). In total, 101 USNIC sea ice analysis charts were processed, spanning the spatiotemporal extent of the 2018-2019 S-AIS data set. Once joined, each AIS report in our data set contained additional columns of data containing the sea ice analysis attributes at the time of the AIS report. The RIO score was then computed for each AIS report using Equation 1 (see Section 1.2.1).

2.2.3 Descriptive Statistics for Vessel Speed in Different RIO Result Categories

Using the results from Section 2.2.2 it is possible to compute descriptive statistics of the AIS reported vessel speed in different POLARIS RIO result categories. POLARIS RIO values were grouped into five categories to support this method, including; (1) RIO = 30: Open Water Operation, (2) 0 <= RIO < 30: Normal Ice Operations, (3) -10 <= RIO < 0: Elevated Operational Risk, (4) -30 < RIO < -10: High Risk Operations, and (5) RIO = -30: Extreme Risk Operations. The selection of POLARIS RIO result categories to produce descriptive statistics is discussed in detail in PIII and will be discussed in Section 3.1.2.

2.3 Computing the Expected Transit Time (ETT) in Ice Covered Waters (RO1 / RQ3 / PIII)

The most basic approach to transit time estimation is a simple distance divided by speed calculation, where distance is known, and the speed is fixed. This calculation assumes that, without environmental or other external factors, a ship has a planned transit speed that remains constant for the duration of a transit.

$$T = \frac{D}{S} \qquad \text{Equation 2}$$

where,

T = Transportation Time (hours)

D = Distance (nautical miles)

S = Ship Speed (knots)

Unfortunately, simple transit time estimation methods used to estimate transit time do not allow for the formal consideration of variable sea ice conditions along a route, and their impact on ship speed. PII previously showed the use of POLARIS and open access sea ice analysis products to evaluate the expected POLARIS RIO along routes in polar waters. We now introduce a new computational method that combines the POLARIS RIO results along a route, with the RIO speed curves discussed in Section 1.2.2.1, to compute the Expected Transit Time (ETT) in ice-covered water.

ETT is computed using the conventional distance divided by speed approach previously discussed, except we now account for the impact of varying expected sea ice conditions along a route. This is achieved by computing the distance a polar class ship must transit through each of the pre-defined POLARIS RIO categories, divided by a specified ship speed associated with each of the POLARIS RIO categories. The ETT is then determined by performing a linear sum of these results. Equation 3 provides a generalized mathematical formulation for computing ETT using POLARIS.

$$ETT_{jt} = \sum_{k=1}^{4} \frac{D_{jtk}}{S_k} \quad \forall\, j \in J, t \in T \qquad \text{Equation 3}$$

In Equation 3, the estimated transit time, ETT_{jt} , is the estimated transit time by a ship with ice class *j*, in analysis period *t*. To compute ETT_{jt} we first generate D_{jtk}, which is a sparse matrix containing the distances travelled through POLARIS RIO category k, by ship ice class *j*, in analysis period *t*. The ship speed, S_k , represents the specified ship speed through POLARIS RIO category *k*. The indexes J, and T represent the set of all ship ice class j, and analysis period t. This mathematical formulation can be used to calculate the ETT for all ship ice classes, and analysis periods. Currently, our analysis is completed on a bi-weekly basis, which results in 26 bi-weekly analysis periods. A necessary assumption is that the route being evaluated can be completed within the analysis period being considered.

2.4 Computing the Ice Risk-Adjusted Estimated Time of Arrival (I-ETA) (RO2 / RQ4 / PIV)

2.4.1 Arctic Transportation Graph Construction

To facilitate the computation of the Ice-Risk Adjusted Estimated Time of Arrival (I-ETA) it was necessary to first construct a network graph, consisting of nodes and arcs that overlap with the coverage area of our gridded POLARIS RIO results vector layer. Similar to (Smith & Stephenson, 2013), a vector layer of nodes was first created by generating a point at the centroid of each grid cell of the gridded POLARIS RIO results vector layer. To produce the transportation graph, each node was then linked to the nodes in the surrounding square neighborhood by the 8 shortest line segments (arcs). Figure 5 illustrates the process of creating the transportation graph used for this study.

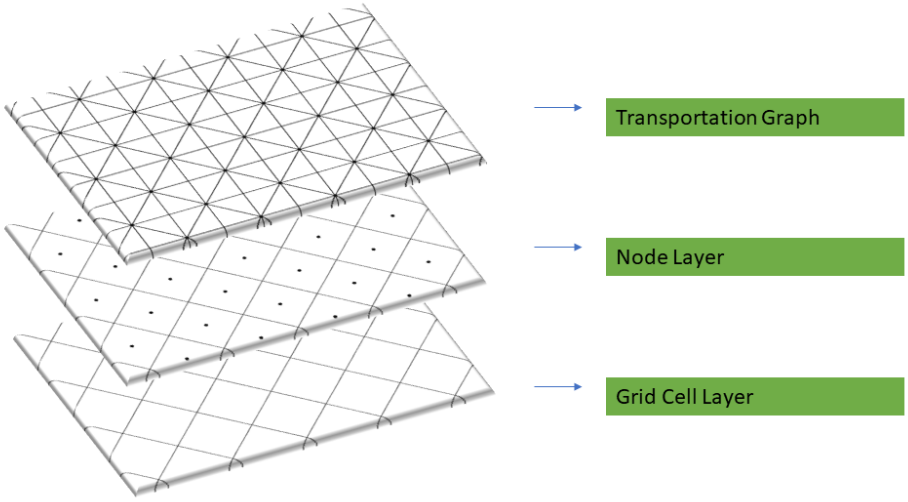

Figure 5: Spatial processing stack to produce the transportation graph (PIV)

The graph was then geospatially processed to remove nodes and arcs in water depths less than 30 m, or within 5 nm of the coastline. The resulting arctic transportation graph consists of 140,817 nodes and 1,099,952 arcs. Figure 6 shows a zoomed in part of the arctic transportation graph.

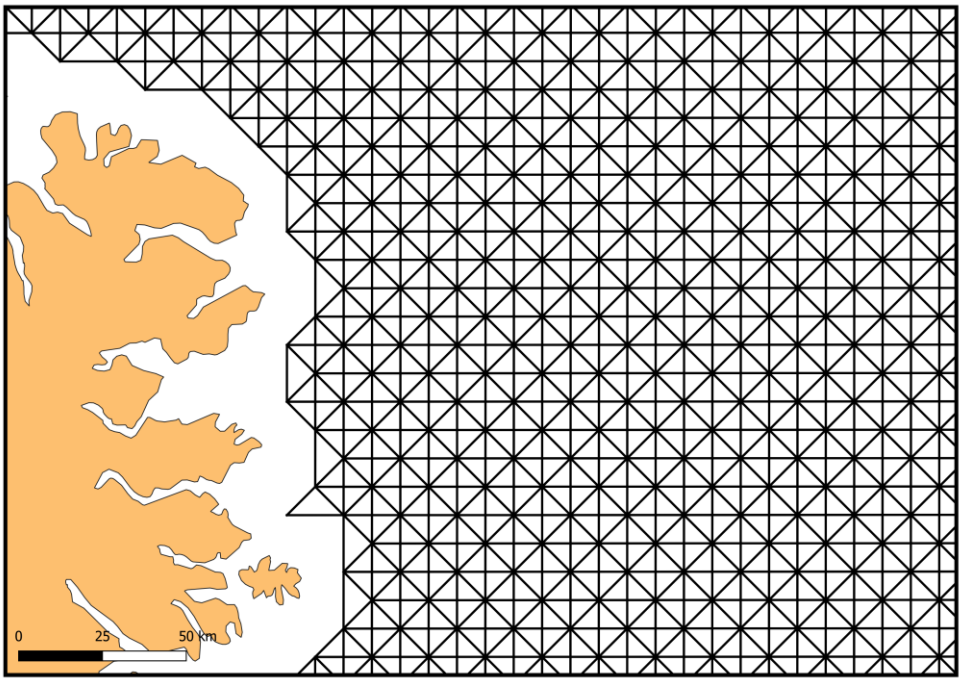

Figure 6: Arctic transportation graph constructed from uniformly spaced nodes and 8 shortest lines connecting neighboring nodes (PIV)

After we created the arctic transportation graph, we then generated the POLARIS RIO results for each arc in the graph. This required a two-step process. The first step was to join the gridded POLARIS RIO results layer with the nodes of our arctic transportation graph. The second step was to compute the POLARIS RIO value for each arc in the graph. This was done by taking the average of the POLARIS RIO value of the start node and the end node of the arc, see Equation 4. The final arc cost is the arc length divided by the expected speed associated with the POLARIS RIO value of the arc, see Equation 5.

$$Arc\ RIO = \frac{RIO_{arc\ start\ node} + RIO_{arc\ end\ node}}{2} \qquad \text{Equation 4}$$

$$Arc\ Cost = \frac{Arc\ Length\ (nm)}{Speed_k(kts)} \quad k = POLARIS\ RIO\ Result\ Category \qquad \text{Equation 5}$$

It is important to note that there are RIO values associated with each arc for every ship ice class and analysis period. This is because the selection of POLARIS RIO result depends on the ship ice class and period being considered. As ice conditions change throughout the year, so does the POLARIS RIO value for a specific arc in the arctic transportation graph. The POLARIS result also changes based on the selection of ship ice class. Ships with more capability to operate in ice will have a higher POLARIS RIO value, indicating a more favorable operating condition. Ships with less capability will have a lower POLARIS RIO value, indicating a less favorable operating condition. Figure 7 provides a high-level overview of the geospatial processing stack and resulting graph with joined RIO analysis for each arc.

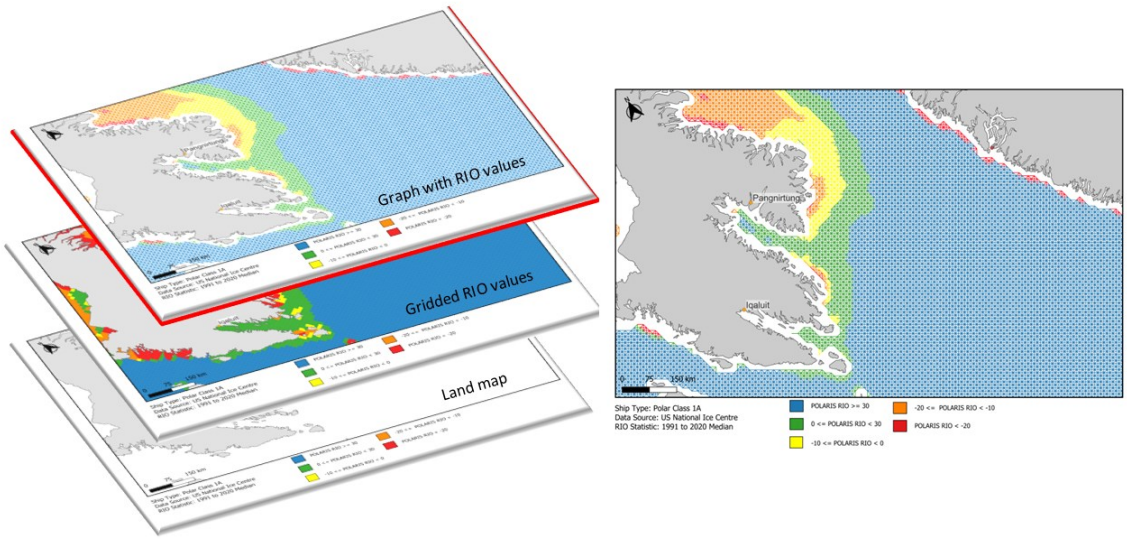

Figure 7: Geospatial processing stack to generate the arctic transportation graph with arc RIO values (PIV)

2.4.2 Fastest Path Network Optimization

Let $G = (V, E)$ be our undirected transportation graph, consisting of nodes (V) and arcs (E). Let $s, t \in V$ be nodes such that there is a feasible path from a specified origin node of voyage (s) to a specified destination node of voyage (t). Let T be the set of transshipment nodes in our graph. The RIO value for each arc in our graph is determined by averaging the RIO value of the start and end node of each arc in the graph (Equation 4). The

transportation cost, $c_{i,j,y,z}$, of each arc in our graph is then computed by dividing the cartesian distance between any two connected nodes by the expected ship speed along the specified arc (Equation 5). Below is the general linear program formulation of the fastest path problem presented in this thesis to compute the I-ETA.

$$Minimize: \sum_{i \in I} \sum_{j \in J} c_{i,j,y,z} x_{i,j}$$

Subject to:

$$\sum_{(s,j) \in E} x_{s,j} = 1 \qquad (1)$$

$$\sum_{i,k} x_{i,k} - \sum_{k,j} x_{k,j} = 0 \quad \forall\, k \in T \qquad (2)$$

$$\sum_{(i,t) \in E} x_{i,t} = 1 \qquad (3)$$

$$x_{i,j} \in \{0,1\} \quad \forall\, (i,j) \in E \qquad (4)$$

Where:

T = Set of transshipment nodes

E = Set of arcs in graph

I = Set of feasible start nodes

J = Set of feasible end nodes

Y = Set of ship ice classes

Z = Set of analysis time periods

s = Specified origin node of voyage

t = Specified destination node of voyage

k = feasible transshipment node

$x_{i,j}$ = ship transit from node *i* to node *j*

$c_{i,j,y,z}$ = Expected Transit Time (ETT) from start node *i* to end node *j*, for ship ice class y, in analysis time period z

(1) = One outgoing edge from start location must be selected

(2) = One incoming edge and one outgoing edge must be selected for each transshipment node

(3) = One incoming edge to end location must be selected

(4) = Binary Integer Constraint on selection of edges

By exploiting the total unimodularity of our fastest path problem formulation we are able to relax the binary integer constraint (4) to a linear non-negativity constraint. The total unimodularity our constraint matrix guarantees that the solution will be an integer solution (Schrijver, 1998).

To compute the fastest path, we use the QGIS fastest path (point to point) function from the network analysis function list in the processing toolbox (QGIS, 2023). This function calculates the fastest path between any specified origin and destination in our arctic transportation graph using a commercial implementation of Dijkstra's algorithm (Dijkstra, 1959). The fastest path is then the selection of arcs from a start point to an end point that minimizes the total transit time. The total transit time is the linear sum of the transit time of all selected arcs forming the path from start to end location. We refer to the total transit time of the fastest path as the Ice Risk-Adjusted Estimated Transit Time (I-ETA). The I-ETA combines the results of the ETT calculation with network path optimization to produce an estimate of the expected total transit time of the optimal path between two locations in ice-covered waters.

2.4.3 Fastest Path Route Analysis

Once a route has been generated, we can use the POLARIS assessment to determine the proportion of a total transit through different POLARIS RIO result categories. This knowledge allows for the strategic analysis of routes based on a desired risk profile/tolerance for a route. For example, it is possible to set threshold values for each POLARIS RIO result category to limit a ship's exposure to negative RIO conditions. Our method for calculating the fastest route does not currently constrain routes to favorable RIO result categories, rather, it applies a higher arc cost (transit time) to segments of a transit through areas of higher risk. This approach ensures that routes can still cross areas of higher

risk, but with the obvious consequence of increasing the total transit time. The use of the fastest path route analysis method allows one to quantitatively assess and visualize the overall risk of the route, based on the distribution to the total transit distance through each of RIO result categories encountered during the voyage.

2.5 Marine-Based Incident Response using I-ETA (RO3 / RQ5 / PVI)

In addition to computing the fastest path, we are also interested in computing Incident Response Service Areas (IRSA) and Incident Response Isochrones (IRI) in the Canadian Arctic. To simplify the following discussion, we first introduce the concept of the Service Area Analysis Scenario (SAAS). The SAAS refers to the selection of, (1) Polar Class ship type, (2) analysis period, (3) RIO value statistical aggregation, (4) expected ship speed in each RIO result category, (5) Maximum Response Time Cut-off (MRTC), and (6) a specified SAR incident location. The IRSA contains all the nodes and arcs of our transportation network that can be reached for a given SAAS. The IRI is a curve of equal travel time (isochrone) formed at the furthest locations in our network that can be reached for given SAAS. Mathematically, the IRSA is the concave hull formed from all nodes in the transportation graph that can be reached within the specified time cut-off. Figure 8 illustrates the relationship between the transportation graph, incident response service area, and incident response isochrone.

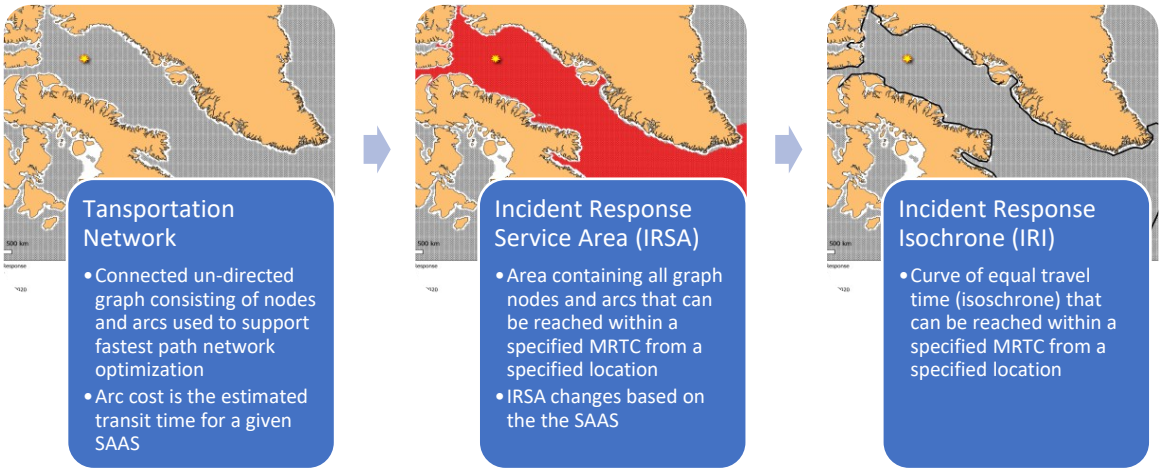

Figure 8: Relationship between transportation network, incident response service area, and incident response isochrone (PVI)

CHAPTER 3: Results

This section is divided into three parts, each dedicated to one of the three research objectives presented in Section 1.3. Section 3.1 discusses the key results from the effort to produce a new computational method to estimate expected transit time in ice-covered waters. Section 3.2 shows the results produced using the graph-theoretic approach to strategic route planning proposed in this thesis. Lastly, Section 3.3 discusses the application of the I-ETA methodology for SAR response planning in the Canadian Arctic.

3.1 Estimating Marine-Based Transit Time in Ice-Covered Waters (RO1/RQ2,3/PIII)

3.1.1 AIS Data Processing

Approximately 12.4M AIS messages in the S-AIS data set were successfully matched with the FS ice classification data, representing 45% of the reports contained in the full AIS dataset. The matched AIS reports were associated with 116 vessels (unique IMO), leaving 68 vessels in the AIS data set that could not be associated with an FS ice class. The remaining AIS messages formed the AIS data set used for the analysis described in this section.

Table 1 provides a detailed breakdown of the 12.4M AIS messages that were successfully matched with FS ice classification. To support the ship speed analysis discussed later in this thesis, the AIS data was further reduced to only include vessels with a ship classification of Finnish Class 1A and 1A Super. This action was needed because the Finnish Transport Safety Agency only provides official IACS Polar Class (PC) equivalency for Finnish Ice Class 1A (PC 7) and 1A Super (PC 6) (Finnish Transport Safety Agency, 2017). Following this last filtering step, approximately 8.1M AIS reports from FS 1A and 1A Super vessels remain from the original AIS data set.

Table 1: Breakdown of received AIS messages by available Finnish Swedish (FS) Ice Classification

Ice Class	# of Messages	Unique IMO
FS Ice Class 1A Super	2,252,394	7
FS Ice Class 1A	5,850,853	52
FS Ice Class 1B	1,409,845	12
FS Ice Class 1C	2,725,304	42
FS Ice Class II	161,268	3
No FS Ice Classification	10,188,462	68
Total	22,588,106	184

3.1.2 POLARIS RIO Category Statistics

Figure 9 shows the distribution of the frequency of vessel speed over ground in the S-AIS data set. The distribution shows multiple modes in the distribution of the frequency of reported vessel speed. We see peaks in the frequency of vessel speeds around 14 kts, 8.5 kts, 5 knots, and 1.5 knots. The average design speed of various categories of ships operating in the Arctic were reported in the Arctic Council's Arctic Maritime Shipping Assessment (AMSA) 2009 report (Arctic Council, 2009). A total of 1477 ships were examined in the AMSA report, and the average ship speed in polar waters was determined to be 14kts (Lack & Corbett, 2012). The average ship speed reported in the AMSA 2009

report agrees with the maximum speeds shown in Figure 9. While understanding average ship speed may be useful for strategic planning, without knowledge of the corresponding environmental conditions, it is hard to use this information in practice. It also provides little help in explaining the observed peaks in vessel speeds around 8.5 kts, 5 kts, and 1.5 kts.

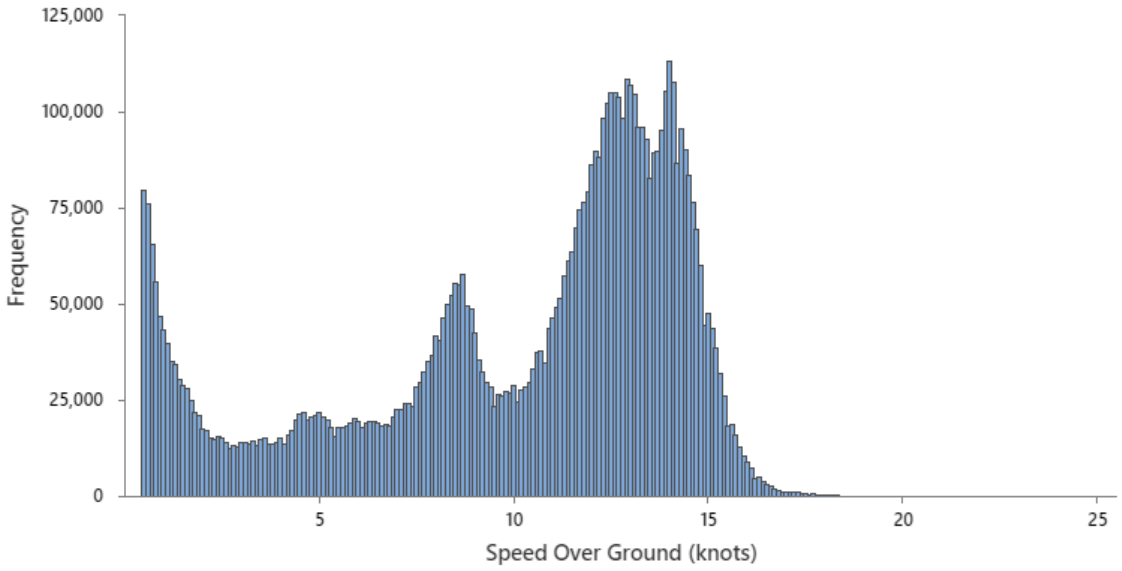

Figure 9: Distribution of the frequency of speed over ground reported in the 2018-2019 S-AIS data set

Figure 10 shows a statistical box plot of the observed vessel speed over ground in different POLARIS RIO result categories using the processed S-AIS data set. The line value in each box is the median speed observed in each RIO category. Since the speed is specified based on the RIO result category, it is not necessary to consider the Polar Class of vessel when deciding the expected ship speed. This is because the ice classification of the vessel has already been considered when computing the appropriate RIO value for the ship. Table 2 provides a summary of the descriptive statistics computed for observed ship speed in different RIO result categories.

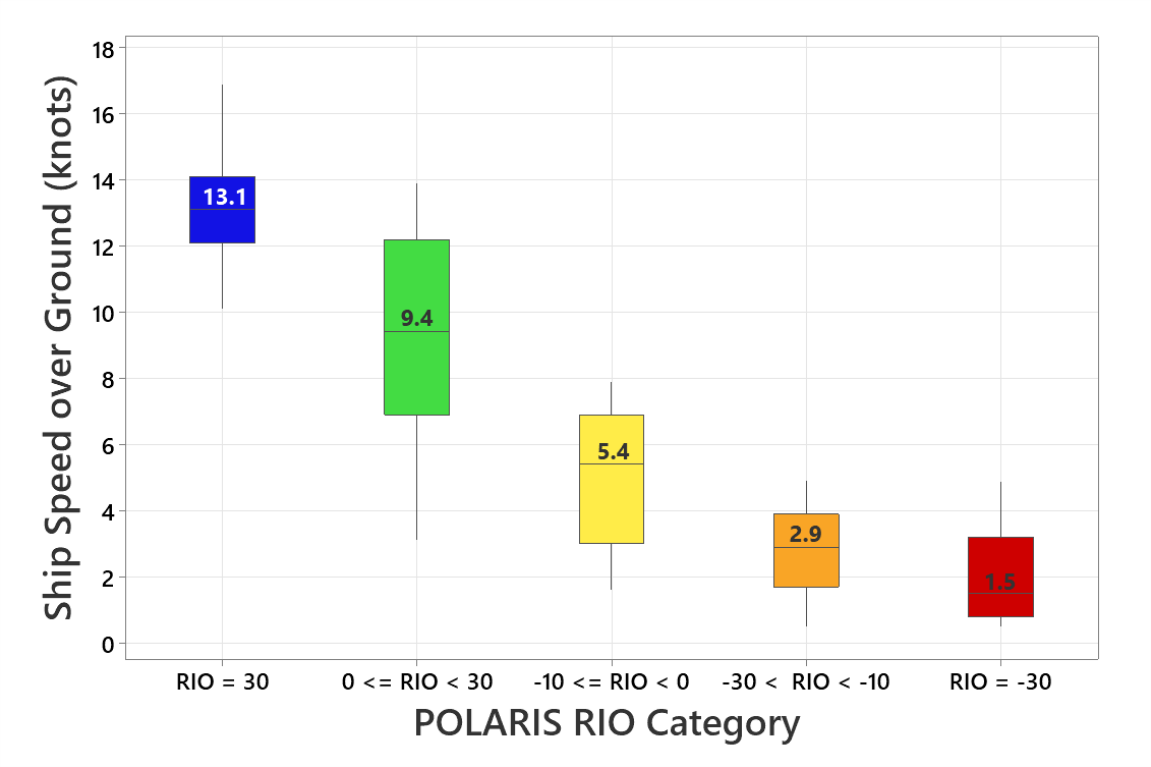

Figure 10: Box plot of the observed vessel speed over ground in different POLARIS RIO categories

Table 2: Summary of AIS reported ship speed in different POLARIS RIO categories. N is the number of unique AIS reports in the corresponding RIO category.

RIO Category	Median Ship Speed (knots)	Q1 Ship Speed (knots)	Q3 Ship Speed (knots)
RIO = 30 (N=3,539,558)	13.1	12.1	14.1
0 <= RIO < 30 (N=656,125)	9.4	6.9	12.2
-10 <= RIO < 0 (N=45,836)	5.4	3	6.9
-30 < RIO < -10 (N=20,682)	2.9	1.7	3.9
RIO = -30 (N=808,176)	1.5	0.8	3.2

3.1.3 Transit Time Validation Case Study

The following validation case study relies on historical AIS data and POLARIS RIO results to validate the ETT approach discussed in Section 2.3. We focus on an Eastern Arctic transit completed by Canadian Forces Auxiliary Vessel (CFAV) QUEST, during July 2012. CFAV QUEST was a Polar Class 1A vessel, with a maximum economic speed of 14 knots. The leg of the voyage that was analyzed was from Nuuk, Greenland to Gascoyne Inlet, Northwest Territories. The voyage was a continuous transit, covering 1,119 nautical miles. The total reported transiting time from origin to destination was 101 hours (about 4 days), confirmed by analysis of the ships GPS and AIS position reporting. Figure 11 provides a high-level overview of the CFAV QUEST arctic transit, as reported by the ships GPS and AIS. The rest of this section focuses on the computation of the ETT for this transit using CFAV QUEST's GPS track, and the USNIC sea ice analysis chart issued on 16 JULY 2012.

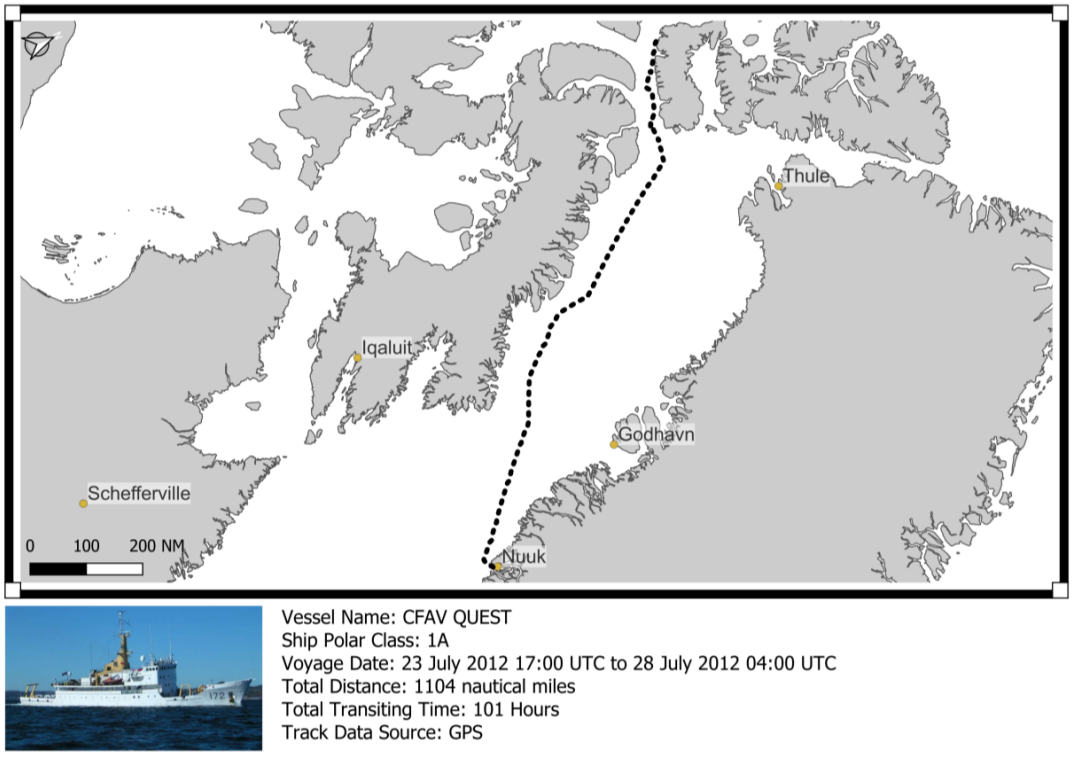

Figure 11: Overview of CFAV QUEST transit from Nuuk, Greenland to Gascoyne Inlet, Northwest Territories (NWT). Ship image from Canadian Broadcast Corporation (CBC), posted Feb 01, 2014

Figure 12 provides a map overview of the POLARIS RIO results for CFAV QUEST in the area of operations, computed using available USNIC sea ice analysis published close to the

time of the transit. For this transit, 65.7% of the total transit was in open water (RIO = 30 / 735.6 nm), 33.1% was in normal ice conditions for a Polar Class 1A ship (0 <= RIO < 30 / 370.4 nm), and 1.2% was in the high operational risk category (-10 <= RIO < -30 / 13 nm).

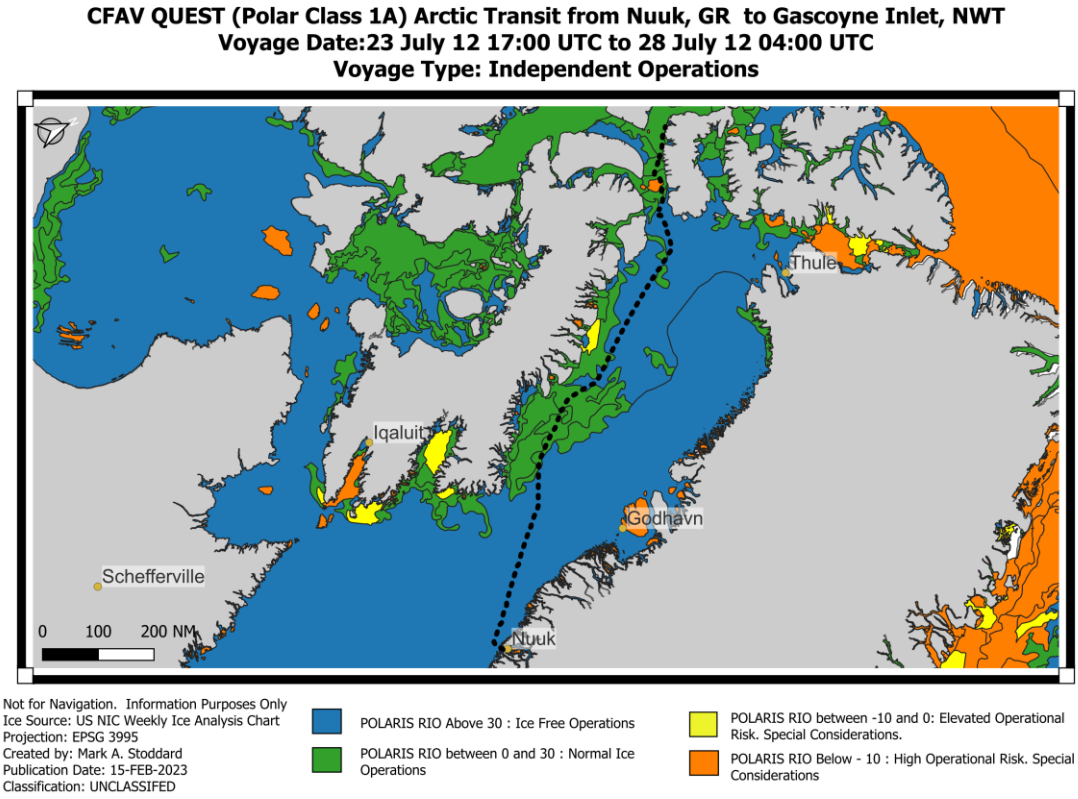

Figure 12: Overview of POLARIO RIO results for CFAV QUEST transit from Nuuk, GL to Gascoyne Inlet, NWT

We can compute the ETT from Nuuk, GL to Gascoyne Inlet for CFAV Quest using Equation 3. To better illustrate the computation of the ETT, we provide the completed calculation below. In this case we have calculated the ETT using the POLARIS RIO results derived from the USNIC sea ice analysis chart issued on 16-JUL-2012 (calendar week 29) and the median expected ship speed in different RIO categories from Table 2.

$$ETT_{jt} = \sum_{k=1}^{4} \frac{D_{jtk}}{S_k} = ETT_{1A,29} = \frac{735.6}{13.1} + \frac{370.4}{9.4} + \frac{0}{5.4} + \frac{13.0}{2.9} + \frac{0}{1.5} = \mathbf{100.1\ hrs\ (4.17\ days)}$$

The actual transit time for CFAV QUEST to complete this transit was approximately 101 hours (about 4 days). The actual transit time was derived from the ship's GPS log, by selecting a start and end location that corresponds with the route shown in Figure 11 and

Figure 12. For this case, the ETT underestimated the actual transit time by 0.9 hours, which is an error of less than 1%.

In an effort to further validate the ETT calculation, 10 routes executed in ice-covered water were evaluated. S-AIS data was used to reconstruct the ship route, and to determine the continuous transiting time required to complete the route. The S-AIS data points were linearly interpolated to produce the route, which was then evaluated using the ETT methodology with the most temporally aligned USNIC sea ice analysis chart. The percentage error was computed between the actual transit time and the estimated transit time using the ETT methodology (see Table 3). The percentage error was then statistically analyzed to support the validation of the method (see Table 4). Figure 13 provides a map overview of the 10 routes that were used to support the validation of the ETT methodology. The average route length used for validation was 991 nautical miles, with an average total transit time of 103.3 hours.

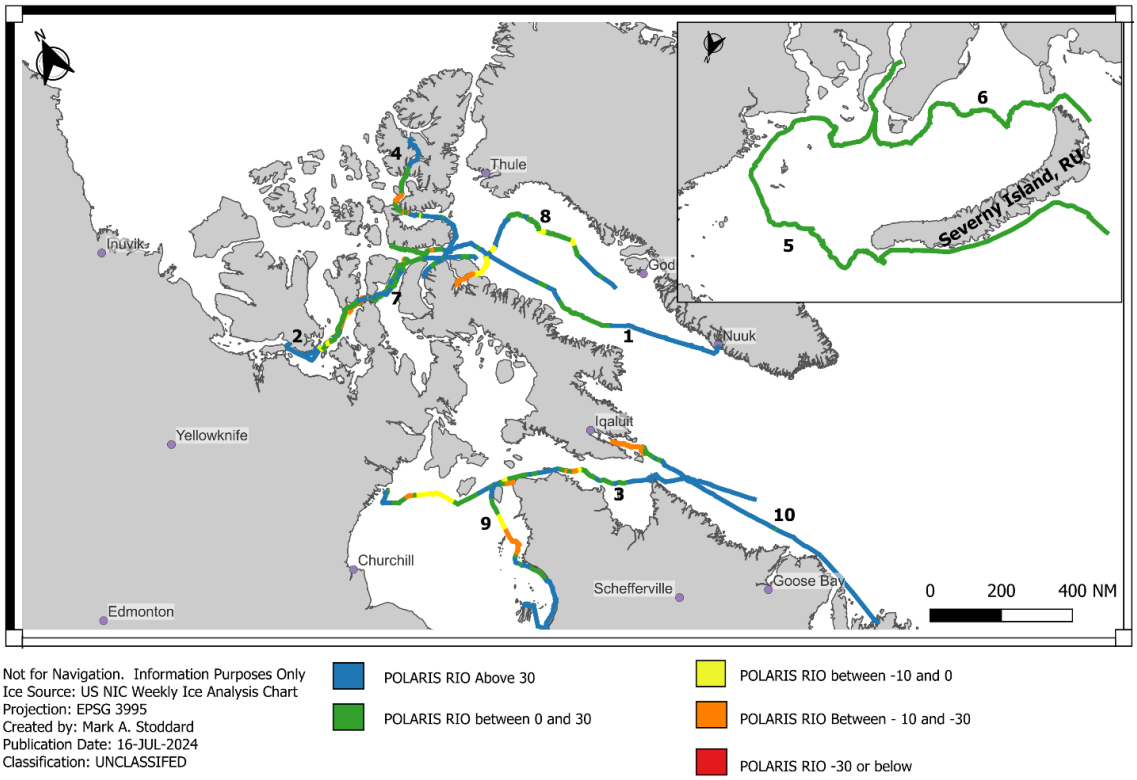

Figure 13: Overview of 10 routes executed in ice-covered waters to support the validation of the ETT methodology.

Table 3: Detailed analysis of 10 routes in-covered waters using the ETT methodology. Comparison is between estimated transit time and actual transit time as reported by S-AIS.

Voyage ID	Ship Name	Ice Class	Distance (nm)	Actual Transit Time (hours)	Estimated Transit Time (Hours)	Percentage Error
1	CFAV Quest	FS 1A / PC1A	1121	107.5	100.1	6.44
2	MV Claude A. Desgagnes	FS 1A / PC7	967	89.2	96.3	7.96
3	MV Miena Desgagnes	FS 1A / PC7	1254	145.7	138.8	-4.74
4	MV Qamutik	FS 1A / PC7	1212	58.5	70.1	19.83
5	MT UIKKU*	FS 1AS / PC6	1334	151.0	142.1	-5.89
6	MT UIKKU*	FS 1AS / PC6	691	82.3	73.5	-10.69
7	MV Claude A. Desgagnes	FS 1A / PC7	792	68.1	77.3	13.51
8	MV Ocean Raynald T	FS 1A / PC7	747	107.7	101.5	-5.76
9	MV Rosaire A. Desgagnes	FS 1A / PC7	732	111.5	99.2	-11.03
10	MV QIKIQTAALUK W.	FS 1A / PC7	1063	112	123.58	10.34

* MT UIKKU was escorted during transit, therefore RIO +10 used in POLARIS Assessment

Table 4: Descriptive statistics for transit time estimation percentage error using ETT methodology

N	Mean	SE Mean	StDev	Minimum	Q1	Median	Q3	Maximum
10	2.00	3.45	10.92	-11.03	-7.09	0.85	11.13	19.83

3.2 A Graph-Theoretic Approach to Strategic Route Planning (RO3/RQ5/PIV)

Figure 14 provides an overview of the fastest route between a start and end location in the Eastern Arctic for a Polar Class 1A ship during four different bi-weekly analysis periods.

The 1991 to 2020 median RIO value was used to assess the navigational risk throughout the year for a Polar Class 1A ship. The figure shows how the fastest route changes throughout the year depending on the POLARIS RIO values present during the specified analysis period. We can also see that at certain times of the year there is no feasible path between the specified start and end location of the route.

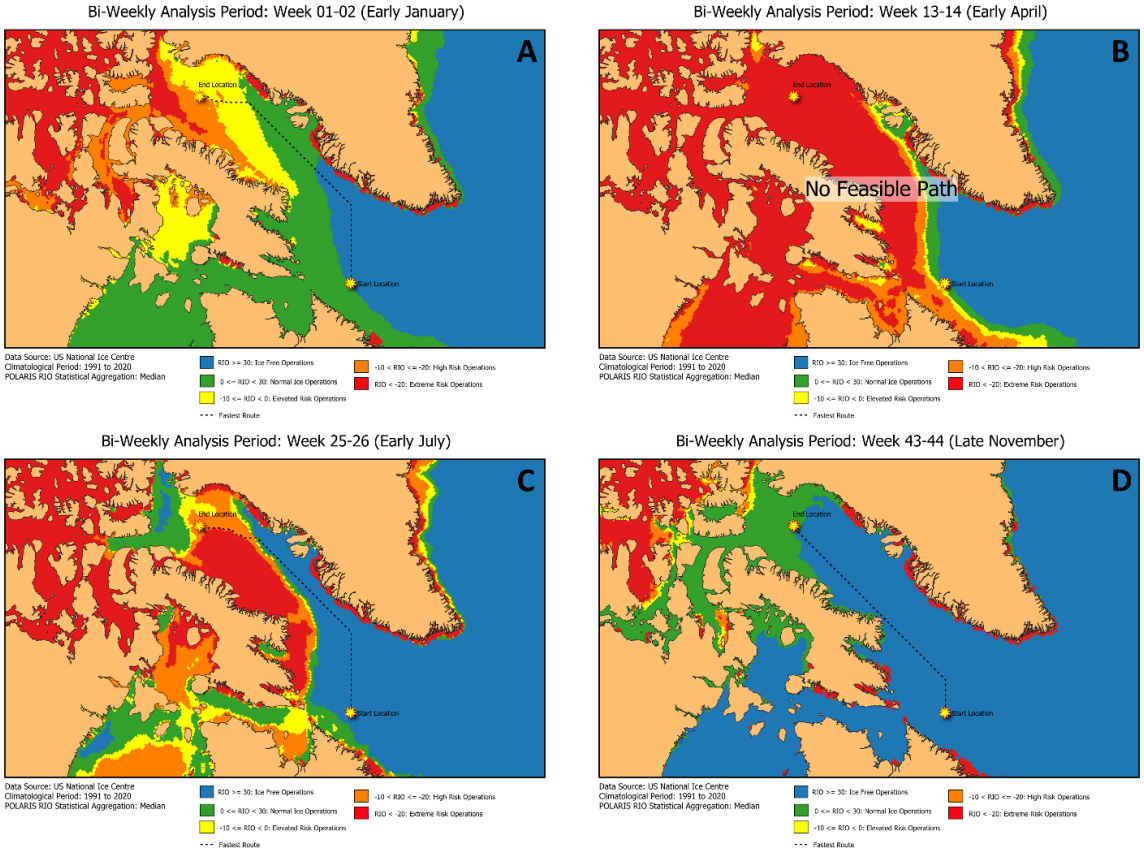

Figure 14: Overview of the fastest route and expected transit time between two locations in the Arctic.

Figure 15 provides a bar chart of the year-round I-ETA between the start and end location shown in the previous figure. We can observe that for a sizable part of the year there is no feasible route for a Polar Class 1A ship between the start and end location. This would indicate that the severity of sea ice conditions, and associated navigational risk, exceeds the safe operating limits of a Polar Class 1A ship during that time.

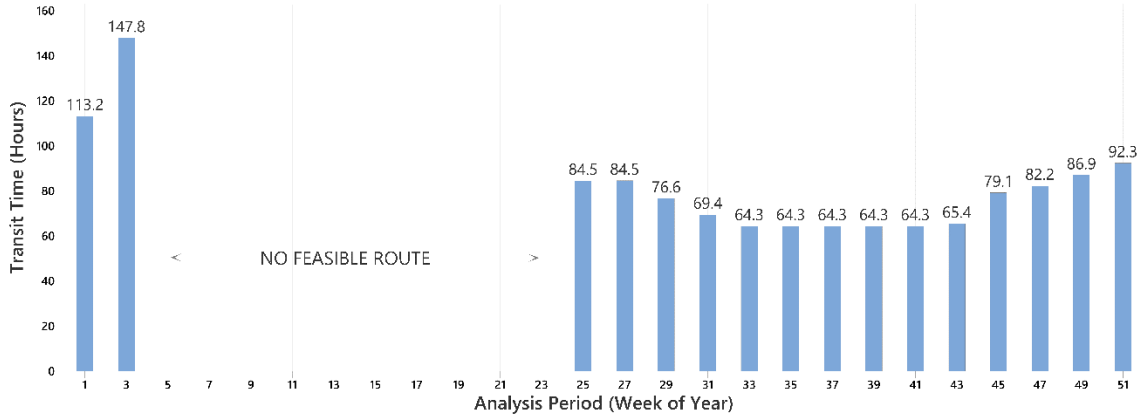

Figure 15: Summary of the year-round I-ETA results between the start and end location shown in Figure 16.

It is also possible to compare I-ETA results for different ship ice classes. In Figure 16 we compare the year-round I-ETA for the same start and end location for a Polar Class 1A and Polar Class PC5 ship using a multi-line plot. For awareness, a Polar Class 1A is capable of summer/autumn operation in thin first-year ice (ice thickness from 30 to 70cm), while a Polar Class PC5 is capable of year-round operation in medium first-year ice (ice thickness from 70 to 120cm). The enhanced ice operating capabilities of the PC5 vessel allow it to operate safely over a much wider range of sea ice conditions than a 1A vessel. The result is twofold; (1) A PC5 vessel can typically operate at higher speed when sea ice is present when compared to a 1A vessel, and (2) A PC5 vessel has a longer operating season, when compared to a 1A vessel.

We can see from Figure 16, that for a sizable portion of the year there is no feasible route between the start and end location for the Polar Class 1A vessel; starting in late January / early February (Week 5) and ending in late June (Week 25). Periods where no feasible route exists appear as areas of discontinuity in the line plot. Notable observations from the comparison of Polar Class 1A and PC5 ships are summarized in Table 5.

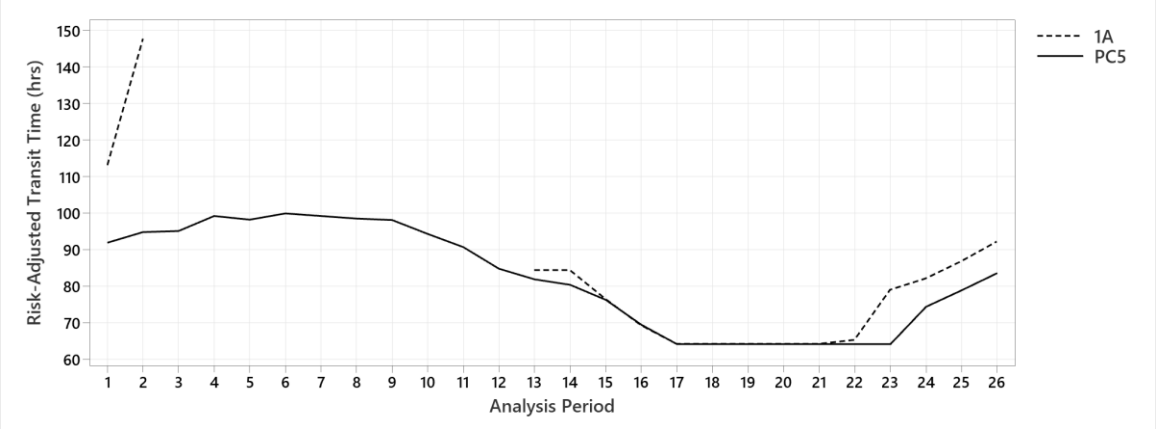

Figure 16: Comparison of the year-round I-ETA for a Polar Class 1A and PC5 ship between the same start and end location in the Eastern Arctic for each bi-weekly analysis period. Note: When no feasible route exists, the line is not drawn for that ship class.

Table 5: Summary of year-round I-ETA results for Polar Class 1A and PC5

	Polar Class 1A	**Polar Class PC5**
No Feasible Route (Bi-Weekly Period)	3 to 12	N/A
Maximum I-ETA (hours)	147.8	100.0
Maximum I-ETA (Bi-Weekly Period(s) of Occurrence)	2	6
Minimum I-ETA (hours)	64.3	64.3
Minimum I-ETA (Bi-Weekly Period(s) of Occurrence)	17 to 21	17 to 23

Trans-arctic routes provide a challenging case for our strategic route analysis method due to the vastness of the area to be transited. The complex geography, and varied sea ice conditions one would expect to encounter, create a unique challenge for computing the fastest route. Using the I-ETA method discussed, we can automatically generate the fastest path between a specified start location in the Northwest Atlantic, south of Greenland, and end location in the Chukchi Sea, North of Alaska. Figure 17 provides a map overview of the computer-generated fastest route between the specified start location and end location. The trans-arctic route shown in this figure was generated for Polar Class PC6 ship departing in Week 37-38 (mid-September). The I-ETA for the fastest route was 275 hours (11.5 days), with a total transit distance was 3670 nautical miles.

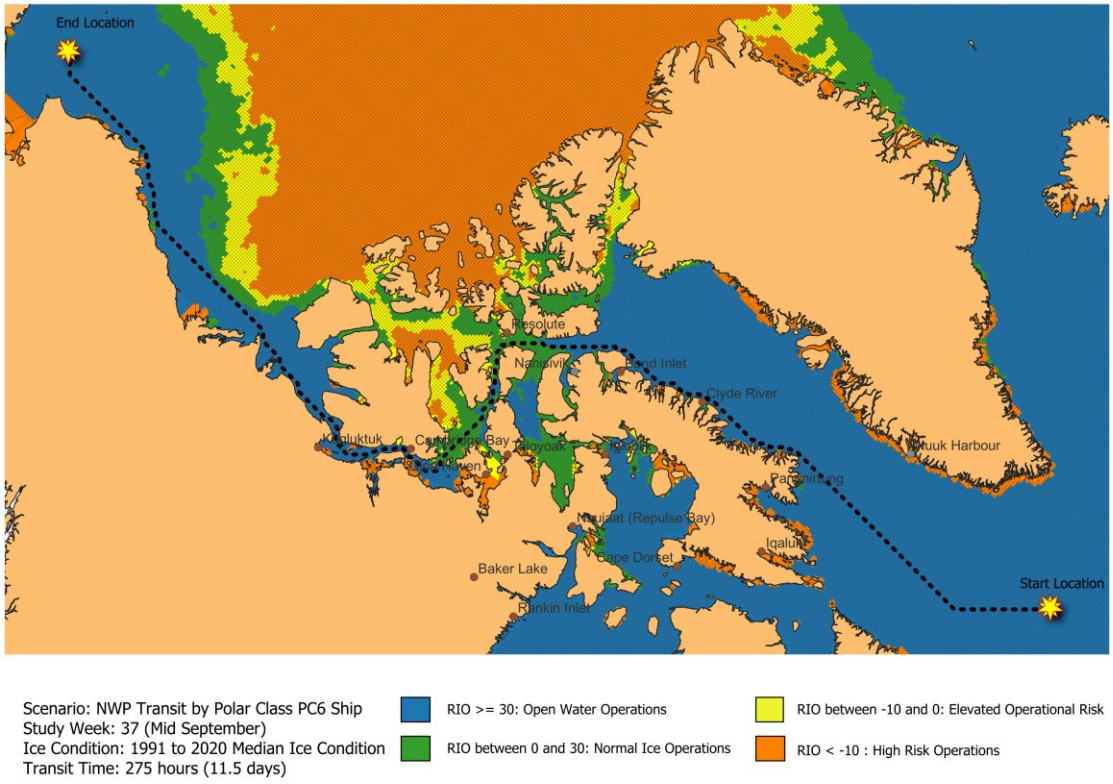

Figure 17: Computer-generated route from a specified start location in the Northwest Atlantic to end location in the Western Arctic using our strategic route analysis method for a Polar Class PC6 ship in Week 37-38 (minimum ice extent)

In addition to computing the I-ETA and total transit distance, we also compute summary statistics for the RIO categories encountered along the fastest route. For this transit, 89.1% of the route is in open water, and 10.9% is in RIO values between 0 and 29. The results show that for a PC6 ship navigating the NWP in Week 37 (mid-September), most of the route is in open water, with only 10.9 percent of the total transit distance occurring in areas where normal ice operations would be expected.

Figure 18 provides a composite map plot of the fastest route generated between the same start and end location in each of the 26 bi-weekly analysis periods. The route through the NWP with the shortest transit time is highlighted in green, occurring in analysis period 19 (~mid-September). The route through the NWP with the longest transit time is highlighted in red, occurring in analysis period 8 (~mid-April). We also see that at certain times of the year, using the alternative NSR route is slightly faster than the much shorter NWP route. The NSR is only marginally favored during analysis periods 1, 5 and 6 (March). Figure 19

shows the year-round I-ETA, and polar route choice (NSR vs. NWP), for a Polar Class PC6 ship. The maximum I-ETA is observed in late March /early April (maximum ice extent), and the minimum I-ETA is in mid-September (minimum ice extent).

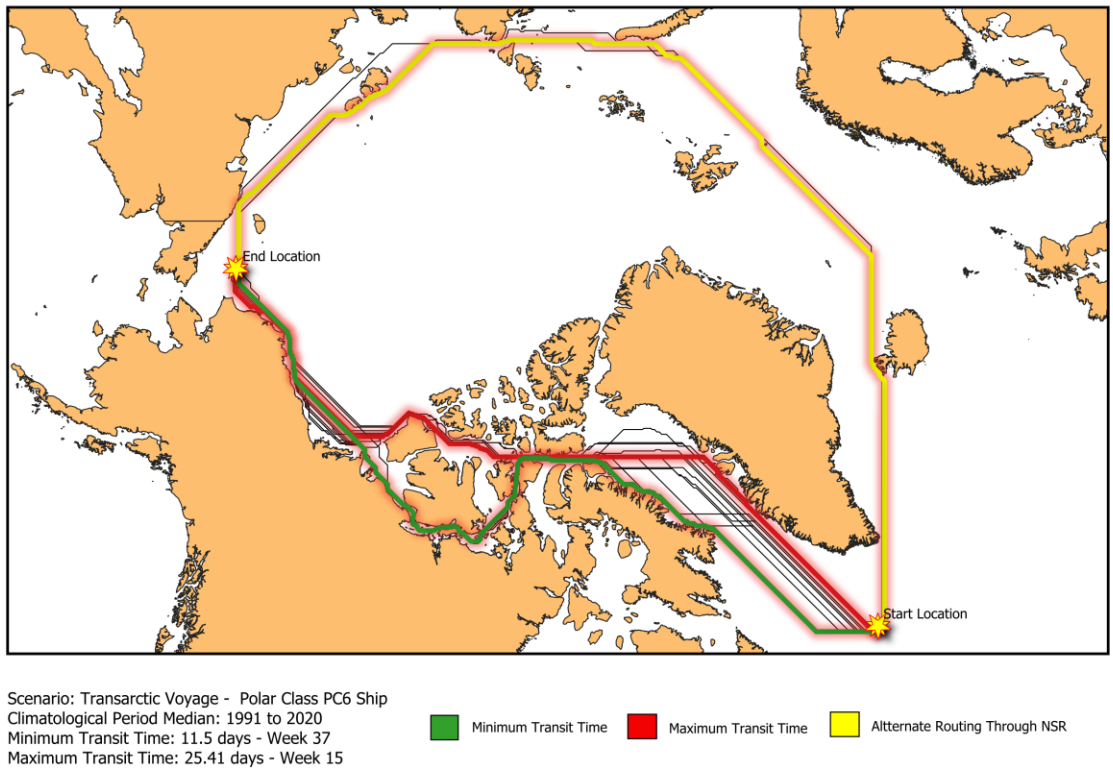

Figure 18: Composite plot of the fastest route through the Arctic, generated for each of the 26 bi-weekly analysis periods

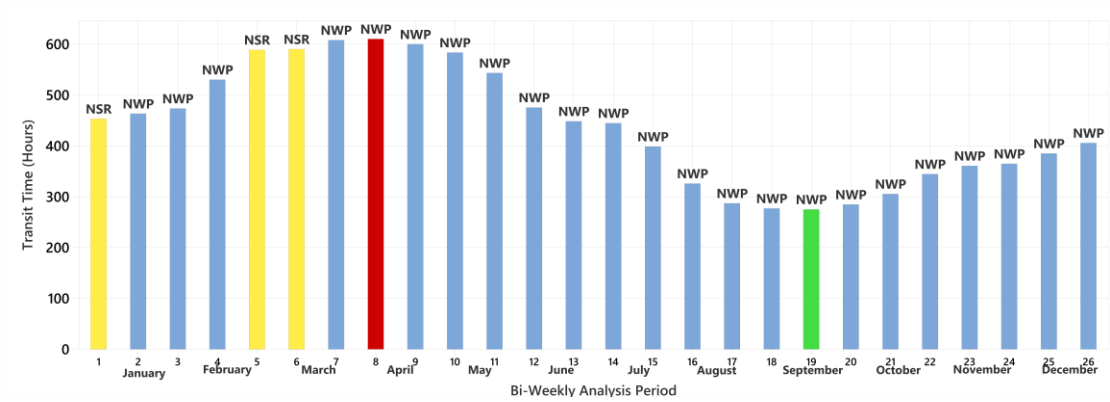

Figure 19: Bar chart of I-ETA results for a PC6 ship transiting from Southwest Greenland to Chukchi Sea in each of the 26 bi-weekly analysis periods. The green bar shows the minimum I-ETA. The red bar shows the maximum I-ETA. The yellow bar shows the use of the NSR. The blue bar shows all other I-ETA results

3.2.1 Comparison of I-ETA Results and Commonly Accepted Strategic Routes Through the Arctic

This study focused on developing a strategic route analysis method that could be used to compute routes in ice-covered waters and to estimate the expected transit time. We referred to the expected transit time of the fastest route between two locations as the I-ETA. The results show the use and utility of the I-ETA method in the support of strategic route analysis. We are now able to compute the fastest routes throughout the polar region at various times of the year, for all ship ice classes. One unexpected outcome of this study was the high degree of agreement between our computer -generated fastest routes and the customary strategic routes used to transit the polar region. This is especially true for strategic routes through the NWP and NSR.

Figure 20 shows a high-level representation of the common routes through the NWP and NSR, adapted from the Arctic Council AMSA report (Arctic Council, 2009). The computer-generated routes produced for our study follow these three paths, with subtle deviations in response to varying sea ice conditions throughout the year.

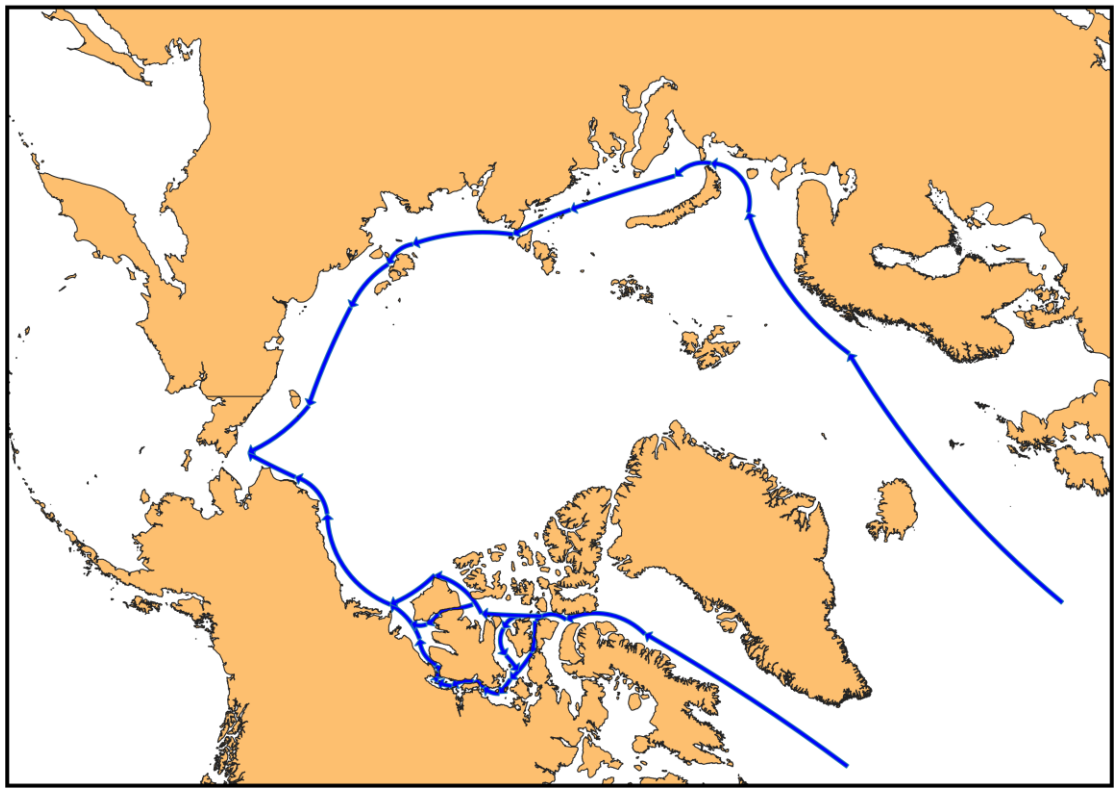

Figure 20: High-level representation of the most used routes through the Northwest Passage and the Northern Sea Route (Data Source: Arctic Council, 2009)

Figure 21 provides a heatmap visualization of the computer-generated routes for a PC6 ship over 26 bi-weekly analysis periods, with a general overlay of the commonly accepted routes through the NWP previously discussed (Arctic Council, 2009). We see the convergence of the computer-generated routes on two of primary routes through the NWP (Headland, 2022):

1. Davis Strait, Lancaster Sound, Barrow Strait, Viscount Melville Sound, McClure Strait, Beaufort Sea, and Chukchi Sea. This route is often described as the shortest but most difficult way through the NWP due to severe ice near McClure Strait.
2. Davis Strait, Lancaster Sound, Barrow Strait, Peel Sound, Franklin Strait, Victoria Strait, Coronation Gulf, Amundsen Gulf, Beaufort Sea, and Chukchi Sea. This route is considered by many as the principal route through the NWP.

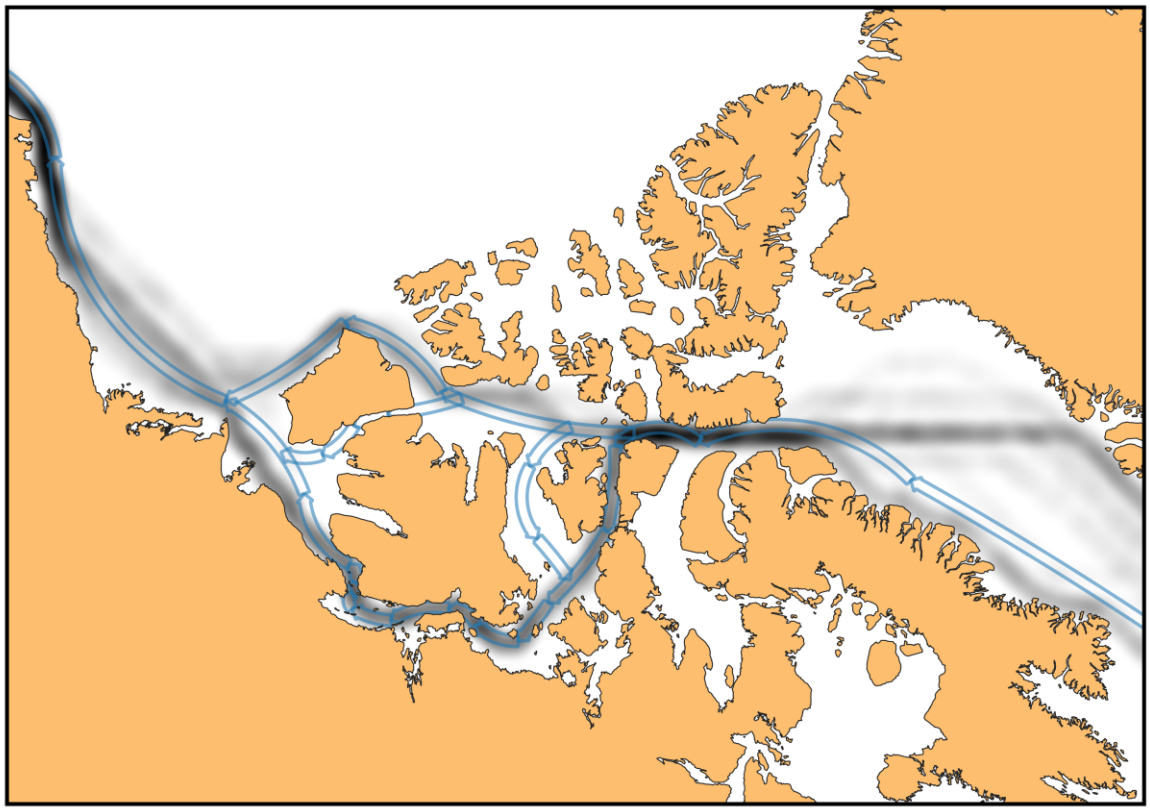

Figure 21: Heatmap of computer-generated routes for a PC6 ship in each of the 26 bi-weekly analysis periods with an overlay of the commonly accepted routes through the NWP

Greater than 60% of the routes generated for a PC6 transiting through the Canadian Arctic Archipelago followed the route through Davis Strait, Lancaster Sound, Barrow Strait, Peel Sound, Franklin Strait, Victoria Strait, Coronation Gulf, Amundsen Gulf, Beaufort Sea, and Chukchi Sea. This route was consistently shown to be the fastest route during the Summer and Fall period (Weeks 29 to Week 43). These results support the claim by (Headland, 2022), that this route is the principal route through the NWP.

The fastest routes generated for the winter months are not possible for a PC6 ship when navigational risk is carefully considered. The transit times during December and June are more than double the fastest route generated during the minimum ice extent period. This would indicate a high degree of navigational risk associated with the route. Figure 22 illustrates the infeasibility of the routes generated during the winter months for a PC6 ship. The distribution of RIO categories encountered along the fastest path for a PC6 in Week 15 (mid-March) highlights the elevated navigational risk of the route. 48.4% (~ 1615 nm) of the total transit would be considered elevated risk (-10 <= RIO < 0), with 15.3% (~ 500

nm) of the total transit in the high-risk category (-10 < RIO < -30). It is obvious that given the risk profile of the Week 15 fastest route, that the ships prolonged exposure to the elevated navigational risk would be intolerable.

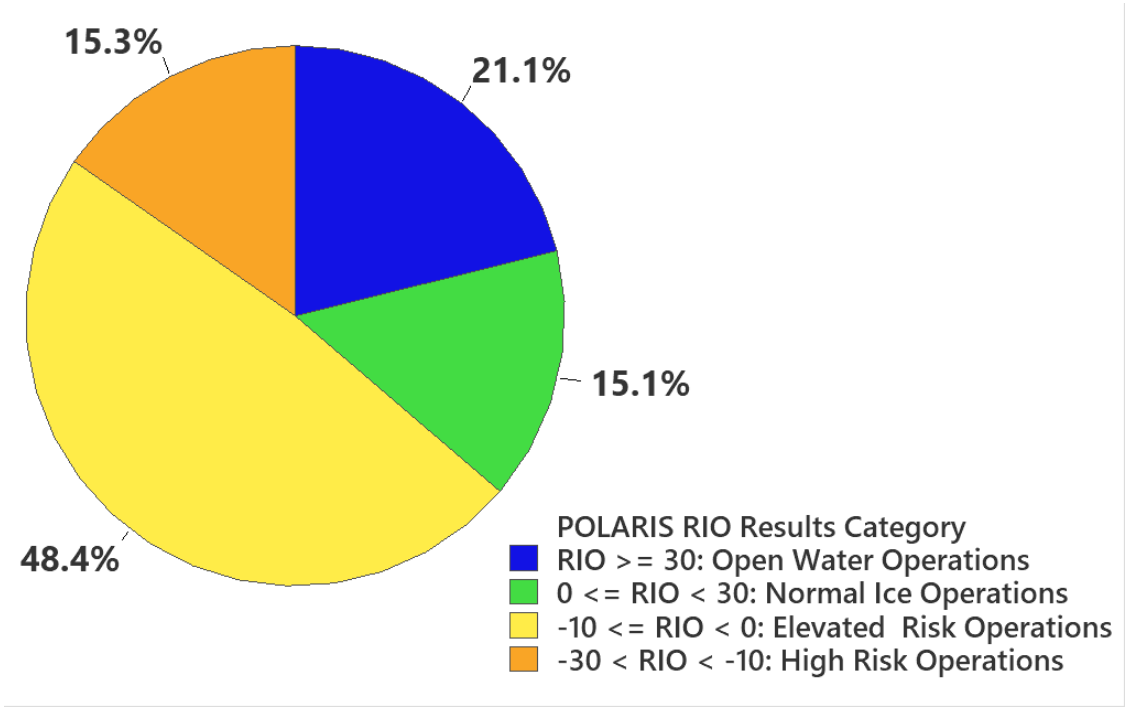

Figure 22: Distribution of RIO categories encountered along the fastest path for a PC6 ship in Week 15, expressed as a percentage of total transit distance

Computing the fastest route during the winter months does offer some insight into the inter-annual variation in transit time through the year in the Arctic. As expected, we see transit times follow the same general trend as sea ice conditions. I-ETA is minimal when the sea ice is historically at its minimal extent. I-ETA is maximal when the sea ice is historically at its maximum extent.

There are several limitations to the results of this study that should also be mentioned. While we have computed several different statistical aggregations of POLARIS RIO results, the route analysis completed so far has focused on the median RIO value observed over the 1990 to 2020 climatological period. A useful follow-on analysis could take a deeper look at the use of other statistical aggregations of the RIO value, or climatological periods, to see their impact on the I-ETA. Also, we have not discussed the impact of escort operations on I-ETA. In some situations, it might be possible that a short escort through

high-risk ice conditions could significantly alter the optimal fastest route. The current method to compute the fastest route using Dijkstra's algorithm will not support this form of analysis. The POLARIS assessment does have provisions to support escort operations, but these have not been considered in this study. Future work could also focus on evaluating the quality of the computer-generated fastest routes using the method proposed in this study, and the accuracy of the I-ETA calculation.

3.2.2 Impact of Temporal Resolution of Sea Ice Analysis on Strategic Navigation Planning

Currently, the USNIC is the only authoritative source of detailed characterizations of sea ice that provide circumpolar coverage of the Arctic and Antarctic regions. The USNIC takes imagery and ancillary data from a variety of space-based and terrestrial sensor systems, such as synthetic aperture radar and passive microwave, to produce detailed characterizations of ice concentration, ice type, and general ice thickness. Once the ice analysis is complete, many products are created and provided open access to a broad user community. USNIC sea ice analysis products are grouped by region, and produced for different time periods, depending on the nature of analysis contained in the product. The USNIC product relied on for this study is the arctic sea ice GIS Shapefile, produced bi-weekly. This product has the desired coverage area, and sea ice analysis attribute data, to compute POLARIS RIO values throughout the Arctic.

While suitable for strategic navigation assessment, it may be more desirable to assess navigational risk using a daily product for tactical navigation assessment. The use of daily sea ice analysis products in our network analysis would make the fastest path optimization and transit time estimation results more applicable at the tactical level. Figure 23 compares the fastest path and transit time results, using USNIC bi-weekly sea ice analysis and Canadian Ice Service (CIS) daily sea ice analysis, produced at the start and end of the bi-weekly analysis period. We see good agreement between the fastest route and transit time produced from the USNIC and CIS sea ice analysis products at the beginning of the bi-weekly analysis period. When we compare the results using the same USNIC bi-weekly chart and a CIS daily product issued toward the end of the USNIC bi-weekly period, we start to observe significant differences between the fastest route and transit time. It should

be noted that ice conditions are known to change rapidly in the June / July period, so we would expect the greatest differences between the use of bi-weekly and daily products to be observed during the yearly sea ice break-up and freeze-up periods.

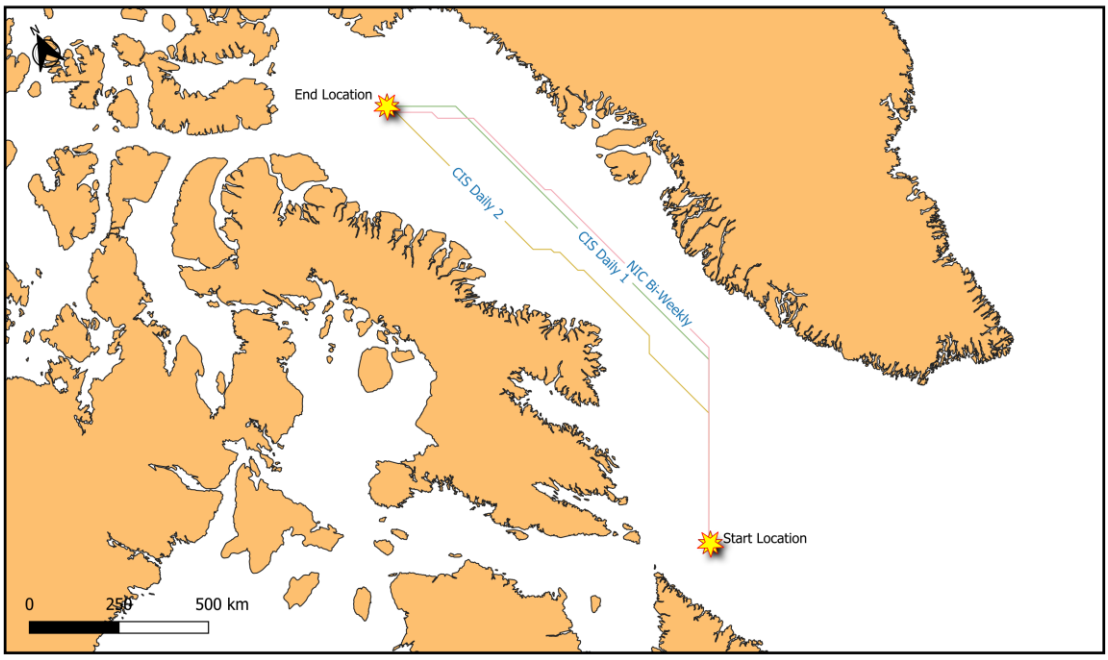

Data Source 1: US National Ice Centre
Data Source 2: Canadian Ice Service

POLARIS RIO Source	US NIC Bi-Weekly - 2020-07-09	CIS Daily 1 - 2020-07-09	CIS Daily 2 - 2020-07-23
Transit Time (hrs)	67.5	67.1	64.9

Figure 23: Comparison of fastest route and transit time using the USNIC bi-weekly ice chart issued on 09 July 2020, and the CIS daily ice chart issued at the start and end of the USNIC bi-weekly analysis period (09 and 23 July 2020).

3.2.3 Choice of Historical POLARIS RIO Summary Statistics

For strategic planning, it is often necessary to plan voyages based on the ice conditions expected to be met during a planned voyage. The selection of the proper sea ice analysis to use for strategic planning is a challenging task, and often relies on expert judgement and the selection of sea ice analysis from similar years. Our analysis has so far relied on the use of summary statistics of historical POLARIS RIO values over a given climatological period to support strategic planning. There are two commonly used 30-year climatology period used for strategic sea ice analysis, (1) 1981 to 2010, and (2) 1991 to 2020. The USNIC moved to a baseline period of 1981 to 2010 starting July 1, 2013 (National Snow and Ice Data Center, 2013). The Canadian Ice Service (CIS) have adopted a different approach,

updating their 30-year ice climate normal every 10 years, with the current period being 1991 to 2020.

In this study we have chosen to use the 1991 to 2020 climatological period when examining historical sea ice conditions, and their expected impact on polar ship operations. The results in this thesis focus on the 1991 to 2020 median RIO value when computing sea ice risk and its impact on ship routing, transit time, and incident response service areas. The other statistical aggregations that have been computed include; (1) minimum RIO value, (2) first quartile RIO value, (3) mean RIO value, (4) third quartile RIO value, and (5) maximum RIO value. Future studies could compare ship routing and transit time results using different statistical aggregations of POLARIS RIO values to better understand the impact this has on route generation and transit time.

The choice of RIO value affects both the fastest route optimization and expected transit time. When selecting the maximum RIO value (most positive) the resulting optimal route is expected to be the most direct route possible between the start and end location, achieving the minimum expected transit time. One would also expect this voyage to also have the highest average ship speed. Figure 24 shows the fastest route and transit time computed using different statistical aggregations of historical RIO values observed over the climatological period from 1991 to 2020. This figure also shows the spatial variability in the fastest route based on the selected RIO value statistic. The maximum RIO corresponds to the highest RIO value observed during the climatological period, representing the most favorable operating conditions observed.

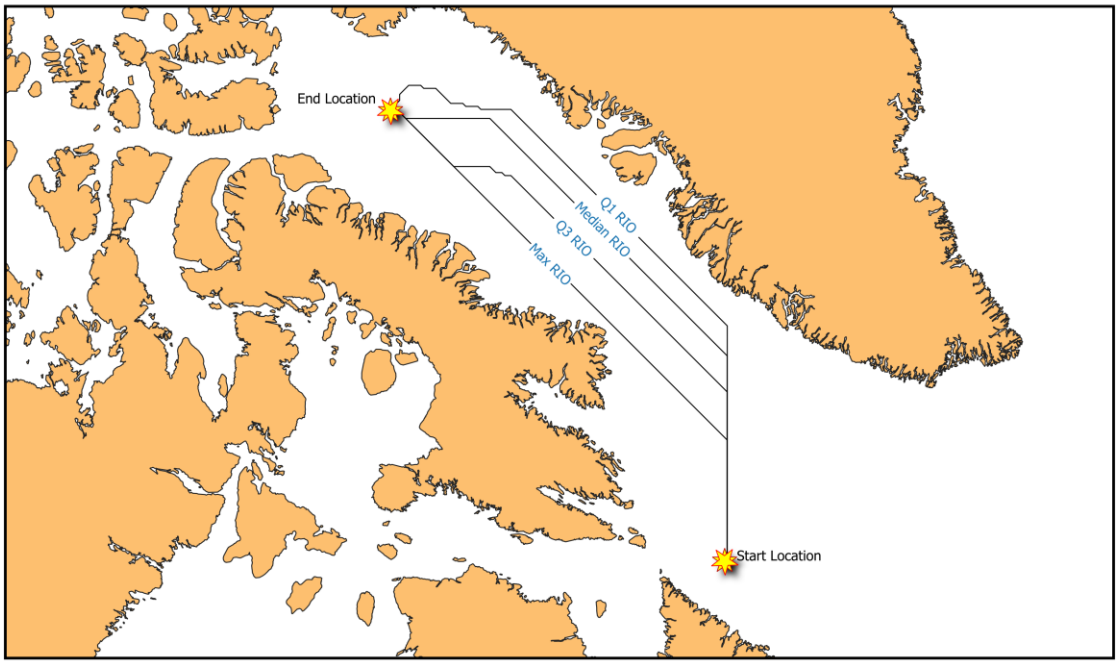

Data Source: US National Ice Centre
Climatological Analysis Period: 1991 to 2020
Bi-Weekly Analysis Period: Week 29-30 (Early July)

POLARIS RIO Summary Statistic	Min RIO	Q1 RIO	Median RIO	Q3 RIO	Max RIO
Transit Time (hrs)	No Solution	90.5	72.7	67.4	64.3

Figure 24: Comparison of fastest route and transit time using different statistical aggregations of historical RIO values observed over the climatological period from 1991 to 2020

Figure 25 compares the fastest route between the same two points using (1) a single USNIC sea ice chart produced on 16-JUL-2020, and (2) the 1991 to 2020 median RIO value. In this case, we see that the fastest route and transit time using the sea ice chart from 16-JUL-2020 is faster, arriving at the end location 6.4 hours earlier. This would indicate that the RIO values derived from the sea ice chart from 16-JUL-2020 are more favorable than the 1991-2020 median RIO.

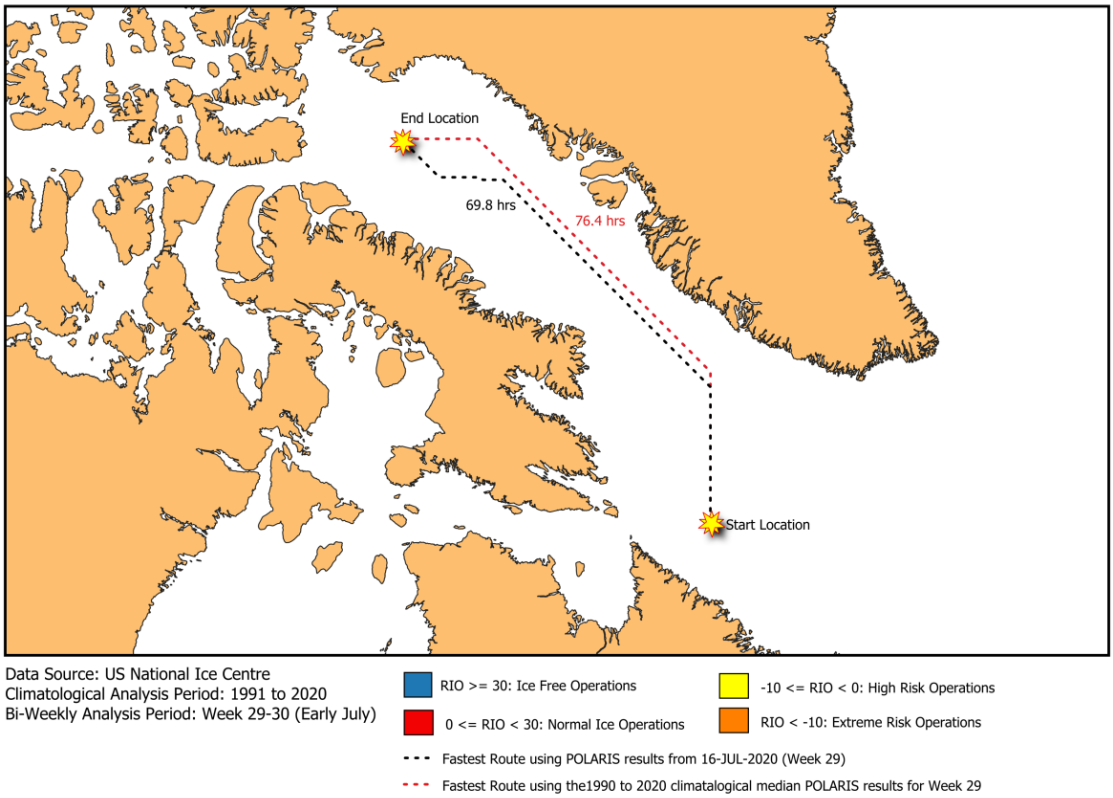

Figure 25: Comparison of risk-adjusted transit time between two points in the Eastern Arctic using the 1991 to 2020 climatological median POLARIS RIO and the POLARIS RIO from a single USNIC sea ice chart for the same bi-weekly period

3.3 Marine-Based Incident Response

In Section 2.4 we presented a method to compute the fastest route between two locations in ice-covered waters. We will now discuss the use of the I-ETA method to study of SAR incident response in the Eastern Arctic. All results were produced for the same incident location (central Baffin Bay) to simplify the comparison of results, and follow-on discussion. All POLARIS risk maps, ISRA, and IRI have been computed for an IACS Polar Class 1A ship, with some exception when comparing modeling results for different ship ice classes. The 1A ship ice class was chosen because it is one of the most common ship ice classes found operating in the Canadian Arctic during the navigable summer season. In practice, IRSA and IRI can be produced for any incident location, time of year, ship ice class, and choice of RIO value summary statistic. The two results presented and discussed in this section include:

1. Incident Response Service Areas
2. Incident Response Isochrones

Using the I-ETA method, it is possible to compute the fastest path between any start and end node in the arctic transportation network, which is a required step to compute the IRSA. The IRSA shown in Figure 26 was generated for a Polar Class 1A ship operating in the Eastern Arctic during Week 29-30 using a 96-hour maximum response time cut-off (MRTC). The IRSA can be interpreted as containing all start nodes in our graph that can reach our incident location (end node) within the specified MRTC. The MRTC used for the analysis in this section is 96 hours (~ 4 days). Figure 27 shows how the IRSA size changes throughout the year as the RIO changes due to varying sea ice conditions throughout the year. Other factors that influence service area size are the MRTC (see Figure 28) and ship ice class (see Figure 29).

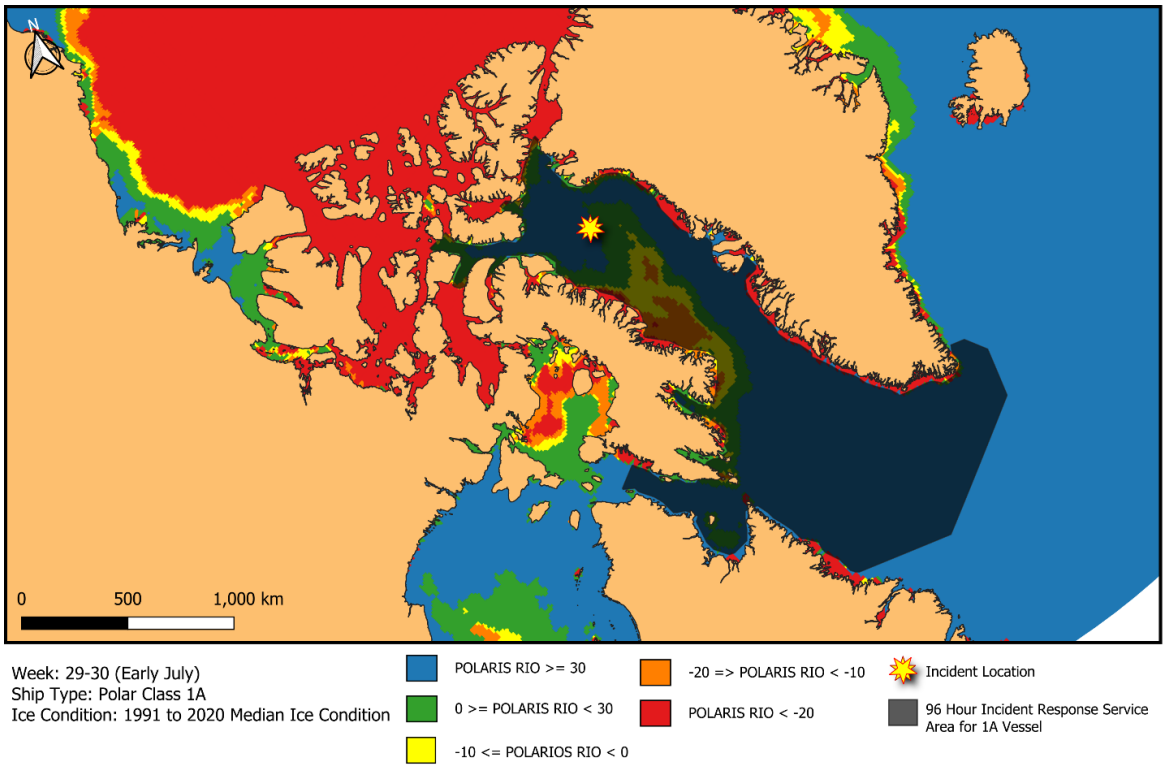

Figure 26: Computed IRSA for a Polar Class 1A ship in week 29-30.

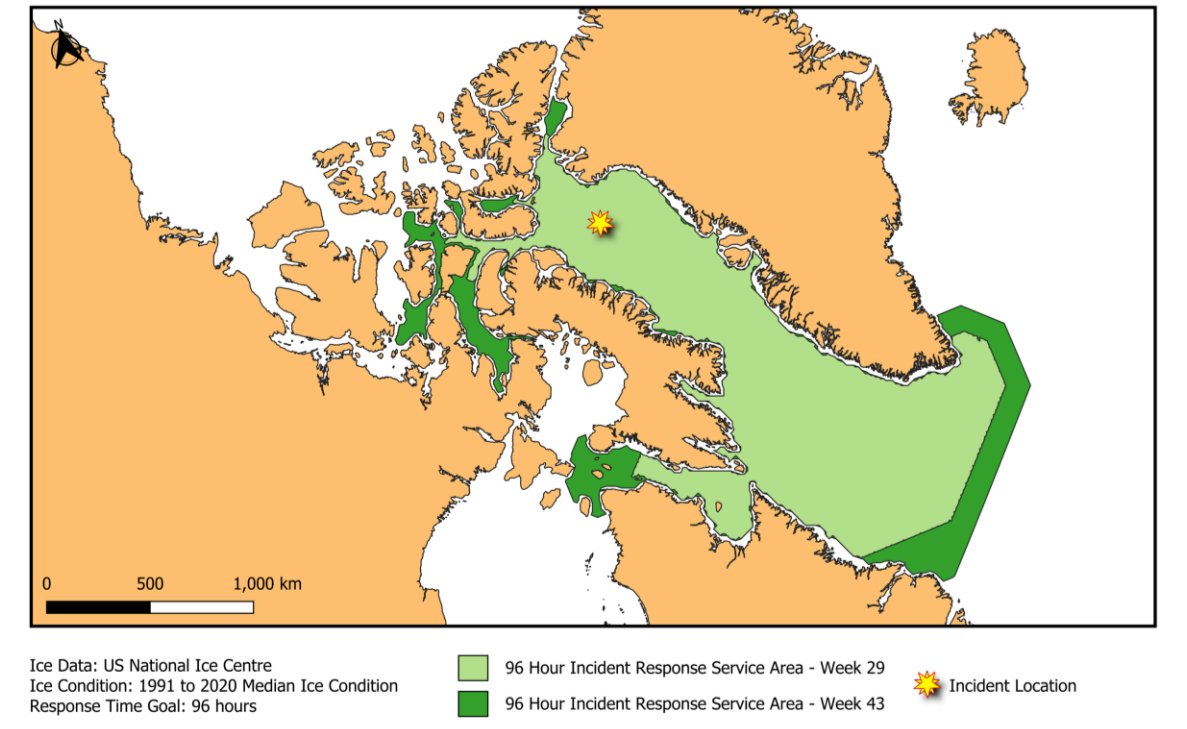

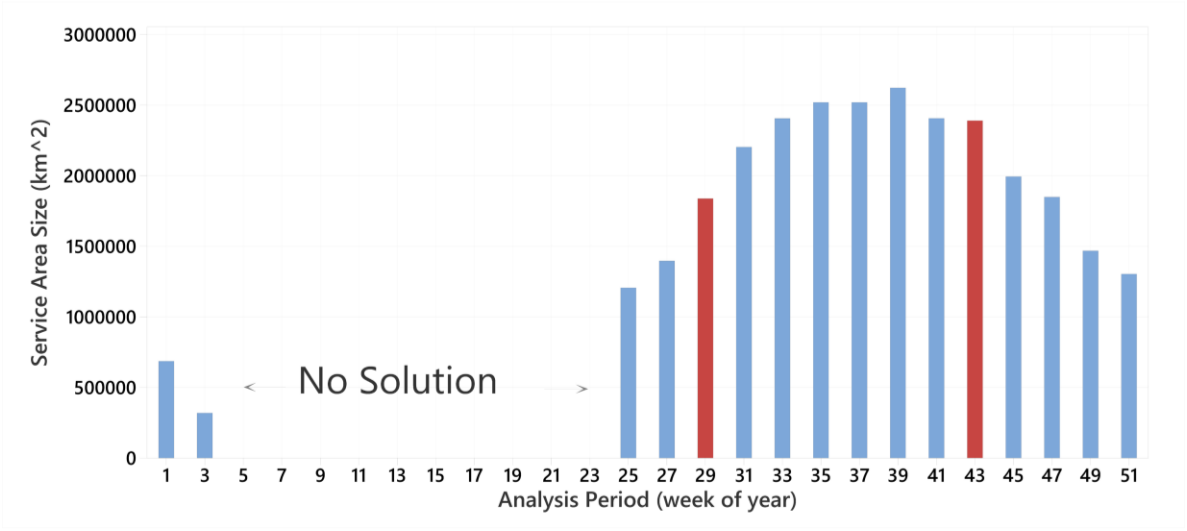

Figure 27: Comparison of geographic size of the IRSA for a Polar Class 1A vessel throughout the year, for a given Service Area Analysis Scenario (SAAS).

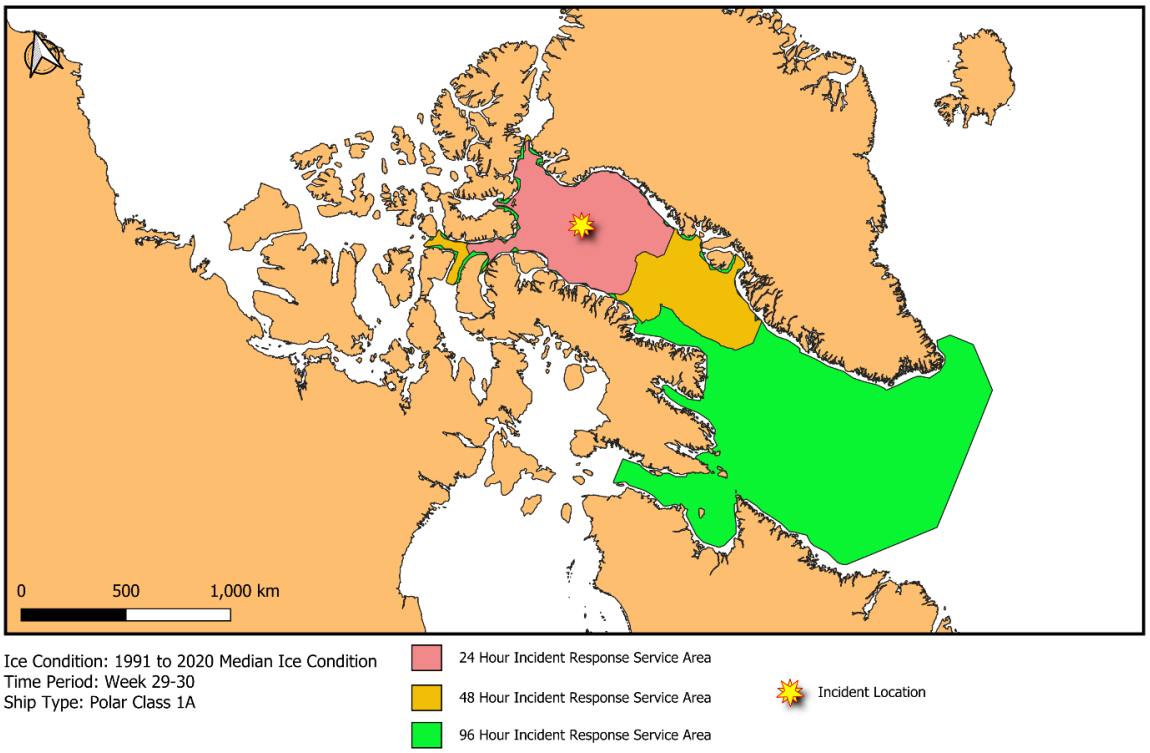

Figure 28: Comparison of the IRSA size for a Polar Class 1A ship in Week 29-30 for 24 h, 48 h, and 96 h MRTC.

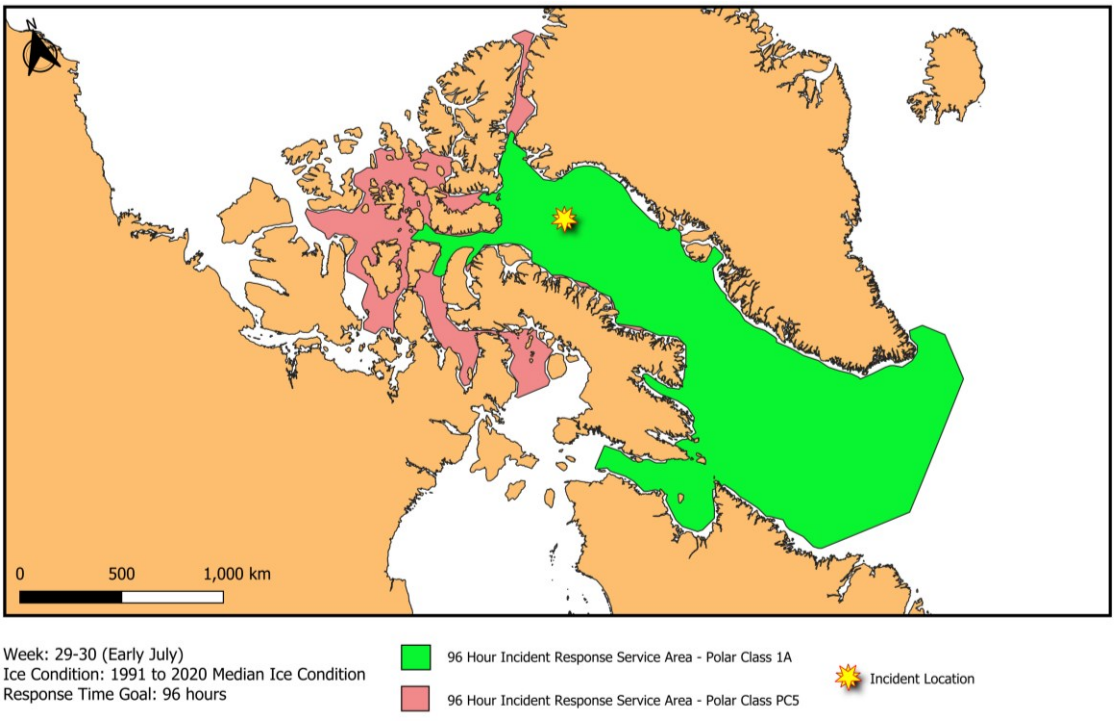

Figure 29: Comparison of the IRSA for a Polar Class 1A and PC5 ship in Week 29-30.

Sometimes it might be more convenient to visualize the isoline formed at the MRTC value, referred to in this study as the IRI. This is the isoline formed around the maximum extent of the service area. The travel time from any arbitrary point on the isochrone to the incident location is equal to the MRTC. Figure 30 compares the 96-hour incident response isochrone for a Polar Class 1A and PC5 ship in week 29-30.

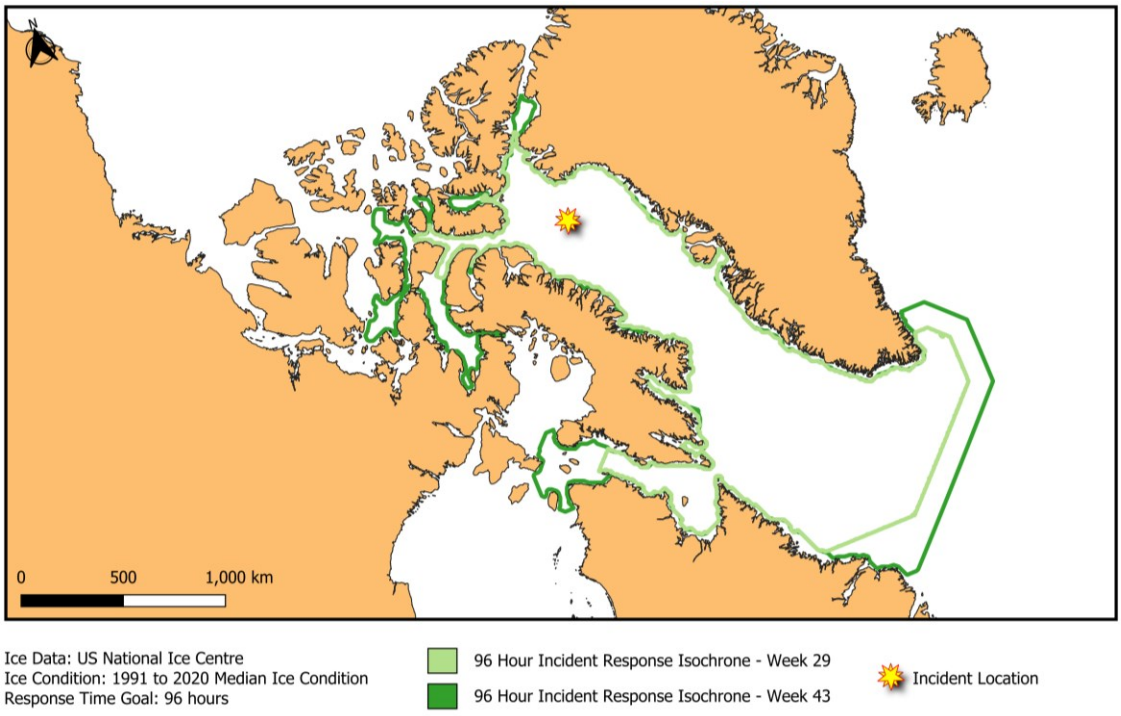

Figure 30: Comparison of 96-hour IRI for a Polar Class 1A in week 29 and week 43.

The application of traditional network analysis methods to compute optimal routes in polar waters has resulted in several useful analytics and metrics with potential to support quantitative studies related to incident response and ABM in the Canadian Arctic. Our approach integrates sea ice analysis, navigation risk assessment, and network optimization to compute the expected transit time between two points in polar waters. Once computed, the expected transit time provides an objective measure to examine surface ship incident response in polar waters. The results show that incident response times are heavily influenced by the geographic location of the incident and responding vessel, time of year, sea ice conditions, and the ship ice class of the vessel responding to the incident.

The complex geography and variable sea ice conditions found in the Canadian Arctic Archipelago are significant contributors to the spatiotemporal variability of emergency response time and overall maritime mobility. The remoteness of the Canadian Arctic and lack of infrastructure affects the timeliness of SAR response, especially maritime-based SAR response. Ships must be prepared to wait days before maritime-based SAR resources arrive at the incident location. Currently, the Polar Code requires that all vessels operating in polar waters be prepared to wait at least 5 days for SAR resources to arrive on-scene (International Maritime Organization, 2016). The National Research Council of Canada (NRC) has previously evaluated the expected time until recovery for several geographic locations in the Arctic ((Kennedy, Gallagher, & Aylward, 2013), (Piercey, Kennedy, & Power, 2019)). The NRC study examined emergency response at 8 locations dispersed throughout northern Canada, but was limited to two hypothetical emergency scenarios, (1) mild August environmental conditions, and (2) severe August environmental conditions. The geographical locations selected by NRC were based on several considerations. The first was to ensure that locations were selected throughout the Canadian Arctic, to provide results that cover the vastness of the region. The second consideration involved the frequency of travel based on current shipping routes and maritime traffic and expected future shipping activity. The third consideration was to ensure the selected locations were positioned at varying distances from existing infrastructure, such as airports, communities, and ports.

Error! Reference source not found. shows the location of the NRC maximum exposure e valuation sites overlayed on historical SAR incident data from the Canadian Coast Guard (CCG) Search and Rescue Program Information Management System (SISAR). SISAR incident data is one of the primary data sources used to capture statistics relating to maritime SAR cases to inform demand for program services and the achievement of outcomes (Government of Canada, 2019). SAR incident data provides a rich multivariate spatiotemporal dataset that can support a wide range of analysis (Stoddard & Pelot, 2020). PV provided a location analysis of historical maritime incidents to give a better understanding of the spatial distribution of historical incident locations in the Canadian Arctic, which broadly supported the ABM goals of the CCG.

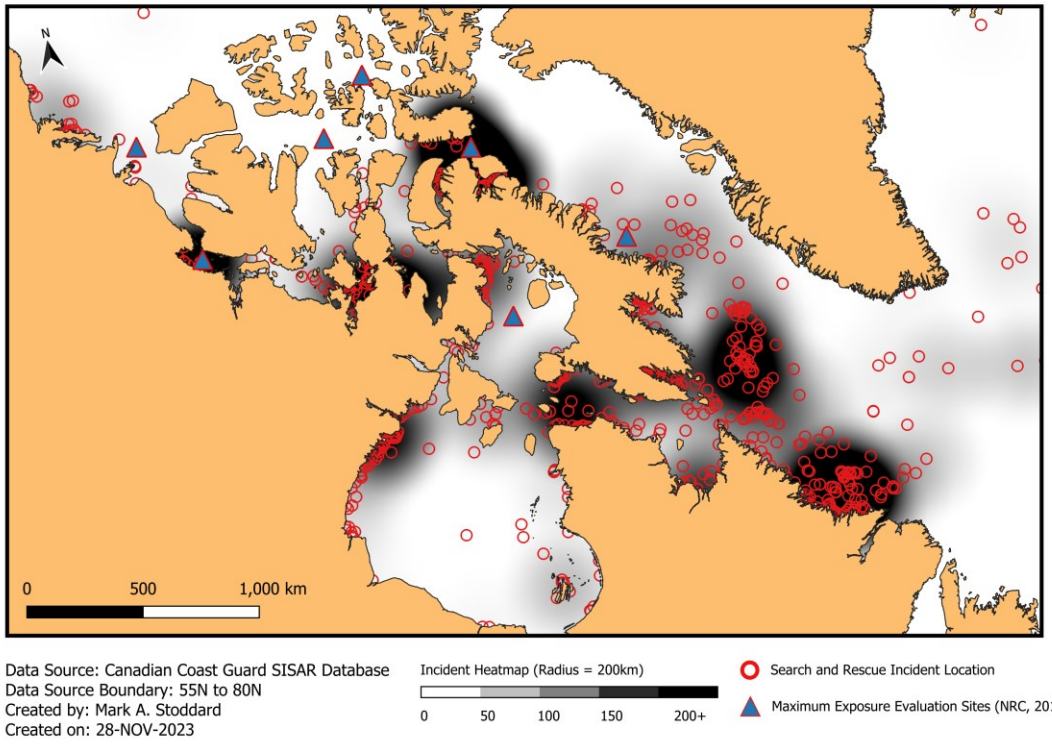

Figure 31: SISAR incident data from 2001 to 2020 with an overlay of the NRC maximum exposure time evaluation sites

The use of IRSA and IRI to quantify and visualize the expected transit time for marine-based assets would be another extension to the NRC study of maximum exposure time in the Arctic. This added analysis would allow for a greater consideration of the spatiotemporal variability of expected response time for marine-based SAR assets throughout the year. The use of IRSA and IRI computed on a bi-weekly basis would allow for a more complete analysis of expected transit time for marine-based response assets throughout the year, and its impact on expected exposure time. Figure 32 shows Week 33 (mid-August) 12-hour, 24-hour, and 48-hour IRSA for a selected NRC maximum exposure evaluation site. A Polar Class 1A vessel found anywhere in a selected IRSA polygon could reach the location of interest within the associated time cut-off. While the IRSA results shown in Figure 32 are specifically for a Polar Class 1A vessel, the same method can be used to visualize the IRSA results for any chosen Polar Class vessel to reach the NRC evaluation site.

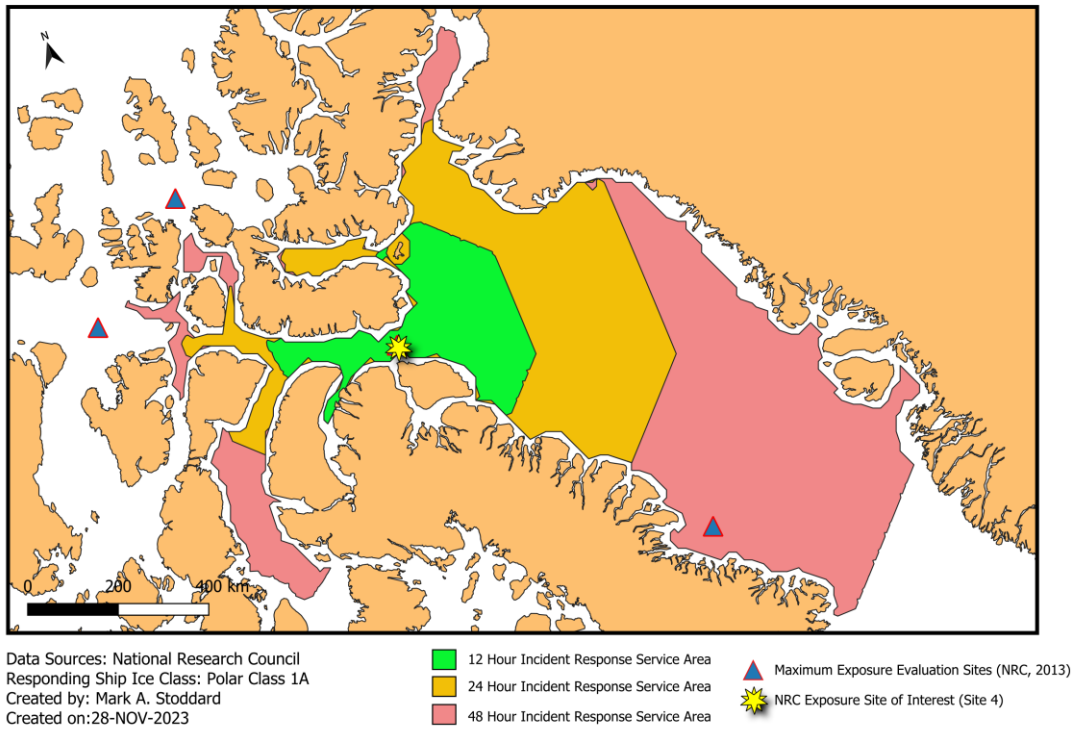

Figure 32: 12-hour, 24-hour, and 48-hour IRSA for a Polar Class 1A vessel operating in Week 33, assuming 1990 to 2021 median RIO value for Week 33-34.

More specifically, IRSA and IRI concepts could be used to extend the study results for marine-based SAR response to explicitly consider the contribution of Vessels of Opportunity (VOO) in the analysis. This added analysis would not require a significant change in the study method. This could be achieved by combining the analysis of historical shipping activity data (Polar Class ship type, time, and location), and IRSA results, to find the probability of a VOO being available and able to respond to an incident within the specified MRTC. This approach could also support a wide variety of ABM tools that aim to incorporate historical shipping activity into the overall assessment of marine-based SAR response for pre-selected evaluation sites in the Canadian Arctic. Figure 33 shows how observations of shipping activity can be combined with IRSA to quantify the expected contribution of VOO to incident response and maximum exposure time. In this case, we see that no VOO can reach the evaluation site within 12 hours, three VOO can reach the site within 12 to 24 hours, and forty-nine VOO can reach the site within 24 to 48 hours. The location, and number of VOO, shown in Figure 33 are representative of a single instant

in time. By analyzing shipping traffic data over multiple years, it would be possible to statistically characterize VOO availability to support this form of analysis.

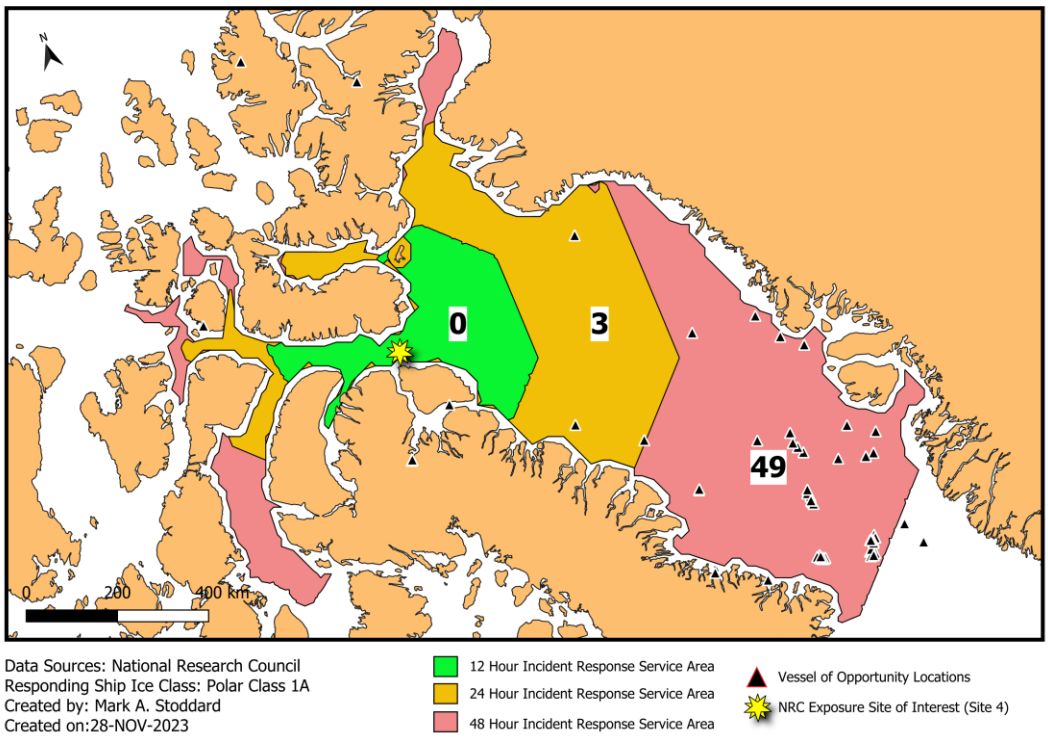

Figure 33: 12-hour, 24-hour, and 48-hour IRSA for a Polar Class 1A vessel operating in Week 33, with an example overlay of vessel of opportunity locations and total vessel counts in each IRSA

CHAPTER 4: Discussion and Future Research

4.1 Thesis contribution and Reached Objectives

This section discusses the contributions of this thesis to marine-based transit time in ice-covered waters and strategic ship routing and analysis in the Arctic. The research objectives and questions found in Section 1.3, and graphically represented in Figure 1, have guided the development of new computational methods, spatial data processing techniques, and the application of network analysis methods to support strategic route planning and analysis in the Arctic. The contribution of the new computational methods and completed analysis, and its links to strategic route analysis and SAR response planning, are assessed.

4.1.1 Marine-Based Transit Time Estimation in Ice-Covered Waters (PI/PII/PII)

Estimating transit time between the origin and destination of a planned voyage is a common task in maritime navigation. Marine-based transit time estimation in the Canadian Arctic is particularly challenging because of the great distances that must often be traversed, the navigational complexity of the Canadian Archipelago, and the variable sea ice conditions that are expected to be encountered. (McCallum, 1996) first proposed the use of polynomial fitting between minimum and maximum expected ship speeds for several Canadian Arctic Class (CAC) ships in different ice risk regimes. A scaling procedure was then used to produce speed curves for different ice class ships in different ice risk regimes. As more sources of data become available to make sense of maritime activity in ice-covered waters, such as S-AIS, researchers are now relying more on the use of semi-empirical, empirical, and data-driven models to estimate vessel speed in different ice regimes ((Lehtola, Montewka, Goerlandt, Guinness, & Lensu, 2019), (Tremblett, Garvin, & Oldford, 2021), and (Liu, Musharraf, Li, & Kujala, A data mining method for automatic identification and analysis of, 2022)).

To date, most of the data-driven methods used to determine vessel speeds in ice found in the literature are limited to specific geographic areas, such as the Baltic Sea, or have only considered a small number of ice regimes or ship ice classes in their analysis. The S-AIS data set used for this thesis covers the entire Canadian Arctic, and spans two calendar years.

It includes many ice class ships operating in a wide range of ice regimes. When combined with circumpolar sea ice analysis from the USNIC it was possible to generate analysis results not previously reported in the literature, simply due to the scope and scale of the analysis and the range of ice regimes considered.

In Section 2.2 we presented a new data-driven method that combined our S-AIS data set with outputs from the POLARIS sea ice risk assessment method to characterize the expected ship speed in different POLARIS RIO categories. The results show that the POLARIS RIO value provides essential information to interpret AIS reported speeds in ice-covered waters, and to characterize expected ship speed in different RIO categories. When combined with knowledge of the POLARIS RIO results along a planned route, we were able to carry out **Objective 1** of this thesis and produce a new computational method to estimate marine-based transit times in ice-covered waters that considers the risk from sea ice and its impact on ship speed. This result was referred to as the Expected Transit Time (ETT).

The use of the ETT calculation allows a navigator to explicitly account for the expected transit delays along a planned route in ice-covered waters due to varying sea ice risk along the route. The transit time validation case study presented in Section 3.1.3, and found in PIII, has also shown that the proposed method produces a reasonable estimate of ship transit time for independent ship operations in ice-covered waters.

4.1.2 Strategic Route Planning in Ice-Covered Waters (PIV)

POLARIS has proven to be a useful tool not only for tactical decision-making onboard ships, but also for the strategic appraisal of navigational risk over wide areas. The challenge is incorporating the results from navigational risk assessment into a modeling framework that can be used to support strategic route planning. (Smith & Stephenson, 2013) give an example of incorporating sea ice risk assessment in a maritime transportation model to study the future navigability of trans-arctic polar routes. The authors constructed a transportation graph and were able to compute optimal navigation routes through the Arctic using a least-cost path algorithm. Their study focused on the use of modeled data and results were only generated for the month of September. Their results offer little insight into optimal routing at other times of the year. More recently, (Lehtola, Montewka, Goerlandt,

Guinness, & Lensu, 2019) discuss the use of semi-empirical (simulation) models, and data-driven models to estimate vessel transit speed in different ice regimes. While several examples exist in the literature discussing vessel transit speed in ice-covered waters, far fewer have presented a model that can directly use these results to support strategic route planning over wide areas.

Section 2.4 presented a methodology that accomplishes **Objective 2** of this thesis, successfully combining POLARIS sea ice risk assessment, expected ship speeds in different POLARIS risk categories, and network optimization, to compute the fastest route and expected transit time between two locations in ice-covered waters, referred to as Ice Risk-Adjusted Estimated Time of Arrival (I-ETA). The results shown in Section 3.2 showed the utility of the I-ETA method and its potential to support a variety of strategic decision applications, such as wide-area strategic ship routing and SAR response planning.

The results shown in Section 3.2 and PIV suggest that the fastest routes generated through the Canadian Archipelago using the I-ETA method converge on the commonly accepted strategic routes through the Canadian Arctic. Using these new methods to support strategic route planning in ice-covered waters can reduce the expected transit time and increase ship safety. The accomplishment of Objective 2 provides a new method to help ensure voyage planners and ship navigators have the necessary methods to find the fastest route through ice-covered waters that minimize the total time a ship is exposed to unfavorable ice conditions.

4.1.3 Marine-Based SAR Response Planning (PV/PVI)

The aim of **Objective 3** of this thesis was to combine the I-ETA method with existing network analysis concepts to generate new analysis techniques to support marine-based SAR response planning. The accomplishment of Objectives 1 and 2 provided the necessary tools to achieve this objective. Section 3.3 introduced two new network analysis concepts, namely IRSA and IRI, to support marine-based SAR response planning. The IRSA is a region that encompasses all ship locations that reach an incident location within a specified amount of time. Ships outside the IRSA cannot reach the location within a specified maximum time cut-off. The IRI is closely concept that is the isoline formed using the maximum time cut-off. Ships outside of the IRSA and beyond the IRI are unable to reach

the incident location within a user-specified time. Incorporating IRSA and IRI results into area-based management tools would provide decision makers with a useful tool to help plan and coordinate incident response in polar waters, support ABM of commercial vessel operation, and Search and Rescue provision.

4.2 Limitations of the Utilized Data, Methods, and Thesis Outputs

4.2.1 Further Improvements in Sea Ice Risk Assessment and Transit Time Estimation

In Section 3.1, we presented the results of a statistical analysis on two years of historical S-AIS reports and POLARIS RIO results to gain new insights on the expected ship speed in ice-covered waters. The RIO value has been shown to provide the necessary information to interpret AIS reported speeds in ice-covered waters, and to characterize expected ship speed in varying sea ice conditions. The approach presented in this thesis combined S-AIS geospatial data analysis techniques, sea ice risk assessment, and statistical methods to produce an expected ship speed curve. The POLARIS RIO speed curve can be used to figure out the expected ship speed in different POLARIS RIO categories, allowing ship navigators to directly incorporate POLARIS RIO results into their transit time estimation process. The result is a transit time estimate that incorporates the expected increase and decrease in ship speed due to varying sea ice conditions and navigational risk.

There are several limitations to the current work that may limit the use of these results. The first major limitation is the S-AIS data set used for this study. The AIS data set only covered two years and was geographically constrained to the Canadian Arctic. A fair criticism is that the results are not statistically significant, and that the expected ship speed results may only apply to the Canadian Arctic, due to the geographic limitation of the AIS data set. Another limitation relates to the temporal resolution of the USNIC sea ice analysis used to compute the POLARIS RIO value for each AIS report. In our analysis, we were forced to associate an AIS report with GPS time precision, with an analysis product produced bi-weekly. The difference in temporal resolution undoubtedly creates some errors in analysis. Lastly, due to the limited availability of ship ice class information we had to remove many of the AIS reports from our data set because the ice class of the ship could not be found.

Future efforts to improve the results of this study could focus on expanding the size of the historical AIS data set used for the analysis of vessel speed. This could be achieved by increasing both the temporal range, and geographic extent. For example, including AIS reports from the Russian Arctic would significantly increase the amount of AIS reports from ships operating in ice covered waters, which would help increase the statistical significance of the expected ship speed results. Another potential improvement to this study would be to use daily sea ice analysis products (with the required geographical coverage area), or even in-situ ship observations, to improve the accuracy of the POLARIS RIO value computed for each AIS report. Increasing the accuracy of the POLARIS RIO result associated with each AIS report would help ensure that the reported ship speed is associated with correct RIO result category. More work is also needed to examine more historical transits in ice-covered waters to better confirm our method of computing the ETT.

It is also worth discussing how these results could be used to broadly support efforts to improve strategic navigation planning, and maritime Area-Based Management (ABM). The complex geography, and variable sea ice conditions, found in the Canadian Arctic Archipelago has a significant impact on maritime mobility and transit time. Estimating ship speeds in different ice regimes is critical to improving the estimation of travel time, fuel consumption, and emissions. Providing strategic planners with better tools to estimate the expected transit time for a voyage at various times of the year, and for different ship ice classes, has the potential to increase safety, save time and money, and to reduce shipping emissions. This is achieved by ensuring that ships have the necessary tools to plan to sail at more optimal times of the year, and that the right ship ice class is considered for the voyage.

4.2.2 Improving Marine-Based SAR Response Planning using IRSA and IRI

Two major limitations of our approach to analyzing incident response using IRSA and IRI are (1) the temporal resolution of sea ice analysis, and (2) the use of bi-weekly median RIO values over the 1991 to 2020 climatological period for route generation and transit time estimation. Our method relies on the use of bi-weekly sea ice analysis from the USNIC to assess navigational risk. The consequence of relying on bi-weekly sea ice analysis is that all later analysis products derived from this sea ice analysis must also be produced on a bi-

weekly basis, to avoid over-resolving the data. It also means that our network optimization model assumes that sea ice conditions do not change over a two-week period. For short transits this should not create much concern, but when examining trans-arctic routes through that could exceed 10+ days it may seem unreasonable to assume sea ice condition will remain static during voyage execution. This issue is less of a concern when conducting strategic planning but is of greater concern at the tactical ship operations level. Secondly, the use of the climatological median RIO value in our analysis will limit the usefulness of our results for tactical applications.

4.3 Future Research

This thesis has identified several opportunities to continue the research developed and to support the validation of the proposed research methods and results. The first is to expand the geographic size and temporal extent of the S-AIS data set used to characterize ship speeds in different POLARIS RIO result categories (PIII). Expanding the geographic extent of the S-AIS to match the extent of the USNIC bi-weekly ice analysis chart would maximize the number of AIS reports used in this analysis. This would increase the statistical significance of the vessel speed results and offer greater opportunity to observe vessel activity in more ice regimes.

The second is to expand on the effort to validate ETT results using historical ship tracking data and sea ice analysis charts. AIS data can be used to reconstruct ship voyages in ice-covered water, providing the necessary data to compare actual transit time and the ETT results. The potential exists to automate the validation of the ETT method through the careful processing of historical ship tracking data and its intersection with temporally aligned sea ice analysis. Every voyage executed in ice-covered waters could potentially be used to confirm the ETT results. Special consideration would be needed to ensure that all voyages used for validation correspond to continuous transit, independent ship operations.

Lastly, further exploration of the use of IRSA and IRI for other Area-Based Management (ABM) applications is called for. This thesis has focused exclusively on the use of IRSA and IRI for SAR response planning in ice-covered waters, but a variety of other potential use cases exist. Other potential uses of IRSA and IRI include:

1. Study of year-round marine-based remoteness of coastal communities in the Arctic,
2. Environmental response planning and evaluation
3. Maritime security response planning and interdiction
4. SAR resource selection and deployment planning
5. Realtime vessel monitoring and risk assessment

CHAPTER 5: Conclusion

The computational results and analysis published in PI and P2, and summarized in this thesis, show how open-access sea ice data can be used to support the strategic assessment of ship operational limits in ice. The combination of the POLARIS sea ice risk assessment method with open-access sea-ice information has made it easy to assess and visualize ship operational limits in ice over a large area of interest or along a particular route. The resulting POLARIS scenario risk maps provide a user-friendly visualization of the RIO results for a particular polar ship ice classification. We have generated several statistical aggregations of RIO results over the 1991 to 2020 climatological period, supporting a more rigorous assessment of the available historical sea-ice information. In addition to assessing ship operational limits in sea ice, the POLARIS scenario risk maps and underlying results can also be used to support a variety of strategic decisions relating to fleet mix, ship allocation, or ship scheduling and strategic routing. We have also shown how the POLARIS RIO can be used to make sense of observed vessel kinematic behavior when operating in sea ice. Efforts to improve our ability to make sense of unusual or unexpected shipping behavior are highly desired by the shipping safety and security centers, who handle observing and monitoring maritime activity. The use of the POLARIS scenario risk map in this case allows the user to anticipate how ice may influence a particular vessel's behavior based on the design of the ship and its capability to operate in different sea ice conditions.

The results presented in PIII and summarized in this thesis, provide an original approach to estimating transit time between two locations in ice covered waters. Estimating transit time in the maritime domain, especially in the Arctic region, is complicated by many environmental and other external factors affecting ship speed and its follow-on impact on transit time. The great distances often traversed, and the variable sea ice conditions expected to be encountered in the polar region, are both major factors that complicate arctic navigation and planning. PIII demonstrated a data-driven approach to estimating expected ship speed in different POLARIS RIO result categories using S-AIS data, USNIC sea ice analysis, and the POLARIS sea ice risk assessment method. When the expected ship speed in different RIO result categories is combined with knowledge of the POLARIS RIO results along a route, it is possible to calculate accurate expected transit times in ice covered

waters. The ETT calculation presented in this thesis allows a navigator to explicitly account for the expected transit delays along a route due to varying sea ice risk and its relationship with safe ship speed. The transit time validation case study presented in this thesis showed how the proposed method produces accurate estimated transit times for independent ship operations in ice-covered waters. The proposed methods and results of this study have provided a step forward in overcoming the complexity of computing accurate transit time estimates in ice-covered waters.

The results presented in PIV and summarized in this thesis, introduce several methods to enable strategic route analysis in ice-covered waters. By combining geospatial processing techniques, with statistical analysis, we produced several different statistical aggregations of POLARIS RIO results observed over the climatological period from 1991 to 2020. We combined these results with network analysis methods, to compute the fastest route between two locations in ice-covered waters at various times of the year. The output of this calculation was referred to as the I-ETA. The resulting computer-generated fastest routes through the NWP showed good agreement with the commonly accepted strategic routes through the NWP. These results appear to show that navigational risk, assessed using POLARIS and USNIC sea ice analysis, has a strong influence on strategic ship routing through ice-covered waters and polar regions. Generating acceptable strategic routes through complex navigation environments, such as the Canadian Arctic Archipelago, is a challenging problem. Our study has shown that understanding sea ice risk, and its impact on ship speed, is critical when generating strategic routes in ice-covered waters.

A current limitation of our model is that it generates fastest routes with little consideration for the overall risk associated with the route. We relied on a cost function that increases the time to transit through areas of higher navigational risk. This has the unfortunate consequence of leaving it up to the navigator to then assess the feasibility of safely executing the computer-generated route. With this consequence in mind, we have provided a method to evaluate a route based on the proportion of the total transit distance through different RIO result categories. This analysis occurs only after a route has been created and does not help inform the calculation of the fastest route. The choice of best routes in polar waters is still a hard problem, requiring a combination of ice navigation experience, high

quality data, and robust decision support tools. The methods and results presented in this thesis provide insight into the tools and techniques needed to advance research in strategic route analysis in ice-covered waters. Future work could focus on the inclusion of other planning considerations when generating strategic routes, such as avoiding marine protected areas, calving grounds, and northern community ice bridges, or by rewarding routes that follow corridors with increased service provision, such as ice breaking, communications, and SAR. This would be achieved by applying additional spatial processing of our transportation graph and updates to the cost matrix, $c_{i,j}$ in our fastest path optimization model (see Section 2.4.2).

The results presented in PVI and summarized in this thesis, show how network analysis techniques can be used to compute IRSA and IRI in ice-covered waters. These results offer several valuable insights into the spatiotemporal variability of marine-based transit time and incident response time in polar waters. The use of IRSA and IRI to determine the expected response time for marine-based SAR assets was discussed and discussed as an extension to a 2013 study of maximum exposure time in the Canadian Arctic completed by the NRC. The use of IRSA and IRI to support ABM tools that aim to formally incorporate historical observations of shipping activity into quantitative assessments was also discussed. Incorporating IRSA and IRI results into ABM tools would provide decision makers with a useful tool to help plan and coordinate incident response in polar waters, supporting the management of commercial vessel operation, and Search and Rescue provision.

Future technical work on IRSA and IRI could concentrate on exploring the use of diverse sources of sea ice analysis to better understand how changing the source data can affect the fastest route and expected transit time results. The use of modeled sea ice data from ice forecasting and GCM systems also offers a particularly interesting opportunity to compare expected RIO values derived from the statistical analysis of historical observations, and from the model results. Computing IRSA and IRI using the RIO values derived from forecasted, and/or modeled sea ice conditions, may give decision makers a better understanding of the future navigability of the Canadian Arctic, and its impact on strategic

ship routing and expected transit times. These insights could be used to update policies, industry practices, and regulations that aim to improve shipping safety and SAR response.

Overall, this thesis has stressed the importance of accurately estimating transit time in ice-covered waters to support a variety of strategic decision-making applications in the polar region. The ability to incorporate sea ice risk assessment into quantitative methods supporting route generation and evaluation was seen as a necessary step to improve transit time estimation in the polar region. Through the conduct of this research, several new quantitative methods and information visualizations have been developed to advance the state of the art in the general study of arctic maritime transportation and navigational risk assessment. While several technical advances have been reported in this thesis, much work remains to assess the overall quality and robustness of these contribution to the literature. It is expected that the proposed methods and results presented in this thesis will stimulate new research and technical advances in research related to polar navigation, emergency preparedness, and SAR response.

REFERENCES

Aksenov, Y., Popova, E. E., Yool, A., Nurser, G., Williams, T. D., Bertino, L., & Bergh, J. (2017). On the future navigability of Arctic sea routes: High-resolution projections of the Arctic Ocean and sea ice. *Marine Policy, 75*, 300-317.

Alasia, A., Bedard, F., Belanger, J., Guimond, E., & Penny, C. (2017). *Measuring remoteness and accessibility: A set of indicies for Canadian Communities.* Statistics Canada. Retrieved from www.publications.gc.ca/pub?id=9.835126&sl=0

Andersson, M., & Johansson, R. (2010). Multiple Sensor Fusion for Effection Abnormal Behavior Detection in Counter Piracy Operations. *Proceedings of International Waterside Security Conference.*

ARCDEV. (1998). *Final Public report of the ARCDEV Project.* Retrieved from https://trimis.ec.europa.eu/sites/default/files/project/documents/arcdev.pdf

Arctic Council. (2009). *Arctic Marine Shipping Assessment 2009 Report.* Arctic Council.

Bilge, T. A., Fournier, N., Mignac, D., Hume-Wright, L., Bertino, L., Williams, T., & Teitsche, S. (2022). An Evaluation of the Performance of Sea Ice Thickness Forecasts to Support Arctic Marine Transport. *Journal of Marine Science and Engineering*(10), 265.

Boylan, B. (2021, September). Increased maritime traffic in the Arctic: Implications for governance of Arctic sea routes. *Marine Policy, 131*.

Cairns, W. (2005). AIS and Long Range Identification and Tracking. *Journal of Navigation*, 58:181-189.

Canadian Ice Service. (2009). *Canadian Ice Service Arctic Regional Sea Ice Charts in SIGRID-3 Format.* Boulder, CO: Natinoal Snow and Ice Data Centre.

Canadian Ice Service. (2021). *Ice climate normals for the northern Canadian waters 1991 to 2020.* Governement of Canada.

Cau, Y., Liang, S., Sun, L., Liu, J., Cheng, X., Wang, D., . . . Feng, K. (2022). Trans-Arctic shipping routes expanding faster than the model projections. *Global Evironmental Change, 73*.

Chamberlain, J., Yue, B., Parsons, G., & Mulvie, J. (2008). Advanced Remote Sensing for Better Bottom-Fast Ice Identification. *RADARSAT-2 Workshop.*

Chircop, A., Goerlandt, F., Pelot, R., & Aporta, C. (2024). *Area-Based Management of Shipping: Canadian and Comparative Perspectives.* Springer Cham. doi:https://doi.org/10.1007/978-3-031-60053-1

Collard, F., Mouche, A., Danilo, C., Chapron, B., Isern-Fontanet, J., Johannessen, J., & Backberg, B. (2008). *Routine High Resolution Observation of Selected Major Surface Currents from Space.* SEASAR.

Crawford, A., Stroeve, J., Smith, A., & Jahn, A. (2021). Arctic open-water periods are projected to lengthen dramatically by 2100. *Communications Earth & Environment, 2*(109). doi:https://doi.org/10.1038/s43247-021-00183-x

Crisp, D. (2004). *The State-of-the-Art in Ship Detection in Syntehtic Aperature Radar Imagery.* Adelaide, AS: Defence Science and Technology Organization.

Dahlbom, A., & Niklasson, L. (2007). Tragectory Clustering for Coastal Surveillance. *10th Conference of the International Soceity for Information Fusion.*

Department of Health and Aged Care. (2001). *Measuring remoteness: Accessibility/Remoteness Index of Australia (ARIA).* Government of Australia. Retrieved April 10, 2024, from https://www.nintione.com.au/?p=5335

Dijkstra, E. (1959). A note on two problems in connxion with graphs. *Numerische Mathematik, 1*(1), 269-271.

DNV-GL. (2014). *The Arctic - The nex frontier.*

Dolny, J. (2018). *Methodology for Defining Technical Safe Speeds for Light Ice-Strengthened Government Vessels Operating in Ice.* Ship Structure Committee. United States Coast Guard.

Dovey, K., Woodcock, I., & Pike, L. (2017). Isochrone Mapping of Urban Transport: Car-dependency, Mode-choice, and Design Research. *Planning Practice & Research, 32*(4), 402 - 416.

Eriksen, T., Hoye, G., Narheim, B., & Jenslokken, M. (2006). Maritime Traffic Monitoring using space-based AIS Recevier. *Acta Astronautica*, 58(10): 537-549.

Etienne, L., & Pelot, R. (2013). Simulation of maritime paths taking into account ice conditions in the Arctic. *Symposium for GIS and Computer Cartography for Coastal Zone Management (CoastGIS)*, (pp. 116-119).

European Commission. (2014). *Defining Proxy Indicators for Rural Development Programs.* Journal of the European Union.

Fedi, L., Etienne, L., Haury, O., Rigot-Muller, P., Stephenson, S., & Cheaitou, A. (2018). POLARIS in the Arctic. *Journal of Ocean Technology, 13*(4), 58-71.

Fedi, L., Faury, O., & Etienne, L. (2020). Mapping and analysis of maritime accidents in the Russian Arctic through the lens of the Polar Code and POLARIS system. *Marine Policy*(118), 1-9.

Finnish Transport Safety Agency. (2017). *Finnish ice classes equivalent to class notations of recognized classification societies and the determination of the ice classes of ships.* Helsinki, Finland: Trafi.

Fraser, D. (2020). A Change in the Ice Regime: Polar Code Implementation in Canada. In A. Chircop, F. Goerlandt, C. Aporta, & R. Pelot, *Governance of Arctic Shipping.* Springer Polar Sciences.

Fu, S., Zhang, D., Montewka, J., Yan, X., & Zio, E. (2016). Towards a probabilistic model for predicting ship besetting in ice in Arctic waters. *Reliability Engineering & System Safety*, 124-136.

Georlandt, F., Montewka, J., Zhang, W., & Kujala, P. (2017). An analysis of ship escort and convoy operations in ice conditions. *Safety Science, 95*, 198-209.

Goerlandt, F., & Pelot, R. (2020). An Exploratory Application of the International Risk Governance Council's Risk Governance Framework to Shipping Risks in the Canadian Arcitc. In A. Chircop, *Governance in Arctic Shipping.* Springer Polar Sciences.

Goerlandt, F., Montewka, J., Zhang, W., & Kujala, P. (2017). An analysis of ship escort and convoy operations in ice conditions. *Safety Science, 95*, 198-209.

Goerlandt, F., Montewka, J., Zhang, W., & Kujala, P. (2017). An analysis of ship escort and convoy operations in ice conditions. *Safety Science, 95*, 198-209.

Goerlandt, F., Montewka, J., Zhang, W., & Kujala, P. (2017). An Analysis of Ship Escort and Convoy Operations in ice Conditions. *Safety Science*, 198-209.

Government of Canada. (2019, June 25). *Canadian Coast Guard Search and Rescue and Canadian Coast Guard Auxiliary Evaluation Report*. Retrieved from Department of Fisheries and Oceans Canada: https://www.dfo-mpo.gc.ca/ae-ve/evaluations/11-12/SAR-CCGA-eng.htm#2.1

Greidanus, H., & Kourti, N. (2006). Findings of the CELIMS Project - Detection and Classification of Marine Traffic from Space. *Proceedings of SEASAR 2006.* Frascati, Italy.

Headland, R. (2022). *Transits of the Northwest Passage to End of the 2022 Navigation Season: Atlantic Ocean to Arctic Ocean to Pacific Ocean.* Scott Polar Research Institute. Cambridge University.

Heiberg, H. B., Reistad, M., & A., B. (2006). *Use of ASAR wave spectra in operational wave analysis and forcasting: report from the EnviWave project.* Oslo: Norweigian Meteorological Institute.

Higginbotham, J., & Grosu, M. (2014). The Northwest Territories and Arctic Maritime Development in the Beaufort Regimes. *CIGI Policy Brief*, 40:1-12.

Hirose, T., Kapfer, M., Bennett, J., Cott, P., Manson, G., & Solomon, S. (2008). Bottomfast Ice Mapping and the Measurement of Ice Thickness on Tundra Lakes using C-Band SAR Remote Sensing. *Journal of the American Water Resources Association*, 44(2): 285-292.

Howell, S., & Yackel, J. (2004). A Vessel Transit Assessment of Sea Ice Variability in the Western Arctic, 1969-2002: Implications for ship navigation. *Canadian Journal of Remote Sensing*, 30(2):205-215.

IACS. (2009). *International Association of Classification Societies Charter.* International Association of Classificaiton Socieities.

IACS. (2023). *Requires Concerning POLAR CLASS.* International Association of Classification Socieities.

Intergovernmental Oceanographic Commission of UNESCO. (2004). *SIGRID-3: A Vector archive formate for sea ice charts.* JCOMM Technical Report.

International Maritime Organization. (2004). *Regulation 19 - Carriage requirements for shipborne navigational systems and equipment.* London: International Maritime Organization.

International Maritime Organization. (2016). *International Code for Ships Operating in Polar Waters (POLAR CODE).* International Maritime Organization.

International Telecommunication Union. (2014). *Technical characteristics for an automatic identification system using time division multiple access in the VHF maritime mobile frequency band.* Geneva: International Telecommunication Union.

Kang, M., Lee, H., Yang, C., & Yoon, W. (2008). Estimation of Ocean Current Velocity in Coastal Area using RADARSAT-1 SAR Images and HF-Radar Data. IGRASS 2008.

Kazemi, S., Abhari, S., Lavesson, N., Johnson, H., & Ryman, P. (2013). Open Data for Anomaly Detection in Maritime Surveillance. *Expert Systems with Applications*, 40: 5719 - 5729.

Kennedy, A., Gallagher, J., & Aylward, K. (2013). *Evaluating Exposure Time Until Recovery by Location.* Ottawa, Ontario: National Research Council Canada.

Khan, B., Khan, F., Veitch, B., & Yang, M. (2018). An operational risk analysis tool to analyze marine transportation in Arctic waters. *Reliability Engineering & System Safety, 169*, 485-502. doi:https://doi.org/10.1016/j.ress.2017.09.014.

Kim, H., Jeong, S.-Y., Woo, S.-H., & Han, D. (2018). Study on the procedure to obtain an attainable speed in pack ice. *International Journal of Naval Architecture and Ocean Engineering*(10), 491-498. doi:https://doi.org/10.1016/j.ijnaoe.2017.09.004

Kotovirta, V., Jalonen, R., Axell, L., Riska, K., & Berglund, R. (2009). A system for Route Optimization in Ice-Covered Waters. *Cold Regions Science and Technology*(55), 52-62.

Kubat, I., & Timco, G. (2003). *Vessel Damage in the Canadian Arctic.* National Research Council of Canada.

Lack, D. A., & Corbett, J. J. (2012). Black carbon from ships: a review of the effects of ship speed, fuel. *Atmostpheric Chemistry and Physics*(12), 3985-4000.

Laxhammer, R. (2008). Anomaly Detection for Sea Surveillance. *11th International Conference on Information Fusion* (pp. 47-54). Fusion 2008.

Lee, H.-W., Roh, M.-I., & Kim, K.-S. (2021). Ship Route Planning in Arctic Ocean based on POLARIS. *Ocean Engineering*(234), 1-14.

Lehtola, V., Montewka, J., Goerlandt, F., Guinness, R., & Lensu, M. (2019). Finding safe and efficient shipping routes in ice-covered waters: A framework and a model. *Cold Regions Science and Technology*(165), 1-14. doi:https://doi.org/10.1016/j.coldregions.2019.102795

Lensu, M., & Goerlandt, F. (2019). Big Maritime Data for the Baltic Sea with a Focus on the Winter navigation System. *Marine Policy*, 53-65.

Li, F., Goerlandt, F., Kujala, P., Lehtiranta, J., & Lensu, M. (2018). Evaluation of selected state-of-the-art methods for ship transit simulation in various ice conditions based on full-scale measurement. *Cold Regions Science and Technology, 151*, 94-108. doi:10.1016/j.coldregions.2018.03.008

Liu, C., Musharraf, M., Li, F., & Kujala, P. (2022). A data mining method for automatic identification and analysis of. *Ocean Engineering*(266).

Liu, C., Musharraf, M., Li, F., & kujala, P. (2022). A data mining method for automatic identification and analysis of icebreaker assistance operation in ice-covered waters. *Ocean Engineering, 266*. doi:https://doi.org/10.1016/j.oceaneng.2022.112914

Lloyds of London. (2014). *Arctic Opening: Opportunity and risk inthe high north.* London.

Loptien, U., & Axell, L. (2014). Ice and AIS: ship speed data and sea ice forecasts in the Baltic Sea. *The Cryosphere*(8), 2409-2418.

Marchenko, N. A., Aandreassen, N., Kuznetsova, S. Y., Ingimundarson, V., & Jakobsen, U. (2018, March). TransNav. *Arctic Shipping and Risks: Emergency Categories and Response Capacities*.

Marchenko, N., Borch, O., Markov, S., & Andreassen, N. (2015). Maritime activity in the high north - The range of unwanted incidents and risk patterns. *International Conference on Port and Ocean Engineering under Arctic Conditions 2015.* POAC. Retrieved from http://hdl.handle.net/11250/2392588

Maritime Safety Committee. (2014a). *POLARIS – proposed system for determining operational limitations in ice.* IACS.

Maritime Safety Committee. (2014b). *Technical background to POLARIS.* IACS.

McCallum, J. (1996). *Safe Speed in Ice - An analysis of transit speed and ice decision numerals.* Ottawa, ON: Transport Canada.

Melia, N., Haines, K., & Hawkins, E. (2015). Improved Arctic sea ice thickness projections using bias-corrected CMIP5 simulations. *The Cryoshpere*, 2237-2251.

Melia, N., Haines, K., & Hawkins, E. (2016). Sea ice decline and 21st century trans-Arctic shipping routes. *Geophyscial Research Letters*(43), 9720-9728.

Monroe, K. R., & Maher, K. H. (1995). Psychology and Rational Actor Theory. *Political Psychology, 16*(1), 1-21. doi:https://doi.org/10.2307/3791447

Montewka, J., Goerlandt, F., Kujala, P., & Lensu, M. (2015). Towards probabilistic models for the prediction of a ship performance in dynamic ice. *Cold Regions Science and Technology*(112), 14-28.

Montewka, J., Goerlandt, F., Kujala, P., & Lensu, M. (2015). Towards Probabilitic Models for the Prediction of a Ship Performance in Dynamic Ice. *Cold Regions Science and Technology*(112), 14-28.

Montewka, J., Goerlandt, F., Lensu, M., & Guinness, R. (2019). Towards a hybrid model of ship performance in ice suitable for route planning purpose. *Proceedings of the Instituation of Mechanical Engineers, Part O: Journal of Risk and Reliability, 233*(1), 18-34. doi:10.1177/1748006X18764511

Mudryk, L. R., Dawson, J., Howell, S. E., Derksen, C., Zagon, T. A., & Brady, M. (2021, August). Impact of 1, 2, and 4 Degrees Celcius of Global Climate Wharing on Ship Navigation in the Canadian Arctic. *Nature Climate Change, 11*, 673 to 679.

Muller, M., Knol-Kauffman, M., Jeuring, J., & Palerme, C. (2023). Arctic shipping trends during hazardous weather and sea-ice conditions and the Polar Code's effectiveness. *npj Ocean Sustainability, 2*(12). doi:https://doi.org/10.1038/s44183-023-00021-x

National Snow and Ice Data Center. (2013, July 13). *Frequently Asked Questions on Arctic Sea Ice*. Retrieved April 19, 2023, from Arctic Sea Ice News and Analysis: https://nsidc.org/arcticseaicenews/faq/#1979average

National Snow and Ice Data Centre. (2015a). *Format for gridded sea ice information (SIGRID).* Boulder, CO: National Snow and Ice Data Centre.

Olsen, R., & Wahl, T. (2000). The Role of Wide Swath SAR in High-Latitude Coastal Management. *John Hopkins APL Technical Digest*, 20(1) 136-140.

Piercey, C., Kennedy, A., & Power, J. (2019). *Methodology for Estimating Exposure Time in Polar Regions.* National Research Council. doi:https://doi.org/10.4224/40002043

QGIS. (2023). *QGIS: A free and open source geographic information system*. Retrieved from https://qgis.org/en/site/

Renn, O., & Sellke, P. (2011). Risk, Society and Policy Making: Risk governance in a complex world. *International Journal of Performability engineering, 7*(4), 349-366.

Renn, O., Jaeger, C. C., Rosa, E. A., & Webler, T. (2000). The Rational Actor Paradigm in Risk Theories: Analysis and Critique. In M. Cohen, *RIsk in the Modern Age.* London: Palgrave Macmillan. doi:https://doi.org/10.1007/978-1-349-62201-6_2

Rhodes, B., Bomberger, N., Seibert, M., & Waxman, A. (2005). Maritime Situation Monitoring and Awareness using Learning Mechanisms. *Proceedings of IEEE Military Communications Conference.*

Roy, J. (2010). Rule-Based Expert Systems for Maritime Anomaly Detection. *SPIE 7666, Sensors and Command, Control, Communications, and Intelligence (C3I) Technologies for Homeland Security and Homeland Defense.*

Runge, H., Breit, H., Eineder, M., Schulz-Stellenfleth, J., Bard, J., & Romeiser, R. (2004). Mapping of Tidal Currents with SAR Along Track Interferometry. *IGARSS '04*.

Schrijver, A. (1998). *Theory of Linear and Interger Programming.* John Wiley $ Sons.

Siljander, M., Venalainen, E., Goerlandt, F., & Pellikka, P. (2015). GIS-based cost distance modelling to support strategic maritime search and rescue planning: A feasibility study. *Applied Geography, 57*, 54-70.

Simila, M., & Lensu, M. (2018). Estimated the Speed of Ice-Going Ships by Integrating SAR Imagery and Ship Data from an Automatic Identification System. *Remote Sensing*(10), 1-23.

Smith, C., & Stephenson, S. (2013). New tans-arctic shipping routes navigable by mid-century. *Proceedings of the National Academy of Sciences of the United States of America (PNAS)*, 110:E1191.

Smith, L., & Stephenson, S. (2013). New Trans-Arctic Shipping Routes Navigable by Midcentury. *Proceedings of the National Academy of Sciences - PNAS*, 1191-1195.

Snider, D. (2012). *Polar Ship Operations - A practical guide.* London: The Nautical Institute.

Somanathan, S., Flynn, P. C., & Szymanski, J. (2006). The Northwest Passage: A Simulation. *Proceedings of the 2006 Winter Simulation Conference*, (p. 7).

Spire Maritime. (2023). *Historical AIS Data*. Retrieved from Spire: https://spire.com/maritime/solutions/historical-ais-data/

Statistics Canada. (2016). *Data Products, 2016 Census*. Retrieved from Statistics Canada Census Program: https://www12.statcan.gc.ca/census-recensement/2016/dp-pd/index-eng.cfm

Stephenson, S. R., Smith, L. C., & Agnew, J. A. (2011). Divergent long-term tranjectories of human access to the Arctic. *Nature Climate Change*, 156-160.

Stoddard, M. A., & Pelot, R. (2020). Historical Maritime Search and Rescue Incident Data Analysis. In *Governance of Arctic Shipping.* Springer Polar Sciences.

Stoddard, M. A., Etienne, L., Pelot, R., Fournier, M., & Beveridge, L. (2018). From Sensing to Sense-making: Assessing and Visualizing Ship Operational Limitations in the Canadian Arctic Using Open-Access Ice Data. In L. P. Hidlebrand, L. W. Brigham, & T. M. Johansson, *Sustainable Shipping in a Changing Arctic* (pp. 99-113). Springer.

Stoddard, M. A., Pelot, R., Etienne, L., & Goerlandt, F. (2023). Determining Ship Speeds in Ice using the Polar Operational Limitation Assessment Risk Indexing System (POLARIS). *TBD*, 1-18.

Stoddard, M. A., Pelot, R., Etienne, L., & Goerlandt, F. (2023). Polar Class Ship Speeds in Ice: Obersvation and Analysis. *TBD*, 1-7.

Stoddard, M., Etienne, L., Fournier, M., Pelot, R., & Beveridge, L. (2016). Making sense of Arctic maritime traffic using the Polar Operational Limits Assessment Risk Indexing System (POLARIS). *Earth and Environmental Science*, 1-8.

Stoddard, M., Pelot, R., Goerlandt, F., & Etienne, L. (2023). Making Sense of Marine-Based Search and Rescue Response Time using Network Analysis. *TBD*, 1-29.

Tan, X., Su, B., Riska, K., & Moan, T. (2013). A six-degree-of-freedom numerical model for level ice-ship interaction. *Cold Regions Science and Technology, 92*, 1-16.

Tran, T., Browne, T., Musharraf, M., & Veitch, B. (2023). Pathfinding and Optimization for Vessels in Ice: a literature review. *Cold Regions Science and Technology*(211), 1-8.

Transport Canada. (1998). *Arctic Ice Regime Shipping System (AIRSS) Standards, TP 12259E.* Ottawa: Government of Canada.

Tremblett, A. J., Garvin, M. J., & Oldford, D. (2021). Preliminary Study on the Applicability of the POLARIS Methodology for Ships Operating in Lake Ice. *Proceedsings of the 26th International Conference on Port and Ocean Engineering under Arctic Conditions*, (p. 12). Moscow.

U.S. National Ice Center. (2022). *U.S. National Ice Center Arctic and Antarctic Sea Ice Charts in SIGRID-3 Format, Version 1.* Boulder, Colorado.

U.S. National Ice Centre. (2023). *Arctic Ice Products*. Retrieved from https://usicecenter.gov/Products/ArcticHome

Vachon, P. (2006). Ship Detection in SAR Imagery. *Proceedings of OceanSAR 2006 - Third Workshop on Coastal and Marine Applications of SAR.* St. John's, NL.

Wang, C., Ding, C., Yang, Y., & Dou, T. (2022). Risk Assessment of Ship Navigation in the Northwest Passage: Historical and Projection. *Sustainability*(14). doi:https://doi.org/10.3390/su14095591

Wang, F., & Xu, Y. (2011). Estimating O–D travel time matrix by Google Maps API: implementation, advantages, and implications. *Annals of GIS, 17*(4), 199-209.

Wang, Y., Zhang, R., & Qian, L. (2018). An Improved A* Algorithm Based on Hesitant Fuzzy Set Theory for Multi-Criteria Arctic Route Planning. *Symmetry*(10), 1-20.

Wei, T., Yan, Q., Qi, W., Ding, M., & Wang, C. (2020). Projections of Arctic sea ice conditions and shipping routes in the twenty-first century using CMIP6 forcing scenarios. *Evironmental Research Letters*(15), 1-10.

Weick, K. E., & Sutcliffe, K. M. (2005). Organizing and the Process of Sensemaking. *Organization Science, 16*(4), 409-421.

Wilbrink, J. G. (2017). *Remoteness as a proxy for social vulnerability in Malawian Traditional Authorities: An open data and open-source approach.* The Hague - Netherlands: Delft University.

Williams, T., Korosov, A., Rampal, P., & Olason, E. (2021). Presentation and Evaluation of the Arctic Sea Ice Forecasting System neXtSIM-F. *The Cryoshpere*(15), 3207-3227.

Wilson, K. (2004). Shipping in the Canadian Arctic: Other possible climate change scenarios. *Proceedings of IGARSS'04: Geoscience and Remote Sensing*, 3: 1853.

Wilson, K., Falkingham, H., Melling, H., & De Abreu, R. (2004). Shipping in the Canadian Arctic: Other possible climate change scenarios. *Proceedings of IEEE International Symposium on Geoscience and Remote Sensing*, 3: 1853-1856.

World Maritime Organization. (2016). *International Code for Ships Operating in Polar Waters (POLAR CODE).* World Maritime Oganization.

Wright, C. (2016). *Arctic Cargo: A history of marine transportation in Canada's North.* Marquis Book Printing.

Xi, Y., Miller, E. J., & Saxe, S. (2018). Exploring the Impact of Different Cut-Off Times on Isochrone Measurements of Accessibility. *Transportation Research Record, 2672*(49), 113-124.

Appendix 1: From Sensing to Sense-Making: Assessing and Visualizing Ship Operational Limitations in the Canadian Arctic Using Open-Access Ice Data

Stoddard, M.A., Etienne, L., Pelot, R., Fournier, M., Beveridge, L. (2018). From Sensing to Sense-Making: Assessing and Visualizing Ship Operational Limitations in the Canadian Arctic Using Open-Access Ice Data. In: Hildebrand, L., Brigham, L., Johansson, T. (eds) Sustainable Shipping in a Changing Arctic. WMU Studies in Maritime Affairs, vol 7. Springer, Cham. https://doi.org/10.1007/978-3-319-78425-0_6

From sensing to sense-making: assessing and visualizing ship operational limitations in the Canadian arctic using open-access ice data

Mark A. Stoddard[2], Laurent Etienne, Ronald Pelot, Melanie Fournier and Leah Beveridge

Abstract

Vessels planning a passage in the Canadian Arctic face many risks, most notably from ice, extreme weather, remoteness, and uncharted or poorly charted bathymetry. For ship operators who view the Arctic as a relatively untouched area of opportunity, the desire to operate vessels in the Arctic brings new challenges and risks. This study introduces the Polar Operational Limitations Assessment Risk Indexing System (POLARIS) and demonstrates its use for assessing ship operational limitations using open-access historical ice information. The analysis of ship operational limitations in ice was aided by the construction of POLARIS scenario risk maps which were clearly demonstrated as a useful tool to support the strategic appraisal of ice conditions. Lastly, several use cases are provided to demonstrate how POLARIS and historical ice information can be used to support the strategic appraisal of ship operational limitations in ice.

[1]M.A. Stoddard
Department of Industrial Engineering, Dalhousie University, Halifax, NS, Canada
e-mail: mark.stoddard@dal.ca

Introduction

Maritime traffic in the Canadian Arctic is expected to increase in coming years as northern communities grow, tourism increases, and large resource development projects enter into operation (Higginbotham et al 2012). Potentially accelerating this growth is evidence of a decline in ice coverage in the Canadian Arctic (Vihma 2014). As activity increases, the number of vessels exposed to the navigational risks in Canada's Arctic will rise. Additionally, it is a rather self-explanatory fact that the vulnerability of a vessel to these risks depends heavily on the type and class of the ship, the training and experience of the crew, and access to high quality information to support decision making, both during the planning and execution phase of an operation.

Passage planning for Polar Regions involves navigational practices typically accepted as standard, with additional considerations based on the expectation of the presence of ice (Snider 2012). The Canadian Ice Service (CIS), a division of the Meteorological Service of Canada, is the leading authority for information about ice in Canada's navigable waters. Currently, the CIS provides open-access to digital Arctic regional sea ice charts for marine navigation, climate research, and input to the Global Digital Sea Ice Data Bank (GDSIDB) (Canadian Ice Service 2009). CIS sea-ice charts provide information on the ice concentration, stage of development, and form of ice within the Canadian Arctic. Open-access weekly sea-ice charts covering the Canadian Arctic are available from the National Snow and Ice Data Centre (NSDIC). Weekly sea-ice charts are stored in the standard World Maritime Organization (WMO) ice chart archive vector format, Sea Ice Grid (SIGRID-3). Originally proposed in 1981 and adopted by the WMO, the SIGRID format was designed to meet larger scale climate requirements, providing a computer-compatible sea-ice data bank (National Snow and Ice Data Centre 2015a). The CIS SIGRID-3 vector format provides information about ice conditions in a specific geographic area. It can handle three different forms of ice (Fa, Fb, Fc), the stage of development (Sa, Sb, Sc), and the concentration (Ca, Cb, Cc) for each location (World Meteorological Organization 2004; Etienne and Pelot 2013).

This chapter will show how archived SIGRID-3 ice data can be used to evaluate ship operational limits in ice. Operational limitations were assessed using the Polar Operational

Limitations Assessment Risk Indexing System (POLARIS), which is currently being considered for inclusion in the new International Code for Ships Operating in Polar Water (Polar Code) for use in both the Arctic and the Antarctic (Maritime Safety Committee 2014a, 2014b). The study period covers Canadian Arctic ice conditions observed from 2007 to 2014. The Area of Interest (AOI) is largely driven by the Canadian Shipping Safety Control Zones delineated by the Shipping Safety Control Zones Order of the Arctic Waters Pollution Prevention Act, with the addition of a new Zone 0 to include the southernmost extent of Hudson Bay (Transport Canada 1998, 2003). Figure 1 provides a geographical outline of the study AOI.

A total of 3,744 POLARIS scenario risk maps were generated for the study AOI: for each of 12 ship types (PC1-7, IA, IA Super, IB, IC, no ice strengthening (NOT IS)), using 6 statistical aggregations (minimum, 1st quartile, median, average, 3rd quartile, maximum) of POLARIS results over our study period (2007-2014), and calculated for each of the 52 weeks of the year. Discussion of the results is aided by an example use case that clearly demonstrates how POLARIS scenario risk maps can be used to support the strategic appraisal of ice conditions and ice risk across a large AOI.

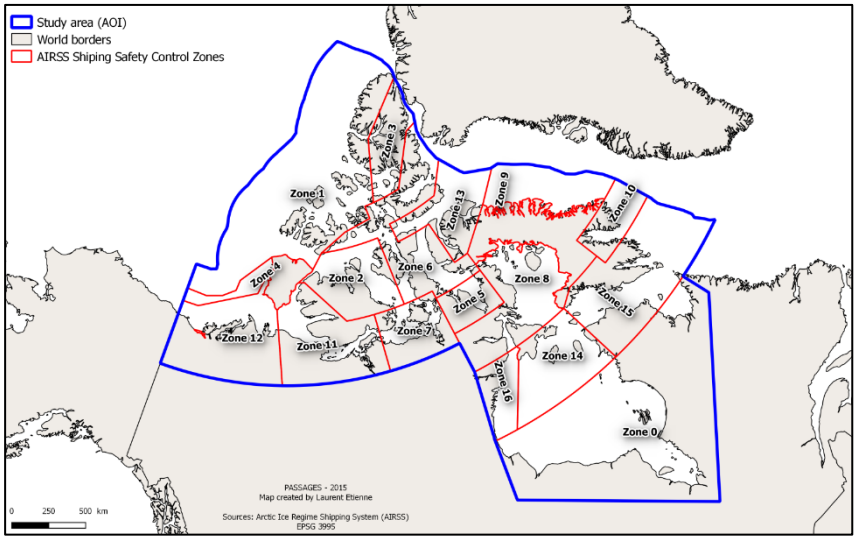

Fig. 1 Study AOI based on the Transport Canada Shipping Safety Control Zones with the addition of a Zone 0 to include Hudson Bay

Assessing Ship Operational Limits in Ice

Transport Canada has provided mariners with a quantitative method to characterize the relative risk which various ice conditions pose to the structure of different ships, referred to as the Arctic Ice Regime Shipping System (AIRSS) (Transport Canada 1998). AIRSS is a widely used maritime framework to assess navigation safety in a given ice regime as a function of ice conditions (see Section 2.1) and the structural and engineering capabilities of a particular vessel class (Smith and Stephenson 2013). The system uses a basic algorithm to determine a result called the Ice Numeral (IN). A positive IN indicates that a vessel can proceed under the given operational conditions; a negative number indicates that a vessel cannot proceed under the given operational conditions (Snider 2012). Transport Canada (1998) provides a complete description of AIRSS and its use to assess ship operational limitations.

Many researchers have incorporated AIRSS into modeling and simulation studies to examine shipping in the Canadian Arctic. The efforts of Howell and Yackel (2004) demonstrated how the use of AIRSS and historical CIS digital ice charts could be used to assess navigational variability over three defined Western Arctic transit routes from 1969 to 2002. Transit routes were sampled at 5km spacing and assigned an IN from a pre-computed IN raster grid. The results were used to visualize the spatial variability of the IN for a Canadian Arctic Class 3 (CAC3) ship throughout their study AOI and along each Western Arctic transit route. Each route was also examined based on the INs encountered during transit. A route containing a negative IN indicated that a section of the route was not suitable for operations. In Wilson et al. (2004), the authors further examined the AOI presented in Howell and Yackel (2004) using several Global Climate Models (GCMs) to predict future ice conditions. Their conclusion was that the future sea-ice conditions in the Canadian Arctic remain highly variable and there could still be seasons of occasional heavy ice conditions that will present a significant navigational challenge to ships.

The work of Somanathan, Flynn and Szymanski (2007) incorporated AIRSS into a simulation to compare the relative economics of shipping through the Northwest Passage and shipping through the Panama Canal. Using historical ice regime data for the Canadian Arctic they prepared probabilistic ice regimes that could be used in AIRSS. IN and ship

type where then used to calculate transit speeds through the Northwest Passage in their simulation. The major conclusion of their study was that for the ice conditions in the Canadian Arctic for the period of 1999 through 2003 the use of the Northwest Passage is economically favored over the traditional route through the Panama Canal. The results were for a CAC3 ship where transit time was the main economic consideration. They qualify this result by saying that the difference is not very compelling, especially given the uncertainty and risk associated with transiting the Northwest Passage.

More recently, Etienne and Pelot (2013) presented a simulation tool that can be used to determine feasible paths throughout the Canadian Arctic based on historical sea ice conditions. The feasibility of a shipping path was determined using AIRSS, where historical ice data and ship classification are used to calculate the IN and resulting "Go" or "No Go" ship limit along a given route. In Smith and Stephenson (2013), the authors provide a similar analysis of shipping route feasibility using AIRSS. Instead of focusing on the use of historical sea ice data, the authors considered several leading Global Climate Models (GCMs) to construct future ice regimes for use in AIRSS. AIRSS was then used to determine the feasibility of trans-Arctic routes for Polar Class (PC) 6 and open-water (OW) vessels. A feasible navigational route consisted of a least-cost path (minimum total voyage time) from a start point to an end point, avoiding areas where the IN would obstruct a particular vessel class (IN < 0). A major conclusion of their paper was that by mid-century, September sea-ice conditions will have changed sufficiently in the Northwest Passage (NWP) such that trans-Arctic shipping to/from North America could commonly capitalize on the approximately 30% geographic distance savings that this route offers over the Northern Sea Route (NSR) which follows the Russian coastline.

Polar Operational Limitations Assessment Risk Indexing System (POLARIS)

POLARIS, a proposed risk assessment framework for determining ship operational limits in ice, was produced by the International Association of Classification Societies (IACS). Similar to the Transport Canada AIRSS system, POLARIS provides a risk assessment

framework to assess navigation safety in a given ice regime, using observed or historical ice conditions and concentration and the vessel classification (Maritime Safety Committee 2014b). An ice regime is used to describe an area with a relatively consistent distribution of a number of ice types, including open water. The concentration of each ice type within an ice regime is reported in tenths. Also, for each ice type there is an associated ice type score defined for each ship ice classification.

In POLARIS, the ice type score is referred to as a Risk Value (RV), and a collection of RVs that correspond to a particular ice regime is referred to as a Risk Index Outcome (RIO). Using POLARIS, RIO is determined by summing the RVs for each ice type present in the ice regime encountered, multiplied by its respective concentration:

$$RIO = C_1RV_1 + C_2RV_2 + \cdots + C_nRV_n$$

where $C_1, C_2, \ldots, C_n$ are the concentrations (in tenths) of ice types within the ice regime and $RV_1, RV_2, \ldots, RV_n$ are the risk values corresponding to each ice type and for a given ship ice class classification. The resulting RIO value is then evaluated for either independent operations or icebreaker escorted operations to determine the appropriate operational limitation (see Table 1).

Table 1 POLARIS evaluation criteria and associated Risk index Outcome (RIO) condition, as defined in Tables 1.1 and 1.2 from the Maritime Safety Committee (2014b)

Evaluation Criteria	**Group A (PC1 – PC5)**	**Group B (PC6 – PC7)**	**Group C (IA Super - IA)**	**Group C (Below IA)**
Operations Not Permitted	$RIO_{ship} < -10$ or $RIO_{escorted} + 10 < -10$	$RIO_{ship} < -10$ or $RIO_{escorted} + 10 < -10$	$RIO_{ship} < -10$ or $RIO_{escorted} + 10 < -10$	$RIO_{ship} < 0$ or $RIO_{escorted} + 10 < -10$
Escorted Operations	$-10 \leq RIO_{escorted} + 10 < 0$	$-10 \leq RIO_{escorted} + 10 < 0$	$-10 \leq RIO_{escorted} + 10 < 0$	Not Permitted

Permitted - Limited Speed				
Escorted Operations Permitted	$RIO_{escorted} + 10 \geq 0$	$RIO_{escorted} + 10 \geq 0$	$RIO_{escorted} + 10 >= 0$	$RIO_{escorted} + 10 \geq 0$
Limited Speed Operation Permitted	$-10 \leq RIO_{ship} < 0$	$-10 \leq RIO_{ship} < 0$	Not Permitted	Not Permitted
Operations Permitted	$RIO_{ship} > 0$	$RIO_{ship} > 0$	$RIO_{ship} > 0$	$RIO_{ship} > 0$

Ice Risk Visualization using POLARIS Scenario Risk Maps

To facilitate the calculation and visualization of risk within the study AOI an Archimedean (uniform) tessellation was used to produce a rectangular mesh grid of the study AOI (Okabe et al. 1992). This tessellation was chosen for its ease of calculation and simplicity of the resulting data structure. The resulting quantized AOI contains approximately 16 million grid cells at a 1 km^2 resolution. The quantized AOI was further processed using a vector layer of the Canadian shoreline to delete grid cells that are outside of the AOI or inland. These spatial processing steps yielded an AOI containing 4 million grid cells. Next, CIS SIGRID-3 sea ice information was filtered to only include ice polygons within the study AOI and the resulting sea ice information was associated with the 1km x 1km grid cells of our quantized AOI. For illustration purposes, Figure 2 contains the Bellot Strait area of the study AOI with the associated gridded overlay at a 1 km^2 resolution.

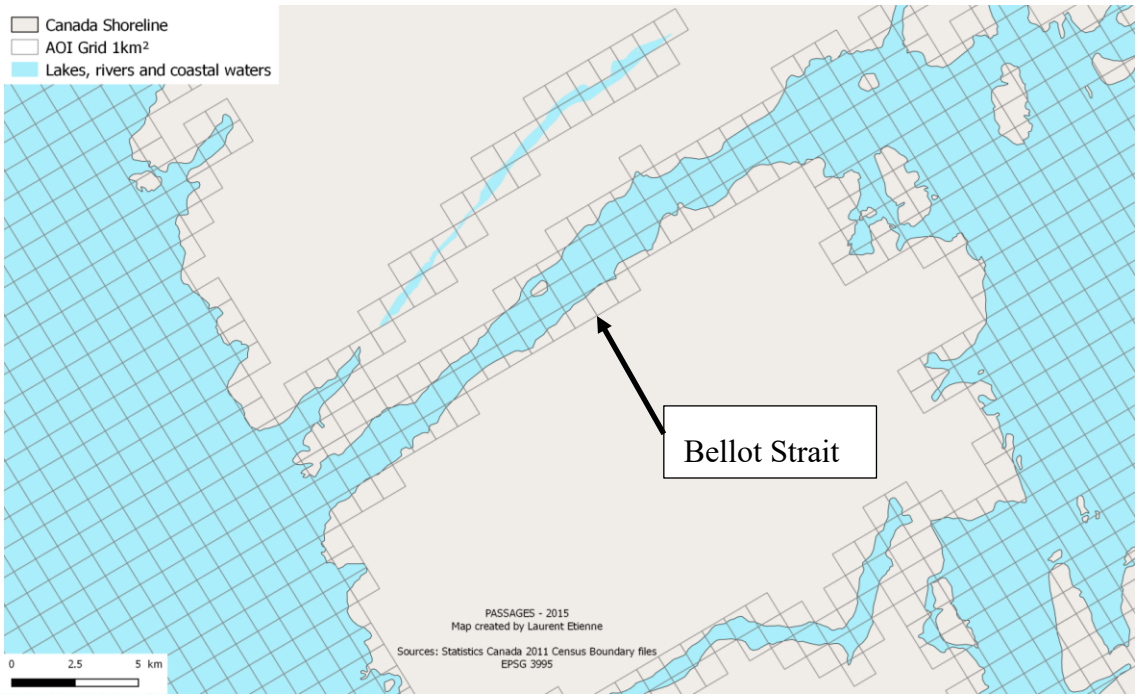

Figure 2 Example of the gridded (tessellated) overlay produced for the study AOI. The area shown contains the Bellot Strait area with a rectangular grid resolution of 1 km^2

In order to use CIS SIGRID-3 ice regime information within POLARIS, a processing step was required to convert SIGRID-3 ice stage into POLARIS ice type. The Maritime Safety Committee (2014) defines 12 ice types that are used by POLARIS. Table 2 provides the mapping of POLARIS ice type to the CIS SIGRID-3 ice types used in this study. *The mapping of POLARIS and CIS SIGRID-3 ice types provided in Table 2 is intended for academic purposes only and is to be considered UNOFFICIAL.*

Table 2 POLARIS / SIGRID-3 ice type conversion table

Polaris Ice Type	SIGRID-3 codes	SIGRID-3 stage of development
Ice Free	00, 80	Ice Free
New Ice	81, 82	New Ice < 10cm
Grey Ice	84	Grey Ice (10 to 15 cm)
Grey White Ice	83, 85	Young Ice (10 to 30 cm)
Thin First Year Ice, 1st stage	88	Thin First Year Ice (stage 1)
Thin First Year Ice, 2nd stage	86, 87, 89	Thin First Year Ice (>30cm) or Brash Ice
Medium First Year Ice 2nd stage	91	Medium First Year Ice (70 to 120cm)
Thick First Year Ice	93	Thick First Year Ice (>120cm)
Second Year Ice	96	Second Year Ice
Light Multi Year Ice	95	Old Ice
Heavy Multi Year Ice	97, 98	Multi Year Ice

Using the POLARIS ice type and ship class information, a RIO for each grid cell in the study AOI can be calculated. The last step is to use the evaluation criteria for operational limitations (see Table 1) and apply an ordinal color scheme to convey the following evaluation results: (1) Operation Permitted (GREEN), (2) Limited Speed Operations Permitted (YELLOW), (3) Escorted Operations Permitted (ORANGE), (4) Escorted Operations Permitted - Low Speed (DARK ORANGE), and (5) Operations Not Permitted (RED).

Figure 3a summarizes the results of the POLARIS risk assessment for a IA class vessel as a thematic map, hereafter referred to as a POLARIS scenario risk map. For comparison, Figure 3b provides an AIRSS scenario risk map for a Type B vessel to highlight the differences between POLARIS and AIRSS evaluations. Table 3 provides the vessel classification mapping that was used in this study to compare the results from AIRSS and POLARIS for Category C ships (below PC7). The Maritime Safety Committee (2014b) discusses modifications that could offer better alignment of the AIRSS system with the Polar Code and Polar Classes. These discussions, and potential impact on the mapping provided in Table 3, are outside of the scope of this study. *The vessel classification mapping provided in Table 3 is intended for academic purposes only and is to be considered UNOFFICIAL.*

Table 3 Vessel classification mapping for Polar Code Category C (below PC7) classed vessels

Type of Ship (Canada)	**Lloyd's Register of Shipping**	**Finnish-Swedish Ice Class Rules**
Type A	100 A1 Ice Class 1 LMC or 100A1 Ice Class 1A Super LMC	IA Super
Type B	100 A1 Ice Class 1 LMC or 100A1 Ice Class 1A LMC	IA
Type C	100 A1 Ice Class 2 LMC or 100A1 Ice Class 1B LMC	IB
Type D	100 A1 Ice Class 3 LMC or 100A1 Ice Class 1D LMC	IC/II
Type E	100 A1 LMC	II

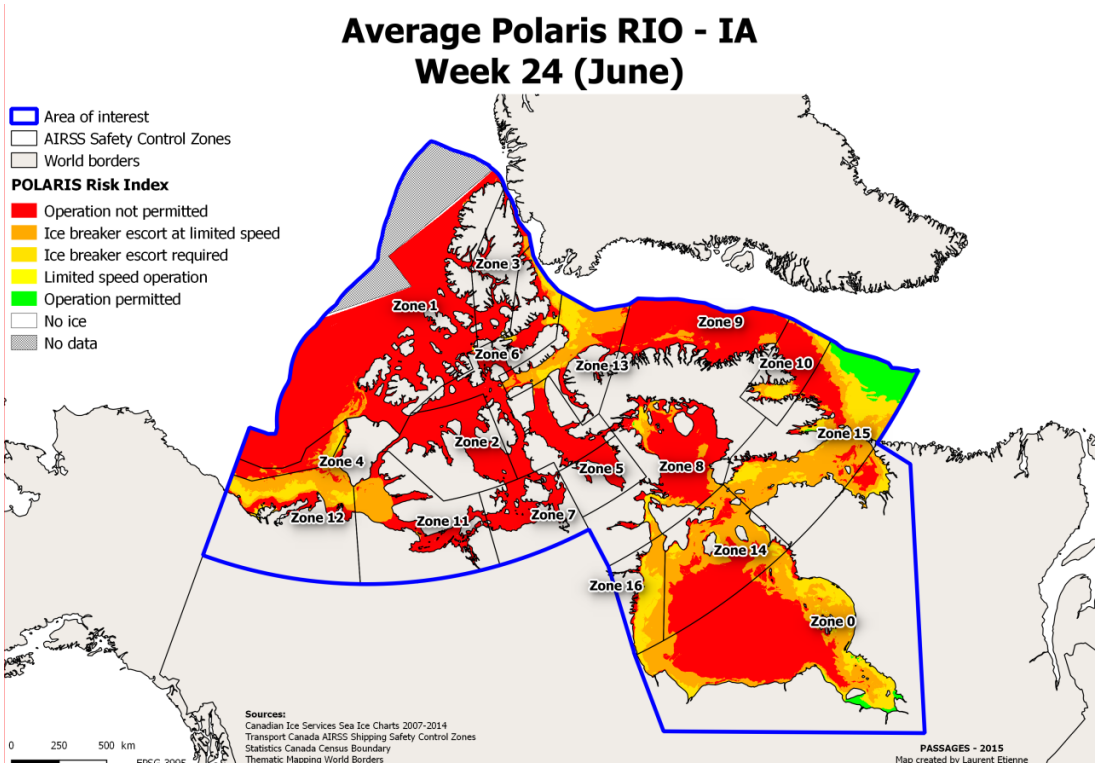

(a) POLARIS ship limitations for a IA classed vessel operating in the AOI during week

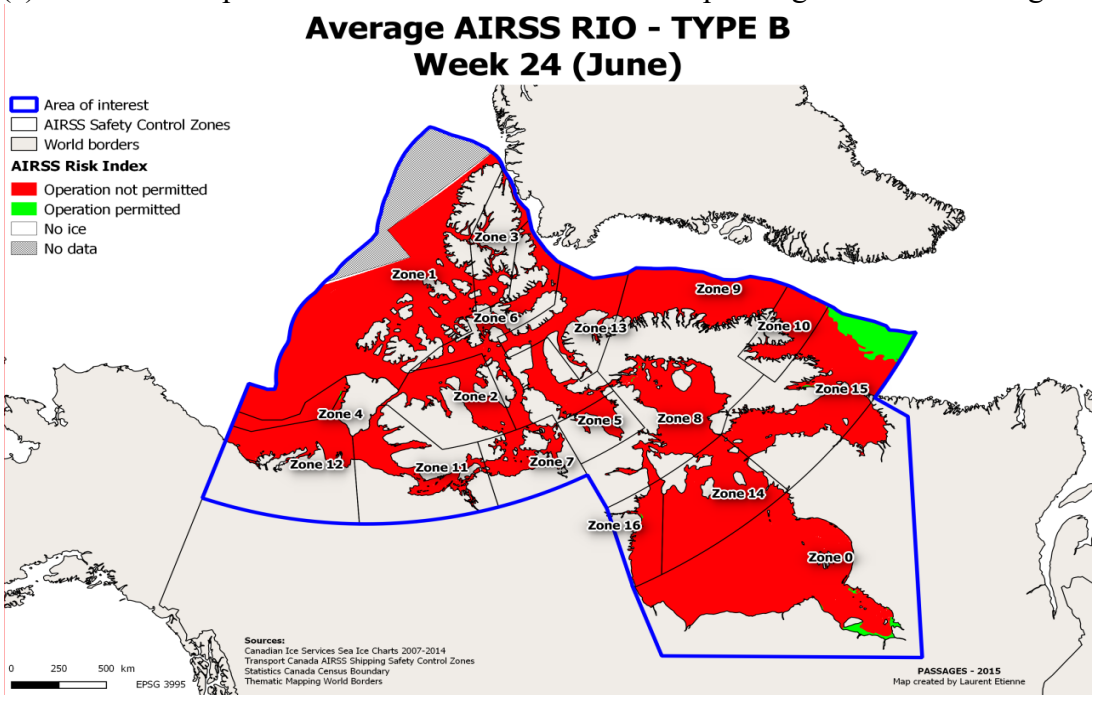

(b) AIRSS Ship limitations for a IA classed vessel operating in the AOI during week 24

Figure 34 (***a***) Summary plot of the POLARIS ship limitations for a IA vessel operating in the study AOI during week 24 using the 2007-2014 average Risk Index Outcome (RIO). For comparison, (***b)*** shows the AIRSS ship limitations for an equivalent classed vessel (Type B) during week 24 using the 2007 – 2014 average Ice Numeral (IN).

Example Use Case – Strategic Appraisal of Ice Conditions

The strategic appraisal of ice conditions involves the use of all information sources to give the most complete picture of the ice conditions possible (Canadian Coast Guard 2012). CIS SIGRID-3 ice data was discussed in Section 1 as a high-quality source of historical ice conditions suitable for strategic appraisal of ice conditions and that can be easily accessed. While historical ice charts and knowledge of historical ice conditions can be combined towards the creation of a picture of the sea ice conditions possible in an area, the use of POLARIS improves sense-making for ship operators by visualizing the expected impact of ice on ship operations. In order to illustrate the use of the POLARIS scenario risk maps three potential uses for strategic appraisal are discussed, including the effect of: (1) varying polar ship classification when ice regime remains constant; (2) varying the transit/study period when polar ship classification and statistical aggregation of the RIO remains constant; and (3) varying the statistical aggregation of the RIO when ship classification and transit/study period remains constant.

Use 1: Varying Ship Classification

POLARIS scenario risk maps can be used to visualize the effect of varying polar ship classification in the AOI. The obvious result is that the more ice capable a ship is, the greater the freedom to maneuver it will have within the AOI. What remains of interest is the comparison of multiple ship classifications over the entire AOI. POLARIS RIO provides a consistent method to compare the capabilities of ships of varying polar ice classification within an AOI. The POLARIS scenario risk maps provide a visually

appealing method to examine spatio-temporal phenomena within the AOI that vary in response to changing ship class. Figure 4 provides some insight to how the POLARIS risk index changes when the Polar Ship classification is varied within the study AOI.

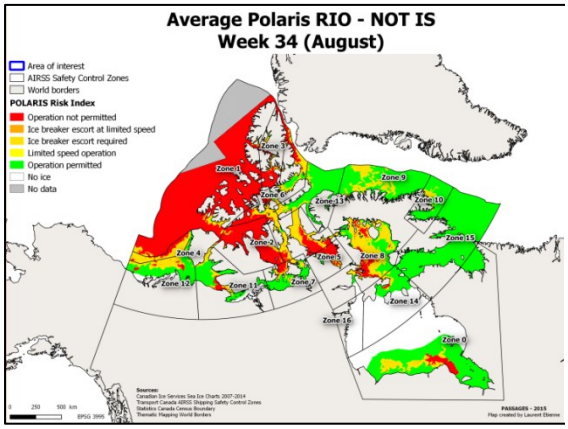

(**a**) Average RIO for Not Ice Strengthened

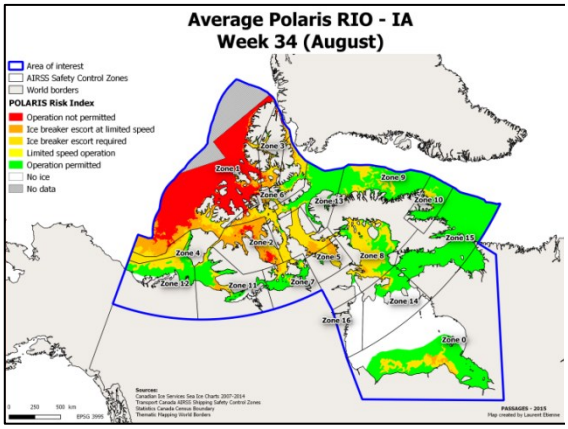

(**b**) Average RIO for IA vessel

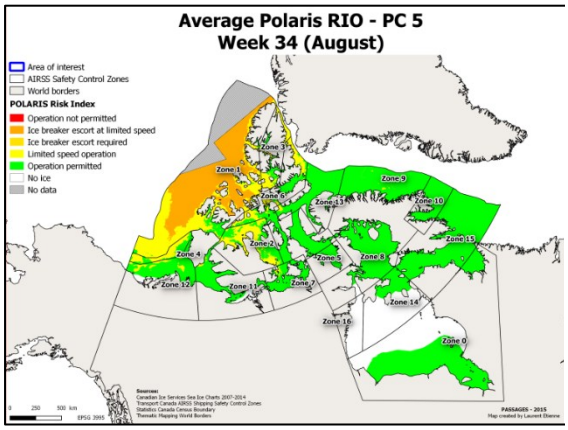

(**c**) Average RIO for PC5 vessel

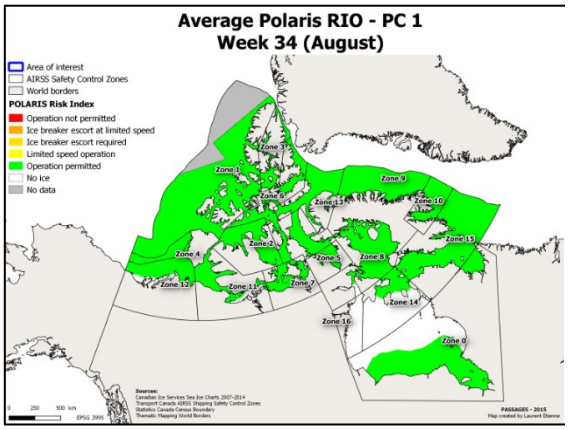

(**d**) Average RIO for PC1 vessel

Figure 4 Average POLARIS RIO results for four ship classifications operating in the study AOI during week 34, using the average RIO result from 2007 to 2014

Use 2: Temporal variation of RIO

The second use examines the temporal variation in RIO for a given ship class and ice regime over a four-week period in the AOI. Ice loss typically quickens in June with the largest loss rate occurring in July, the warmest month of the year (National Snow and Ice Data Center 2015b]. The computational results shown in Figure 5 illustrate the temporal variation in average RIO results during the July time frame (week 27 to week 30). By isolating Transport Canada Shipping Safety Control Zone 13, temporal variation in ship limitations, based on the percentage (%) of the Zone's total surface area corresponding to a particular ship type's operational limitation, can be examined. With the help of Figure 6, it is evident that there is a steady increase in the extent of operations permitted starting around week 29 and gradually declining towards week 44 for an IA class vessel.

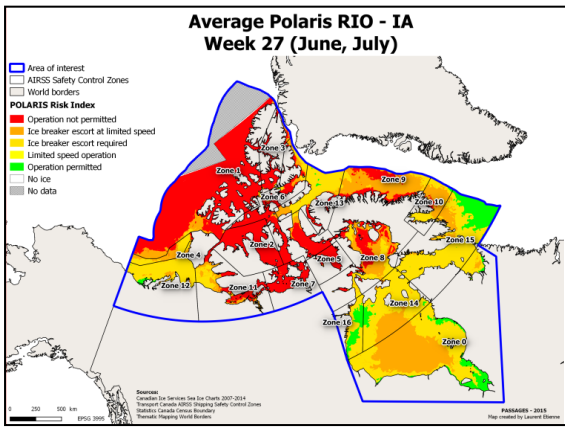

(**a**) Average RIO for an IA vessel in week

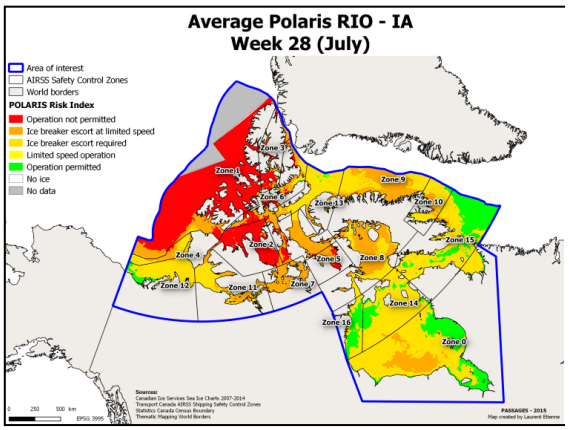

(**b**) Average RIO for an IA vessel in week

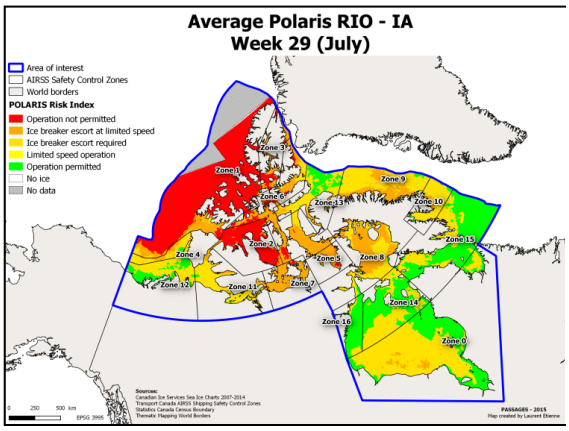

(**c**) Average RIO for an IA vessel in week

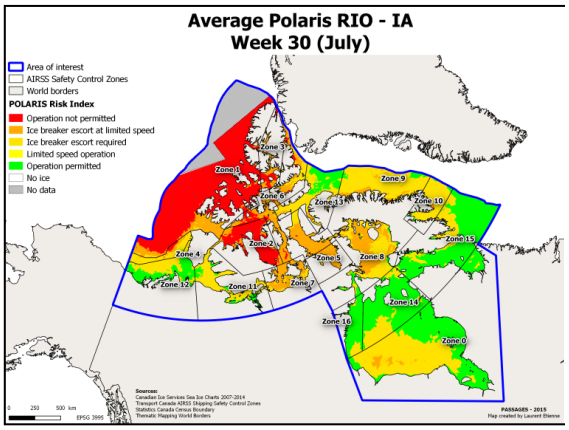

(**d**) Average RIO for an IA vessel in week

Figure 5 Polaris Risk Index Outcome (RIO) for an IA class vessel operating in the defined Area of Interest (AOI) for week 27 to week 30 (month = June/July) using the 2007-2014 average RIO result

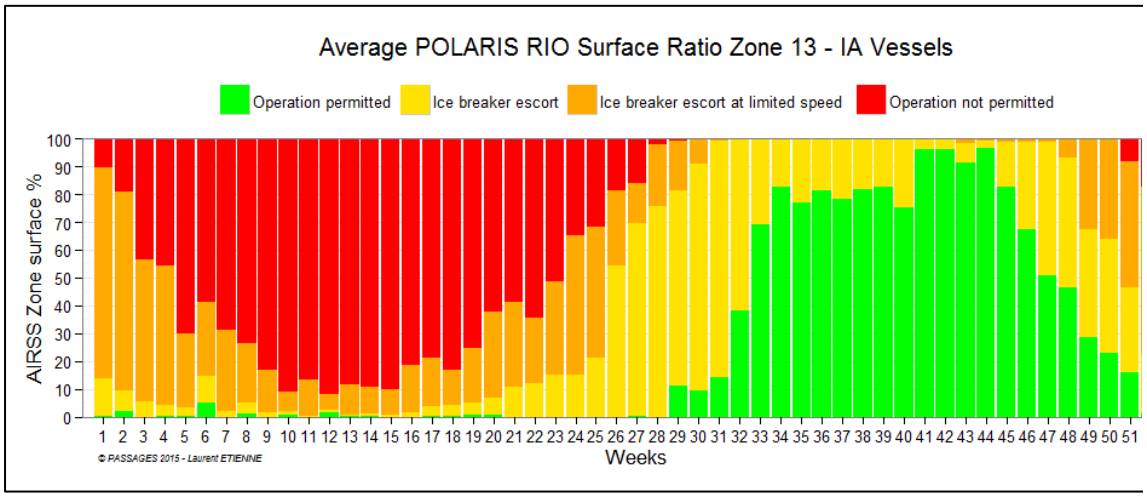

(**a**) POLARIS operational limitations for Transport Canada Shipping Safety Control

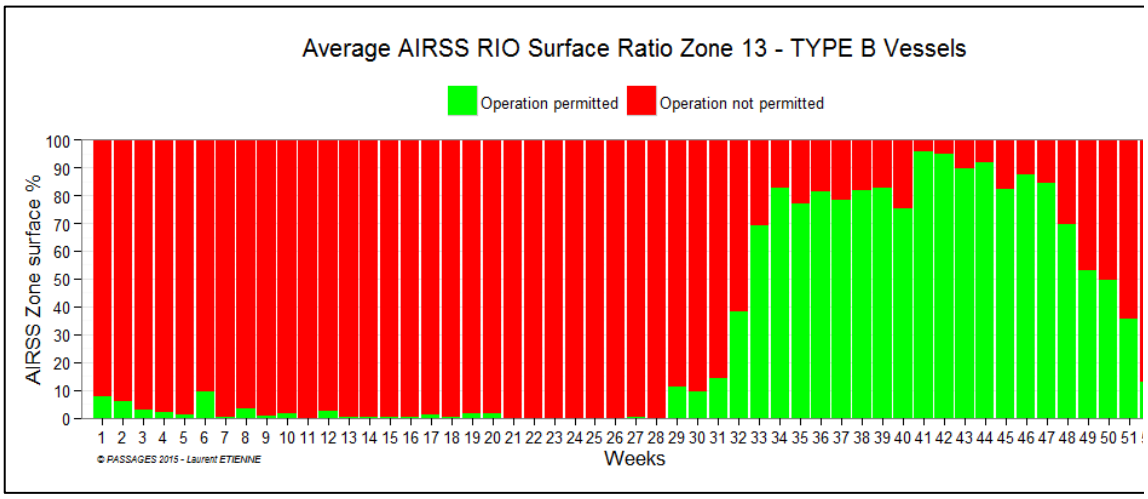

(**b**) AIRSS operational limitations for Transport Canada Shipping Safety Control Zone

Figure 6 (***a***) shows the temporal variation in ship operational limitations given by POLARIS for a IA vessel operating in Zone 13. Operational limitations are given as a percentage of the Zone 13 total surface area. (***b)*** shows the temporal variation in ship operational limitations given by AIRSS for an IA equivalent Type B vessel (see Table 3) operating in zone 13.

Use 3: Impact of statistical aggregation on RIO

The last use examines the impact of six different statistical aggregations of the RIO results from 2007 to 2014. Six different statistical aggregations are considered: (1) maximum RIO, (2) 1st quartile RIO, (3) average RIO, (4) median RIO, (5) 3rd quartile RIO, and (6) minimum RIO. The selection of the best aggregation is a question that cannot be easily answered; minimum and maximum statistical aggregations indicate the worst case and best case RIO results, while the average and percentiles are useful to understand the distribution of RIO scores over the study period (2007-2014). Further research and validation with expert Ice Navigators could shed light on the best statistical aggregation for route planning and evaluation.

The POLARIS scenario risk maps that correspond to each of the six chosen statistical aggregation methods are shown in Figure 7. The maximum RIO score corresponds to the

least severe ice conditions, while the minimum RIO score corresponds to the most severe ice conditions. The area of the study AOI most affected by the selection of statistical aggregation method is the Western entrance to the Northwest Passage. In the Maximum RIO score scenario, the entrance is open and operations are permitted. For the Minimum RIO score scenario (Figure 7.f.), the entrance is closed and operations are not permitted.

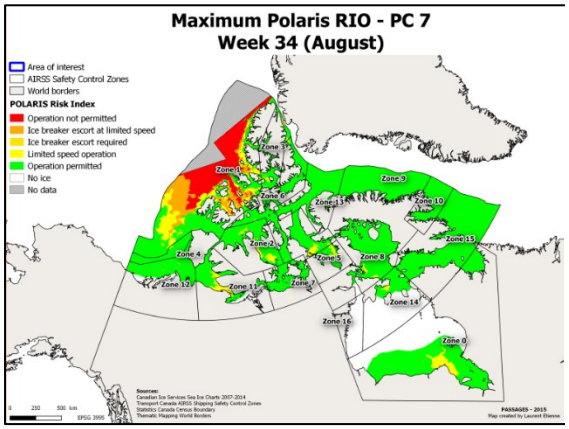

(**a**) Maximum RIO statistical aggregation

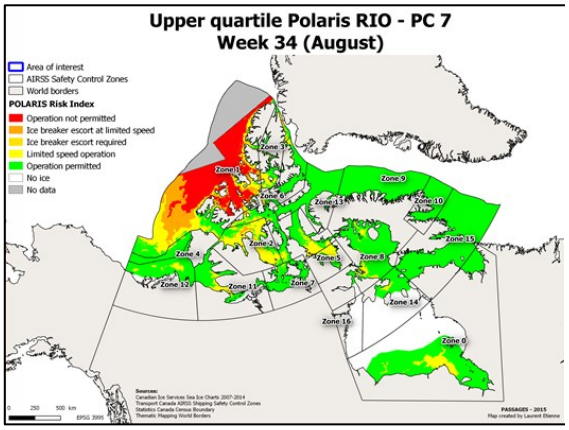

(**b**) 75th percentile RIO statistical

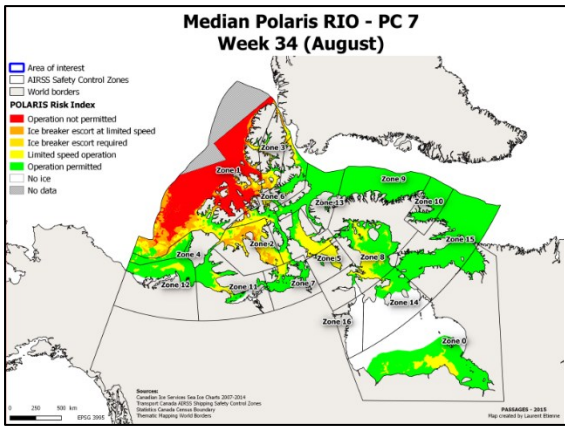

(**c**) 50th percentile RIO statistical

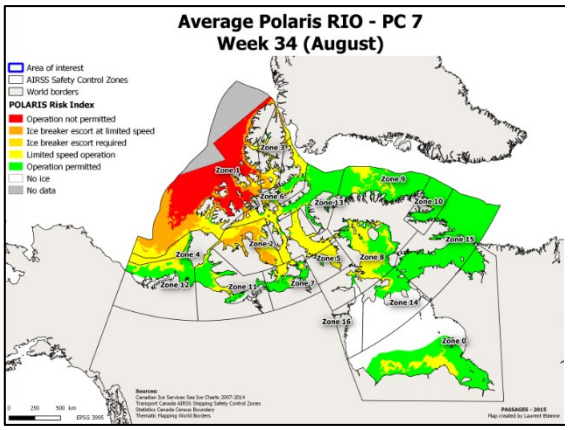

(**d**) Average RIO statistical aggregation

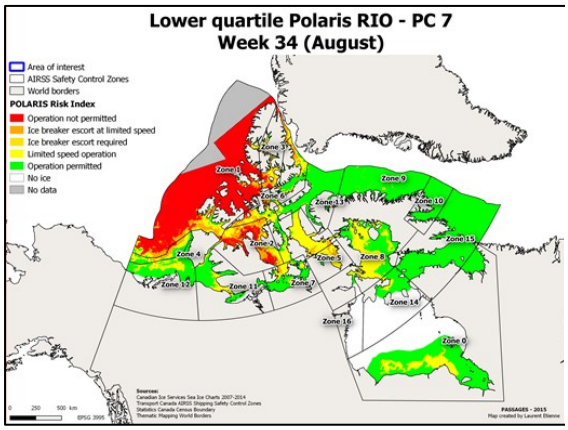

(**e**) 25th percential RIO statistical

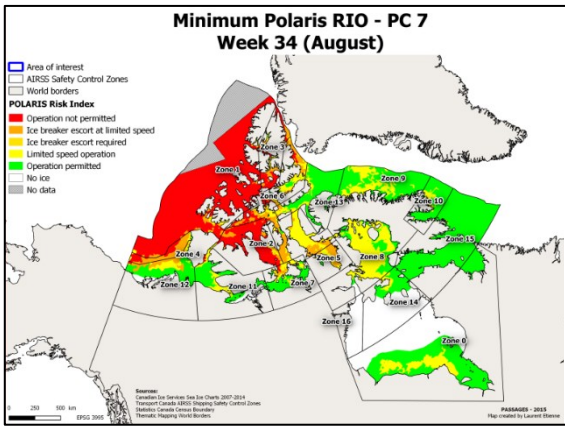

(**f**) Minimum RIO statistical aggregation

Figure 7 RIO results for a PC7 vessel operating in the AOI during week 34 using six different statistical aggregation methods, including (***a***) Maximum RIO, (***b***) 75th Percentile RIO, (***c***) 50th Percentile / Median RIO, (***d***) Average RIO, (***e***) 25th Percentile RIO, and (***f***) Minimum RIO

Discussion

The preceding section illustrated how POLARIS and CIS SIGRID-3 ice information can be used to support the strategic appraisal of ship operational limitations over a large AOI. Polar ship classification was identified as a variable that significantly influences ship operational limitations throughout the AOI, as expected. These results could be used by decision makers to examine the selection of a particular polar classification for a planned route, or the feasibility of operations in a particular region of the Canadian Arctic during a specific time of the year. Varying the transit period/study week also significantly impacts ship operational limitations. Figure 5 was used to visualize a four-week period within our study AOI for a PC7 vessel. Figure 6 extended this analysis and examined ship operational limitations over a 52-week period for a particular Transport Canada Shipping Safety Control Zone of interest (Zone 13), using both POLARIS and AIRSS. An example of this use is demonstrated in Stoddard et al (2016), comparing an actual vessel trip route with the

POLARIS rating along the route, and noting the implications of altering the trip timing to avoid anticipated navigation problems. Lastly, six different statistical aggregation methods of RIO results for the study AOI were compared. Figure 7 provided a visualization for each of the statistical aggregation methods. Based on a visual analysis of Figure 7, the operational limitations in Zone 1 (Western Arctic) appear to be most influenced by the chosen statistical aggregation method. More detailed analysis would be required to substantiate this statement and could be considered in future studies.

The POLARIS scenario risk maps developed as part of this study served as a useful tool to support the strategic appraisal of ice conditions; however, the use of historical ice data inherently limits their tactical use. POLARIS and the Transport Canada AIRSS system both rely on an accurate assessment of ice conditions [Transport Canada, 2003]. Predicting navigational feasibility based on the historical ice regime information remains difficult due to the vast array of other explanatory atmospheric and oceanic factors (Howell and Yackel 2004). Some other major factors that influence passage planning in the Canadian Arctic include operating area remoteness, locations of nearby support, extreme weather, daylight, presence of multi-year and glacial ice, and location of historical incidents (Snider 2012). With respect to sea ice, the conditions in the Canadian Arctic are characterized by substantial inter-annual variability (Lasserre 2011). The resulting unpredictability of ice conditions is often cited as a major hindrance for shipping in the Arctic (O'Rourke 2010). For this reason, both systems require that the ice regime be assessed in-situ by a qualified ice navigator to ensure that ship operational limitations are accurately determined during execution.

Conclusions

The computational results and analysis at hand clearly demonstrate how open-access SIGRID-3 ice data can be used to support the strategic assessment of ship operational limits in ice. Where appropriate, ship operational limits using POLARIS were compared to the operational limits determined by using the Transport Canada AIRSS assessment. Several thematic risk maps were produced to visualize operational limitations in the study AOI. A use case was constructed to facilitate the discussion on the use of Polaris Scenario Risk

Maps to support the strategic appraisal of ice conditions and associated ship operational limitations. POLARIS has been clearly demonstrated as an excellent risk assessment framework to assess and visualize ship operational limits over large geographic areas. In addition to assessing ship operational limits, the POLARIS scenario risk maps and underlying data presented in this chapter could be used by decision makers to examine fleet mix, ship allocation, or ship scheduling and routing within a large AOI.

Acknowledgments

Funding for this research was provided by the Natural Sciences and Engineering Research Council of Canada, exactEarth Ltd., the German Ministry of Economy and Technology, and Airbus Defence & Space.

References

Canadian Coast Guard (2012) Ice navigation in Canadian waters: navigation in ice covered waters. Government of Canada, Ottawa

Canadian Ice Service (2009) Canadian Ice Service Arctic regional sea ice charts in SIGRID-3 Format, (2007-2014). National Snow and Ice Data Center, Boulder, Colorado

Etienne L, Pelot R (2013) Simulation of maritime paths taking into account ice conditions in the Arctic. In: Devillers R, Lee C, Canessa R, Sherin A (eds) CoastGIS conference 2013: monitoring and adapting to change on the coast. 11th international symposium for GIS and computer cartography for coastal zone management, Victoria BC, June 2013. University of Victoria, Victoria, British Columbia, p 116

Higginbotham J, Charron A, Manicom J (2012) Canada – US Arctic Marine Corridors and Resource Development. The Centre for International Governance Innovation, Policy Brief No 24, November 2012. Available from www.cigionline.org/publications

Howell SEL, Yackel JJ (2004) A vessel transit assessment of sea ice variability in the western Arctic, 1969-2002: implications for ship navigation. Can J Remote Sens 30:205-215

Lasserre F (2011) Arctic shipping routes: from the Panama myth to reality. Int J, 66 (4): 793-808

Maritime Safety Committee (2014a) POLARIS – proposed system for determining operational limitations in ice. International Association of Classification Societies (IACS), International Martime Organization.

Maritime Safety Committee (2014b) Technical background to POLARIS. International Association of Classification Societies (IACS), International Maritime Organization

National Snow and Ice Data Centre (2015a) Format for gridded sea ice information (SIGRID). Boulder, Colorado USA: National Snow and Ice Data Center, Boulder

National Snow and Ice Data Centre (2015b), Downwardly mobile. Arctic sea ice news and analysis. Accessed 8 July 2015.

Okabe A, Boots B, Sugihara K (1992) Spatial tessellations: concepts and applications of Voronoi diagrams. J. Wiley and Sons, Chichester

O'Rourke R (2010) Changes in the Arctic: background and issues for congress. Congressional Research Service, 7-5700, R41153, p. 13. Accessed 08 July 2015

Transport Canada (1998) Arctic Ice Regime Shipping System (AIRSS) Standards, TP 12259E. Government of Canada, Ottawa

Transport Canada (2003) Arctic Ice Regime Shipping System (AIRSS): A pictorial guide. TP 14044E Government of Canada, Ottawa

Smith CL, Stephenson SR (2013) New trans-Arctic shipping routes navigable by midcentury. In: Mosley-Thompson ES (ed) Proceedings of the National Academy of Sciences of the United States of America (PNAS), vol 110. p E1191. Available via www.pnas.org. Accessed 28 July 2015

Snider D (2012) Polar ship operations: a practical guide. The Nautical Institute, London

Somanathan S, Flynn PC, Szymanski JK (2007) Feasibility of a sea route through the Canadian Arctic. Maritime Economics and Logistics 9:324-334

Stoddard, MA, Etienne L, Fournier M, Pelot R, Beveridge L (2016) Making sense of Arctic maritime traffic using the Polar Operational Limits Assessment Risk Indexing System (POLARIS). IOP Conf. Ser.: Earth Environ. Sci. 34 012034, pp 9.

Vihma, T. (2014) Effects of Arctic Sea Ice Decline on Weather and Climate: A Review. Surv Geophys 35: 1175. doi:10.1007/s10712-014-9284-0

Wilson KJ et al (2004) Shipping in the Canadian Arctic: other possible climate change scenarios. In: Proceedings of IGARSS '04: Geoscience and Remote Sensing, Anchorage, Alaska, September 2004. Vol 3. IEEE International, New York, p 1853

World Meteorological Organization (2004) SIGRID-3: A vector archive format for sea ice charts, JCOMM Technical Report No. 23, WMO/TD-No. 1214, Available via ftp://ftp.wmo.int/. Accessed 10 Oct 2016.

Appendix 2: Making sense of Arctic maritime traffic using the Polar Operational Limits Assessment Risk Indexing System (POLARIS)

Stoddard, M.A., Etienne, L., Pelot, R., Fournier, M., Beveridge, L. (2016). Making sense of Arctic maritime traffic using the Polar Operational Limits Assessment Risk Indexing System (POLARIS). IOP Conference Series: Earth and Environmental Science. Issue 34. https://doi.org/10.1088/1755-1315/34/1/012034

Making sense of maritime traffic in the Arctic using the Polar Operational Limits Assessment Risk Indexing System (POLARIS)

M A Stoddard[1], L Etienne[2], M Fournier[1], R Pelot[1] and L Beveridge[1]

[1]Department of Industrial Engineer, Dalhousie University, Halifax, NS, Canada
[2]Department of Planning and Environment, University of Tours, Tours, France

E-mail: mastodda@dal.ca

Abstract. Maritime traffic volume in the Arctic is growing for several reasons: climate change is resulting in less ice in extent, duration, and thickness; economic drivers are inducing growth in resource extraction traffic, community size (affecting resupply) and adventure tourism. This dynamic situation, coupled with harsh weather, variable operating conditions, remoteness, and lack of straightforward emergency response options, demand robust risk management processes. The requirements for risk management for polar ship operations are specified in the new International Maritime Organization (IMO) International Code for Ships Operating in Polar Waters (Polar Code). The goal of the Polar Code is to provide for safe ship operations and protection of the polar environment by addressing the risk present in polar waters. Risk management is supported by evidence-based models, including threat identification (types and frequency of hazards), exposure levels, and receptor characterization. Most of the information used to perform risk management in polar waters is attained in-situ, but increasingly is being augmented with open-access remote sensing information. In this paper we focus on the use of open-access historical ice charts as an integral part of northern navigation, especially for route planning and evaluation.

1. Introduction

Maritime traffic in the Canadian Arctic is expected to increase in coming years as northern communities grow, tourism increases, and large resource development projects enter into operation. As Arctic maritime traffic increases, a greater number of vessels are exposed to the navigational risks in Canada's Arctic. The vulnerability of a vessel to these navigational

risks depends heavily on the type and class of ship, crew training and experience, and access to high quality information to support decision making. Efforts to improve our knowledge and understanding of the Arctic maritime domain are required to ensure the safety and sustainability of increased maritime activity in the Canadian Arctic.

Observation and monitoring of the changing environment is critical to achieving Maritime Situational Awareness (MSA) in the Arctic. Traditional efforts to achieve MSA have focused on building accurate and timely knowledge of anything within the maritime domain that could impact the security, safety, economy, or environment. In the Canadian Arctic, environmental factors strongly influence maritime activity, including but not limited to, extreme weather, ice conditions, and daylight [1]. The Arctic environment is not uniform; there are large seasonal variations in ice, light and weather and these factors vary greatly throughout the Arctic [2]. Characterizing these factors and their impact of vessel activity in the Arctic presents a significant challenge due to the remoteness and vastness of the region. These challenges have driven major advancements in sensors and systems supporting MSA and the observation and monitoring of maritime traffic in the Arctic.

AIS (Automatic Identification System), LRIT (Long Range Identification and Tracking) and VMS (Vessel Monitoring System) now allow an observer to determine what types of ships are navigating, as well as their position at any time during their course [3,4]. These systems are now integral to the security and safety of the global maritime domain. Remote sensing systems also offer a very attractive tool for providing relevant and timely data from which a variety of shipping information products can be developed for decision makers.

Common applications of remote sensing in the Canadian Arctic include the characterization of ocean waves [5], coastlines [6], ocean currents [7-9], ice [10, 11], and shipping activity. Since the launch of the first civilian SAR satellite, SEASAT, there have been many research contributions to ship detection in SAR imagery [12-15]. Sensors such as RADARSAT-1, RADARSAT-2, ENVISAT, COSMO-SkyMed and Sentinel-1 have routinely been used to monitor the ice in the Arctic. These same sensors are also used to detect and monitor maritime traffic. The challenge we are now routinely faced with is how do we move past simply detecting and locating vessels and begin to achieve higher level sense-making of observed maritime activity. Increasingly, we must expand our awareness

of non-traditional data sources and types to improve our understanding of maritime activity, and the risks it may pose.

In this paper we will introduce the Polar Operational Limitations Assessment Risk Indexing System (POLARIS). We will demonstrate how it can be used with open-access historical ice information to preform maritime risk assessment and subsequent risk visualization. Lastly, we will provide two examples of how POLARIS can be used to support both the planning and evaluation of maritime activity in the Canadian Arctic.

2. The Polar Code and POLARIS

The International Maritime Organization (IMO) has adopted the International Code for Ships Operating in Polar Waters (Polar Code) [16] and related amendments to make it mandatory under both the International Convention for the Safety of Life at Sea (SOLAS) [17] and the International Convention for the Prevention of Pollution from Ships (MARPOL) [18]. The Polar Code will aid Arctic marine transportation in a number of ways. Not only does it address safety of navigation and environmental protection from the mariner's point of view, but it also provides a way for classification societies and underwriters to appropriately assess the risks along a desired voyage and the readiness of the company, ship, master, and crew to embark on the journey. The Polar Code will establish new guidelines beyond those contained in the SOLAS and MARPOL conventions, helping to define customary behaviour in polar waters [19]. Associated with the Polar Code is a proposed methodology to determine a ships capabilities and limitations in ice, referred to as the Polar Operational Limitations Risk Indexing System (POLARIS).

2.1. Polar Operational Limitations Assessment Risk Indexing System (POLARIS)

POLARIS provides a risk assessment framework to assess navigational safety in a given ice regime, using observed or historical ice conditions and concentration and a polar ship classification [16, 20]. Many researchers may compare POLARIS to the Transport Canada Arctic Ice Regime Shipping System (AIRSS) [21], as discussed in [12,25]. A major difference is that POLARIS allows for the consideration of limited speed / escort operations, as well as the effects of seasonal ice decay on ice strength. The addition of limited speed operations reflects known feedback from operators in the Arctic where they

met conditions they could operate in with due caution, although above the nominal limits given by AIRSS [26].

Both POLARIS and AIRSS rely on the use of an ice regime to describe an area with a number of relatively consistent ice types, including open water. The concentration of each ice type within an ice regime is reported in tenths. For each ice type there is an associated ice type score defined for each particular polar ship classification. The ice type score is referred to as a Risk Value (RV), and a collection of RVs that correspond to a particular ice regime is referred to as a Risk Index Outcome (RIO). Using POLARIS, RIO is determined by summing the RVs for each ice type present in the ice regime encountered, multiplied by its concentration (equation 1):

$$RIO = C_1RV_1 + C_2RV_2 + \ldots + C_nRV_n \qquad \text{Equation 1}$$

Where C_1, C_2,..., C_n are the concentrations (in tenths) of ice types within the ice regime and RV_1, RV_2,...,RV_n are the risk values corresponding to each ice type and for a given ship ice class classification. The resulting RIO value is then evaluated to determine the appropriate polar ship operational limits in ice.

2.2. Visualization of RIO Results using SIGRID-3 Ice Data

Integral to the calculation of the RIO is the availability of accurate information of the ice regime. As was previously mentioned, an ice regime is used to describe an area with a number of relatively consistent ice types, including open water. The ice regime can be determined in two ways, (1) in-situ by a qualified ice navigator on the bridge of a ship operating in polar waters, or (2) using open-access historical Sea Ice data. Historical sea-ice charts covering the Canadian Arctic are available from the National Snow and Ice Data Centre (NSDIC). Weekly sea-ice charts are stored in the standard World Maritime Organization (WMO) ice chart archive vector format, Sea Ice Grid (SIGRID-3). Originally proposed in 1981 and adopted by the World Maritime Organization, the SIGRID format was designed to meet larger scale climate requirements, providing a computer-compatible sea-ice data bank [27]. The CIS SIGRID-3 vector format provides information about ice conditions in a specific geographic area.

To facilitate the calculation and visualization of risk, a 1km x 1km rectangular mesh grid was generated for a defined Area of Interest (AOI) in the Canadian Arctic. This tessellation was chosen for its ease of calculation and simplicity of the resulting data structure. The resulting quantized AOI contained approximately 16 million grid cells at a 1 km^2 resolution. The AOI was further processed using a vector layer of the Canadian shoreline to delete gird cells that are outside of our AOI or inland. These spatial processing steps produced an AOI containing 4 million grid cells. Next, we filtered the CIS SIGRID-3 sea ice information to only include ice polygons within our AOI and associated this information with all intersecting grid cell from the quantized AOI. Now, for a given polar ship classification, we are able to determine the RIO for each grid cell. Six different statistical aggregations of RIO results have been generated using historical sea ice information from 2007 to 2014, including, (1) minimum RIO, (2) 25^{th} percentile RIO, (3) average RIO, (4) median RIO, (5) 75^{th} percentile, and (6) maximum RIO. Figure 1 provides a visualization of the Average POLARIS RIO from 2007 to 2014 for a Polar Class (PC) 6 vessel operating in the defined AOI during week 23.

3. Arctic Maritime Traffic Analysis

There have been many recent studies examining maritime traffic in the Canadian Arctic. Howell and Yackell provide an early example of a temporal and spatial assessment of ship navigation variability in the Canadian Arctic using historical ice information and the Arctic Ice Regime Shipping system (AIRSS) [22]. Etienne and Pelot discuss the development and use of a network graph model to determine shortest paths between an origin and destination in the Canadian Arctic, with consideration for historical ice conditions and ship capabilities in ice [25]. This model can be used to simulate maritime traffic in the Canadian Arctic. Somanathan et al. defined several alternative shipping routes through the Canadian Arctic, evaluating the relative economics of each route. By correlating ship speed to historical ice condition, and simulating year-round transits of the North West Passage (NWP) - a sea route connecting the northern Atlantic and Pacific Oceans through the Arctic Ocean, along the northern coast of North America via waterways through the Canadian Arctic Archipelago - using the

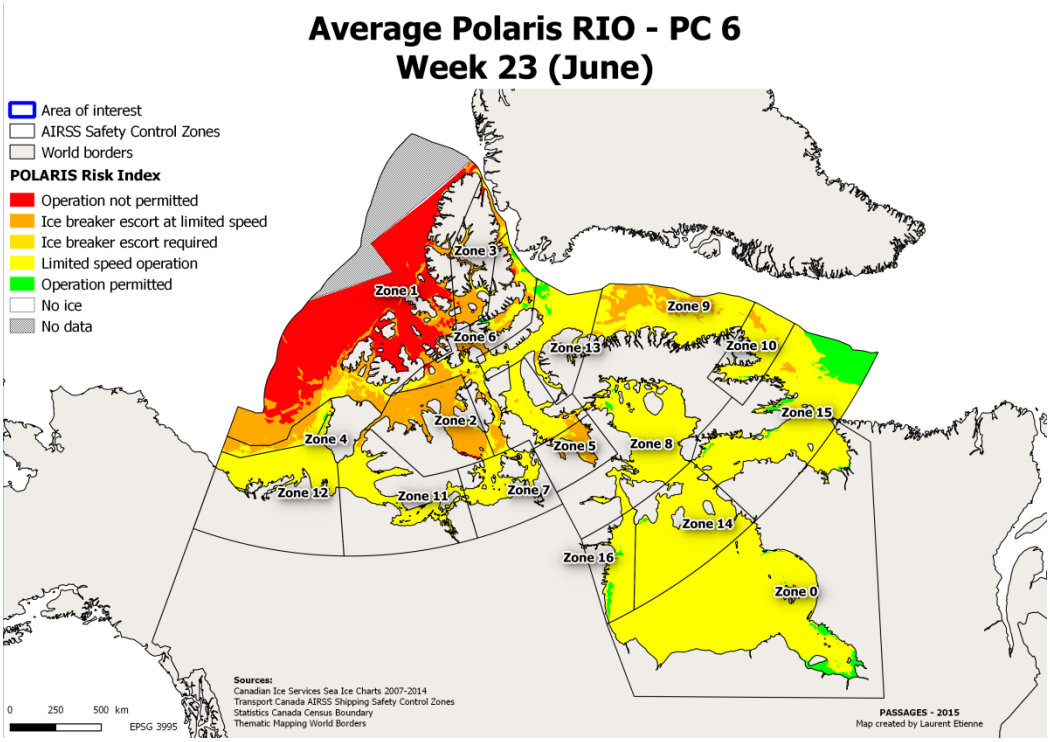

Figure 1. POLARIS scenario risk map for a PC 6 vessel operating in the defined AOI during Week 23, using the average RIO result from 2007 - 2014.

traffic simulation software Visual Simulation for Alternative Modelling (VSLAM™), the researchers were able to estimate a common measure of shipping performance, Required Freight Rate (RFR). The authors reasoned that continued thinning of Arctic ice will have the effect of increasing the economic benefit of taking the NWP when compared to conventional shipping routes [22]. Lastly, Smith and Stephenson examined the feasibility of new shipping routes through the Arctic based on the prediction of sea ice thickness and concentration from several leading Global Climate Change Models (GCMs) [24].

In this paper we will discuss the use of POLARIS and open-access ice information to evaluate the risk along a shipping route in the Canadian Arctic. We rely on the RIO to provide context when trying to make sense of erratic or unexpected kinematic behaviour along an executed route. We provide two examples, (1) Route evaluation with historical data, and (2) Route evaluation with near-real time data.

3.1.1. Route Evaluation with Historical Data

Passage planning for the Canadian Arctic region continues to be based on typical accepted standard navigational practice, with additional consideration placed on the expectation of ice presence and uncertain bathymetric charting information. Many factors influence route planning, including, operating area remoteness, locations of nearby support, extreme weather, daylight, presence of multi-year and glacial ice, and location of historical incidents [28]. For the purposes of this example we will evaluate and visualize the expected Risk Index Outcome (RIO) along a planned route. Using our AOI grid containing pre-computed RIO values, we are able to assess the risk along the route using the POLARIS evaluation criteria. Figure 2 provides an overview of the three types of visualizations that can support route planning and evaluation for a Polar Ship Ice Class 1A (IA), as defined in [18].

Figure 2 (a) provides a strategic appraisal of the RIO for a given ship class and voyage week, in this case it is an IA vessel transiting the AOI during week thirty using the median RIO value. Using this image, a planner can assess their route visually, using the median RIO results for the area they intend to transit in a particular week. Figure 2 (b) simply colour codes the route based on the median

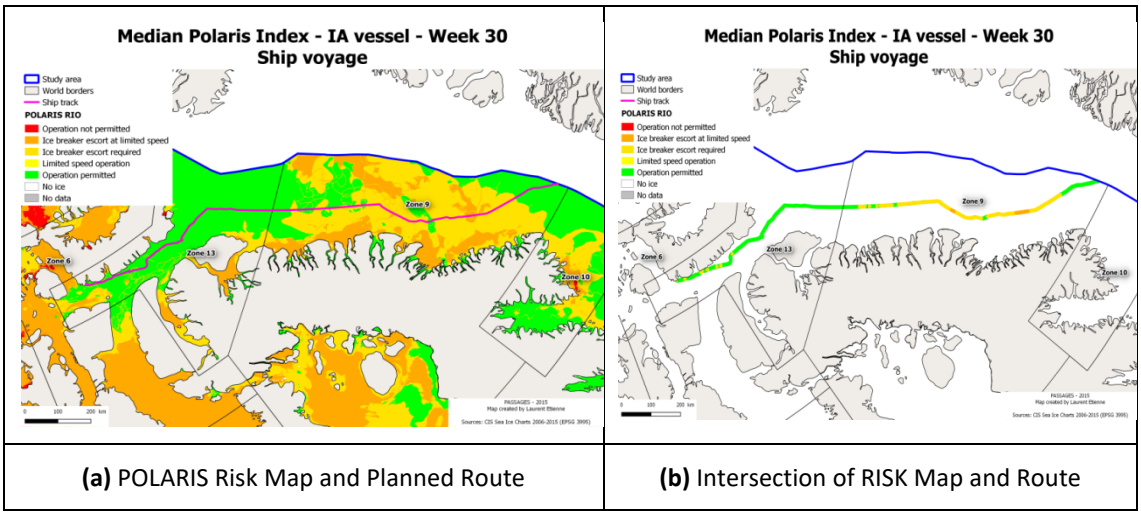

(a) POLARIS Risk Map and Planned Route

(b) Intersection of RISK Map and Route

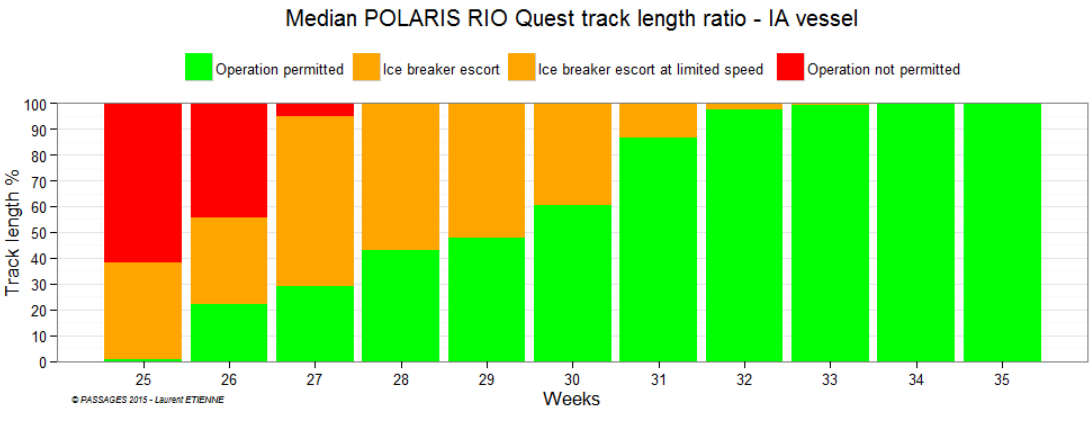

(c) Percentage of total track length corresponding to each POLARIS ship limitation for a number of potential execution weeks.

Figure 2. Route planning and evaluation visualizations for an IA vessel enter the defined AOI during week 30 using the median POLARIS RIO score.

RIO results. This simplified view can be used to quickly identify the portions of the route that are higher risk. Lastly, figure 2 (c) provides a route summary based on the proportion of the planned route that corresponds to each of the POLARIS RIO evaluation criteria. In this case we see that for an IA ship executing this planned route during week 30 that roughly 60% of the route is GREEN (operations permitted), while the other 40% may require ice breaker escort, based on median POLARIS RIO results. Of interest is that if the trip was to be be moved from week 30 to week 31 we see that conditions are much more favourable, with 86% of the track is GREEN (operations permitted), while only 14% may require ice breaker escort.

When interpreting the results shown in figure 2 one must always consider both the sea ice variation – the natural spatiotemporal variation in sea ice conditions, and the ship limit (RIO) uncertainty – the degree of precision with which ship limitations (RIO) can be measured, assessed, or evaluated. The inter-annual variation of sea ice conditions throughout the Canadian Arctic has been studied ever since Arctic-wide data for the extent of sea ice was first computed in 1979 [29]. This inter-annual variability provides a significant challenge to effective route planning and evaluation in Arctic waters. In response, figure 3 provides a box plot visualization that can be used to examine the impact

of sea ice variation (inter-annual) on each of the RIO categories. The variation is expressed in terms of the percentage of the total surface area of a given TC zone associated with a particular RIO category, for each of the 52 weeks of the year. The box plot visualization shown in figure 3 was constructed for an IA vessel operating in TC zone 13, using CIS multi-year sea ice information from 2007 and 2014.

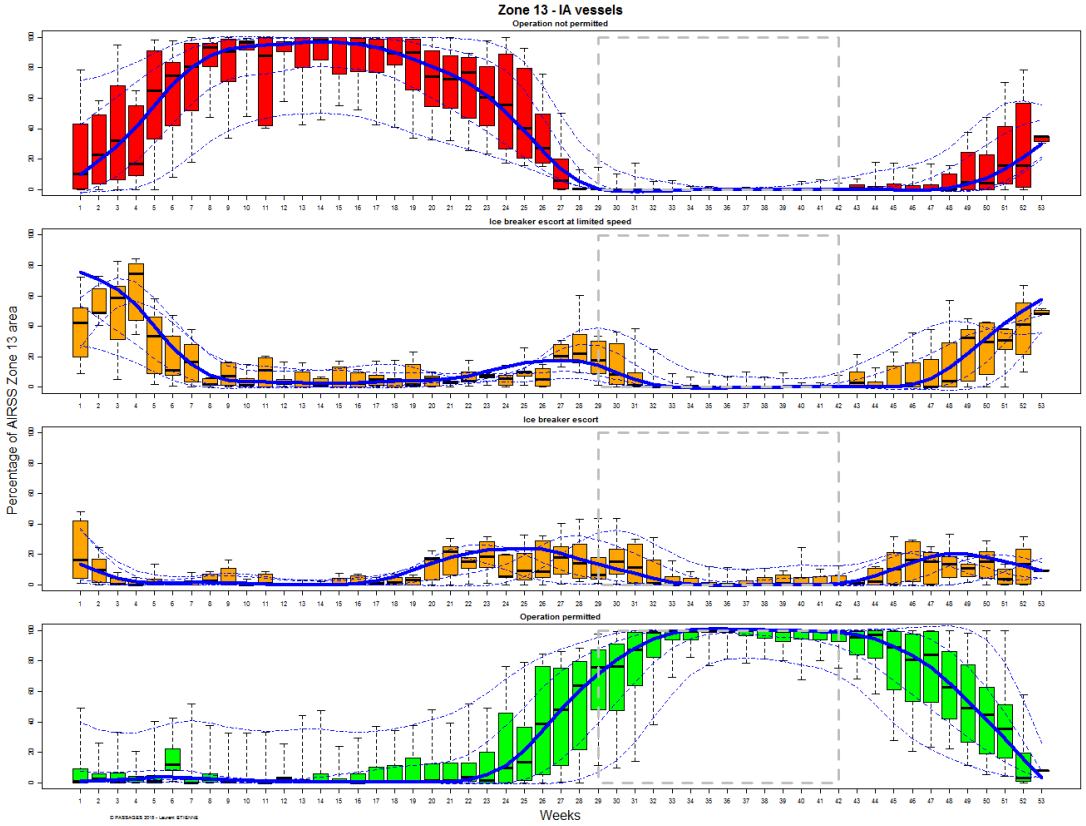

Figure 3. Box plot visualization of variability in RIO for Zone 13 using CIS ice information from 2007 - 2014. Interpolation lines are given for the minimum, 1st quartile, mean (thick blue), median, 3rd quartile, and maximum RIO value.

3.1.2. Route Evaluation with Near - Real Time Data

When presented with a recently executed or planned route it is possible to assess this route using the ice chart most closely matched in time. The approach can be used to determine the expected impact of ice along a ship route. The resulting POLARIS risk map will highlight areas where unusual kinematic ship behaviour may be observed due to the

presence of ice. In figure 4 we show a POLARIS scenario risk map for a particular IA vessel observed operating in the Canadian Arctic during week 30 of 2012. The pink line represents the ships track, as reported by an on-board Global Positioning System (GPS). Using the corresponding 2012 week 30 sea-ice information from the CIS SIGRID-3 ice database we can associate this vessel route with reported ice conditions. Instead of simply displaying the reported ice conditions, we use our knowledge of the vessels polar classification to determine the ships RIO (and associated operational limits in ice) and visualize the result over the entire AOI. Using the resulting visualization, we can associate unusual kinematic behaviour along the executed route with the ship operational limits determined using POLARIS. The two black boxes shown in figure 4 highlight areas along the route where erratic kinematic behaviour was observed, and expected, due to the presence of ice.

4. Discussion

In the previous section we illustrated the use of POLARIS to evaluate a route. The significance of this work is that it allows an observer of maritime activity, such as the Canadian Coast Guard, to identify areas along a route where unexpected kinematic behaviour may occur due to the presence of ice. This approach takes in to account the complex interaction of ice type, ice concentration, and ship design

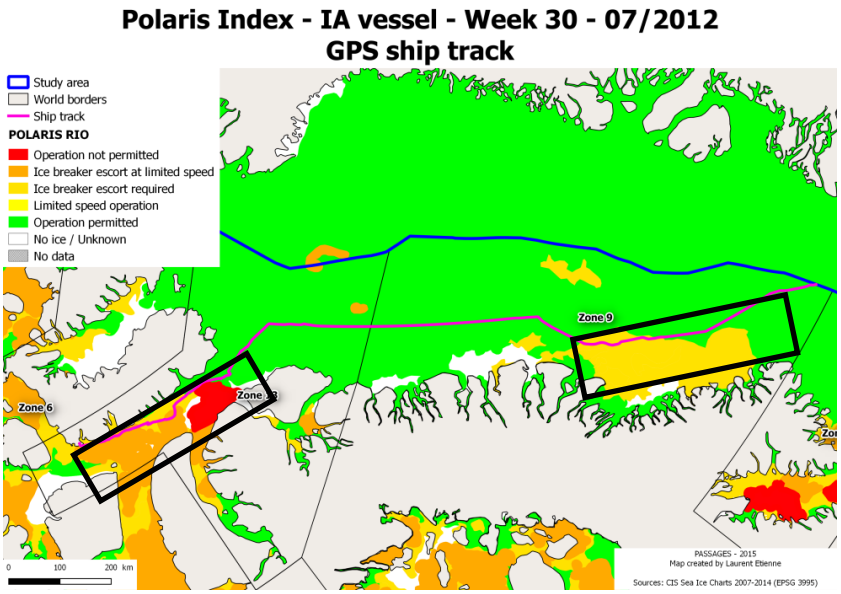

Figure 4. POLARIS Scenario risk map for 2012 week 30 for a 1A vessel operating in the Eastern Arctic.

limitations; ultimately providing a rich visualization of ship operational limits. This information can potentially be used to support three functions, (1) monitoring of vessels to ensure they remain safely within their operational limitations in ice, (2) aid in route planning and evaluation using historical ice information, and (3) identification of vessels exhibiting unexpected kinematic behaviour.

5. Conclusion

The use of POLARIS with open-access sea-ice information has made it easy to assess and visualize ship operational limits in ice over a large area of interest or along a particular route. The resulting POLARIS scenario risk maps provide a user-friendly visualization of the RIO for a particular polar ship ice classification. We have generated several statistical aggregations of RIO results from 2007 to 2014, supporting a more rigorous assessment of the available historical sea-ice information. We have also shown how using a sea-ice chart that most closely matches a series of observations from an executed route can help make sense of observed vessel kinematic behaviour. The use of the POLARIS scenario risk map in this case allows the user to understand how ice may influence a particular vessel's behaviour.

References

[1] DNV GL 2014 *The Arctic: The next risk frontier*. Hovik, Norway, 94 p.

[2] Lloyds 2012 *Arctic Opening: Opportunity and risk in the high north*. Chatham House, UK, 59 p.

[3] Eriksen T, Hoye G, Narheim B, Jenslokken Meland B 2006 Maritime traffic monitoring using a space-based AIS receiver. *Acta Astronautica* **58** (10) 537-549.

[4] Cairns W R 2005 AIS and Long Range Identification & Tracking. *J. Navigation* **58** 181-189.

[5] Heiberg H, Breivik L-A, Reistad M and Brattli A 2006 Use of ASAR wave spectra in operational wave analysis and forecasting: report form the EnviWave project. *Met.no Report* **10**, Norwegian Meteorological Institute, Oslo, Norway.

[6] Olsen R B and Wahl T 2000 The role of wide swath SAR in high-latitude coastal management. *John Hopkins APL Technical Digest* **20** (1) 136-140.

[7] Runge H, Breit H, Eineder M, Schulz-Stellenfleth J, Bard J and Romeiser R 2004 Mapping of tidal currents with SAR along track interferometry. *IGARSS 2004*.

[8] Collard F, Mouche A, Danilo C, Chapron B, Isern-Fontanet J, Johannessen J and Backeberg B 2008 Routine high resolution observation of selected major surface currents from space. *SEASAR 2008*.

[9] Kang, M K, Lee H, Yang C S, Yoon W J 2008 Estimation of ocean current velocity in coastal area using RADARSAT-1 SAR images and HF-Radar data. *IGARSS 2008*.

[10] Hirose, T, Kapfer M, Bennett J, Cott P, Manson G and Solomon S 2008 Bottomfast ice mapping and the measurement of ice thickness on tundra lakes using C-Band Synthetic Aperture Radar remote sensing. *Journal of the American Water Resources Association* **44** (2) 285 - 292.

[11] Chamberlain J, Yue B, Parsons G and Mulvie J 2010 Advanced remote sensing for better bottom-fast ice identification. *RADARSAT-2 Workshop*, September 2008.

[12] Vachon, P W 2006 Ship detection in Synthetic Aperture Radar imagery. *Proceedings OceanSAR 2006 – Third Workshop on Coastal and Marine Applications of SAR*, St. John's, NL, Canada.

[13] Crisp, D J 2004 The state-of-the-art in ship detection in Synthetic Aperture Radar imagery. *Defence Science and Technology Organisation Report* (DSTO-RR-0272, May 2004).

[14] Greidanus, H and Kourti N 2006 Findings of the DECLIMS Project – Detection and classification of marine traffic from space. *Proceedings of SEASAR 2006*, Frascati, Italy.

[15] Power D, Howell C, Lane K, Youden J, Randell C, Staples G and MacDonald B 2005 ENVISAT ASAR and RADARSAT-2 based iceberg and ship discrimination for application in maritime surveillance. *8th Int. Conf. Rem. Sens. Marine & Coastal Environments,* Halifax, NS, Canada.

[16] International Maritime Organization 2015 *International Code for Ship Operating in Polar Waters (POLAR CODE).* https://edocs.imo.org/FinalDocuments/English/MEPC68-21-ADD.1(E).doc, retrieved 2016.03.03.

[17] International Maritime Organization 1974 *International Convention for the Safety of Life at Sea (SOLAS).* http://www.imo.org/en/About/Conventions/ListOfConventions/Pages/International-Convention-for-the-Safety-of-Life-at-Sea-%28SOLAS%29,-1974.aspx, retrieved 2016.03.03.

[18] International Maritime Organization 1974 *International Convention for the Prevention of Pollution from Ships (MARPOL)* http://www.imo.org/en/About/conventions/listofconventions/ pages/international-convention-for-the-prevention-of-pollution-from-ships%28marpol% 29.aspx, retrieved 2016.03.03.

[19] Maritime Safety Committee 2014 *International Code for Ships Operating in Polar Waters (POLAR CODE).* (International Maritime Organization).

[20] Maritime Safety Committee 2014 *POLARIS: Proposed system for determining operational limitations in ice* (International Maritime Organization).

[21] Transport Canada 1998 *Arctic Ice Regime Shipping System (AIRSS) Standards.* Transport Canada, Ottawa, TP 12259E)

[22] Howell S and Yackel J J 2004 A vessel transit assessment of sea ice variability in the Western Arctic, 1969 – 2002: Implications for ship navigation. *Cdn. J. Rem. Sensing* **30** (2) 205-215

[23] Somanathan S, Flynn P C and Szymanski J K 2007 Feasibility of a sea route through the Canadian Arctic. *Maritime Economics and Logistics* **9** 324-334.

[24] Smith C L and Stephenson S R 2013 New Trans-Arctic shipping routes navigable by midcentury. *Proceedings of the National Academy of Sciences of the United States of America (PNAS)* (www.pnas.org/cgi/doi/10.1073/pnas.1214212110, March, E1191-E1195.)

[25] Etienne L and Pelot R 2013 Simulation of maritime paths taking into account ice conditions in the Arctic. *11th International Symposium for GIS and Computer Cartography for Coastal Zone Management (CoastGIS)*, 116-119.

[26] Maritime Safety Committee 2014 *Technical background to POLARIS* (International Maritime Organization*)*

[27] National Snow and Ice Data Centre 2015 *Format for gridded sea ice information (SIGRID)* (Boulder, Colorado USA: National Snow and Ice Data Center)

[28] Snider, D 2012 *Polar ship operations - A practical guide* (London: The Nautical Institute)

[29] Lasserre, F 2011 Arctic Shipping Routes. *International Journal* **66** (4) 793-808.

Appendix 3: Determining Ship Speeds in Ice using the Polar Operational Limitation Assessment Risk Indexing System (POLARIS)

Stoddard, M.A., Pelot, R., Etienne, L., and Goerlandt, F. (2024). Determining Ship Speeds in Ice using the Polar Operational Limitation Assessment Risk Indexing System (POLARIS). **DRAFT.**

Title: Determining Ship Speeds in Ice using the Polar Operational Limitation Assessment Risk Indexing System (POLARIS)

Authors: Mr. Mark A. Stoddard, Dalhousie University

Dr. Ron Pelot, Dalhousie University

Dr. Floris Goerlandt, Dalhousie University

Dr. Laurent Etienne, ISEN University

Abstract

Determining the expected ship speed through varying sea ice conditions is critical to improving the estimation of travel time, fuel consumption, and emissions in ice-covered waters. It is expected that as the risk to a ship from sea ice increases, ship speed is reduced to increase safety, and minimize damage to a ship's hull. Several risk assessment methodologies exist to assist ship operators with determining the sea ice risk, but all offer very little guidance on the reduction of ship speed to increase shipping safety and prevent damage. The International Maritime Organization's Polar Code currently recommends the use of the Polar Operational Limits Assessment Risk Indexing System (POLARIS) to assess sea ice risk to ships. POLARIS combines knowledge of sea ice conditions, and a ship's ice classification, to determine the risk to a ship from sea ice. The output from POLARIS is referred to as the Risk Index Outcome (RIO). This study focuses on combining AIS data with US National Ice Centre (USNIC) sea ice analysis charts to produce a POLARIS RIO-based ship speed curve. The resulting speed curve can be used to determine the expected speed of a ship operating in different POLARIS RIO result categories, which enables the computation of an Estimated Transit Time (ETT) that accounts for changes in ship speed along a route due to varying ice conditions. The results of this study provide a step forward in overcoming the complexity of computing accurate ETT in ice-covered waters with varying sea ice conditions.

KEYWORDS: POLARIS, Risk Assessment, Automated Identification System, Arctic, Navigation, transit time

1. Introduction

Navigation in the Canadian Arctic follows standard navigational practice, with special consideration for the presence of sea ice (Snider, 2012). Sea ice conditions have a strong influence on ship routing and the expected transit time between maritime locations (Howell & Yackel, 2004). To improve navigation safety in the Canadian Arctic, ships are subject to entry and exit date requirements for different maritime areas (commonly referred to as zones), that are based of a ship's ice class (Transport Canada, 1998). A ships ice class is determined by organizations and national authorities which develop and apply technical standards for the design, construction and survey of ships. Many different ship classification societies exist around the world that establish and maintain technical standards for the construction and inspection of polar vessels. Examples of ship classification societies include the American Bureau of Shipping (ABS), Llyod's Register, Bureau Verita, and the International Association of Classification Societies (IACS).

Several sea ice risk assessment frameworks exist to assist ship operators with navigational decision making, discussed further in Section 2. The International Maritime Organization (IMO)'s Polar Code promotes the use of the Polar Operational Limit Assessment Risk Indexing System (POLARIS) to determine sea ice risk (Maritime Safety Committee, 2014b). POLARIS has a built-in 4-year review period, set by the IMO, to evaluate its efficacy (Fraser, 2020). The result from POLARIS is referred to as the Risk Index Outcome (RIO). POLARIS has proven to be a useful tool for not only tactical decision-making onboard ships, but also for the strategic appraisal of navigational risk over wide areas in the Canadian Arctic and other polar and ice-covered regions (Stoddard M. A., Etienne, Pelot, Fournier, & Beveridge, 2018), (Fedi, et al., 2018), (Tremblett, Garvin, & Oldford, 2021), and (Wang, Ding, Yang, & Dou, 2022).

While very useful for assessing the ice risk throughout an area of operation, the POLARIS methodology only provides general recommendations for safe speed limits in elevated risk operations (RIO values between 0 and -10). To date, there have been no empirical studies that have produced results that can be used to specify ship speeds over the full range of POLARIS RIO results. This study aims to close this gap in the literature by performing spatiotemporal analysis of historical AIS data and sea ice analysis to produce a POLARIS

RIO-based speed curve that can be used to specify expected ship speeds in different RIO result categories.

Section 2 presents background research published on estimating ship speed in ice, covering several different approaches to this complex problem. Section 3 provides an overview of the quantitative methods proposed by this study to determine the expected ship speed in different RIO result categories. We also introduce a new computational method that combines the POLARIS RIO results along a planned route, with the RIO speed curves discussed in the previous section, to compute the Expected Transit Time (ETT) in ice-covered water on a pre-determined route. Section 4 presents the results of our study, finishing with a transit time validation case study. Section 5 provides a discussion on the limitations of the methods and results presented in this study and opportunities for future research. Lastly, Section 6 provides concluding remarks and last thoughts on the research topic of ship speed in ice-covered waters.

2. Background

Estimating ship speeds in varying sea ice conditions is critical to improving the estimation of travel time, fuel consumption, and emissions in ice-covered waters. Much research has been devoted to this topic, focusing on the development of quantitative methods to explain the complex relationship between ice features and ship design and operational characteristics of independent ship operations, convoy, and ice breaker escort. The primary use of these methods is shipping route generation and optimization in ice-covered waters for the detailed study of arctic maritime traffic.

(McCallum, 1996) proposed the use of polynomial fitting between minimum and maximum expected ship speeds for several Canadian Arctic Class (CAC) ships in different ice risk regimes, determined using the Transport Canada Arctic Ice Regime Shipping System (AIRSS). A scaling procedure was used to produce speed curves for different ice class ships in different ice risk regimes. However, these curves were only produced for ships below a Canadian Arctic Class (CAC) rating, with a maximum speed of 11 knots. The curves were also only produced for positive Ice Numerals (IN). (Somanathan, Flynn, & Szymanski, 2006) build on the methods proposed by (McCallum, 1996), further discussing the use of

AIRSS to predict ship speed decreases in different ice risk regimes. Their study evaluated the relative economics of shipping through the Northwest Passage and shipping through the Panama Canal. The authors used historical sea ice analysis to prepare probabilistic ice regimes along shipping routes in the arctic. Ice conditions were simulated throughout the year and the impact of ice on ship operations was estimated by the AIRSS Ice Numeral (IN). The authors then specified a relationship between IN and ship ice class to calculate a speed through ice.

(Kotovirta, Jalonen, Axell, Riska, & Berglund, 2009) examined the use of computer-based optimization to determine optimal routes in ice-covered waters. Their model combined the gridded outputs from an ice prediction model, with a ship performance model to determine ship speed in different ice conditions. The ship speed in various ice thickness was determined using a mathematical relationship between ship net thrust and ice thickness/resistance. AIS data was used for statistical validation of the transit times calculated by their method. The authors note that the quality of optimal routes depends greatly on the quality and resolution of the ice condition data.

((Stephenson, Smith, & Agnew, 2011), (Smith & Stephenson, 2013), (Melia, Haines, & Hawkins, Sea ice decline and 21st century trans-Arctic shipping routes, 2016), (Aksenov, et al., 2017)) all discuss the use of coupled atmosphere-ocean General Circulation Models (GCMs) to project future sea ice thickness and concentration to study the future navigability of trans-arctic polar routes. Ship speed and transit time were calculated using the Arctic Transport Accessibility Model (ATAM), which combines high resolution projections of sea ice conditions from a GCM with the AIRSS algorithm to determine navigability and ship speed over wide areas. Ship travel times were specified using the IN versus Ship Speed relationship first published in (McCallum, 1996).

(Loptien & Axell, 2014) examined the relationship between AIS ship speed data and sea ice forecasts in the Baltic Sea. By analyzing over 14,000 AIS vessel speed reports, and comparing with Baltic Sea ice charts, the authors were able to produce a mixed-effects model to predict vessel speed from forecasted ice properties (ice concentration, ice thickness, and ridge density). The authors observed decreases in ship speed, without consideration for ship ice class, when sea ice concentration and ice thickness increased

from 0 cm to 30 cm. Interestingly, no further systematic speed drops occurred for ice thicknesses above 30 cm were reported. Their analysis shows that a large part of observed ship speed variation can be well explained by the corresponding forecasted sea ice properties, for average ice thicknesses less than 30cm.

(Montewka, Goerlandt, Kujala, & Lensu, Towards Probabilitic Models for the Prediction of a Ship Performance in Dynamic Ice, 2015) reviewed the use of semi-empirical methods that estimate ship resistance and ship speed in sea ice. The authors noted that most prior work in this area characterized the ice conditions only by the average level ice thickness. In response, the authors developed a Bayesian network that could represent the probabilistic relationship between the speed of the ship and a multitude of surrounding ice features. Given a set of ice features, the model could be used to compute the probability for a ship to attain a certain speed. Ice features were determined using the state-of-the-art HELMI ice model, allowing the authors to considers the joint effect of various ice features on ship performance.

(Kim, Jeong, Woo, & Han, 2018) present a physics-based method to calculate attainable speed in ice, defined as the speed that is possible to achieve in certain ice types and properties if the ship power level is fixed. Their method combines measures of resistance, self-propulsion (thruster performance), and resistance overload to calculate the attainable speed of a vessel in different ice thicknesses. Tank trials were conducted at the Korean Research Institute of Ship and Ocean Engineering (KRISO) in an effort to validate results from their calculation, showing good agreement between computed and measured results during tank testing.

(Simila & Lensu, 2018) discuss estimating the speed of ice-going ships by integrating Synthetic Aperture Radar (SAR) imagery and ship data from AIS. Their study focused on associating the reported vessel location and speed from AIS with features in the SAR imagery. A random forest regression model was constructed to estimate ship speed from the features of SAR images. In essence, their method translates SAR images collected over ice cover to expected ship speed maps which can be used for follow-on analysis, such as route planning and optimization. The authors were able to generate useful speed maps from a limited training set, although several uncertainties involved in the use of AIS data were

noted. These uncertainties included; (1) changes in speed not due to ice condition, (2) uniformity of ice-going capabilities of observed ships, and (3) the use of frequently navigated channels with different ice properties.

(Lehtola, Montewka, Goerlandt, Guinness, & Lensu, 2019) discuss the use of semi-empirical (simulation) models, and data-driven models to estimate vessel transit speed in different ice regimes. These models are used to estimate the attainable speed of a vessel based on the characteristics of both the ice field and the ship. A ship operating outside of the ice field in open water is expected to transit at its design speed, where it achieves maximum efficiency. However, a ship operator may choose to operate at slower speeds in polar open water conditions to minimize the risk of high-speed collision with free floating ice.

(Tremblett, Garvin, & Oldford, 2021) provided an example of a data-driven approach to estimate ship speeds in lake ice using POLARIS. Using shore-based AIS data collected in the North American Great Lakes region between 2010 and 2019, they examine the distribution of observed vessel speeds in different RIO risk category. The RIO for each ship was determined by using ships position as reported by AIS, and associating the ship observation with the daily sea ice conditions as reported by the Canadian Ice Service (CIS). Through the use of probability density functions of ship speed in each RIO category, the authors were able to demonstrate a clear trend of speed reduction with decreasing RIO values, both for mild and severe ice conditions. The authors note that for their study they had to assume that there was an approximate ice thickness equivalence between lake ice and ice types used in POLARIS. This assumption was required because POLARIS does not currently provide Risk Values specifically for seasonal lake ice.

Lastly, (Goerlandt, Montewka, Zhang, & Kujala, An Analysis of Ship Escort and Convoy Operations in ice Conditions, 2017) and (Liu, Musharraf, Li, & Kujala, A data mining method for automatic identification and analysis of, 2022) discuss the particular case of expected ship speeds for escort and convoy operations in ice-covered waters. Both studies focus on the analysis of AIS data collected in the Baltic Sea during the winter months. (Liu, Musharraf, Li, & Kujala, A data mining method for automatic identification and analysis of, 2022) provide results for expected escort and convoy operation speeds for different

average sea ice thickness and concentration. The authors reported that as average sea ice thickness increases, transit speed is reduced. The mean value for a merchant vessel under escort was reported as 5.5 knots, increasing to 10 knots when escort was no longer required. Similarly, (Goerlandt, Montewka, Zhang, & Kujala, An Analysis of Ship Escort and Convoy Operations in ice Conditions, 2017) also utilized AIS data to analyze ship escort and convoy operations. Their analysis aimed to provide new insights into ship escort and convoy operations by combining AIS data and environmental data to contextualize reports of vessel speed in ice-covered waters. Escort and convoy speeds reported by AIS are provided for different sea ice thicknesses. The authors report that a transit speed of 10 knots is reasonable for escort operations, however, in sea ice thicknesses greater than 0.6 meters, a convoy transit speed of 5 knots is recommended for operational planning purposes.

3. Methods

3.1. AIS Reporting and Ship Ice Classification

AIS transponders are designed to be capable of automatically providing position, speed, identification and other information about the ship to other ships, coastal authorities. Since 2004, SOLAS regulation V/19 - ”Carriage requirements for shipborne navigational systems and equipment” has required all ships of 300 gross tonnage to carry AIS (International Maritime Organization, 2004). The early days of AIS vessel tracking were dependent on establishing a network of shore-based AIS receivers to receive the AIS VHF transmissions of passing ships fitted with AIS transponders. The advent of satellite-based AIS receivers, and rapid commercialization of space-based reception, has led to an explosion of global vessel tracking and related research relying on AIS.

The AIS data set used for this study was collected by the ExactEarth Ltd. AIS satellite constellation, covering 2018 and 2019 and containing approximately 22 million AIS position reports from 184 ships (Spire Maritime, 2023). The geographic extent of the AIS data set is approximately 40N to 90N and 45W to 130W, and is shown in Figure 1. Each AIS position report provides information on the vessel identity, type, time, position, speed, and navigation status. Currently, the International Telecommunication Union (ITU) AIS message specification does not include ship ice class, which is a necessary AIS message

attribute to compute sea ice risk using POLARIS (International Telecommunication Union, 2014).

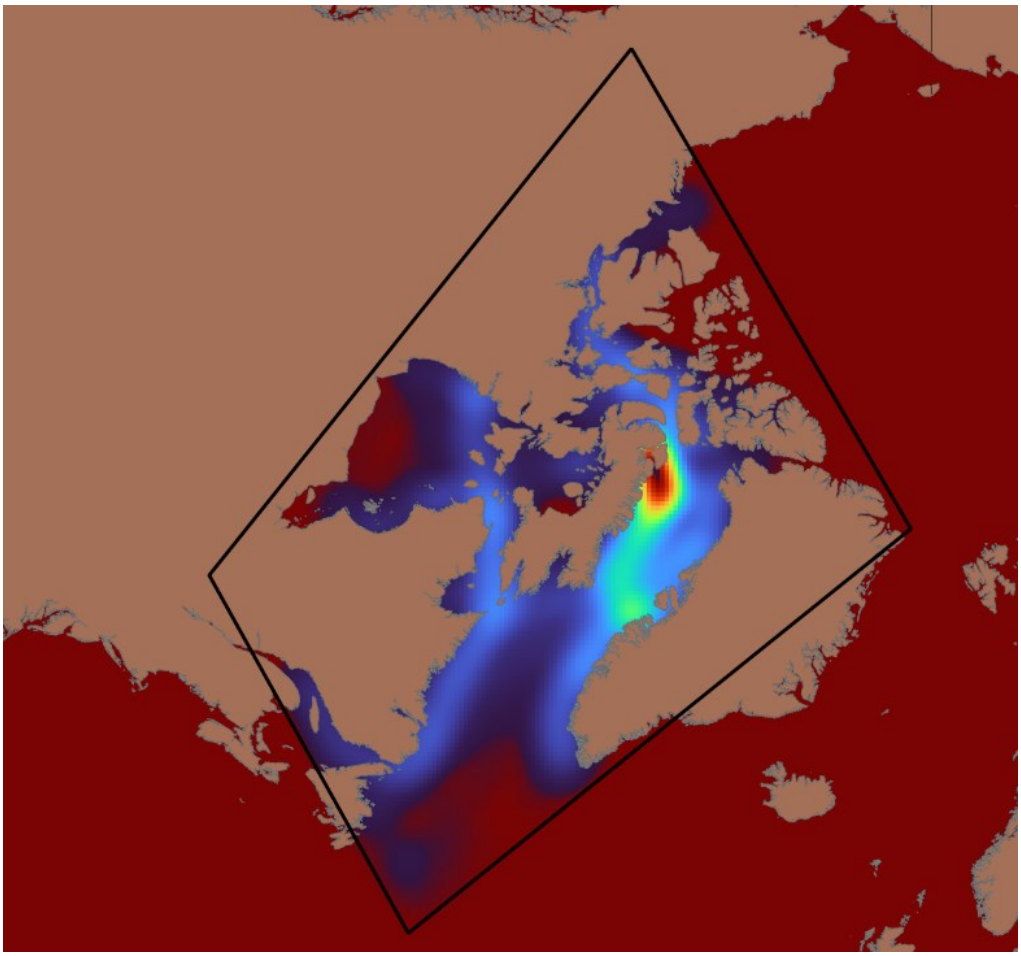

Figure 1: 2018-2019 Geographic extent of the AIS data set and message density

To add the ice class attribute to the AIS data set, we joined our data with a database of Finnish-Swedish (FS) ice class ships. The FS ice class ship database contained ice class information for 12,720 ships. These two data sets were joined by matching the IMO number from each AIS report with the IMO number associated with each of the FS ice class ships in the database. AIS reports that could not be matched were removed from the data set.

3.2. Computing POLARIS RIO using Sea Ice Analysis Charts

POLARIS has been produced by IACS to provide a quantitative framework to assess navigational safety in an ice regime, using observed or historical ice conditions and

concentration and a vessel's ship ice classification (Maritime Safety Committee 2014b). An ice regime is used to describe an area with a relatively consistent distribution of one or more ice types, including open water. The concentration of each ice type within an ice regime is reported in tenths. For each ice type, there is an associated ice type score defined for each ship ice classification. The ice type score is referred to as a Risk Value (RV), and a collection of RVs that correspond to an ice regime is referred to as a Risk Index Outcome (RIO). Using POLARIS, the RIO result is determined by summing the RVs for each ice type present in the ice regime encountered, multiplied by the respective concentration (in tenths):

$$RIO = C_1RV_1 + C_2RV_2 + \cdots + C_nRV_n \qquad \text{Equation 1}$$

where $C_1, C_2, \ldots, C_n$ are the concentrations of the ice types present in an ice regime and $RV_1, RV_2, \ldots, RV_n$ are the risk values corresponding to each ice type, specific to a particular ship ice class. The resulting RIO value is then evaluated to determine an appropriate operational limitation due to the presence of sea ice in an area of operation. The RIO score can be determined using in-situ observations of a local ice regime, or can be computed directly from ice analysis data contained in national sea ice analysis charts.

Weekly sea ice charts for the arctic from the USNIC were used for this study (U.S. National Ice Centre, 2023). USNIC sea ice charts are produced through the detailed analysis of available in-situ, remote sensing and model data sources. Sea ice condition data is digitally stored in Sea Ice Grid (SIGRID)-3 format. The USNIC digital ice analysis charts (hemispheric, regional and daily) are encoded in SIGRID-3, and have two main components: the shapefile containing the ice analysis ice information (ice polygons and related attributes) and the metadata describing the ice analysis data (National Snow and Ice Data Centre, 2015a). Equation 1 can be combined with sea ice analysis information from a USNIC sea ice analysis chart to compute the POLARIS RIO in each ice analysis polygon, commonly referred to as a sea ice risk assessment.

3.3. Joining Historical AIS Messages with the POLARIS RIO Result

QGIS Desktop 3.24.3 was used to perform the necessary geospatial processing steps required to join the attributes of our AIS data set with the USNIC sea ice analysis polygons, and to compute the POLARIS RIO values (QGIS, 2023). In total, 101 bi-weekly sea ice analysis charts were processed, spanning the temporal extent of the 2018-2019 AIS data set. The AIS data set consisted of 22 million AIS messages. The attributes of each sea ice analysis polygon contained in the USNIC bi-weekly sea ice charts were spatiotemporally joined with each AIS report in the data set. To enable the temporal alignment of the AIS reports and bi-weekly sea ice analysis charts, it was necessary to compute the bi-weekly period for each AIS message from the message received date. Once the bi-weekly period was computed, the attributes from the AIS messages and sea ice analysis charts from each bi-weekly analysis period were spatially joined. The RIO score was then computed for each AIS message using Equation 1 and the recently joined sea ice analysis attributes. Lastly, we examined the distribution of the frequency of reported vessel speed over ground and computed descriptive statistics using reported vessel speed in different RIO result categories.

To add the necessary environmental context, we calculate descriptive statistics for the AIS reported vessel speed in different POLARIS RIO result categories. For this analysis, POLARIS RIO values were grouped into five categories; (1) RIO = 30 : Open Water Operation, (2) 0 <= RIO < 30 : Normal Ice Operations, (3) -10 <= RIO < 0 : Elevated Operational Risk, (4) -30 < RIO < -10 : Operation Subject to Special Consideration, and (5) RIO = -30 : Operation Not Recommended. (Fedi, Faury, & Etienne, 2020) provide additional background on the selection of RIO result categories, and their qualitative relationship to ship operations. The minor difference with the RIO categories used for this study is that we have introduced two new RIO categories, (1) RIO = 30 and (2) RIO = -30. These new categories were created to specifically consider ship operations in the best case and worst-case conditions.

3.4. Computing Estimated Transit Time in Ice-Covered Waters using POLARIS RIO Speed Curves

The most basic approach to transit time estimation is a simple distance divided by speed calculation, where distance is known and the speed is fixed (see Equation 2). This

calculation assumes that in the absence of environmental or other external factors, a ship has a planned transit speed that remains constant for the duration of the transit.

$$T = \frac{D}{S} \qquad \text{Equation 2}$$

where,

T = Transportation Time (hours)

D = Distance (nautical miles)

S = Ship Speed (knots)

Estimating ship transit time in ice-covered waters is especially difficult, and continues to be based on typical accepted standard navigational practice, with additional consideration placed on the expectation of ice presence (Snider, 2012). The challenge is that simple methods used to estimate transit time do not allow for the formal consideration of variable sea ice conditions along a route, and their impact on ship speed. (Stoddard M. , Etienne, Fournier, Pelot, & Beveridge, 2016) previously demonstrated the use of POLARIS and open access sea ice analysis products to evaluate the expected POLARIS RIO along routes in polar waters. We now introduce a new computational method that combines the POLARIS RIO results along a route, with the RIO speed curves discussed in the previous section, to compute the Expected Transit Time (ETT) in ice-covered water on a pre-determined route.

ETT is computed using the same simple distance divided by speed approach previously discussed, except we now account for the impact of varying expected sea ice conditions along a route. This is achieved by computing the distance a polar class ship must transit through each of the pre-defined POLARIS RIO categories, divided by the specified ship speed associated with each of the POLARIS RIO categories. The ETT is then determined by performing a linear sum of these results. Equation 3 provides a generalized mathematical formulation for computing ETT using POLARIS.

$$ETT_{jt} = \sum_{k=1}^{4} \frac{D_{jtk}}{S_k} \quad \forall\, j \in J, t \in T \qquad \text{Equation 3}$$

In Equation 3, the estimated transit time, ETT_{jt} , is the estimated transit time by a ship with ice class *j*, in analysis period *t*. To compute ETT_{jt} we first generate D_{jtk}, which is a sparse matrix containing the distances travelled through POLARIS RIO category k on a pre-determined route, by ship ice class *j*, in analysis period *t*. The ship speed, S_k , represents the ship speed through POLARIS RIO category *k*. The indexes J, and T represent the set of all ship ice classes j, and analysis periods t. This mathematical formulation can be used to calculate the ETT for all ship ice classes, for each analysis period. Currently, our analysis is completed on a bi-weekly basis, which results in 26 bi-weekly analysis periods. A necessary assumption is that the route being evaluated can be completed within the analysis period being considered.

4. Results

4.1. AIS Data Processing

Approximately 12.4M AIS messages in the AIS data set were successfully matched with the FS ice classification data, representing 45% of the reports contained in the full AIS dataset. The matched AIS reports were associated with a total of 116 vessels (unique IMO), leaving 68 vessels in the AIS data set that could not be associated with a FS ice class.

Table 1 provides a detailed breakdown of the 12.4M AIS messages that were successfully matched with FS ice classification. To support the ship speed analysis discussed later in this paper, the AIS data was further reduced to only include vessels with a ship classification of Finnish Class 1A and 1A Super. This action was required because the Finnish Transport Safety Agency only provides official IACS Polar Class (PC) equivalency for Finnish Ice Class 1A (PC 7) and 1A Super (PC 6) (Finnish Transport Safety Agency, 2017). Following this last filtering step, approximately 8.4M AIS reports from FS 1A and 1A Super vessels remain from the original AIS data set.

Table 1: Breakdown of received AIS messages by available Finnish Swedish (FS) Ice Classification

Ice Class	# of Messages	Unique IMO

FS Ice Class 1A Super	2,252,394	7
FS Ice Class 1A	5,850,853	52
FS Ice Class 1B	1,409,845	12
FS Ice Class 1C	2,725,304	42
FS Ice Class II	161,268	3
No FS Ice Classification	10,188,462	68
Total	22,588,106	184

4.2. POLARIS RIO Result Statistics

Figure 2 shows the distribution of the frequency of vessel speed over ground in the AIS data set. The distribution shows multiple modes in the distribution of the frequency of reported vessel speed. We see peaks in the frequency of vessel speeds around 14 knots, 8.5 kts, 5 knots, and 1.5 knots. The average design speed of different categories of ships operating in the arctic were reported in the Arctic Council's Arctic Maritime Shipping Assessment (AMSA) 2009 report (Arctic Council, 2009). A total of 1477 ships were examined in the AMSA report, and the average ship speed in polar waters was determined to be 14kts. The average ship speed reported in the AMSA 2009 report agrees with the maximum speeds shown in Figure 4. While understanding average ship speed may be useful for strategic planning, without the environmental context, and in particular the prevailing ice conditions, it is hard to use this information in practice. It also provides little help in explaining the observed peaks in vessel speeds around 8.5 kts, 5 kts, and 1.5 kts.

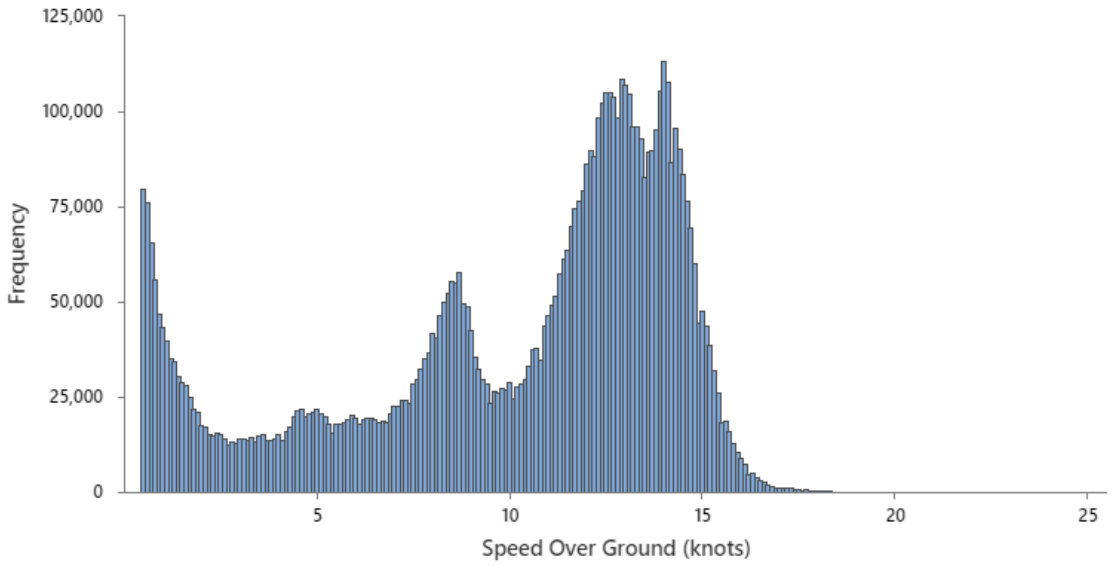

Figure 2: Distribution of the frequency of speed over ground reported in the 2018-2019 AIS data set

Figure 3 shows a statistical box plot of the observed vessel speed over ground in different POLARIS RIO result categories using the processed AIS data set. The line value in each box represents the median speed observed in each RIO category. The top value of the box represents the 3rd quartile of observed vessel speed, and the bottom value of the box represents the 1st quartile of observed vessel speed. The length of the vertical line in the box plot represents the range of vessel speeds overserved in each of the POLARIS RIO result categories specified. Since the speed is specified based on the RIO result category, it is not necessary to consider the Polar Class of vessel when determining the expected ship speed. This is because the ice classification of the vessel has already been considered during the selection of POLARIS used to compute the appropriate RIO value for the ship (see Equation 1). Table 2 provides a summary of the descriptive statistics computed for observed ship speed in different RIO result categories.

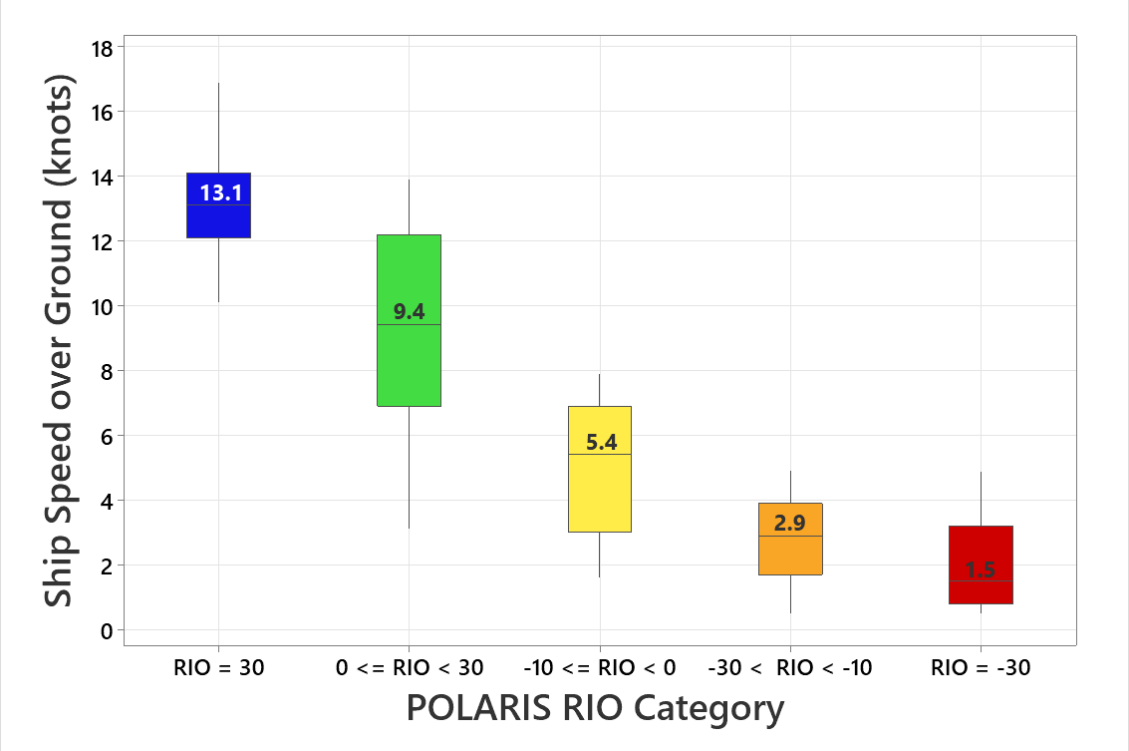

Figure 3: Box plot of the observed vessel speed over ground in different POLARIS RIO categories

Table 2: Summary of AIS reported ship speed in different POLARIS RIO categories

RIO Category	Median Ship Speed (knots)	Q1 Ship Speed (knots)*	Q3 Ship Speed (knots)**
RIO = 30 (N=3,539,558)	13.1	12.1	14.1
0 <= RIO < 30 (N=656,125)	9.4	6.9	12.2
-10 <= RIO < 0 (N=45,836)	5.4	3	6.9
-30 < RIO < -10 (N=20,682)	2.9	1.7	3.9
RIO = -30 (N=808,176)	1.5	0.8	3.2

* The first quartile (Q1, or the lowest quartile) is the 25th percentile, meaning that 25% of the observed vessel speeds in this RIO category falls below the first quartile.

**The third quartile (Q3, or the upper quartile) is the 75th percentile, meaning that 75% of the observed vessel speeds in this RIO category falls below the first quartile.

4.3. Transit Time Validation Case Study

The following case study relies on historical AIS data and POLARIS RIO results to validate the Estimated Transit Time (ETT) approach introduced in Section 3.4. We focus on an Eastern Arctic transit completed by Canadian Forces Auxiliary Vessel (CFAV) QUEST, during July 2012. CFAV QUEST was a Polar Class 1A vessel, with a maximum economic speed of 14 knots. The leg of the voyage analyzed was from Nuuk, Greenland to Gascoyne Inlet, Northwest Territories. The voyage was a continuous transit, covering a total distance of 1119 nautical miles. The total reported transiting time from origin to destination was 101 hours, confirmed by analysis of the ships GPS and AIS position reporting. Figure 4 provides a high-level overview of the CFAV QUEST arctic transit, as reported by the ships GPS. The remainder of this section focuses on the computation of the ETT for this transit using CFAV QUEST's GPS track and the USNIC weekly sea ice analysis chart issued on 16 JULY 2012.

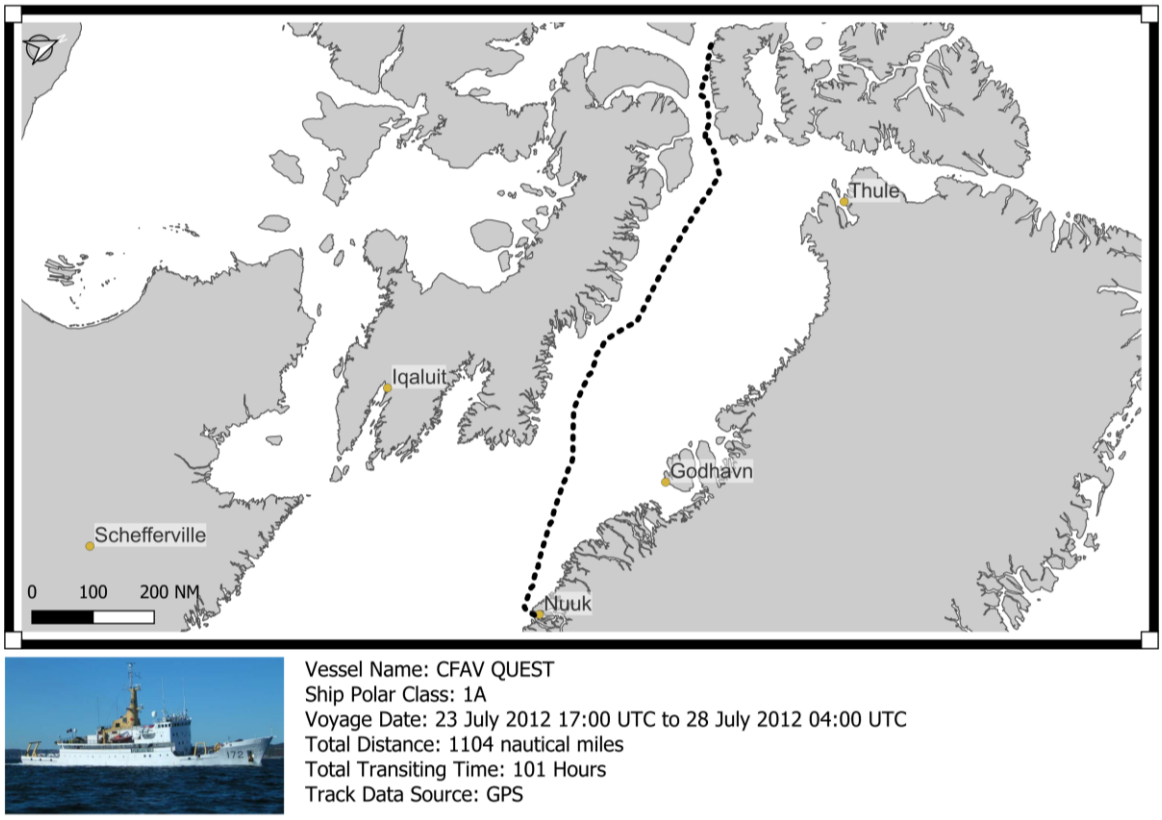

Figure 4: Overview of CFAV QUEST transit from Nuuk, Greenland to Gascoyne Inlet, Northwest Territories (NWT)

Figure 5 provides a map overview of the POLARIS RIO results for CFAV QUEST in the area of operations, computed using available USNIC sea ice analysis. For this particular transit, 65.7% of the total transit was in predominately ice-free water (RIO = 30), 33.1% was in normal ice conditions (0 <= RIO < 30) for a Polar Class 1A ship (370.4 nm), and 1.2% was in the high operational risk category (-30 < RIO <= -10).

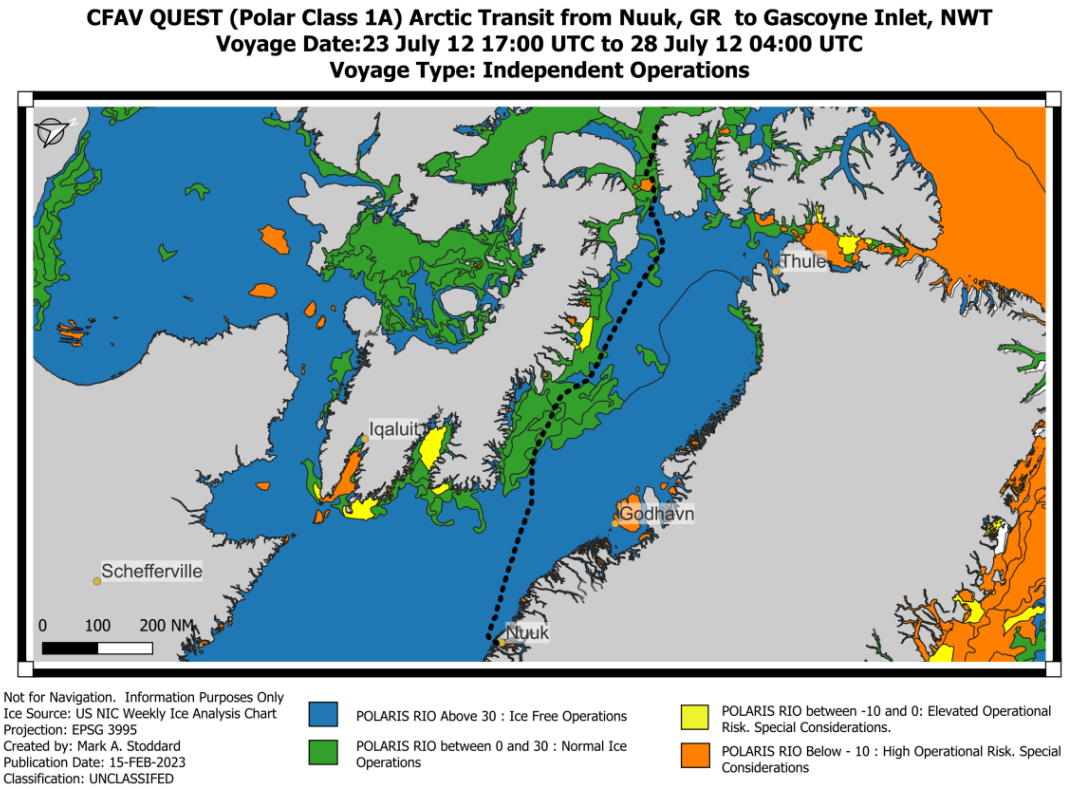

Figure 5: Overview of POLARIO RIO results for CFAV QUEST transit from Nuuk, GL to Gascoyne Inlet, NWT

We are able compute the ETT from Nuuk, GL to Gascoyne Inlet for CFAV Quest using Equation 3. To better illustrate the computation of the ETT, we provide the completed calculation below. In this case we have calculated the ETT using the POLARIS RIO results derived from the USNIC sea ice analysis chart issued on 16-JUL-2012 (calendar week 29) and the expected ship speed in different RIO categories from Table 3.

$$ETT_{jt} = \sum_{k=1}^{4} \frac{D_{jtk}}{S_k} = ETT_{1A,29} = \frac{735.6}{13.1} + \frac{370.4}{9.4} + \frac{0}{5.4} + \frac{13.0}{2.9} + \frac{0}{1.5} = 100.1 \text{ hrs (4.17 days)}$$

The actual transit time for CFAV QUEST to complete this transit was approximately 101 hours. The actual transit time was derived from the ships GPS log, by selecting a start and end location that corresponds with the route shown in Figure 4 and 5. For this case, the ETT underestimated the actual transit time by 0.9 hours, which is an error of less than 1%.

5. Discussion

In this study we combined two years of historical AIS reports and POLARIS RIO results in an attempt to gain new insights into expected ship speed in ice-covered waters. The RIO value has been shown to provide the necessary environmental context to interpret AIS reported speeds in ice-covered waters, and to characterize expected ship speed in varying sea ice conditions. Our approach combines AIS geospatial data analysis techniques, sea ice risk assessment, and statistical methods to produce an expected ship speed curve. The POLARIS RIO speed curve can be used to determine the expected ship speed in different POLARIS RIO categories, allowing ship navigators to directly incorporate POLARIS RIO results into their transit time estimation process. The result is a transit time estimate for a pre-determined route that incorporates the expected increase and decrease in ship speed due to varying sea ice conditions and navigational risk.

There are several limitations to the current work that may limit the use of the results reported in this study. The first major limitation has to do with the AIS data set that was used for this study. The AIS data set only covered two years, and was geographically constrained to the Canadian Arctic. The results of this study could be improved by processing a larger AIS data set. Another limitation relates to the temporal resolution of the USNIC sea ice analysis used to compute the POLARIS RIO value for each AIS report. In our analysis we were forced to associate an AIS report with GPS time precision, with an analysis product that is produced on a weekly basis. The difference in temporal resolution undoubtedly creates some error in analysis. Lastly, due to the limited availability of ship ice class information we had to remove many of the AIS reports from our data set because the ice class of the ship could not be determined.

Future efforts to improve the results of this study could focus on expanding the size of the historical AIS data set used for the analysis of vessel speed. This could be achieved by increasing both the coverage time period, and geographic extent. For example, including AIS reports from the Russian Arctic would significantly increase the amount of AIS reports from ships operating in ice covered waters, which would help increase the statistical significance of the expected ship speed results. Another potential improvement to this study would be to use daily sea ice analysis products (with the required geographical coverage area), or even in-situ ship observations, to improve the accuracy of the POLARIS

RIO value computed for each AIS report. Increasing the accuracy of the POLARIS RIO result associated with each AIS report would help ensure that the reported ship speed is associated with correct RIO result category. More work is also required to examine a larger number of historical transits in ice-covered waters and to compare our results with the results of other studies examining ship speed prediction in ice to better validate our ETT method.

It is also worth discussing how these results could be used to broadly support efforts to improve strategic navigation planning, and maritime Area-Based Management (ABM). The complex geography, and variable sea ice conditions, found in the Canadian Arctic Archipelago has a significant impact on maritime mobility and transit time. Estimating ship speeds in different ice regimes is critical to improving the estimation of travel time, fuel consumption, and emissions. Providing strategic planners with better tools to estimate the expected transit time for a voyage at different times of the year, and for different ship ice classes, has the potential to increase safety, save time and money, and to reduce shipping emissions. This is achieved by ensuring that ships have the necessary tools to plan to sail at more optimal times of the year, and that the most appropriate ship ice class is considered for the voyage.

Another use of these methods is to gain a better understanding of remoteness and accessibility of locations in ice-covered waters for a variety of ABM applications. For example, the remoteness of the Canadian Arctic, and lack of infrastructure, affects the timeliness of SAR response, especially maritime-based SAR response. Ships must be prepared to wait days before maritime-based SAR resources arrive at the incident location. SAR response time in ice-covered waters is heavily influenced by the geographic location of the incident and responding vessel, time of year, sea ice conditions, and the ship ice class of the vessel responding to the incident. Currently, the Polar Code requires that all vessels operating in polar waters be prepared to wait at least 5 days for SAR resources to arrive on-scene (World Maritime Organization, 2016). The methods presented in this study could be combined with the statistical analysis of historical POLARIS RIO results, SAR resource locations, and historical vessel traffic data, to compute the expected SAR response time for different incident locations in the arctic at different times of the year. Once computed, the

expected transit time would provide an objective measure to examine marine-based SAR response, and the expected time to rescue.

6. Concluding Remarks

Estimating transit time between the origin and destination of a planned voyage is a common task in maritime navigation. The process of estimating transit time in the maritime domain is complicated by a multitude of environmental, and other external factors, affecting ship speed and its follow-on impact on transit time. In the Canadian Arctic, the great distances that are often traversed, and the variable sea ice conditions that are expected to be encountered, is another major factor that complicate arctic navigation and planning. In this paper we have presented a data-driven method to estimate expected ship speed in different POLARIS RIO categories using AIS data, USNIC sea ice analysis, and the POLARIS sea ice risk assessment methodology. When combined with knowledge of the POLARIS RIO results along a route, these results enable the computation of an accurate estimate of transit time. The proposed transit time calculation allows a navigator to explicitly account for the expected transit delays along a route due to varying sea ice risk and its impact on safe ship speed. The transit time validation case study has shown that the use of the proposed method produces accurate estimated transit times for independent ship operations in ice-covered waters. The proposed methods and results of this study have provided a step forward in overcoming the complexity of computing accurate transit time estimates in ice-covered waters.

REFERENCES

Aksenov, Y., Popova, E. E., Yool, A., Nurser, G., Williams, T. D., Bertino, L., & Bergh, J. (2017). On the future navigability of Arctic sea routes: High-resolution projections of the Arctic Ocean and sea ice. *Marine Policy, 75*, 300-317.

Alasia, A., Bedard, F., Belanger, J., Guimond, E., & Penny, C. (2017). *Measuring remoteness and accessibility: A set of indicies for Canadian Communities.* Statistics Canada. Retrieved from www.publications.gc.ca/pub?id=9.835126&sl=0

Andersson, M., & Johansson, R. (2010). Multiple Sensor Fusion for Effection Abnormal Behavior Detection in Counter Piracy Operations. *Proceedings of International Waterside Security Conference.*

ARCDEV. (1998). *Final Public report of the ARCDEV Project.* Retrieved from https://trimis.ec.europa.eu/sites/default/files/project/documents/arcdev.pdf

Arctic Council. (2009). *Arctic Marine Shipping Assessment 2009 Report.* Arctic Council.

Bilge, T. A., Fournier, N., Mignac, D., Hume-Wright, L., Bertino, L., Williams, T., & Teitsche, S. (2022). An Evaluation of the Performance of Sea Ice Thickness Forecasts to Support Arctic Marine Transport. *Journal of Marine Science and Engineering*(10), 265.

Boylan, B. (2021, September). Increased maritime traffic in the Arctic: Implications for governance of Arctic sea routes. *Marine Policy, 131*.

Cairns, W. (2005). AIS and Long Range Identification and Tracking. *Journal of Navigation*, 58:181-189.

Canadian Ice Service. (2009). *Canadian Ice Service Arctic Regional Sea Ice Charts in SIGRID-3 Format.* Boulder, CO: Natinoal Snow and Ice Data Centre.

Canadian Ice Service. (2021). *Ice climate normals for the northern Canadian waters 1991 to 2020.* Governement of Canada.

Cau, Y., Liang, S., Sun, L., Liu, J., Cheng, X., Wang, D., . . . Feng, K. (2022). Trans-Arctic shipping routes expanding faster than the model projections. *Global Evironmental Change, 73*.

Chamberlain, J., Yue, B., Parsons, G., & Mulvie, J. (2008). Advanced Remote Sensing for Better Bottom-Fast Ice Identification. *RADARSAT-2 Workshop.*

Chircop, A., Goerlandt, F., Pelot, R., & Aporta, C. (2024). *Area-Based Management of Shipping: Canadian and Comparative Perspectives.* Springer Cham. doi:https://doi.org/10.1007/978-3-031-60053-1

Collard, F., Mouche, A., Danilo, C., Chapron, B., Isern-Fontanet, J., Johannessen, J., & Backberg, B. (2008). *Routine High Resolution Observation of Selected Major Surface Currents from Space.* SEASAR.

Crawford, A., Stroeve, J., Smith, A., & Jahn, A. (2021). Arctic open-water periods are projected to lengthen dramatically by 2100. *Communications Earth & Environment, 2*(109). doi:https://doi.org/10.1038/s43247-021-00183-x

Crisp, D. (2004). *The State-of-the-Art in Ship Detection in Syntehtic Aperature Radar Imagery.* Adelaide, AS: Defence Science and Technology Organization.

Dahlbom, A., & Niklasson, L. (2007). Tragectory Clustering for Coastal Surveillance. *10th Conference of the International Soceity for Information Fusion.*

Department of Health and Aged Care. (2001). *Measuring remoteness: Accessibility/Remoteness Index of Australia (ARIA).* Government of Australia. Retrieved April 10, 2024, from https://www.nintione.com.au/?p=5335

Dijkstra, E. (1959). A note on two problems in connxion with graphs. *Numerische Mathematik, 1*(1), 269-271.

DNV-GL. (2014). *The Arctic - The nex frontier.*

Dolny, J. (2018). *Methodology for Defining Technical Safe Speeds for Light Ice-Strengthened Government Vessels Operating in Ice.* Ship Structure Committee. United States Coast Guard.

Dovey, K., Woodcock, I., & Pike, L. (2017). Isochrone Mapping of Urban Transport: Car-dependency, Mode-choice, and Design Research. *Planning Practice & Research, 32*(4), 402 - 416.

Eriksen, T., Hoye, G., Narheim, B., & Jenslokken, M. (2006). Maritime Traffic Monitoring using space-based AIS Recevier. *Acta Astronautica*, 58(10): 537-549.

Etienne, L., & Pelot, R. (2013). Simulation of maritime paths taking into account ice conditions in the Arctic. *Symposium for GIS and Computer Cartography for Coastal Zone Management (CoastGIS)*, (pp. 116-119).

European Commission. (2014). *Defining Proxy Indicators for Rural Development Programs.* Journal of the European Union.

Fedi, L., Etienne, L., Haury, O., Rigot-Muller, P., Stephenson, S., & Cheaitou, A. (2018). POLARIS in the Arctic. *Journal of Ocean Technology, 13*(4), 58-71.

Fedi, L., Faury, O., & Etienne, L. (2020). Mapping and analysis of maritime accidents in the Russian Arctic through the lens of the Polar Code and POLARIS system. *Marine Policy*(118), 1-9.

Finnish Transport Safety Agency. (2017). *Finnish ice classes equivalent to class notations of recognized classification societies and the determination of the ice classes of ships.* Helsinki, Finland: Trafi.

Fraser, D. (2020). A Change in the Ice Regime: Polar Code Implementation in Canada. In A. Chircop, F. Goerlandt, C. Aporta, & R. Pelot, *Governance of Arctic Shipping.* Springer Polar Sciences.

Fu, S., Zhang, D., Montewka, J., Yan, X., & Zio, E. (2016). Towards a probabilistic model for predicting ship besetting in ice in Arctic waters. *Reliability Engineering & System Safety*, 124-136.

Georlandt, F., Montewka, J., Zhang, W., & Kujala, P. (2017). An analysis of ship escort and convoy operations in ice conditions. *Safety Science, 95*, 198-209.

Goerlandt, F., & Pelot, R. (2020). An Exploratory Application of the International Risk Governance Council's Risk Governance Framework to Shipping Risks in the Canadian Arcitc. In A. Chircop, *Governance in Arctic Shipping.* Springer Polar Sciences.

Goerlandt, F., Montewka, J., Zhang, W., & Kujala, P. (2017). An analysis of ship escort and convoy operations in ice conditions. *Safety Science, 95*, 198-209.

Goerlandt, F., Montewka, J., Zhang, W., & Kujala, P. (2017). An analysis of ship escort and convoy operations in ice conditions. *Safety Science, 95*, 198-209.

Goerlandt, F., Montewka, J., Zhang, W., & Kujala, P. (2017). An Analysis of Ship Escort and Convoy Operations in ice Conditions. *Safety Science*, 198-209.

Government of Canada. (2019, June 25). *Canadian Coast Guard Search and Rescue and Canadian Coast Guard Auxiliary Evaluation Report*. Retrieved from Department of Fisheries and Oceans Canada: https://www.dfo-mpo.gc.ca/ae-ve/evaluations/11-12/SAR-CCGA-eng.htm#2.1

Greidanus, H., & Kourti, N. (2006). Findings of the CELIMS Project - Detection and Classification of Marine Traffic from Space. *Proceedings of SEASAR 2006.* Frascati, Italy.

Headland, R. (2022). *Transits of the Northwest Passage to End of the 2022 Navigation Season: Atlantic Ocean to Arctic Ocean to Pacific Ocean.* Scott Polar Research Institute. Cambridge University.

Heiberg, H. B., Reistad, M., & A., B. (2006). *Use of ASAR wave spectra in operational wave analysis and forcasting: report from the EnviWave project.* Oslo: Norweigian Meteorological Institute.

Higginbotham, J., & Grosu, M. (2014). The Northwest Territories and Arctic Maritime Development in the Beaufort Regimes. *CIGI Policy Brief*, 40:1-12.

Hirose, T., Kapfer, M., Bennett, J., Cott, P., Manson, G., & Solomon, S. (2008). Bottomfast Ice Mapping and the Measurement of Ice Thickness on Tundra Lakes using C-Band SAR Remote Sensing. *Journal of the American Water Resources Association*, 44(2): 285-292.

Howell, S., & Yackel, J. (2004). A Vessel Transit Assessment of Sea Ice Variability in the Western Arctic, 1969-2002: Implications for ship navigation. *Canadian Journal of Remote Sensing*, 30(2):205-215.

IACS. (2009). *International Association of Classification Societies Charter.* International Association of Classificaiton Socieities.

IACS. (2023). *Requires Concerning POLAR CLASS.* International Association of Classification Socieities.

Intergovernmental Oceanographic Commission of UNESCO. (2004). *SIGRID-3: A Vector archive formate for sea ice charts.* JCOMM Technical Report.

International Maritime Organization. (2004). *Regulation 19 - Carriage requirements for shipborne navigational systems and equipment.* London: International Maritime Organization.

International Maritime Organization. (2016). *International Code for Ships Operating in Polar Waters (POLAR CODE).* International Maritime Organization.

International Telecommunication Union. (2014). *Technical characteristics for an automatic identification system using time division multiple access in the VHF maritime mobile frequency band.* Geneva: International Telecommunication Union.

Kang, M., Lee, H., Yang, C., & Yoon, W. (2008). Estimation of Ocean Current Velocity in Coastal Area using RADARSAT-1 SAR Images and HF-Radar Data. IGRASS 2008.

Kazemi, S., Abhari, S., Lavesson, N., Johnson, H., & Ryman, P. (2013). Open Data for Anomaly Detection in Maritime Surveillance. *Expert Systems with Applications*, 40: 5719 - 5729.

Kennedy, A., Gallagher, J., & Aylward, K. (2013). *Evaluating Exposure Time Until Recovery by Location.* Ottawa, Ontario: National Research Council Canada.

Khan, B., Khan, F., Veitch, B., & Yang, M. (2018). An operational risk analysis tool to analyze marine transportation in Arctic waters. *Reliability Engineering & System Safety, 169*, 485-502. doi:https://doi.org/10.1016/j.ress.2017.09.014.

Kim, H., Jeong, S.-Y., Woo, S.-H., & Han, D. (2018). Study on the procedure to obtain an attainable speed in pack ice. *International Journal of Naval Architecture and Ocean Engineering*(10), 491-498. doi:https://doi.org/10.1016/j.ijnaoe.2017.09.004

Kotovirta, V., Jalonen, R., Axell, L., Riska, K., & Berglund, R. (2009). A system for Route Optimization in Ice-Covered Waters. *Cold Regions Science and Technology*(55), 52-62.

Kubat, I., & Timco, G. (2003). *Vessel Damage in the Canadian Arctic.* National Research Council of Canada.

Lack, D. A., & Corbett, J. J. (2012). Black carbon from ships: a review of the effects of ship speed, fuel. *Atmostpheric Chemistry and Physics*(12), 3985-4000.

Laxhammer, R. (2008). Anomaly Detection for Sea Surveillance. *11th International Conference on Information Fusion* (pp. 47-54). Fusion 2008.

Lee, H.-W., Roh, M.-I., & Kim, K.-S. (2021). Ship Route Planning in Arctic Ocean based on POLARIS. *Ocean Engineering*(234), 1-14.

Lehtola, V., Montewka, J., Goerlandt, F., Guinness, R., & Lensu, M. (2019). Finding safe and efficient shipping routes in ice-covered waters: A framework and a model. *Cold Regions Science and Technology*(165), 1-14. doi:https://doi.org/10.1016/j.coldregions.2019.102795

Lensu, M., & Goerlandt, F. (2019). Big Maritime Data for the Baltic Sea with a Focus on the Winter navigation System. *Marine Policy*, 53-65.

Li, F., Goerlandt, F., Kujala, P., Lehtiranta, J., & Lensu, M. (2018). Evaluation of selected state-of-the-art methods for ship transit simulation in various ice conditions based on full-scale measurement. *Cold Regions Science and Technology, 151*, 94-108. doi:10.1016/j.coldregions.2018.03.008

Liu, C., Musharraf, M., Li, F., & Kujala, P. (2022). A data mining method for automatic identification and analysis of. *Ocean Engineering*(266).

Liu, C., Musharraf, M., Li, F., & kujala, P. (2022). A data mining method for automatic identification and analysis of icebreaker assistance operation in ice-covered waters. *Ocean Engineering, 266*. doi:https://doi.org/10.1016/j.oceaneng.2022.112914

Lloyds of London. (2014). *Arctic Opening: Opportunity and risk inthe high north.* London.

Loptien, U., & Axell, L. (2014). Ice and AIS: ship speed data and sea ice forecasts in the Baltic Sea. *The Cryosphere*(8), 2409-2418.

Marchenko, N. A., Aandreassen, N., Kuznetsova, S. Y., Ingimundarson, V., & Jakobsen, U. (2018, March). TransNav. *Arctic Shipping and Risks: Emergency Categories and Response Capacities*.

Marchenko, N., Borch, O., Markov, S., & Andreassen, N. (2015). Maritime activity in the high north - The range of unwanted incidents and risk patterns. *International Conference on Port and Ocean Engineering under Arctic Conditions 2015.* POAC. Retrieved from http://hdl.handle.net/11250/2392588

Maritime Safety Committee. (2014a). *POLARIS – proposed system for determining operational limitations in ice.* IACS.

Maritime Safety Committee. (2014b). *Technical background to POLARIS.* IACS.

McCallum, J. (1996). *Safe Speed in Ice - An analysis of transit speed and ice decision numerals.* Ottawa, ON: Transport Canada.

Melia, N., Haines, K., & Hawkins, E. (2015). Improved Arctic sea ice thickness projections using bias-corrected CMIP5 simulations. *The Cryoshpere*, 2237-2251.

Melia, N., Haines, K., & Hawkins, E. (2016). Sea ice decline and 21st century trans-Arctic shipping routes. *Geophyscial Research Letters*(43), 9720-9728.

Monroe, K. R., & Maher, K. H. (1995). Psychology and Rational Actor Theory. *Political Psychology, 16*(1), 1-21. doi:https://doi.org/10.2307/3791447

Montewka, J., Goerlandt, F., Kujala, P., & Lensu, M. (2015). Towards probabilistic models for the prediction of a ship performance in dynamic ice. *Cold Regions Science and Technology*(112), 14-28.

Montewka, J., Goerlandt, F., Kujala, P., & Lensu, M. (2015). Towards Probabilitic Models for the Prediction of a Ship Performance in Dynamic Ice. *Cold Regions Science and Technology*(112), 14-28.

Montewka, J., Goerlandt, F., Lensu, M., & Guinness, R. (2019). Towards a hybrid model of ship performance in ice suitable for route planning purpose. *Proceedings of the Instituation of Mechanical Engineers, Part O: Journal of Risk and Reliability, 233*(1), 18-34. doi:10.1177/1748006X18764511

Mudryk, L. R., Dawson, J., Howell, S. E., Derksen, C., Zagon, T. A., & Brady, M. (2021, August). Impact of 1, 2, and 4 Degrees Celcius of Global Climate Wharing on Ship Navigation in the Canadian Arctic. *Nature Climate Change, 11*, 673 to 679.

Muller, M., Knol-Kauffman, M., Jeuring, J., & Palerme, C. (2023). Arctic shipping trends during hazardous weather and sea-ice conditions and the Polar Code's effectiveness. *npj Ocean Sustainability, 2*(12). doi:https://doi.org/10.1038/s44183-023-00021-x

National Snow and Ice Data Center. (2013, July 13). *Frequently Asked Questions on Arctic Sea Ice*. Retrieved April 19, 2023, from Arctic Sea Ice News and Analysis: https://nsidc.org/arcticseaicenews/faq/#1979average

National Snow and Ice Data Centre. (2015a). *Format for gridded sea ice information (SIGRID).* Boulder, CO: National Snow and Ice Data Centre.

Olsen, R., & Wahl, T. (2000). The Role of Wide Swath SAR in High-Latitude Coastal Management. *John Hopkins APL Technical Digest*, 20(1) 136-140.

Piercey, C., Kennedy, A., & Power, J. (2019). *Methodology for Estimating Exposure Time in Polar Regions.* National Research Council. doi:https://doi.org/10.4224/40002043

QGIS. (2023). *QGIS: A free and open source geographic information system*. Retrieved from https://qgis.org/en/site/

Renn, O., & Sellke, P. (2011). Risk, Society and Policy Making: Risk governance in a complex world. *International Journal of Performability engineering, 7*(4), 349-366.

Renn, O., Jaeger, C. C., Rosa, E. A., & Webler, T. (2000). The Rational Actor Paradigm in Risk Theories: Analysis and Critique. In M. Cohen, *RIsk in the Modern Age.* London: Palgrave Macmillan. doi:https://doi.org/10.1007/978-1-349-62201-6_2

Rhodes, B., Bomberger, N., Seibert, M., & Waxman, A. (2005). Maritime Situation Monitoring and Awareness using Learning Mechanisms. *Proceedings of IEEE Military Communications Conference.*

Roy, J. (2010). Rule-Based Expert Systems for Maritime Anomaly Detection. *SPIE 7666, Sensors and Command, Control, Communications, and Intelligence (C3I) Technologies for Homeland Security and Homeland Defense.*

Runge, H., Breit, H., Eineder, M., Schulz-Stellenfleth, J., Bard, J., & Romeiser, R. (2004). Mapping of Tidal Currents with SAR Along Track Interferometry. *IGARSS '04*.

Schrijver, A. (1998). *Theory of Linear and Interger Programming.* John Wiley $ Sons.

Siljander, M., Venalainen, E., Goerlandt, F., & Pellikka, P. (2015). GIS-based cost distance modelling to support strategic maritime search and rescue planning: A feasibility study. *Applied Geography, 57*, 54-70.

Simila, M., & Lensu, M. (2018). Estimated the Speed of Ice-Going Ships by Integrating SAR Imagery and Ship Data from an Automatic Identification System. *Remote Sensing*(10), 1-23.

Smith, C., & Stephenson, S. (2013). New tans-arctic shipping routes navigable by mid-century. *Proceedings of the National Academy of Sciences of the United States of America (PNAS)*, 110:E1191.

Smith, L., & Stephenson, S. (2013). New Trans-Arctic Shipping Routes Navigable by Midcentury. *Proceedings of the National Academy of Sciences - PNAS*, 1191-1195.

Snider, D. (2012). *Polar Ship Operations - A practical guide.* London: The Nautical Institute.

Somanathan, S., Flynn, P. C., & Szymanski, J. (2006). The Northwest Passage: A Simulation. *Proceedings of the 2006 Winter Simulation Conference*, (p. 7).

Spire Maritime. (2023). *Historical AIS Data*. Retrieved from Spire: https://spire.com/maritime/solutions/historical-ais-data/

Statistics Canada. (2016). *Data Products, 2016 Census*. Retrieved from Statistics Canada Census Program: https://www12.statcan.gc.ca/census-recensement/2016/dp-pd/index-eng.cfm

Stephenson, S. R., Smith, L. C., & Agnew, J. A. (2011). Divergent long-term tranjectories of human access to the Arctic. *Nature Climate Change*, 156-160.

Stoddard, M. A., & Pelot, R. (2020). Historical Maritime Search and Rescue Incident Data Analysis. In *Governance of Arctic Shipping.* Springer Polar Sciences.

Stoddard, M. A., Etienne, L., Pelot, R., Fournier, M., & Beveridge, L. (2018). From Sensing to Sense-making: Assessing and Visualizing Ship Operational Limitations in the Canadian Arctic Using Open-Access Ice Data. In L. P. Hidlebrand, L. W. Brigham, & T. M. Johansson, *Sustainable Shipping in a Changing Arctic* (pp. 99-113). Springer.

Stoddard, M. A., Pelot, R., Etienne, L., & Goerlandt, F. (2023). Determining Ship Speeds in Ice using the Polar Operational Limitation Assessment Risk Indexing System (POLARIS). *TBD*, 1-18.

Stoddard, M. A., Pelot, R., Etienne, L., & Goerlandt, F. (2023). Polar Class Ship Speeds in Ice: Obersvation and Analysis. *TBD*, 1-7.

Stoddard, M., Etienne, L., Fournier, M., Pelot, R., & Beveridge, L. (2016). Making sense of Arctic maritime traffic using the Polar Operational Limits Assessment Risk Indexing System (POLARIS). *Earth and Environmental Science*, 1-8.

Stoddard, M., Pelot, R., Goerlandt, F., & Etienne, L. (2023). Making Sense of Marine-Based Search and Rescue Response Time using Network Analysis. *TBD*, 1-29.

Tan, X., Su, B., Riska, K., & Moan, T. (2013). A six-degree-of-freedom numerical model for level ice-ship interaction. *Cold Regions Science and Technology, 92*, 1-16.

Tran, T., Browne, T., Musharraf, M., & Veitch, B. (2023). Pathfinding and Optimization for Vessels in Ice: a literature review. *Cold Regions Science and Technology*(211), 1-8.

Transport Canada. (1998). *Arctic Ice Regime Shipping System (AIRSS) Standards, TP 12259E.* Ottawa: Government of Canada.

Tremblett, A. J., Garvin, M. J., & Oldford, D. (2021). Preliminary Study on the Applicability of the POLARIS Methodology for Ships Operating in Lake Ice. *Proceedsings of the 26th International Conference on Port and Ocean Engineering under Arctic Conditions*, (p. 12). Moscow.

U.S. National Ice Center. (2022). *U.S. National Ice Center Arctic and Antarctic Sea Ice Charts in SIGRID-3 Format, Version 1.* Boulder, Colorado.

U.S. National Ice Centre. (2023). *Arctic Ice Products*. Retrieved from https://usicecenter.gov/Products/ArcticHome

Vachon, P. (2006). Ship Detection in SAR Imagery. *Proceedings of OceanSAR 2006 - Third Workshop on Coastal and Marine Applications of SAR.* St. John's, NL.

Wang, C., Ding, C., Yang, Y., & Dou, T. (2022). Risk Assessment of Ship Navigation in the Northwest Passage: Historical and Projection. *Sustainability*(14). doi:https://doi.org/10.3390/su14095591

Wang, F., & Xu, Y. (2011). Estimating O–D travel time matrix by Google Maps API: implementation, advantages, and implications. *Annals of GIS, 17*(4), 199-209.

Wang, Y., Zhang, R., & Qian, L. (2018). An Improved A* Algorithm Based on Hesitant Fuzzy Set Theory for Multi-Criteria Arctic Route Planning. *Symmetry*(10), 1-20.

Wei, T., Yan, Q., Qi, W., Ding, M., & Wang, C. (2020). Projections of Arctic sea ice conditions and shipping routes in the twenty-first century using CMIP6 forcing scenarios. *Evironmental Research Letters*(15), 1-10.

Weick, K. E., & Sutcliffe, K. M. (2005). Organizing and the Process of Sensemaking. *Organization Science, 16*(4), 409-421.

Wilbrink, J. G. (2017). *Remoteness as a proxy for social vulnerability in Malawian Traditional Authorities: An open data and open-source approach.* The Hague - Netherlands: Delft University.

Williams, T., Korosov, A., Rampal, P., & Olason, E. (2021). Presentation and Evaluation of the Arctic Sea Ice Forecasting System neXtSIM-F. *The Cryoshpere*(15), 3207-3227.

Wilson, K. (2004). Shipping in the Canadian Arctic: Other possible climate change scenarios. *Proceedings of IGARSS'04: Geoscience and Remote Sensing*, 3: 1853.

Wilson, K., Falkingham, H., Melling, H., & De Abreu, R. (2004). Shipping in the Canadian Arctic: Other possible climate change scenarios. *Proceedings of IEEE International Symposium on Geoscience and Remote Sensing*, 3: 1853-1856.

World Maritime Organization. (2016). *International Code for Ships Operating in Polar Waters (POLAR CODE).* World Maritime Oganization.

Wright, C. (2016). *Arctic Cargo: A history of marine transportation in Canada's North.* Marquis Book Printing.

Xi, Y., Miller, E. J., & Saxe, S. (2018). Exploring the Impact of Different Cut-Off Times on Isochrone Measurements of Accessibility. *Transportation Research Record, 2672*(49), 113-124.

Appendix 4: An approach to Support Strategic Route Analysis in ice-covered waters using the Ice Risk-Adjusted Estimated Time of Arrival (I-ETA)

Stoddard, M.A., Pelot, R., Etienne, L., and Goerlandt, F. (2024). An approach to Support Strategic Route Analysis in ice-covered waters using the Ice Risk-Adjusted Estimated Time of Arrival (I-ETA). **DRAFT.**

Title: An Approach to Support Strategic Route Analysis in Ice-Covered Waters using the Ice Risk-Adjusted Estimated Time of Arrival (I-ETA)

Authors: Mr. Mark A. Stoddard, Dalhousie University

Dr. Ron Pelot, Dalhousie University

Dr. Floris Goerlandt, Dalhousie University

Dr. Laurent Etienne, ISEN University

Abstract

Navigation in ice-covered waters follows standard navigational practice, with special consideration for the presence of sea ice. Several risk assessment frameworks exist to assist ship operators with navigational decision-making in ice-covered waters, the most notable being the Polar Operational Limitations Risk Indexing System (POLARIS). POLARIS has proven to be a useful tool for not only tactical decision-making onboard ships, but also for the strategic appraisal of navigational risk over wide areas. This study presents a route generation methodology that combines POLARIS risk assessment, expected ship speeds in different POLARIS risk categories, and network optimization, to compute the fastest route and expected transit time between two locations in ice-covered waters. The end result of this transit analysis methodology is referred to as the Ice Risk-Adjusted Estimated Time of Arrival (I-ETA). Our results show that the fastest routes generated through the Canadian Archipelago using the proposed route analysis methodology converge on the commonly accepted strategic routes through the Canadian Arctic. Our study shows that by carefully accounting for the impact of sea ice risk on expected ship speed, it is possible to compute potential fastest routes and expected transit times over wide areas in the polar region. Using I-ETA method to support strategic route planning in ice-covered waters has the potential to reduce the expected transit time and increase ship safety. This is achieved by ensuring ship navigators have the necessary methods to determine the fastest route through ice-covered waters that minimize the total time a ship is exposed to unfavorable ice conditions.

KEYWORDS: POLARIS, Risk Assessment, Automatic Identification System, Arctic, Navigation, transit time

1. Introduction

Global climate change, particularly its impact on sea ice conditions in the polar regions, continues to drive interest in the evolving economic feasibility of arctic navigation and commercial shipping, see e.g (Melia, Haines, & Hawkins, 2015), (Aksenov, et al., 2017), (Boylan, 2021), and (Cau, et al., 2022). The reported decline in arctic sea ice is projected to continue, and that by mid-century the feasibility of trans-Arctic navigation and commercial shipping by a larger number of polar ship classes will increase. While arctic shipping may be becoming increasingly feasible, uncertain future sea ice conditions will continue to present a significant planning challenge to ship navigators. As the Arctic continues to open it will be increasingly important to have good methods to support strategic route analysis in ice-covered waters ((Crawford, Stroeve, Smith, & Jahn, 2021), (Wei, Yan, Qi, Ding, & Wang, 2020)).

Navigation in the polar regions, such as the Canadian Arctic, involves navigational practices typically accepted as standard, with additional considerations based on the expectation of the presence of ice (Snider 2012). Sea ice conditions exhibit a high degree of spatiotemporal variability, and can create significant disruption to ship movement. National sea ice analysis authorities, such as the Canadian Ice Service (CIS) and US National Ice Centre (USNIC) have been analyzing ice in polar waters for more than 60 years, and have compiled sea ice statistics for different regions in the arctic. Historical Information on the ice is gathered from an archive of weekly, bi-weekly or monthly sea ice analysis charts to compute the sea ice climate normals for polar waters (Canadian Ice Service, 2021). Ice climate normals are used to describe the historical sea ice freeze-up / break-up dates and typical ice conditions (ice concentration and predominant ice type). While useful for building a general understanding of expected sea ice conditions along a route, ice climate normals do not provide much insight into the navigational risk along a planned route due to complex interaction of ships and ice.

Operating ships in sea ice requires specialized knowledge and skill beyond that of many mariners (Snider, 2012). Knowledge of the environment, ice, available infrastructure, polar ship design and equipment, and ship handling in ice are all essential when planning routes in the Arctic. Several knowledge requirements for polar water operations are specified in

the International Maritime Organization (IMO) Polar Code. The Polar Code is the product of years of negotiations at the IMO to improve shipping safety in polar regions. The objective of the Polar Code is to address the unique hazards confronted by ships operating in the Arctic and Antarctic through the introduction of a variety of safety and pollution prevention measures, including those related to design and equipment, operations, crew training, and the protection of the marine environment (Fraser, 2020).

A key component of the Polar Code is the mandatory requirement for all ships intending to operating in the Arctic and Antarctic to carry a ship specific polar water operational manual (PWOM). This defines specific procedures for mitigating risks to and from ships operating in polar waters by ensuring that a vessel operates safely within in ship design limits. To help mitigate the risk to a ship from sea ice, the PWOM requires ship operators to specify a practical methodology for assessing ship operational limits in ice. One methodology accepted by the IMO is the Polar Operational Limit Assessment Risk Indexing System (POLARIS), developed by the International Association of Classification Societies (IACS). POLARIS has already proven to be a useful tool for not only tactical decision-making in ice, but also for the strategic appraisal of navigational risk over wide areas using information from sea ice analysis charts (Stoddard M. A., Etienne, Pelot, Fournier, & Beveridge, 2018), (Fedi, et al., 2018), (Tremblett, Garvin, & Oldford, 2021), and (Wang, Ding, Yang, & Dou, 2022).

In this paper we present a route generation methodology that combines POLARIS, expected ship speeds in ice, and network optimization, to generate the fastest route and expected transit time between two locations in ice-covered waters. We refer to the expected transit time of the fasted route generated using our methodology as the Ice Risk-Adjusted Estimated Time of Arrival (I-ETA). The results from our methodology help to address the challenge of generating routes over wide areas in complex polar navigating environments. Figure 1 provides an overview of the main components of the proposed route analysis methodology.

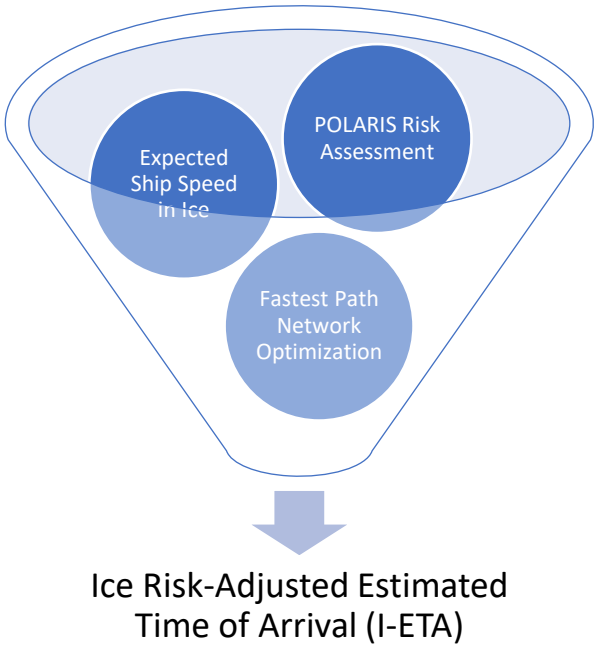

Figure 1: Overview of components of the proposed route generation methodology

The remainder of this paper is organized as follows. Section 2 provides a high-level overview of previous work on sea ice risk assessment, ship speeds in ice, and expected travel time in ice-covered waters, focusing on the unique challenges that complicate polar water navigation, and the tools and information sources used by navigators to overcome these challenges. Section 3 describes the methodologies proposed by this study to, (1) compute historical POLARIS RIO value statistics, (2) construction of an artic transportation analysis graph to support route analysis, and (3) fastest path network optimization. The I-ETA is intended to be used by navigators to support strategic route planning and analysis by providing a useful method to auto-generate routes and estimate transit times in ice-covered waters. Section 4 provides results to illustrate the use and utility of the proposed methods, focusing on their practical application in support of strategic route analysis. Section 5 and 6 provides a discussion and conclusion, respectively.

2. Background

2.1. Sea Ice Analysis

Sea ice exists in a variety of types and forms, which depend on the stage of development and the meteorological and other physical conditions present. Several authoritative sources

of sea ice analysis exist, including the United States National Ice Centre (USNIC), Canadian Ice Service (CIS), Danish Meteorological Institute (DMI), Icelandic Meteorological Office (IMO), and the Norwegian Meteorological Institute (NMI). To promote interoperability and data exchange, all national ice centers publish sea-ice charts in a standard World Maritime Organization (WMO) ice chart archive vector format, Sea Ice Grid (SIGRID-3) (U.S. National Ice Center, 2022). Operational sea ice charts show ice regimes as distinct polygons within a mapped region. Ice analysts working for national ice centers have access to a variety of high-resolution data sources to estimate the partial ice concentrations of various ice types in an ice regime, and encode the information according to a World Meteorological Organization standard (Intergovernmental Oceanographic Commission of UNESCO, 2004). The ice regime is used by ice analysts and navigators to describe the concentrations of one or more ice types in a sea ice analysis polygon.

2.2. Sea Ice Risk Assessment and Route Analysis

POLARIS provides a quantitative framework to assess the navigational risk to a ship operating in an ice regime. The concentration of each ice type within an ice regime is reported in tenths. For each ice type, POLARIS provides a Risk Index Value (RV) that is associated with each International Association of Classification Societies (IACS) Polar Class ship ice class. The collection of RVs present in an ice regime is referred to as the Risk Index Outcome (RIO), and is determined by calculating the linear sum of the RVs associated with each sea ice type present in a given ice regime, multiplied by the respective sea ice type concentration (in tenths):

$$RIO = C_1RV_1 + C_2RV_2 + \cdots + C_nRV_n \qquad \text{Equation 1}$$

where $C_1, C_2, \ldots, C_n$ are the concentrations of the ice types present in an ice regime and $RV_1, RV_2, \ldots, RV_n$ are the risk values provided by POLARIS. The RIO value is then evaluated, and a series of decision rules are applied to determine an appropriate operational limitation due to the presence of sea ice in the area of operation (Maritime Safety Committee, 2014b). The RIO score can be determined using in-situ observations of a local

ice regime, or it can be computed directly from sea ice analysis charts generated by national ice centers, such as the CIS and USNIC.

(Stoddard M. , Etienne, Fournier, Pelot, & Beveridge, 2016) presented a method to compute different statistical aggregations of POLARIS RIO results using a historical archive of CIS sea ice analysis charts. Their results were intended to support year-round strategic route analysis in the Canadian arctic. One limitation noted by the authors was that their results are limited to the Canadian Arctic because of their reliance on CIS sea ice analysis charts, which are only produced for the Canadian Arctic. To overcome national ice center product coverage area and temporal resolution limitations, researchers are increasingly using model data from sea ice forecasting models, and coupled atmosphere-ocean general circulation models (GCM), to determine sea ice thickness and concentration, e.g. (Melia, Haines, & Hawkins, 2015), (Montewka, Goerlandt, Kujala, & Lensu, 2015), and (Williams, Korosov, Rampal, & Olason, 2021). These sources typically provide researchers with a daily estimate of the average sea ice thickness (m) and corresponding sea ice concentration (%) at a specified spatial resolution (Bilge, et al., 2022).

(Smith & Stephenson, 2013) analyzed seven climate model projections of sea ice conditions, assuming two different climate change scenarios, to assess future changes in commercial shipping pathways from the Atlantic Ocean to the Pacific Ocean. Their analysis successfully combined the Transport Canada Arctic Ice Regime Shipping System (AIRSS) navigability assessment (Transport Canada, 1998), and data from different coupled atmosphere-ocean general circulation models (GCM), to generate trans-arctic shipping routes with expected transit time. Their routes, and estimated transit time results, reflect conditions for the peak late-summer shipping season only (September), and are driven solely by the projected reductions in sea ice thickness and concentration.

(Aksenov, et al., 2017) examined the feasibility of transporting cargo from Europe to Asia via trans-arctic shipping routes. The authors examined the navigability of common arctic sea routes, including the North West Passage (NWP), Northern Sea Route (NSR) and North Pole Route (NPR) using high-resolution projections of ocean and sea ice conditions. Arctic sea route accessibility and transit times by different ice class ships were determined using the Arctic Transport Accessibility Model (ATAM) (Stephenson, Smith, & Agnew, 2011).

The ATAM model assumes sea ice conditions are the primary factor impacting safe ship speeds and ship transit time in polar waters, and relies on the use of the AIRSS Ice Numeral (IN) to assess a ships ability to safely navigate in different ice regimes (Transport Canada, 1998). A ship safe speed for different IN was used to estimate the trans-arctic total transit time through varying ice conditions.

(Melia, Haines, & Hawkins, 2016) utilized simulations from several global climate models (GCMs) to examine the future arctic shipping prospects for two polar vessel classes; (1) Open Water (not-ice strengthened), and (2) Polar Class PC6 (capable of operating in medium first year ice). Shipping routes were calculated using a speed of 16 knots in open water and six-degree-of-freedom numerical model to determine slower speeds in ice that account for different polar class vessel capabilities in sea ice (Tan, Su, Riska, & Moan, 2013). The results of their work indicate that traditional trans-arctic routes (NSR, NWP, and NPR) will become faster throughout the 21st century, but interannual variability will remain a significant factor in route availability and selection.

(Fedi, Faury, & Etienne, 2020) discuss the use of the European Union's Copernicus database to produce ice condition statistics (thickness and concentration) over a 28-year period, on a daily basis. To compute the POLARIS RIO using these data sources, researchers must first apply a set of rules to convert average ice thickness to its equivalent ice stage of development. Once this mapping was complete, it was possible to calculate the RIO value by multiplying the risk value that corresponds to the stage of development by the ice concentration ((Wei, Yan, Qi, Ding, & Wang, 2020), (Lee, Roh, & Kim, 2021)). A limitation of this approach is that it does not consider partial concentrations of more than one ice type in an ice regime.

Similar to (Smith & Stephenson, 2013), (Wei, Yan, Qi, Ding, & Wang, 2020) generated arctic shipping routes using a two-step process, (1) calculate the technical accessibility of a grid cell by an ice classed ship, and (2) find the fastest route. Technical accessibility of a grid cell was determined using AIRSS with forecasted ice properties (thickness and concentration) from a GCM. A cell-based, least-cost path algorithm in a GIS was then used to determine the optimal path from origin to destination. More recently, (Lee, Roh, & Kim, 2021) proposed a cell-free seed-based genetic algorithm to obtain safe and economic

shipping routes through the Arctic Ocean, using POLARIS and the prediction of sea ice properties (thickness and concentration) from a GCM.

2.3. Ship Speeds in Ice

Several different approaches to determine the ship speed in ice conditions have been taken over the years, covering a range of empirical, semi-empirical, and data-driven methods. (McCallum, 1996) first proposed the use of polynomial fitting between minimum and maximum expected ship speeds for several Canadian Arctic Class (CAC) ships in different ice risk regimes. Ice risk was determined using the Transport Canada AIRSS. A major limitation of this early work was that the results were only produced for a limited number of ship ice classes, and only for positive AIRSS Ice Numerals. (Somanathan, Flynn, & Szymanski, 2006) were able to extend these early results using probabilistic modeling of sea ice conditions to specify a relationship between the AIRSS Ice Numeral and ship ice classification to calculate the expected ship speed in ice for a larger number of ship ice classes. (Smith & Stephenson, 2013) (Melia, Haines, & Hawkins, 2016), and (Aksenov, et al., 2017) further discuss the use of the AIRSS Ice Numeral to construct ship safe speed curves.

An increasing number of researchers have begun to favor the use Automatic Identification System (AIS) data to better understand expected ship speeds in ice. (Loptien & Axell, 2014) examined the relationship between AIS ship speed data and sea ice forecasts in the Baltic Sea to produce a mixed-effects model to predict vessel speed from forecasted ice properties (ice concentration, ice thickness, and ridge density). (Goerlandt, Montewka, Zhang, & Kujala, An Analysis of Ship Escort and Convoy Operations in ice Conditions, 2017) provide an analysis of AIS data collected in the Baltic Sea during the winter months to determine the expected ship speed for escort and convoy operations in ice-covered waters. (Simila & Lensu, 2018) discuss estimating the speed of ice-going ships by integrating Synthetic Aperture Radar (SAR) imagery and ship data from AIS. (Tremblett, Garvin, & Oldford, 2021) used shore-based AIS data collected in the North American Great Lakes region between 2010 and 2019 to examine the distribution of observed vessel speeds in different POLARIS RIO categories. The authors used CIS sea ice charts for the Great Lakes region to compute the POLARIS RIO values between 2010 and 2019. The authors

note that for their study they had to assume that there was an approximate ice thickness equivalence between lake ice and the sea ice types used in POLARIS. This assumption was required because POLARIS does not currently provide Risk Values for lake ice.

Lastly, (Stoddard M. A., Pelot, Etienne, & Goerlandt, Determining Ship Speeds in Ice using the Polar Operational Limitation Assessment Risk Indexing System (POLARIS), 2023) statistically analyzed two years of satellite AIS data collected in the Canadian Arctic to determine expected ship speed in different POLARIS RIO categories. The results of this study can be used to specify an expected ship speed in different POLARIS RIO result categories, enabling the computation of more realistic expected transit times in ice-covered waters. The expected ship speeds in different RIO result categories used for this study are taken from (Stoddard M. A., Pelot, Etienne, & Goerlandt, Determining Ship Speeds in Ice using the Polar Operational Limitation Assessment Risk Indexing System (POLARIS), 2023), and summarized in Table 1.

Table 1: Speed versus RIO Category (Stoddard M. A., Pelot, Etienne, & Goerlandt, Determining Ship Speeds in Ice using the Polar Operational Limitation Assessment Risk Indexing System (POLARIS), 2023)

RIO Category	Ship Speed (kt)
RIO >= 30	13.1
0 <= RIO < 30	9.4
-10 <= RIO < 0	5.4
-30 < RIO < -10	2.9
RIO = -30	1.5

2.4. Expected Transit Time in Ice Covered Waters

The simplest method used to estimate transit time is a basic distance divided by speed calculation, where total distance is known and the speed is fixed. This approach to transit time estimation is widely used in the maritime environment because ships are designed to operate at a particular speed to maximize fuel efficiency and minimize emissions. Ships may be forced to deviate from the maximum economic speed for a number of reasons, such as adverse weather, but it is expected that these deviations would only affect a small fraction of the total journey, and are therefore not explicitly accounted for in the estimate of expected transit time for a given route.

Unfortunately, this basic speed calculation does not lend itself easily to estimating transit time when varied ice conditions are expected along a route, and their impact on ship speed is unknown. Ship impacts with first year and multi-year are one of the main causes of vessel damage in polar waters (Kubat & Timco, 2003). It has been previously reported that ships will significantly reduce average speed when operating in areas of high total ice concentration in order to reduce the severity of damage from ice impact ((Goerlandt, Montewka, Zhang, & Kujala, 2017), (Fu, Zhang, Montewka, Yan, & Zio, 2016)). To minimize this risk of damage from ship impacts with ice, one approach is to break a voyage up into two primary route segments, (1) route segment to ice edge, and (2) route segment after crossing the ice edge (Snider, 2012). In this case, a ship would use its maximum economic speed up to the ice edge, and then a reduced average speed for the route segment after crossing the ice edge.

Simple route segmentation does not work as well for routes that span vast areas of highly variable sea ice conditions. As access to timely and high-quality sea ice analysis increases, it is becoming increasingly important for ship operators to incorporate this information into their route analysis processes, particularly for calculations of estimated time of arrival. (Stoddard M. A., Pelot, Etienne, & Goerlandt, Determining Ship Speeds in Ice using the Polar Operational Limitation Assessment Risk Indexing System (POLARIS), 2023) describe a computational method for estimating transit time that combines the POLARIS RIO results along a route with the expected vessel speed in different POLARIS RIO result categories. The authors refer to this as the Expected Transit Time (ETT) in ice-covered waters.

ETT is computed using the familiar transit distance divided by speed calculation, but it explicitly accounts for reductions in ship speed due to changing sea ice conditions along a ships route. This was achieved by performing a linear sum of the total distance a ship transits through different POLARIS RIO result categories over an entire route, divided by the expected ship speed in each POLARIS RIO result category (see Equation 2).

$$ETT_{jt} = \sum_{k=1}^{4} \frac{D_{jtk}}{S_k} \quad \forall \, j \in J, t \in T \qquad \text{Equation 2}$$

In Equation 2, the estimated transit time, ETT_{jt} , is the expected transit time by a ship with ice class *j*, in analysis period *t*. To compute ETT_{jt} we first generate D_{jtk}, which is a sparse matrix containing the distances travelled through POLARIS RIO category k, by ship ice class *j*, in analysis period *t*. The ship speed, S_k , represents the ship speed through POLARIS RIO category *k*. The indexes J, and T represent the set of all ship ice class j, and analysis period t. A more complete description of the ETT calculation can be found in (Stoddard M. A., Pelot, Etienne, & Goerlandt, Determining Ship Speeds in Ice using the Polar Operational Limitation Assessment Risk Indexing System (POLARIS), 2023).

3. Methods

3.1. Statistical Aggregation of POLARIS RIO Results

(Stoddard M. , Etienne, Fournier, Pelot, & Beveridge, 2016) presented a method to produce six different statistical aggregations of POLARIS RIO results using an open-access archive of CIS sea ice analysis charts. Their method was limited to the Canadian Arctic due to the CIS product coverage area limitations and only considered sea ice analysis from 2003 to 2014. To overcome this limitation, the proposed method uses the open access archive of USNIC circumpolar sea ice analysis charts to produce statistical aggregations of POLARIS RIO results reported over the climatological period from 1991 to 2020. In total, 1295 USNIC sea ice analysis charts were tessellated using a uniformly spaced analysis grid, with a cell resolution of 12.5 km x 12.5 km. Each sea ice analysis chart produced 4,212,296 georeferenced grid cells containing the sea ice analysis attributes from each chart. Gridded USNIC sea ice analysis charts were then grouped into bi-weekly analysis periods to enable the computation of different bi-weekly statistical aggregations of the POLARIS RIO

values. Figure 2 provides an overview of the processing flow to compute different statistical aggregations of the historical POLARIS RIO results.

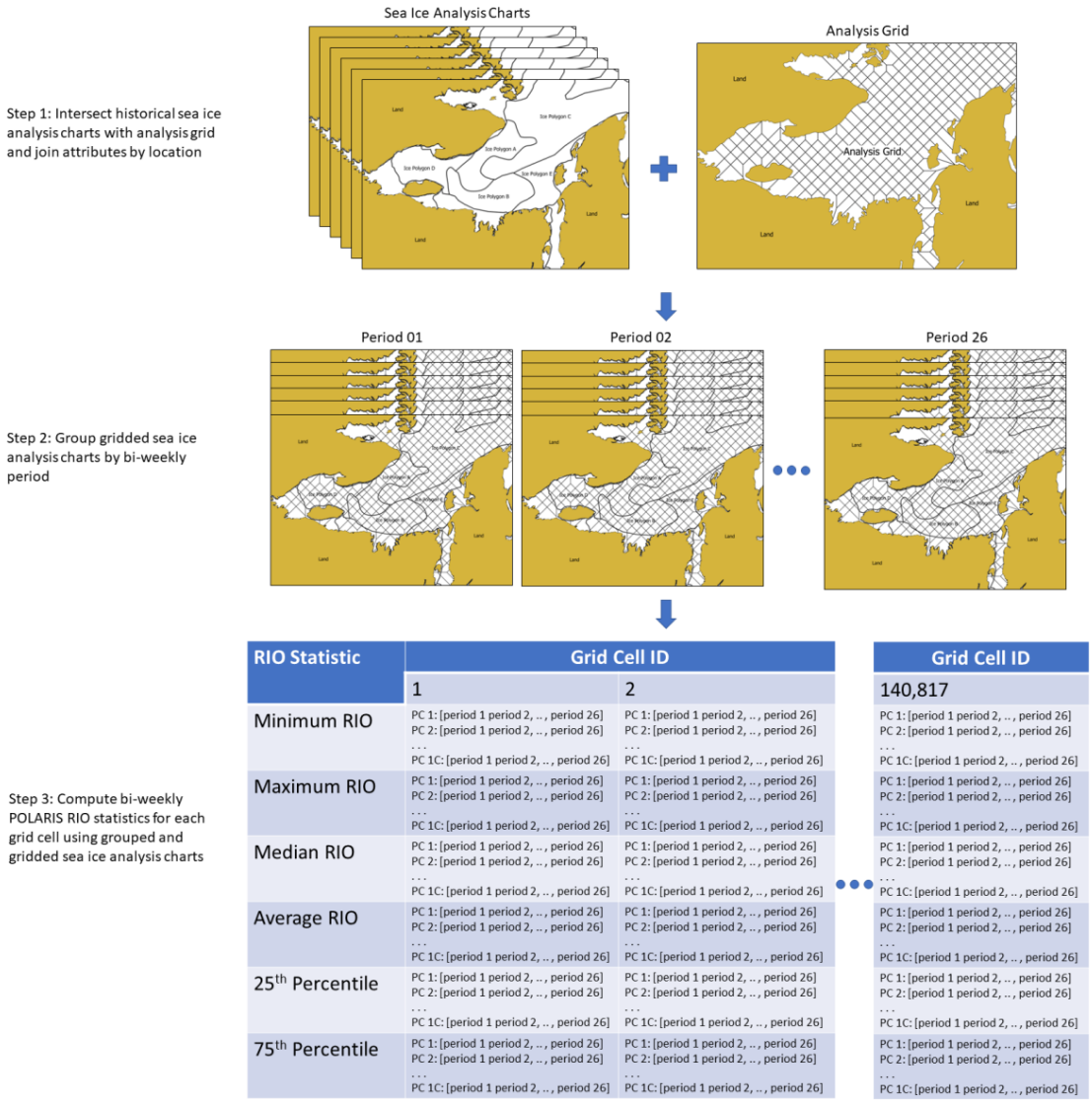

RIO Statistic	Grid Cell ID			Grid Cell ID
	1	2		140,817
Minimum RIO	PC 1: [period 1 period 2, .. , period 26] PC 2: [period 1 period 2, .. , period 26] . . . PC 1C: [period 1 period 2, .. , period 26]	PC 1: [period 1 period 2, .. , period 26] PC 2: [period 1 period 2, .. , period 26] . . . PC 1C: [period 1 period 2, .. , period 26]		PC 1: [period 1 period 2, .. , period 26] PC 2: [period 1 period 2, .. , period 26] . . . PC 1C: [period 1 period 2, .. , period 26]
Maximum RIO	PC 1: [period 1 period 2, .. , period 26] PC 2: [period 1 period 2, .. , period 26] . . . PC 1C: [period 1 period 2, .. , period 26]	PC 1: [period 1 period 2, .. , period 26] PC 2: [period 1 period 2, .. , period 26] . . . PC 1C: [period 1 period 2, .. , period 26]		PC 1: [period 1 period 2, .. , period 26] PC 2: [period 1 period 2, .. , period 26] . . . PC 1C: [period 1 period 2, .. , period 26]
Median RIO	PC 1: [period 1 period 2, .. , period 26] PC 2: [period 1 period 2, .. , period 26] . . . PC 1C: [period 1 period 2, .. , period 26]	PC 1: [period 1 period 2, .. , period 26] PC 2: [period 1 period 2, .. , period 26] . . . PC 1C: [period 1 period 2, .. , period 26]		PC 1: [period 1 period 2, .. , period 26] PC 2: [period 1 period 2, .. , period 26] . . . PC 1C: [period 1 period 2, .. , period 26]
Average RIO	PC 1: [period 1 period 2, .. , period 26] PC 2: [period 1 period 2, .. , period 26] . . . PC 1C: [period 1 period 2, .. , period 26]	PC 1: [period 1 period 2, .. , period 26] PC 2: [period 1 period 2, .. , period 26] . . . PC 1C: [period 1 period 2, .. , period 26]		PC 1: [period 1 period 2, .. , period 26] PC 2: [period 1 period 2, .. , period 26] . . . PC 1C: [period 1 period 2, .. , period 26]
25th Percentile	PC 1: [period 1 period 2, .. , period 26] PC 2: [period 1 period 2, .. , period 26] . . . PC 1C: [period 1 period 2, .. , period 26]	PC 1: [period 1 period 2, .. , period 26] PC 2: [period 1 period 2, .. , period 26] . . . PC 1C: [period 1 period 2, .. , period 26]		PC 1: [period 1 period 2, .. , period 26] PC 2: [period 1 period 2, .. , period 26] . . . PC 1C: [period 1 period 2, .. , period 26]
75th Percentile	PC 1: [period 1 period 2, .. , period 26] PC 2: [period 1 period 2, .. , period 26] . . . PC 1C: [period 1 period 2, .. , period 26]	PC 1: [period 1 period 2, .. , period 26] PC 2: [period 1 period 2, .. , period 26] . . . PC 1C: [period 1 period 2, .. , period 26]		PC 1: [period 1 period 2, .. , period 26] PC 2: [period 1 period 2, .. , period 26] . . . PC 1C: [period 1 period 2, .. , period 26]

Figure 2: Processing flow to compute the statistical aggregations of RIO value using historical archive of USNIC sea ice analysis charts

3.2. Arctic Transportation Graph Construction

To facilitate the computation of the fastest path it was necessary to first construct a network graph, consisting of nodes and arcs that overlap with the coverage area of our gridded POLARIS RIO results vector layer. Similar to (Smith & Stephenson, 2013), a vector layer of nodes was first created by generating a point at the centroid of each grid cell of the

gridded POLARIS RIO results vector layer. To produce the transportation graph, each node was then linked to the nodes in the surrounding square neighborhood by the 8 shortest line segments (arcs). Figure 3 illustrates the process of creating the transportation graph used for this study.

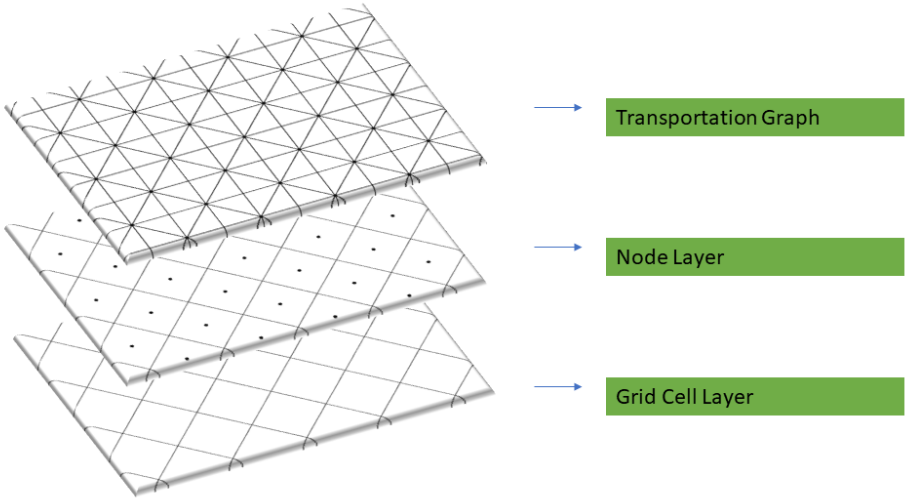

Figure 3: Spatial processing stack to produce the transportation graph

The graph was then geospatially processed to remove nodes and arcs in water depths less than 30 m, or within 5 nm of the coastline. The resulting arctic transportation graph consists of 140,817 nodes and 1,099,952 arcs. Figure 4 shows a zoomed in portion of the arctic transportation graph.

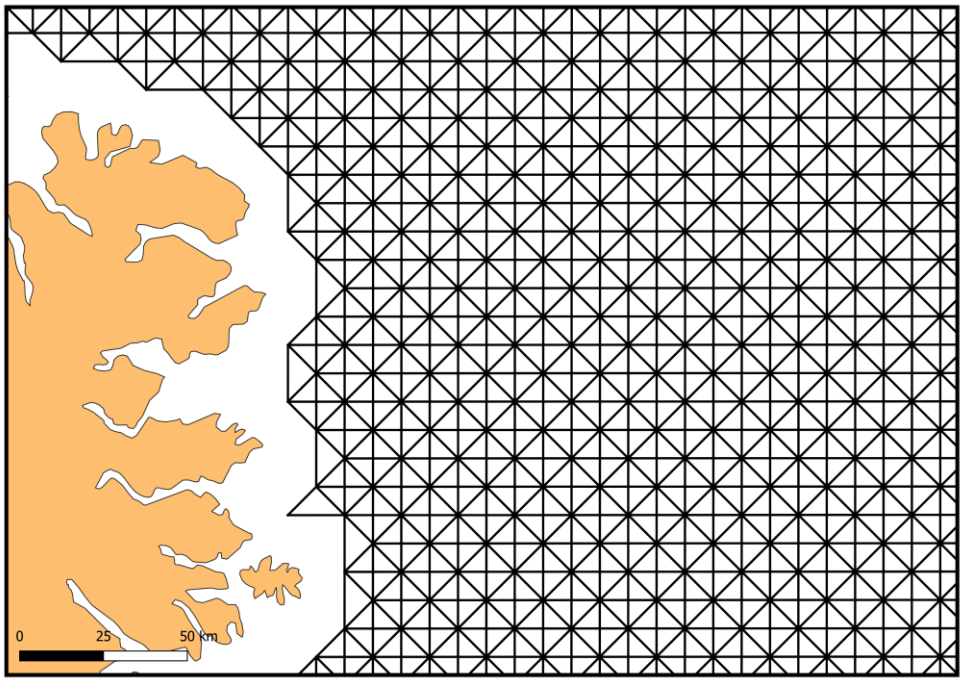

Figure 4: Arctic transportation graph constructed from uniformly spaced nodes and 8 shortest lines connecting neighboring nodes

After we created the arctic transportation graph, we then need to generate the POLARIS RIO results for each arc in the graph. This required a two-step process. The first step was to join the gridded POLARIS RIO results layer with the nodes of our arctic transportation graph. The next step was to compute the POLARIS RIO value for each arc in the graph. This was accomplished by taking the average of the POLARIS RIO value of the start node and the end node of the arc, see Equation 3. The final arc cost is the arc length divided by the expected speed associated with the POLARIS RIO value of the arc, see Equation 4.

$$Arc\ RIO = \frac{RIO_{arc\ start\ node} + RIO_{arc\ end\ node}}{2} \qquad \text{Equation 3}$$

$$Arc\ Cost = \frac{Arc\ Length\ (nm)}{Speed_k(kts)} \quad k = POLARIS\ RIO\ Result\ Category \qquad \text{Equation 4}$$

It is important to note that there are RIO values associated with each arc for every ship ice class and analysis period. This is because the selection of POLARIS RIO result depends on the ship ice class and time period being considered. As ice conditions change throughout the year, so does the POLARIS RIO value for a specific arc in the arctic transportation graph. The POLARIS result also changes based on the selection of ship ice class. Ships with more capability to operate in ice will have a higher POLARIS RIO value, indicating a more favorable operating condition. Ships with less capability will have a lower POLARIS RIO value, indicating a less favorable operating condition. Figure 5 provides a high-level overview of the geospatial processing stack and resulting graph with joined RIO analysis for each arc.

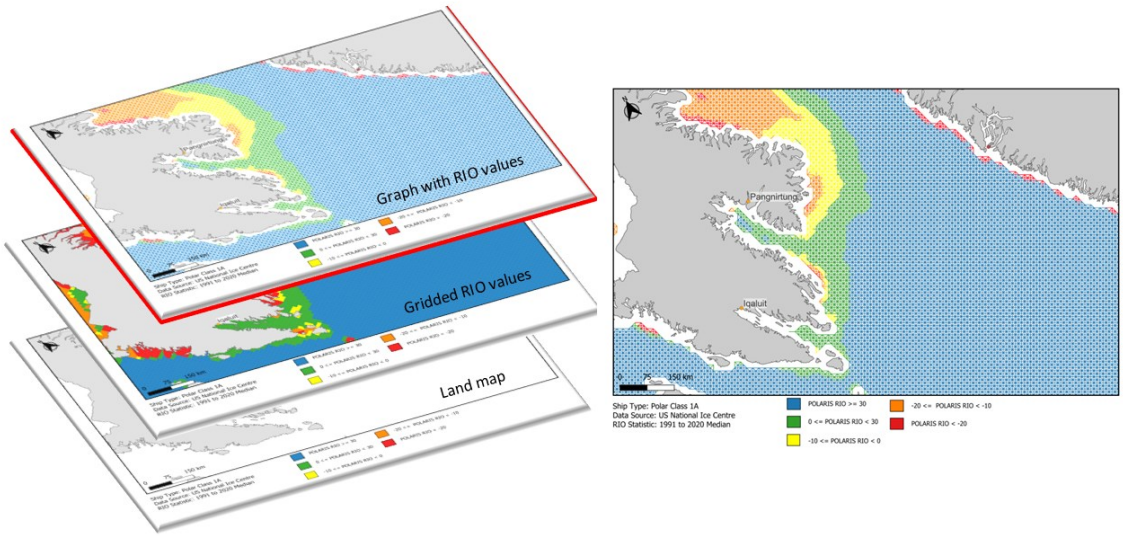

Figure 5: Geospatial processing stack to generate the arctic transportation graph with arc RIO values

3.3. Fastest Path Network Optimization

To compute the fastest path, we use the QGIS fastest path (point to point) function from the network analysis function list in the processing toolbox (QGIS, 2023). This function calculates the fastest path between any two points in our arctic transportation graph using Dijkstra's algorithm (Dijkstra, 1959). For our analysis graph, the arc cost is the expected transit time from the arc start node to end node, and have been pre-computed using Equation

2. The fastest path is then the selection of arcs from a start point to an end point that minimizes the total transit time. The transit time is determined by summing the transit time of all selected arcs forming the path from start to end location. We refer to the total transit time of the fastest path as the Ice Risk-Adjusted Estimated Transit Time (I-ETA). The I-ETA combines the results of the ETT calculation with network path optimization to produce an estimate of the expected total transit time between two locations in ice-covered waters.

1.1 FASTEST PATH ROUTE ANALYSIS

For this study we propose a method to support the strategic analysis of routes in ice-covered waters using the POLARIS RIO results. Once a route has been generated, we can use the POLARIS assessment to determine the proportion of a total transit through different POLARIS RIO result categories. This knowledge allows for the strategic analysis of routes based on a desired risk profile/tolerance for a route. For example, it is possible to set threshold values for each POLARIS RIO result category to limit a ships exposure to negative RIO conditions. Our method for calculating the fastest route does not currently constrain routes to favorable RIO result categories, rather, it applies a higher arc cost (transit time) to segments of a transit through areas of higher risk. This approach ensures that routes can still span areas of higher risk, but with the obvious consequence of increasing the total transit time. The use of the fastest path route analysis method allows one to quantitatively assess and visualize the overall risk of the route, based on the RIO result categories encountered along the voyage.

4. Results

4.1. Statistical Aggregation of POLARIS RIO results

The biggest computational challenge of this study was the calculation of different statistical aggregations of POLARIS RIO results over the climatological period from 1991 to 2020, for the entire circumpolar region. We computed the minimum, 1st quartile (Q1), mean, median, 3rd quartile (Q3), and maximum POLARIS RIO result overserved over our specified climatological period, on a bi-weekly basis. The POLARIS RIO result statistics

were computed for all IACS polar ship ice classes. We use the selection of POLARIS RIO value statistic, ships ice class, and analysis period, to produce a map visualization of the POLARIS RIO results. To further aid the creation of the map visualization, we categorize the POLARIS RIO results into five categories to simplify the map and the ease of interpretation. Figure 6 provides a map visualization of the 1st quartile RIO, Median RIO, and 3rd quartile RIO value for a Polar Class 1A ship in analysis period 15 (mid July). The 1st quartile result represents less a less favorable RIO result, while the 3rd quartile result represents a more favorable RIO result. We can see that the selection of RIO statistic has a significant impact on the expected navigability of the area.

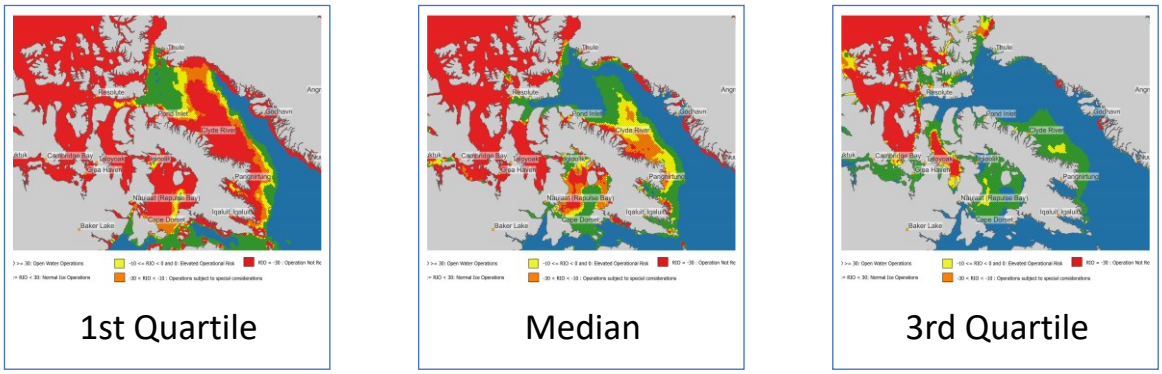

Figure 6: Map visualization of different POLARIS RIO statistics for a Polar Class 1A ship in analysis period 15 (mid-July)

4.2. Fastest Route in Ice-Covered Water

Our method to compute the fastest route in ice-covered water produces the most significant results for this study. Figure 7 provides an overview of the fastest route between a start and end location in the Eastern Arctic for a Polar Class 1A ship during four different bi-weekly analysis periods (1, 7, 13, and 22). The 1991 to 2020 median RIO value was used to assess the navigational risk throughout the year for a Polar Class 1A ship. The figure shows how the fastest route changes throughout the year depending on the POLARIS RIO values present during the specified analysis period. We can also see that at certain times of the year there is no feasible path between the specified start and end location of the route.

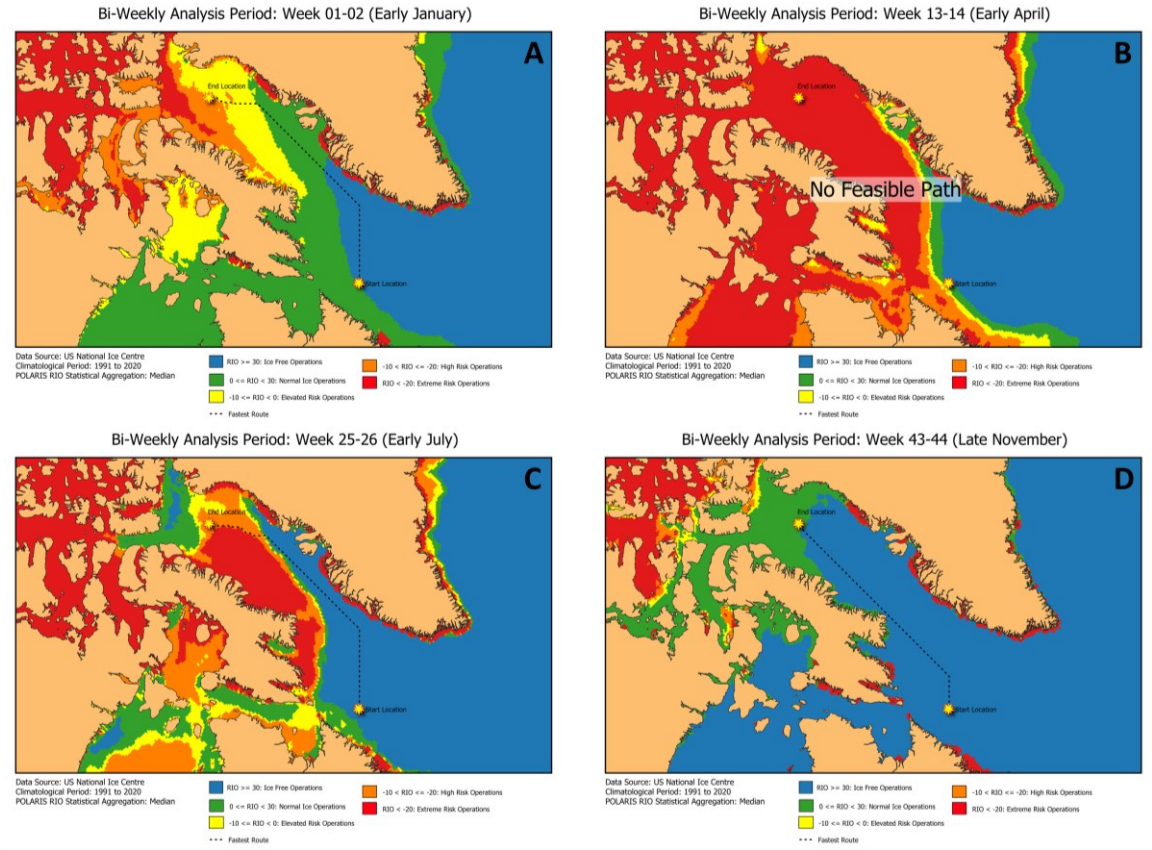

Figure 7: Overview of the fastest route and expected transit time between two locations in the arctic.

Figure 8 provides a bar chart of the year-round I-ETA between the start and end location shown in the previous figure. We can observe that for a significant portion of the year there is no feasible route for a Polar Class 1A ship between the start and end location. This would indicate that the severity of sea ice conditions, and associated navigational risk, exceeds the safe operating limits of a Polar Class 1A ship during that time.

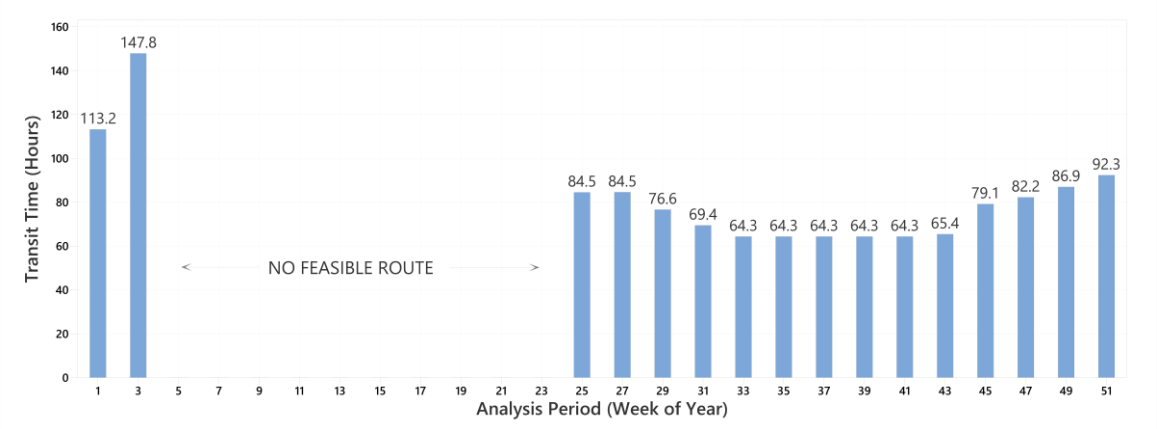

Figure 8: Summary of the year-round I-ETA results between the start and end location identified in Figure 6.

It is also possible to compare I-ETA results for different ship ice classes. In Figure 9 we compare the year-round I-ETA for the same start and end location for a Polar Class 1A and Polar Class PC5 ship using a multi-line plot. For awareness, a Polar Class 1A is capable of summer/autumn operation in thin first-year ice (ice thickness from 30 to 70cm), while a Polar Class PC5 is capable of year-round operation in medium first-year ice (ice thickness from 70 to 120cm). The enhanced ice operating capabilities of the PC5 vessel allow it to operate safely over a much wider range of sea ice conditions than a 1A vessel. The result is twofold; (1) A PC5 vessel can typically operate at higher speed when sea ice is present when compared to a 1A vessel, and (2) A PC5 vessel has a longer operating season, when compared to a 1A vessel.

Using the same start and end location from the Eastern Arctic transit scenario shown in Figure 7, we computed the fastest route and expected transit for Polar Class 1A and PC5. Figure 9 shows the expected transit time results as a multi-line plot. For a sizable portion of the year there is no feasible route between the start and end location for the Polar Class 1A vessel; starting in late January / early February (Week 5) and ending in late June (Week 25). Periods where no feasible route exists appear as areas of discontinuity in the line plot. Notable observations from the comparison of Polar Class 1A and PC5 ships are summarized in Table 2.

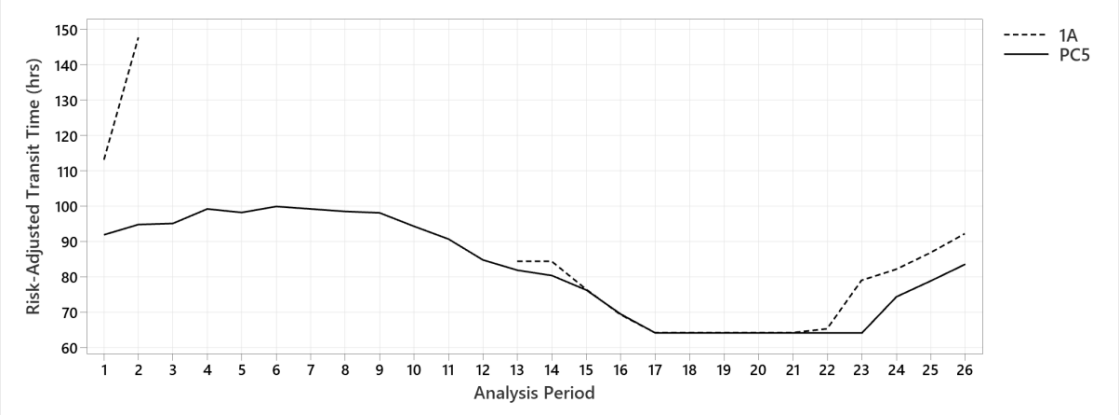

Figure 9: Comparison of the year-round I-ETA for a Polar Class 1A and PC5 ship between the same start and end location in the Eastern Arctic. Note: When no feasible route exists, the line is not drawn for that ship class.

Table 2: Summary of year-round I-ETA results for Polar Class 1A and PC5

	Polar Class 1A	**Polar Class PC5**
No Feasible Route (Period)	3 to 12	N/A
Maximum I-ETA (hours)	147.8	100.0
Maximum I-ETA (Period(s) of Occurrence)	2	6
Minimum I-ETA (hours)	64.3	64.3
Minimum I-ETA (Period(s) of Occurrence)	17 to 21	17 to 23

4.3. Trans-arctic Routes and I-ETA

Trans-arctic routes provide a challenging case for our strategic route analysis method due to the vastness of the area to be transited. The complex geography, and varied sea ice condition one would expect to encounter, creates a unique challenge for computing the fastest route. In this section we focus on the auto-generation of a trans-arctic route between a specified start location in the Northwest Atlantic, south of Greenland, and end location located in the Chukchi Sea, North of Alaska. Figure 10 provides a map overview of the computer-generated fastest route between the specified start location and end location. The trans-arctic route shown in this figure was generated for Polar Class PC6 ship departing in

Week 37-38 (mid-September). The I-ETA for the fastest route was 275 hours (11.5 days), with a total transit distance was 3670 nautical miles.

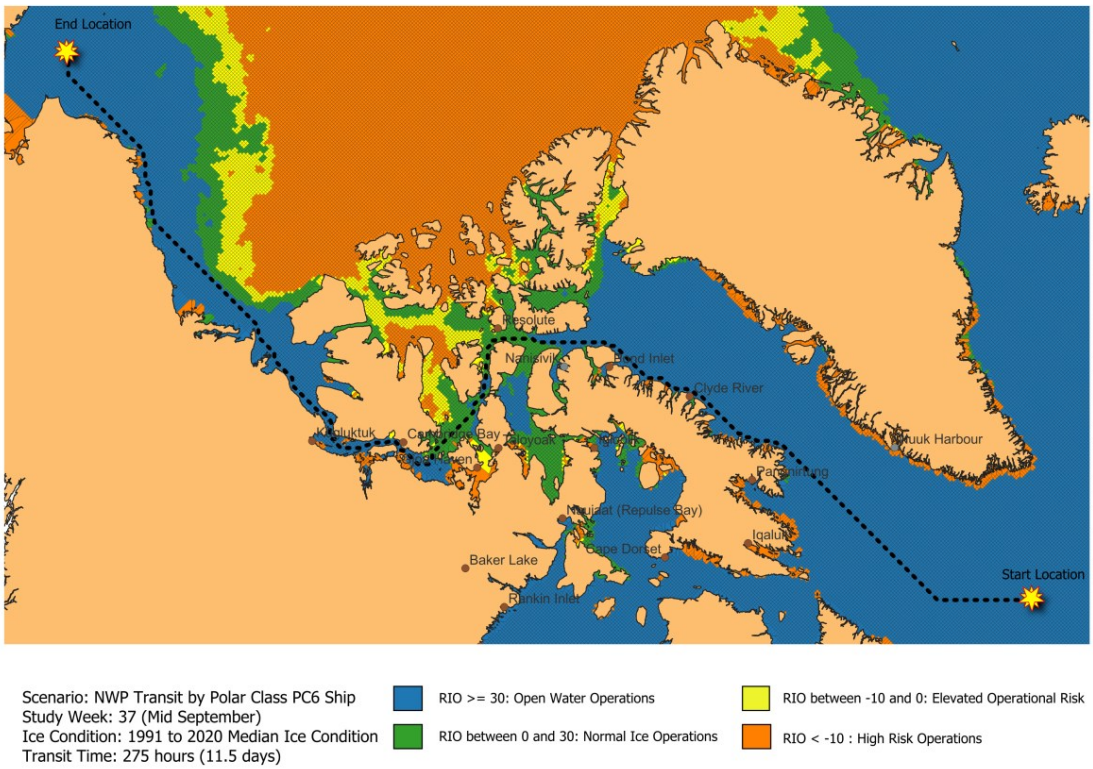

Figure 10: Computer-generated route from a specified start location in the Northwest Atlantic to end location in the Western Arctic using our strategic route analysis method for a Polar Class PC6 ship in Week 37-38 (minimum ice extent)

In addition to computing the I-ETA and total transit distance, we also compute summary statistics for the RIO categories encountered along the fastest route. For this transit, 89.1% of the route is in open water, and 10.9% is in RIO values between 0 and 29. The results show that for a PC6 ship navigating the NWP in Week 37 (mid-September), the majority of the route is in open water, with only 10.9 percent of the total transit distance occurring in areas where normal ice operations would be expected.

Figure 11 provides a composite map plot of the fastest route generated in each of the 26 bi-weekly analysis periods. The route through the NWP with the shortest transit time is highlighted in green, occurring in analysis period 19 (mid-September). The route through

the NWP with the longest transit time is highlighted in red, occurring in analysis period 8 (~mid-April). We also see that at certain times of the year, using the alternative NSR route is actually faster than taking the much shorter NWP route. The NSR is favored during analysis periods 1, 5 and 6 (March). Figure 12 shows the year-round I-ETA and polar route selection (NSR vs. NWP) for a Polar Class 6 ship. The maximum I-ETA is observed in late March /early April (maximum ice extent), and the minimum I-ETA is in mid-September (minimum ice extent).

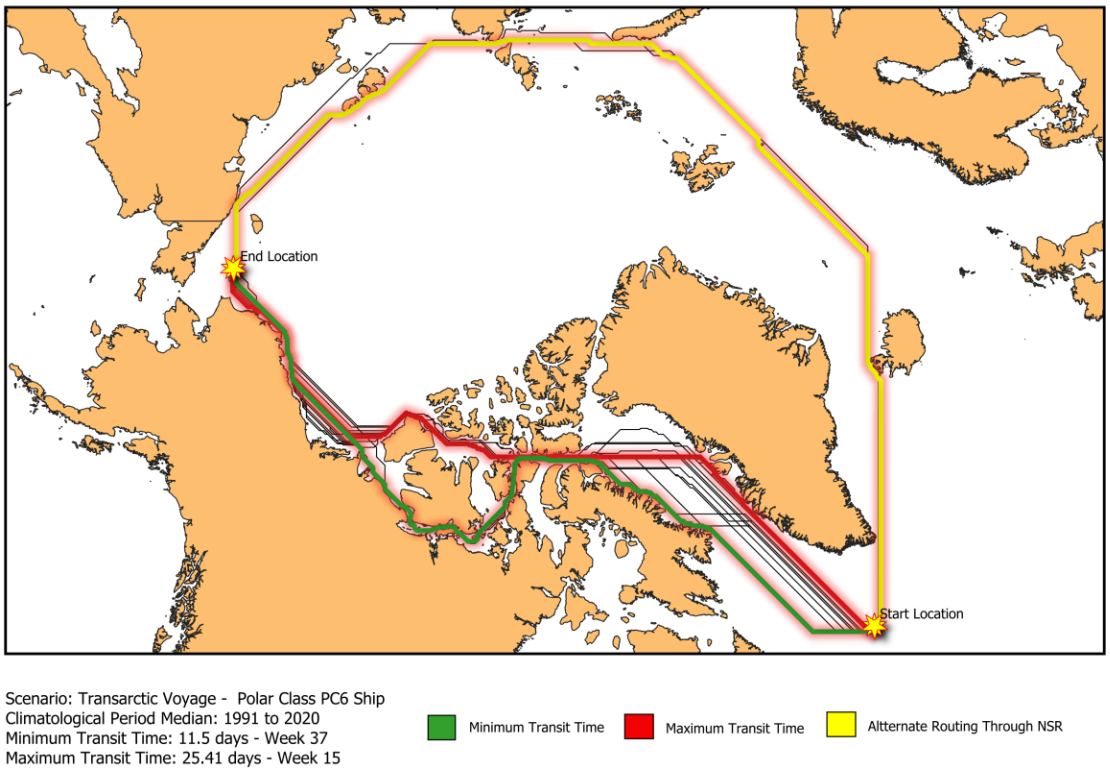

Figure 11: Composite plot of the fastest route through the Arctic, generated for each of the 26 bi-weekly analysis periods

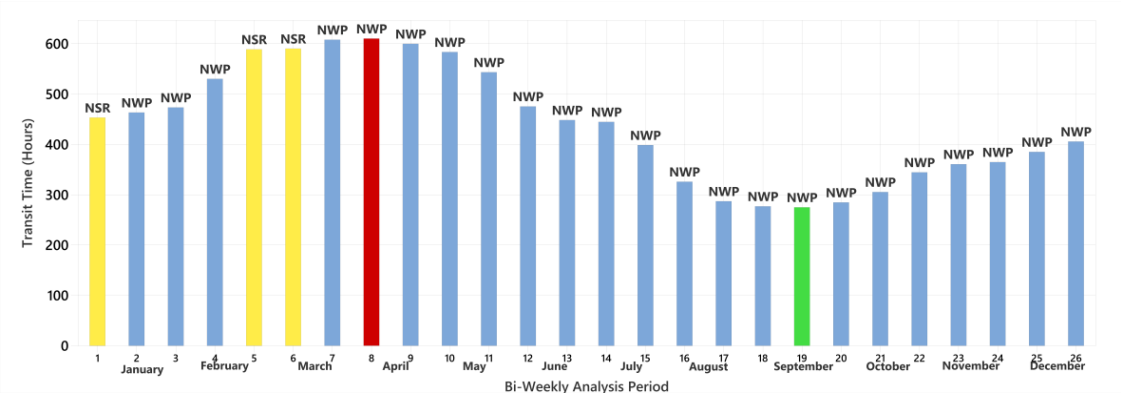

Figure 12: Bar chart of I-ETA results for a PC6 ship transiting from South West Greenland to Chukchi Sea in each of the 26 bi-weekly analysis periods. Green bar indicates minimum I-ETA. Red bar indicates maximum I-ETA. Yellow bar indicates use of the NSR. Blue bars indicate the I-ETA for all other analysis periods

5. Discussion

The focus of this study was on the development of a route generation methodology that can be used to produce fastest routes in ice-covered waters, and to provide an estimate of the expected transit time. We referred to the expected transit time of the fastest route produced using our methodology as the I-ETA. The results demonstrate the use and utility of the I-ETA method in the support of strategic route analysis. We are now able to compute the fastest routes throughout the polar region at different times of the year, for all ship ice classes.

Figure 13 shows a high-level representation of the common routes through the NWP and NSR, adapted from the Arctic Council AMSA report (Arctic Council, 2009). The computer-generated routes produced for our study generally follow these three paths, with subtle deviations in response to varying sea ice conditions through the year.

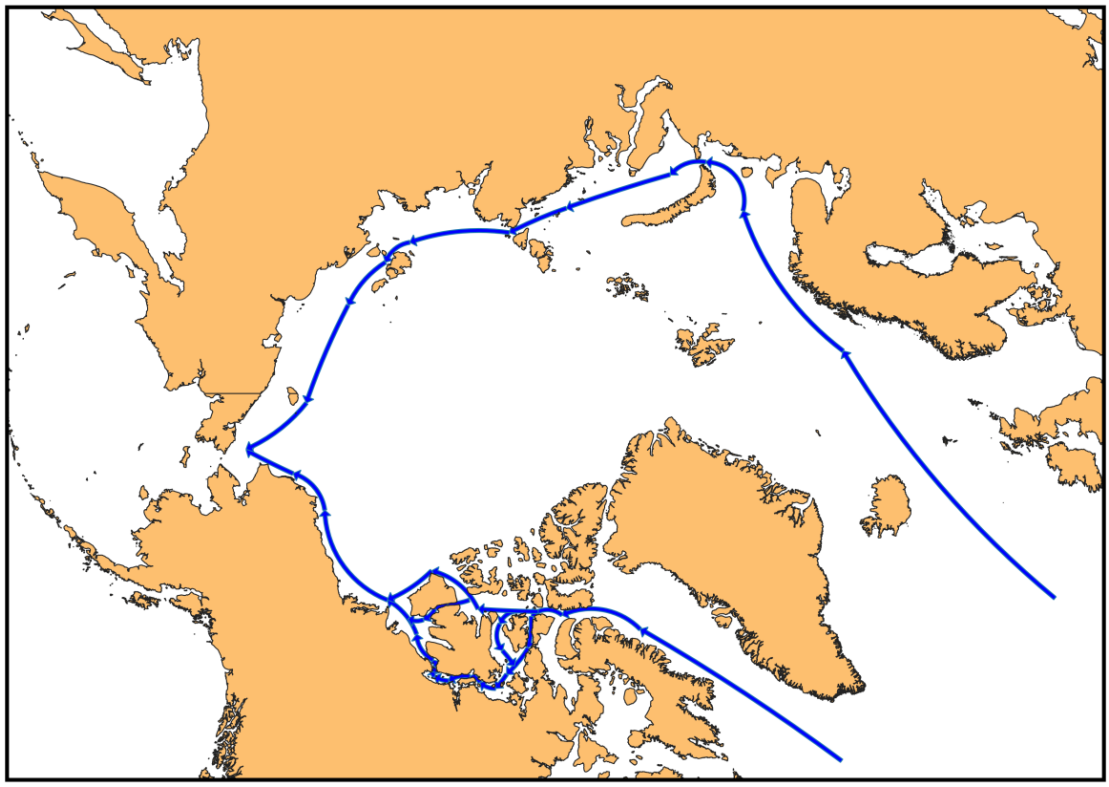

Figure 13: High-level representation of the most commonly used routes through the Northwest Passage and the Northern Sea Route

Figure 14 provides a heatmap visualization of the computer-generated routes for a PC6 ship over the 26 bi-weekly analysis periods, with a general overlay of the commonly accepted routes through the NWP previously discussed (Arctic Council, 2009). We see the convergence of the computer-generated routes on two of the primary routes through the NWP (Headland, 2022):

3. Davis Strait, Lancaster Sound, Barrow Strait, Viscount Melville Sound, McClure Strait, Beaufort Sea, and Chukchi Sea. This route is often characterized as the shortest, but most difficult way through the NWP due severe ice in vicinity of McClure Strait.
4. Davis Strait, Lancaster Sound, Barrow Strait, Peel Sound, Franklin Strait, Victoria Strait, Coronation Gulf, Amundsen Gulf, Beaufort Sea, and Chukchi Sea. This route is considered by many as the principal route through the NWP.

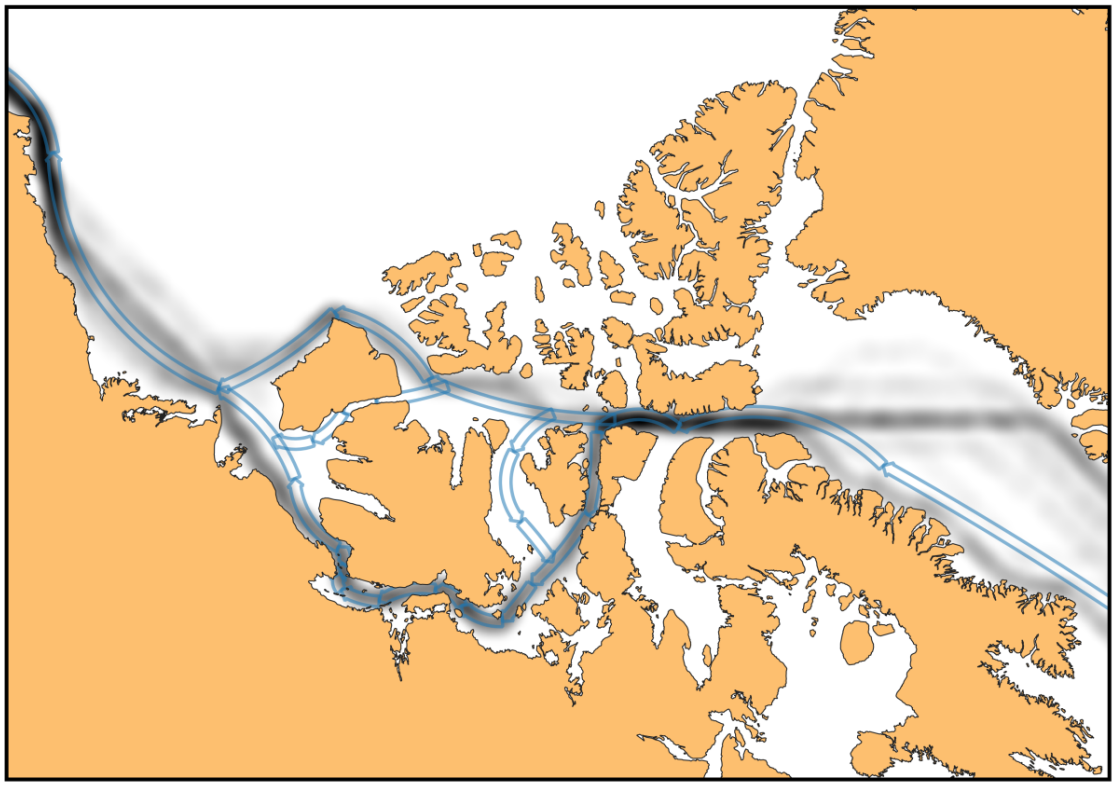

Figure 14: Heatmap of computer-generated routes for a PC6 ship in each of the 26 bi-weekly analysis periods with an overlay of the commonly accepted routes through the NWP

More than 60% of the routes generated for a PC6 transiting through the Canadian Arctic Archipelago followed the second primary route through the NWP previously identified. This route was consistently shown to be the fastest route during the Summer and Fall timeframe (Weeks 29 to Week 43). These results support the claim by (Headland, 2022), that this route is the principal route through the NWP.

The fastest routes generated for the winter months are likely not feasible for a PC6 ship when navigational risk is properly considered. The transit times during the months of December and June are more than double the fastest route generated during the period of minimum ice extent. This would indicate that there is a high degree of navigational risk associated with the route. Figure 15 illustrates the infeasibility of the routes generated during the winter months for a PC6 ship. The distribution of RIO categories encountered along the fastest path for a PC6 in Week 15 (mid-March) highlights the elevated navigational risk of the route. 48.4% (~ 1615 nm) of the total transit would be considered

elevated risk (-10 <= RIO < 0), with 15.3% (~ 500 nm) of the total transit in the high-risk category (-10 < RIO < -30). It is quite obvious that given the risk profile of the Week 15 fastest route, that the ships prolonged exposure to the elevated navigational risk would be intolerable.

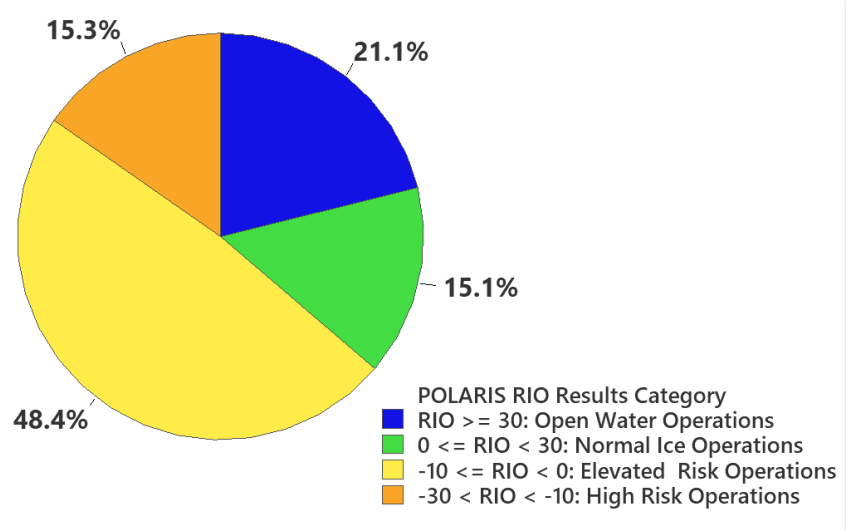

Figure 15: Distribution of RIO categories encountered along the fastest path through the NWP for a PC6 ship in Week 15, expressed as a percentage of total transit distance

Computing the fastest route during the winter months does offer some insight into the inter-annual variation in transit time through the year in the Arctic. As expected, we see transit times follow the same general trend as sea ice conditions. I-ETA is minimal when the sea ice is historically at its minimal extent. I-ETA is maximal when the sea ice is historically at its maximum extent.

There are several limitations to the results of this study that should also be mentioned. While we have computed several different statistical aggregations of historical POLARIS RIO, our results have focused on only the median RIO value. A useful follow-on analysis could take a deeper look at the use of other statistical aggregations of the RIO value to observe their impact on the fastest route and I-ETA. Also, we have not discussed the impact of ice breaker escort operations on the fastest path and I-ETA. In some situations, it might be possible that a short escort through high-risk ice conditions could significantly alter the optimal fastest route. The POLARIS assessment does have provisions to support escort operations, but these have not been considered in this study. (Liu, Musharraf, Li, & kujala,

2022) recently provided a data mining method for the identification and analysis of ice breaker assistance in ice-covered waters. This method could be used to isolate escort operations in our AIS data set to determine a new set of ship speed in different RIO categories that can be applied during escort operations. Future work could also focus on examining the relationship between I-ETA, expected fuel consumption, and emissions. Prolonged transits through harsh sea ice conditions can dramatically increase fuel consumption and emissions due to increases in engine utilization to achieved desired speeds. When these additional factors are considered, the fastest route may quickly become infeasible due to the amount of fuel available to complete the transit.

6. Conclusions

In this paper we have introduced several methods to enable strategic route analysis in ice-covered waters. By combining geospatial processing techniques with statistical analysis, we produced several different statistical aggregations of POLARIS RIO results observed over the climatological period from 1991 to 2020. We were then able to combine these results with network analysis methods, to compute the fastest route and expected transit time between two locations in ice-covered waters at different times of the year and for different ship ice classes. The output of this calculation was referred to as the I-ETA. The resulting computer-generated routes through the NWP showed good agreement with commonly accepted routes through the NWP. These results appear to indicate that navigational risk, assessed using POLARIS and USNIC sea ice analysis, has a strong influence on the computation of the fastest route in ice-covered waters. Generating acceptable shipping routes through complex navigation environments, such as the Canadian Arctic Archipelago, is a challenging problem. Our study has shown that understanding sea ice risk, and its impact on ship speed, is critical when generating strategic routes in ice-covered waters.

A current limitation of our model is that it generates a fastest route, with very little consideration for the overall risk associated with the route. We relied on the use of a cost function that simply increases the time to transit through areas of higher navigational risk. This has the unfortunate consequence of leaving it up to the navigator to then have to assess the feasibility of safely executing the computer-generated route. With this consequence in

mind, we have provided a method to evaluate a route based on the proportion of the total transit distance through different RIO result categories. This analysis occurs only after a route has been created, and does not help inform the calculation of the fastest route. The selection of optimal routes in polar waters remains a hard problem, requiring a combination of ice navigation experience, high quality data, and robust decision support tools. The methods and results presented in this paper provide some insight into the tools and techniques that are required to advance research in the area of strategic route analysis in ice-covered waters.

REFERENCES

Aksenov, Y., Popova, E. E., Yool, A., Nurser, G., Williams, T. D., Bertino, L., & Bergh, J. (2017). On the future navigability of Arctic sea routes: High-resolution projections of the Arctic Ocean and sea ice. *Marine Policy, 75*, 300-317.

Alasia, A., Bedard, F., Belanger, J., Guimond, E., & Penny, C. (2017). *Measuring remoteness and accessibility: A set of indicies for Canadian Communities.* Statistics Canada. Retrieved from www.publications.gc.ca/pub?id=9.835126&sl=0

Andersson, M., & Johansson, R. (2010). Multiple Sensor Fusion for Effection Abnormal Behavior Detection in Counter Piracy Operations. *Proceedings of International Waterside Security Conference.*

ARCDEV. (1998). *Final Public report of the ARCDEV Project.* Retrieved from https://trimis.ec.europa.eu/sites/default/files/project/documents/arcdev.pdf

Arctic Council. (2009). *Arctic Marine Shipping Assessment 2009 Report.* Arctic Council.

Bilge, T. A., Fournier, N., Mignac, D., Hume-Wright, L., Bertino, L., Williams, T., & Teitsche, S. (2022). An Evaluation of the Performance of Sea Ice Thickness Forecasts to Support Arctic Marine Transport. *Journal of Marine Science and Engineering*(10), 265.

Boylan, B. (2021, September). Increased maritime traffic in the Arctic: Implications for governance of Arctic sea routes. *Marine Policy, 131*.

Cairns, W. (2005). AIS and Long Range Identification and Tracking. *Journal of Navigation*, 58:181-189.

Canadian Ice Service. (2009). *Canadian Ice Service Arctic Regional Sea Ice Charts in SIGRID-3 Format.* Boulder, CO: Natinoal Snow and Ice Data Centre.

Canadian Ice Service. (2021). *Ice climate normals for the northern Canadian waters 1991 to 2020.* Governement of Canada.

Cau, Y., Liang, S., Sun, L., Liu, J., Cheng, X., Wang, D., . . . Feng, K. (2022). Trans-Arctic shipping routes expanding faster than the model projections. *Global Evironmental Change, 73*.

Chamberlain, J., Yue, B., Parsons, G., & Mulvie, J. (2008). Advanced Remote Sensing for Better Bottom-Fast Ice Identification. *RADARSAT-2 Workshop.*

Chircop, A., Goerlandt, F., Pelot, R., & Aporta, C. (2024). *Area-Based Management of Shipping: Canadian and Comparative Perspectives.* Springer Cham. doi:https://doi.org/10.1007/978-3-031-60053-1

Collard, F., Mouche, A., Danilo, C., Chapron, B., Isern-Fontanet, J., Johannessen, J., & Backberg, B. (2008). *Routine High Resolution Observation of Selected Major Surface Currents from Space.* SEASAR.

Crawford, A., Stroeve, J., Smith, A., & Jahn, A. (2021). Arctic open-water periods are projected to lengthen dramatically by 2100. *Communications Earth & Environment, 2*(109). doi:https://doi.org/10.1038/s43247-021-00183-x

Crisp, D. (2004). *The State-of-the-Art in Ship Detection in Syntehtic Aperature Radar Imagery.* Adelaide, AS: Defence Science and Technology Organization.

Dahlbom, A., & Niklasson, L. (2007). Tragectory Clustering for Coastal Surveillance. *10th Conference of the International Soceity for Information Fusion.*

Department of Health and Aged Care. (2001). *Measuring remoteness: Accessibility/Remoteness Index of Australia (ARIA).* Government of Australia. Retrieved April 10, 2024, from https://www.nintione.com.au/?p=5335

Dijkstra, E. (1959). A note on two problems in connxion with graphs. *Numerische Mathematik, 1*(1), 269-271.

DNV-GL. (2014). *The Arctic - The nex frontier.*

Dolny, J. (2018). *Methodology for Defining Technical Safe Speeds for Light Ice-Strengthened Government Vessels Operating in Ice.* Ship Structure Committee. United States Coast Guard.

Dovey, K., Woodcock, I., & Pike, L. (2017). Isochrone Mapping of Urban Transport: Car-dependency, Mode-choice, and Design Research. *Planning Practice & Research, 32*(4), 402 - 416.

Eriksen, T., Hoye, G., Narheim, B., & Jenslokken, M. (2006). Maritime Traffic Monitoring using space-based AIS Recevier. *Acta Astronautica*, 58(10): 537-549.

Etienne, L., & Pelot, R. (2013). Simulation of maritime paths taking into account ice conditions in the Arctic. *Symposium for GIS and Computer Cartography for Coastal Zone Management (CoastGIS)*, (pp. 116-119).

European Commission. (2014). *Defining Proxy Indicators for Rural Development Programs.* Journal of the European Union.

Fedi, L., Etienne, L., Haury, O., Rigot-Muller, P., Stephenson, S., & Cheaitou, A. (2018). POLARIS in the Arctic. *Journal of Ocean Technology, 13*(4), 58-71.

Fedi, L., Faury, O., & Etienne, L. (2020). Mapping and analysis of maritime accidents in the Russian Arctic through the lens of the Polar Code and POLARIS system. *Marine Policy*(118), 1-9.

Finnish Transport Safety Agency. (2017). *Finnish ice classes equivalent to class notations of recognized classification societies and the determination of the ice classes of ships.* Helsinki, Finland: Trafi.

Fraser, D. (2020). A Change in the Ice Regime: Polar Code Implementation in Canada. In A. Chircop, F. Goerlandt, C. Aporta, & R. Pelot, *Governance of Arctic Shipping.* Springer Polar Sciences.

Fu, S., Zhang, D., Montewka, J., Yan, X., & Zio, E. (2016). Towards a probabilistic model for predicting ship besetting in ice in Arctic waters. *Reliability Engineering & System Safety*, 124-136.

Georlandt, F., Montewka, J., Zhang, W., & Kujala, P. (2017). An analysis of ship escort and convoy operations in ice conditions. *Safety Science, 95*, 198-209.

Goerlandt, F., & Pelot, R. (2020). An Exploratory Application of the International Risk Governance Council's Risk Governance Framework to Shipping Risks in the Canadian Arcitc. In A. Chircop, *Governance in Arctic Shipping.* Springer Polar Sciences.

Goerlandt, F., Montewka, J., Zhang, W., & Kujala, P. (2017). An analysis of ship escort and convoy operations in ice conditions. *Safety Science, 95*, 198-209.

Goerlandt, F., Montewka, J., Zhang, W., & Kujala, P. (2017). An analysis of ship escort and convoy operations in ice conditions. *Safety Science, 95*, 198-209.

Goerlandt, F., Montewka, J., Zhang, W., & Kujala, P. (2017). An Analysis of Ship Escort and Convoy Operations in ice Conditions. *Safety Science*, 198-209.

Government of Canada. (2019, June 25). *Canadian Coast Guard Search and Rescue and Canadian Coast Guard Auxiliary Evaluation Report*. Retrieved from Department of Fisheries and Oceans Canada: https://www.dfo-mpo.gc.ca/ae-ve/evaluations/11-12/SAR-CCGA-eng.htm#2.1

Greidanus, H., & Kourti, N. (2006). Findings of the CELIMS Project - Detection and Classification of Marine Traffic from Space. *Proceedings of SEASAR 2006.* Frascati, Italy.

Headland, R. (2022). *Transits of the Northwest Passage to End of the 2022 Navigation Season: Atlantic Ocean to Arctic Ocean to Pacific Ocean.* Scott Polar Research Institute. Cambridge University.

Heiberg, H. B., Reistad, M., & A., B. (2006). *Use of ASAR wave spectra in operational wave analysis and forcasting: report from the EnviWave project.* Oslo: Norweigian Meteorological Institute.

Higginbotham, J., & Grosu, M. (2014). The Northwest Territories and Arctic Maritime Development in the Beaufort Regimes. *CIGI Policy Brief*, 40:1-12.

Hirose, T., Kapfer, M., Bennett, J., Cott, P., Manson, G., & Solomon, S. (2008). Bottomfast Ice Mapping and the Measurement of Ice Thickness on Tundra Lakes using C-Band SAR Remote Sensing. *Journal of the American Water Resources Association*, 44(2): 285-292.

Howell, S., & Yackel, J. (2004). A Vessel Transit Assessment of Sea Ice Variability in the Western Arctic, 1969-2002: Implications for ship navigation. *Canadian Journal of Remote Sensing*, 30(2):205-215.

IACS. (2009). *International Association of Classification Societies Charter.* International Association of Classificaiton Socieities.

IACS. (2023). *Requires Concerning POLAR CLASS.* International Association of Classification Socieities.

Intergovernmental Oceanographic Commission of UNESCO. (2004). *SIGRID-3: A Vector archive formate for sea ice charts.* JCOMM Technical Report.

International Maritime Organization. (2004). *Regulation 19 - Carriage requirements for shipborne navigational systems and equipment.* London: International Maritime Organization.

International Maritime Organization. (2016). *International Code for Ships Operating in Polar Waters (POLAR CODE).* International Maritime Organization.

International Telecommunication Union. (2014). *Technical characteristics for an automatic identification system using time division multiple access in the VHF maritime mobile frequency band.* Geneva: International Telecommunication Union.

Kang, M., Lee, H., Yang, C., & Yoon, W. (2008). Estimation of Ocean Current Velocity in Coastal Area using RADARSAT-1 SAR Images and HF-Radar Data. IGRASS 2008.

Kazemi, S., Abhari, S., Lavesson, N., Johnson, H., & Ryman, P. (2013). Open Data for Anomaly Detection in Maritime Surveillance. *Expert Systems with Applications*, 40: 5719 - 5729.

Kennedy, A., Gallagher, J., & Aylward, K. (2013). *Evaluating Exposure Time Until Recovery by Location.* Ottawa, Ontario: National Research Council Canada.

Khan, B., Khan, F., Veitch, B., & Yang, M. (2018). An operational risk analysis tool to analyze marine transportation in Arctic waters. *Reliability Engineering & System Safety, 169*, 485-502. doi:https://doi.org/10.1016/j.ress.2017.09.014.

Kim, H., Jeong, S.-Y., Woo, S.-H., & Han, D. (2018). Study on the procedure to obtain an attainable speed in pack ice. *International Journal of Naval Architecture and Ocean Engineering*(10), 491-498. doi:https://doi.org/10.1016/j.ijnaoe.2017.09.004

Kotovirta, V., Jalonen, R., Axell, L., Riska, K., & Berglund, R. (2009). A system for Route Optimization in Ice-Covered Waters. *Cold Regions Science and Technology*(55), 52-62.

Kubat, I., & Timco, G. (2003). *Vessel Damage in the Canadian Arctic.* National Research Council of Canada.

Lack, D. A., & Corbett, J. J. (2012). Black carbon from ships: a review of the effects of ship speed, fuel. *Atmostpheric Chemistry and Physics*(12), 3985-4000.

Laxhammer, R. (2008). Anomaly Detection for Sea Surveillance. *11th International Conference on Information Fusion* (pp. 47-54). Fusion 2008.

Lee, H.-W., Roh, M.-I., & Kim, K.-S. (2021). Ship Route Planning in Arctic Ocean based on POLARIS. *Ocean Engineering*(234), 1-14.

Lehtola, V., Montewka, J., Goerlandt, F., Guinness, R., & Lensu, M. (2019). Finding safe and efficient shipping routes in ice-covered waters: A framework and a model. *Cold Regions Science and Technology*(165), 1-14. doi:https://doi.org/10.1016/j.coldregions.2019.102795

Lensu, M., & Goerlandt, F. (2019). Big Maritime Data for the Baltic Sea with a Focus on the Winter navigation System. *Marine Policy*, 53-65.

Li, F., Goerlandt, F., Kujala, P., Lehtiranta, J., & Lensu, M. (2018). Evaluation of selected state-of-the-art methods for ship transit simulation in various ice conditions based on full-scale measurement. *Cold Regions Science and Technology, 151*, 94-108. doi:10.1016/j.coldregions.2018.03.008

Liu, C., Musharraf, M., Li, F., & Kujala, P. (2022). A data mining method for automatic identification and analysis of. *Ocean Engineering*(266).

Liu, C., Musharraf, M., Li, F., & kujala, P. (2022). A data mining method for automatic identification and analysis of icebreaker assistance operation in ice-covered waters. *Ocean Engineering, 266*. doi:https://doi.org/10.1016/j.oceaneng.2022.112914

Lloyds of London. (2014). *Arctic Opening: Opportunity and risk inthe high north.* London.

Loptien, U., & Axell, L. (2014). Ice and AIS: ship speed data and sea ice forecasts in the Baltic Sea. *The Cryosphere*(8), 2409-2418.

Marchenko, N. A., Aandreassen, N., Kuznetsova, S. Y., Ingimundarson, V., & Jakobsen, U. (2018, March). TransNav. *Arctic Shipping and Risks: Emergency Categories and Response Capacities*.

Marchenko, N., Borch, O., Markov, S., & Andreassen, N. (2015). Maritime activity in the high north - The range of unwanted incidents and risk patterns. *International Conference on Port and Ocean Engineering under Arctic Conditions 2015.* POAC. Retrieved from http://hdl.handle.net/11250/2392588

Maritime Safety Committee. (2014a). *POLARIS – proposed system for determining operational limitations in ice.* IACS.

Maritime Safety Committee. (2014b). *Technical background to POLARIS.* IACS.

McCallum, J. (1996). *Safe Speed in Ice - An analysis of transit speed and ice decision numerals.* Ottawa, ON: Transport Canada.

Melia, N., Haines, K., & Hawkins, E. (2015). Improved Arctic sea ice thickness projections using bias-corrected CMIP5 simulations. *The Cryoshpere*, 2237-2251.

Melia, N., Haines, K., & Hawkins, E. (2016). Sea ice decline and 21st century trans-Arctic shipping routes. *Geophyscial Research Letters*(43), 9720-9728.

Monroe, K. R., & Maher, K. H. (1995). Psychology and Rational Actor Theory. *Political Psychology, 16*(1), 1-21. doi:https://doi.org/10.2307/3791447

Montewka, J., Goerlandt, F., Kujala, P., & Lensu, M. (2015). Towards probabilistic models for the prediction of a ship performance in dynamic ice. *Cold Regions Science and Technology*(112), 14-28.

Montewka, J., Goerlandt, F., Kujala, P., & Lensu, M. (2015). Towards Probabilitic Models for the Prediction of a Ship Performance in Dynamic Ice. *Cold Regions Science and Technology*(112), 14-28.

Montewka, J., Goerlandt, F., Lensu, M., & Guinness, R. (2019). Towards a hybrid model of ship performance in ice suitable for route planning purpose. *Proceedings of the Instituation of Mechanical Engineers, Part O: Journal of Risk and Reliability, 233*(1), 18-34. doi:10.1177/1748006X18764511

Mudryk, L. R., Dawson, J., Howell, S. E., Derksen, C., Zagon, T. A., & Brady, M. (2021, August). Impact of 1, 2, and 4 Degrees Celcius of Global Climate Wharing on Ship Navigation in the Canadian Arctic. *Nature Climate Change, 11*, 673 to 679.

Muller, M., Knol-Kauffman, M., Jeuring, J., & Palerme, C. (2023). Arctic shipping trends during hazardous weather and sea-ice conditions and the Polar Code's effectiveness. *npj Ocean Sustainability, 2*(12). doi:https://doi.org/10.1038/s44183-023-00021-x

National Snow and Ice Data Center. (2013, July 13). *Frequently Asked Questions on Arctic Sea Ice*. Retrieved April 19, 2023, from Arctic Sea Ice News and Analysis: https://nsidc.org/arcticseaicenews/faq/#1979average

National Snow and Ice Data Centre. (2015a). *Format for gridded sea ice information (SIGRID).* Boulder, CO: National Snow and Ice Data Centre.

Olsen, R., & Wahl, T. (2000). The Role of Wide Swath SAR in High-Latitude Coastal Management. *John Hopkins APL Technical Digest*, 20(1) 136-140.

Piercey, C., Kennedy, A., & Power, J. (2019). *Methodology for Estimating Exposure Time in Polar Regions.* National Research Council. doi:https://doi.org/10.4224/40002043

QGIS. (2023). *QGIS: A free and open source geographic information system*. Retrieved from https://qgis.org/en/site/

Renn, O., & Sellke, P. (2011). Risk, Society and Policy Making: Risk governance in a complex world. *International Journal of Performability engineering, 7*(4), 349-366.

Renn, O., Jaeger, C. C., Rosa, E. A., & Webler, T. (2000). The Rational Actor Paradigm in Risk Theories: Analysis and Critique. In M. Cohen, *RIsk in the Modern Age.* London: Palgrave Macmillan. doi:https://doi.org/10.1007/978-1-349-62201-6_2

Rhodes, B., Bomberger, N., Seibert, M., & Waxman, A. (2005). Maritime Situation Monitoring and Awareness using Learning Mechanisms. *Proceedings of IEEE Military Communications Conference.*

Roy, J. (2010). Rule-Based Expert Systems for Maritime Anomaly Detection. *SPIE 7666, Sensors and Command, Control, Communications, and Intelligence (C3I) Technologies for Homeland Security and Homeland Defense.*

Runge, H., Breit, H., Eineder, M., Schulz-Stellenfleth, J., Bard, J., & Romeiser, R. (2004). Mapping of Tidal Currents with SAR Along Track Interferometry. *IGARSS '04*.

Schrijver, A. (1998). *Theory of Linear and Interger Programming.* John Wiley $ Sons.

Siljander, M., Venalainen, E., Goerlandt, F., & Pellikka, P. (2015). GIS-based cost distance modelling to support strategic maritime search and rescue planning: A feasibility study. *Applied Geography, 57*, 54-70.

Simila, M., & Lensu, M. (2018). Estimated the Speed of Ice-Going Ships by Integrating SAR Imagery and Ship Data from an Automatic Identification System. *Remote Sensing*(10), 1-23.

Smith, C., & Stephenson, S. (2013). New tans-arctic shipping routes navigable by mid-century. *Proceedings of the National Academy of Sciences of the United States of America (PNAS)*, 110:E1191.

Smith, L., & Stephenson, S. (2013). New Trans-Arctic Shipping Routes Navigable by Midcentury. *Proceedings of the National Academy of Sciences - PNAS*, 1191-1195.

Snider, D. (2012). *Polar Ship Operations - A practical guide.* London: The Nautical Institute.

Somanathan, S., Flynn, P. C., & Szymanski, J. (2006). The Northwest Passage: A Simulation. *Proceedings of the 2006 Winter Simulation Conference*, (p. 7).

Spire Maritime. (2023). *Historical AIS Data*. Retrieved from Spire: https://spire.com/maritime/solutions/historical-ais-data/

Statistics Canada. (2016). *Data Products, 2016 Census*. Retrieved from Statistics Canada Census Program: https://www12.statcan.gc.ca/census-recensement/2016/dp-pd/index-eng.cfm

Stephenson, S. R., Smith, L. C., & Agnew, J. A. (2011). Divergent long-term tranjectories of human access to the Arctic. *Nature Climate Change*, 156-160.

Stoddard, M. A., & Pelot, R. (2020). Historical Maritime Search and Rescue Incident Data Analysis. In *Governance of Arctic Shipping.* Springer Polar Sciences.

Stoddard, M. A., Etienne, L., Pelot, R., Fournier, M., & Beveridge, L. (2018). From Sensing to Sense-making: Assessing and Visualizing Ship Operational Limitations in the Canadian Arctic Using Open-Access Ice Data. In L. P. Hidlebrand, L. W. Brigham, & T. M. Johansson, *Sustainable Shipping in a Changing Arctic* (pp. 99-113). Springer.

Stoddard, M. A., Pelot, R., Etienne, L., & Goerlandt, F. (2023). Determining Ship Speeds in Ice using the Polar Operational Limitation Assessment Risk Indexing System (POLARIS). *TBD*, 1-18.

Stoddard, M. A., Pelot, R., Etienne, L., & Goerlandt, F. (2023). Polar Class Ship Speeds in Ice: Obersvation and Analysis. *TBD*, 1-7.

Stoddard, M., Etienne, L., Fournier, M., Pelot, R., & Beveridge, L. (2016). Making sense of Arctic maritime traffic using the Polar Operational Limits Assessment Risk Indexing System (POLARIS). *Earth and Environmental Science*, 1-8.

Stoddard, M., Pelot, R., Goerlandt, F., & Etienne, L. (2023). Making Sense of Marine-Based Search and Rescue Response Time using Network Analysis. *TBD*, 1-29.

Tan, X., Su, B., Riska, K., & Moan, T. (2013). A six-degree-of-freedom numerical model for level ice-ship interaction. *Cold Regions Science and Technology, 92*, 1-16.

Tran, T., Browne, T., Musharraf, M., & Veitch, B. (2023). Pathfinding and Optimization for Vessels in Ice: a literature review. *Cold Regions Science and Technology*(211), 1-8.

Transport Canada. (1998). *Arctic Ice Regime Shipping System (AIRSS) Standards, TP 12259E.* Ottawa: Government of Canada.

Tremblett, A. J., Garvin, M. J., & Oldford, D. (2021). Preliminary Study on the Applicability of the POLARIS Methodology for Ships Operating in Lake Ice. *Proceedsings of the 26th International Conference on Port and Ocean Engineering under Arctic Conditions*, (p. 12). Moscow.

U.S. National Ice Center. (2022). *U.S. National Ice Center Arctic and Antarctic Sea Ice Charts in SIGRID-3 Format, Version 1.* Boulder, Colorado.

U.S. National Ice Centre. (2023). *Arctic Ice Products*. Retrieved from https://usicecenter.gov/Products/ArcticHome

Vachon, P. (2006). Ship Detection in SAR Imagery. *Proceedings of OceanSAR 2006 - Third Workshop on Coastal and Marine Applications of SAR.* St. John's, NL.

Wang, C., Ding, C., Yang, Y., & Dou, T. (2022). Risk Assessment of Ship Navigation in the Northwest Passage: Historical and Projection. *Sustainability*(14). doi:https://doi.org/10.3390/su14095591

Wang, F., & Xu, Y. (2011). Estimating O–D travel time matrix by Google Maps API: implementation, advantages, and implications. *Annals of GIS, 17*(4), 199-209.

Wang, Y., Zhang, R., & Qian, L. (2018). An Improved A* Algorithm Based on Hesitant Fuzzy Set Theory for Multi-Criteria Arctic Route Planning. *Symmetry*(10), 1-20.

Wei, T., Yan, Q., Qi, W., Ding, M., & Wang, C. (2020). Projections of Arctic sea ice conditions and shipping routes in the twenty-first century using CMIP6 forcing scenarios. *Evironmental Research Letters*(15), 1-10.

Weick, K. E., & Sutcliffe, K. M. (2005). Organizing and the Process of Sensemaking. *Organization Science, 16*(4), 409-421.

Wilbrink, J. G. (2017). *Remoteness as a proxy for social vulnerability in Malawian Traditional Authorities: An open data and open-source approach.* The Hague - Netherlands: Delft University.

Williams, T., Korosov, A., Rampal, P., & Olason, E. (2021). Presentation and Evaluation of the Arctic Sea Ice Forecasting System neXtSIM-F. *The Cryoshpere*(15), 3207-3227.

Wilson, K. (2004). Shipping in the Canadian Arctic: Other possible climate change scenarios. *Proceedings of IGARSS'04: Geoscience and Remote Sensing*, 3: 1853.

Wilson, K., Falkingham, H., Melling, H., & De Abreu, R. (2004). Shipping in the Canadian Arctic: Other possible climate change scenarios. *Proceedings of IEEE International Symposium on Geoscience and Remote Sensing*, 3: 1853-1856.

World Maritime Organization. (2016). *International Code for Ships Operating in Polar Waters (POLAR CODE).* World Maritime Oganization.

Wright, C. (2016). *Arctic Cargo: A history of marine transportation in Canada's North.* Marquis Book Printing.

Xi, Y., Miller, E. J., & Saxe, S. (2018). Exploring the Impact of Different Cut-Off Times on Isochrone Measurements of Accessibility. *Transportation Research Record, 2672*(49), 113-124.

Appendix 5: Historical Maritime Search and Rescue Incident Data Analysis

Stoddard, M.A. and Pelot, R. (2020). Historical Maritime Search and Rescue Incident Data Analysis. Book Chapter in A. Chircop et al. (eds.), Governance of Arctic Shipping, Springer Polar Sciences, https://doi.org/10.1007/978-3-030-44975-9_3

Chapter 3

Historical Maritime Search and Rescue Incident Data Analysis

Mark A. Stoddard and Ronald Pelot

Abstract

Since the 1980s the Canadian Coast Guard (CCG) has maintained a database of maritime search and rescue (SAR) incidents involving CCG assets and personnel. This information is stored in a national database known as the Search and Rescue Program Information Management System (SISAR). SISAR contains a spatiotemporal record for all serious incidents that occur within Canada's coastal search and rescue area. In addition to providing the CCG with a record of all response operations, it provides a rich historical dataset for analysts to use to support a wide range of decision-making applications. In this chapter we illustrate the use of SISAR incident data to identify and visualise temporal and spatial patterns in the maritime SAR incident data. Temporal phenomena will be examined at three temporal scales: yearly, monthly, and hourly. Spatial phenomena will be examined using the spatial location and density of incidents. Several useful visualisations to explore and exploit SISAR data are provided. Lastly, we discuss an opportunity that exists to combine SAR incident data in from the Great Lakes region in the United States and Canada. Combining this information may serve to highlight the potential benefits of enhanced cross-border coordination of SAR planning and response.

Keywords

search and rescue, visualisation, incident analysis, data analytics, D3

3.1 Introduction

In Canada, search and rescue (SAR) is one of the primary responsibilities of the Canadian Coast Guard (CCG). The CCG's SAR programme is needed largely due to the size of Canada's coastal search and rescue area (~ 5.3 million km^2), consisting of both extensive inland waterways and open ocean (Government of Canada 2019*a*). Through the effective use of SAR resources, the CCG responds to approximately 6,000 maritime incidents per year (Government of Canada 2019*a*). As with most emergency response services, such as police and fire, incident reporting and record keeping is a critical part of the response. Following each response operation, incident reports and logs are entered in a database known as the Search and Rescue Program Information Management System (SISAR). SISAR, a CCG programme, is a web-based database that integrates all regional response data into one national system. SISAR incident data is one of the primary data sources used to capture statistics relating to SAR cases to inform demand for programme services and the achievement of outcomes (Government of Canada 2019*a*).

This chapter provides an overview of the CCG SISAR database, a short background of spatiotemporal analysis of SAR incident data, and several interactive web visualisations that have been developed to specifically explore and exploit available SISAR incident data. Emphasis has been placed on the development of interactive visualisations to examine temporal and spatial phenomena. Temporal phenomena will be examined at three temporal scales: yearly, monthly, and hourly. Spatial phenomena will be examined using the spatial location, severity, and density of incidents.

3.2 Spatiotemporal Analysis of Search and Rescue Incident Data

SAR incident data provides a rich multivariate spatiotemporal dataset that can support a wide range of analysis. The availability of spatial attribute data enables the use of spatial statistics and geo-referenced data processing techniques (Shaharabi 2003), while temporal attribute data allows for the use of time series analysis and the study of temporal phenomena and trends (Malik et al. 2012). This form of data has been widely used by the CCG and academic researchers to examine issues related to maritime SAR resource planning and

evaluation (Government of Canada 2019; Marven, Canessa and Keller 2007; Akbari, Eiselt and Pelot 2017) .

Shaharabi (2003) completed an early example of spatial and temporal analysis of fishing and marine traffic incidents off the coast of Nova Scotia using available SISAR data. The emphasis of this work was on developing a better understanding of the location of fishing incidents and their time of occurrence. Using a geographic information system (GIS) and a variety of spatial statistical methods, such as kernel density estimation and hierarchical clustering methods, Shaharabi was able to identify areas of higher risk to fisherman off the coast of Nova Scotia. Furthermore, by analysing temporal incident attributes the author was able to highlight times of the year where the likelihood of a SAR event was elevated. Pelot and Plummer (2008) expanded on this work to provide a complete assessment of the risk in the Atlantic coastal zone, largely based on maritime traffic modelling and historical SAR incident data.

In addition to the use of SAR incident data to support spatiotemporal analysis, it can also be used to support decision-making. Marven, Canessa and Keller (2007) show how SAR incident data can be used to support SAR resource planning. Using exploratory spatial data analysis (ESDA) methods suitable for point pattern analysis, these authors proposed several resource allocation modelling approaches based on historical incident data that utilised linear programming, Monte Carlo simulation, and process simulation. More recently, Akbari, Eiselt and Pelot (2017) proposed a goal programming multi-objective model for locating and allocating maritime SAR vessels. The model considered three objectives for the maritime SAR location-allocation problem: (1) primary coverage, (2) backup coverage, and (3) mean access/response time. When considering historical SAR incident data and the current arrangement of SAR vessel type and location in their study area (Atlantic Canada), it was shown that substantial improvements, in terms of access time and coverage, may be possible by using the optimal location-allocation solution from their multi-objective model.

Lastly, (Malik et al. 2012) proposed a visual analytic process for maritime response, asset allocation, and risk assessment. The resulting visual analytic system, Coast Guard Search and Rescue Visual Analytics (cgSARVA), was developed to exploit the United States Coast Guard (USCG) historical response operations database, covering historical response operations in the Great Lakes region from 2002 to 2011. cgSARVA allows USCG

analysts to visually interact with historical SAR incident data, helping to better understand data quality issues and to effectively perform data exploration and analysis. cgSARVA became part of the USCG initiated Station Optimization Process (U.S. Department of Homeland Security 2018). This process was meant to analyse USCG boat stations and identify those that could be closed because they provide overlapping and/or unnecessarily duplicative SAR coverage.

3.3 Search and Rescue Program Information Management System

Currently, when a Joint Rescue Coordination Centre (JRCC) receives a report of a vessel in distress, they dispatch the most appropriate SAR resource to provide assistance. Following each event a new record is added to the SISAR database. SISAR provides a spatiotemporal record of all the serious incidents that required CCG response within Canada's coastal search and rescue area. SISAR was created to provide CCG personnel with easy access to essential information to support SAR planning, management, and operations (Marven, Canessa and Keller 2007). The CCG has provided SISAR data to various Canadian academic institutions to examine historical SAR incidents for a variety of applications, such as assessing manning levels (Marven, Canessa and Keller 2007) and identifying critical locations for permanent SAR resources (Akbari, Eiselt and Pelot 2017; Akbari, Pelot and Eiselt 2018; Pelot and Plummer 2008) .

The CCG SISAR database extraction used for this study contained a total of 36,036 records and covers 2005 to 2013. Records from 2007 were not available due to a database extraction issue. Our analysis is focused on a subset of the available incident attribute data and can be grouped into four general categories: (1) incident description, (2) SAR resource usage, (3) SAR resource deployment, and (4) unit assisted.

The incident description fields of the SISAR database are used primarily for CCG internal accounting of events. A unique ID is assigned to each event and is used for all subsequent reporting. Example incident description attributes include the alert method used by the vessel in distress, location of the incident, start and end date time group (DTG), and a text summary of the event provided by the first responders. The incident description data

that was used in this study included the incident ID, location, start and end DTG, and severity.

The SAR resource usage fields are used to identify the SAR resource used to respond to the incident and details of the mission. These fields try to capture the nature of the response operation. Fields such as distance to the incident, alert time, on-scene time, and distance towed are used to describe CCG resource usage. The SAR resource usage data that was used in this study included the incident distance from shore and alert time.

The SAR resource deployment fields are used to identify the region, base, and squadron of the SAR response asset. Often this information is also associated with a SAR region. Currently, Canada is broken up in to three regions: (1) Eastern, (2) Pacific, and (3) Central and Arctic. Each region is then further broken up into smaller SAR areas. The smaller SAR areas are used for aggregating and reporting marine incident statistics to support resource allocation planning (Marvin 2003). SAR resource deployment data was not used in this study.

The final descriptor, the unit assisted field, describe the various characteristics of the vessel that was involved in the incident, including vessel dimensions, flag state, vessel type, class, and the number of persons on board. This information is used by the JRCC to select the most appropriate asset to respond. This information is useful when examining issues related to asset suitability and capacity given the expected unit characteristics that may be encountered during an incident. The only unit assisted data that was used in this study was the united assisted vessel length (metres).

3.4 Visual Analytics for SISAR Data Analysis

In this section we introduce several visualisations that were implemented in Data-Driven Documents (D3) to explore the SISAR dataset. D3 is an open-source JavaScript library that enables the manipulation of web visualisations, such as charts and graphs, based on underlying data (David and Tauro 2015). D3 accomplishes this by providing a declarative framework for mapping underlying data to visual elements in a web page. This mapping enables the direct inspection and manipulation of a native data representation through user interaction with the web browser (Bostock, Ogievetsky and Heer 2011). Bostock (2019)

provides open access to D3 documentation and a large repository of web visualisation examples submitted by the D3 user community.

Using D3, each SAR incident is treated as an entity with associated attributes, and this information can be used to visualise the temporal and spatial relationships that exist within the data. To identify temporal phenomena in the data, ordinal classes were used to organise entity temporal attributes by year, month, day, and hour to construct a variety of data visualisations. Figure 3.1 provides a simple hierarchical view of the relationship between SAR incidents and attribute data used in this study.

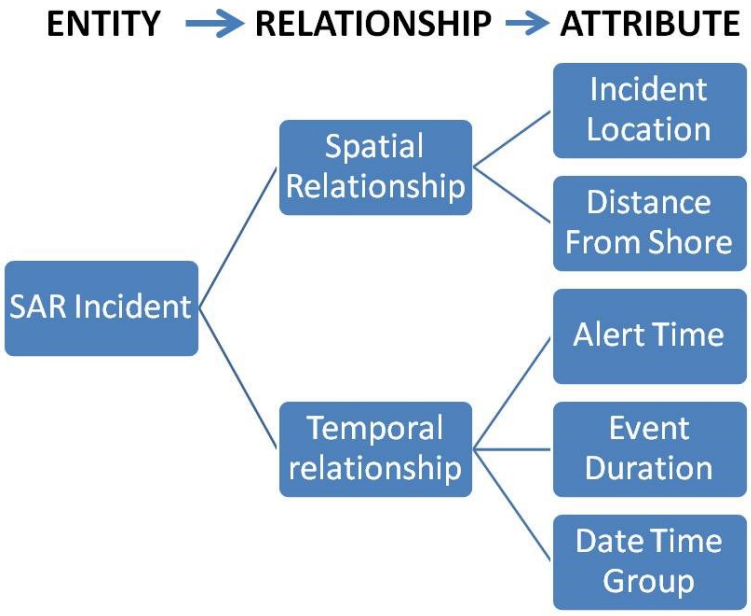

Fig 3.1 Hierarchical view of entity relationship model

3.4.1. Interactive SAR Incident Dashboard

The interactive SAR incident dashboard is the primary web visualisation for exploring the temporal distribution of SAR incidents contained in the SISAR database. This interactive web visualisation allows the user to quickly examine the monthly and daily distribution of total incidents from the SISAR data set using a standard web browser. The data that is visualised in this section is from calendar year 2013 and contains a total of 4,062 SAR incident records. The distribution of monthly total incidents for 2013 is visualised as a bar

chart. The dashboard pie chart is used to visualise the weekday distribution of the total incidents. A 7-sector pie chart is used to conveniently display the information, with each sector representing a day of the week. Initially, the total number of incidents that occurred on each weekday during 2013 was displayed. Figure 3.2 shows the default interactive incident dashboard visualisation of the 2013 monthly and weekday total SAR incidents.

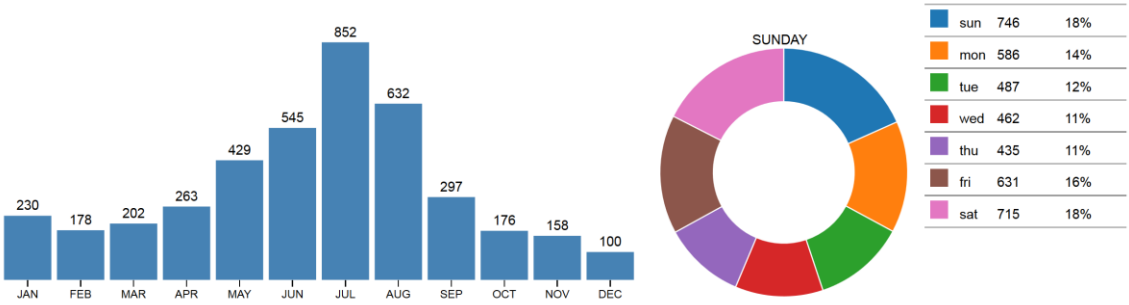

Fig 3.2 SISAR interactive monthly/weekday SAR incident Dashboard for calendar year 2013

A key enabler of the exploration of the temporal distribution of SAR incidents in the SISAR data are the interactive elements of the SAR incident dashboard. These elements of the dashboard allow the user to rapidly sort the SAR incident data by hovering the mouse pointer over a single bar in the bar chart to select a particular month, or hovering over a single sector in the pie chart to select a particular day of the week. Hovering over these elements of the visualisation will automatically render the corresponding analysis result on the webpage. Hovering over a single bar in the bar chart will cause the pie chart to render the distribution of monthly total incidents by day of the week. Hovering over a single sector in the pie chart will cause the bar chart to render the distribution of yearly total incidents for a selected day of the week. Fig and 3.4 illustrate the use of the interactive elements of the SAR incident dashboard.

Figure 3.3 shows the same monthly distribution of SAR incidents as shown in Figure 3.2. In this case, July has been selected by hovering the mouse over the appropriate bar (highlighted column in bar chart). The result of this user interaction is that the corresponding pie chart automatically renders to show the weekday distribution of incidents for the month of July. Figure 3.4 shows the monthly distribution of total SAR incidents that

occurred on Sunday. In this case, Sunday has been selected by hovering the mouse over the sector of the pie chart that corresponds to Sunday. The result of this user interaction is that the bar chart automatically renders to show the monthly distribution of total SAR incidents that occurred on Sunday.

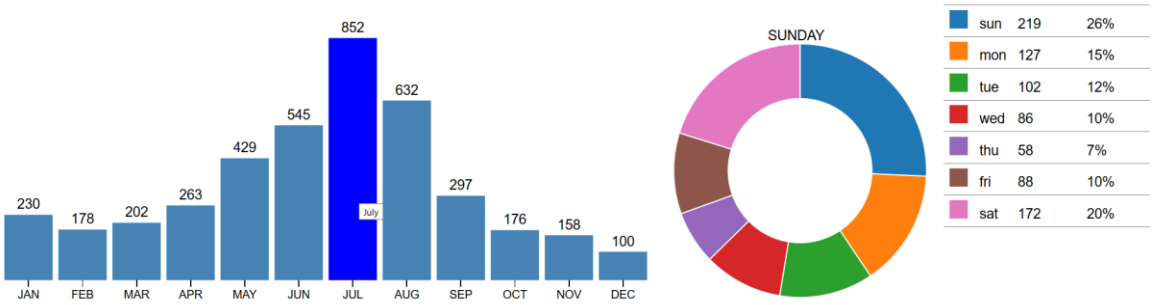

Fig 3.3 Interactive dashboard result showing the weekday distribution of the total number of incidents that occurred during July 2013

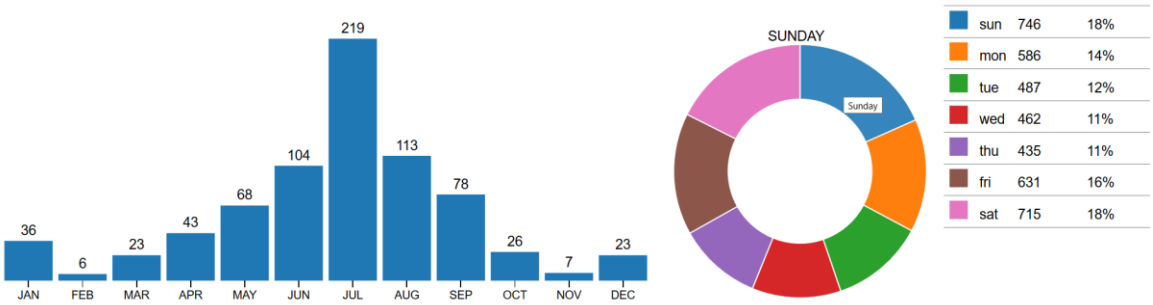

Fig 3.435 Interactive dashboard result showing the monthly distribution of incidents that occurred on Sunday during 2013

3.4.2. Multi-Year Monthly Incident Analysis

The incident dashboard previously described only allows a user to visualise the monthly and weekday distribution of SAR incidents for a single calendar year. In order to satisfy the need to visualise longer term trends in the SISAR incident data three multi-year visualisations were used: (1) multi-year monthly incident time series graph, (2) multi-year monthly incident time series chart, and (3) multi-year monthly incident heat map. All three visualisations display the same information, but use three different approaches. Van Wijk

and Selow (1999) provide an extensive description of calendar-based visualisation of time series data like those presented in this chapter.

3.4.2.1. Multi-Year Monthly Incident Time Series Graph and Chart

Using the DTG associated with a SAR incident enables the visualisation of SAR incident data as a time series. Each month is paired with an incident total and plotted. Using simple linear interpolation, a line is constructed that connects the dots that represent the total incidents for a month. By overlaying multiple years of data, we can compare each of the line plots to get insight into multi-year trends. Figure 3.5 shows a multi-series line chart of monthly total incident data from 2005 to 2013. For comparison, Figure 3.6 shows the same data as a multi-year time series chart. Figure 3.6 more clearly emphasises the cyclical nature of total month SAR incidents over a multi-year period.

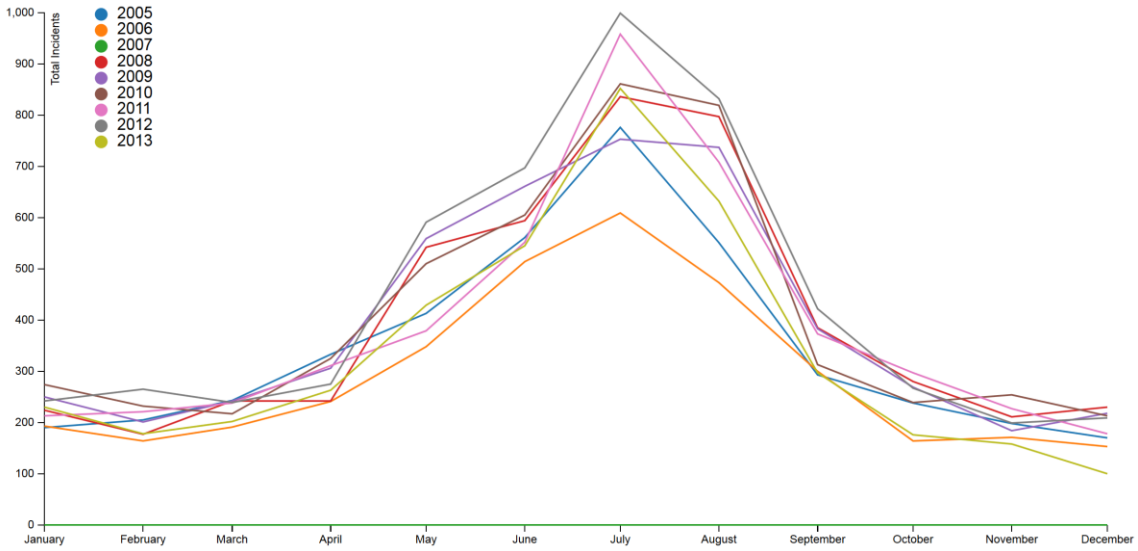

Fig 3.5 Multi-series line chart of monthly incident totals (2005–2013)

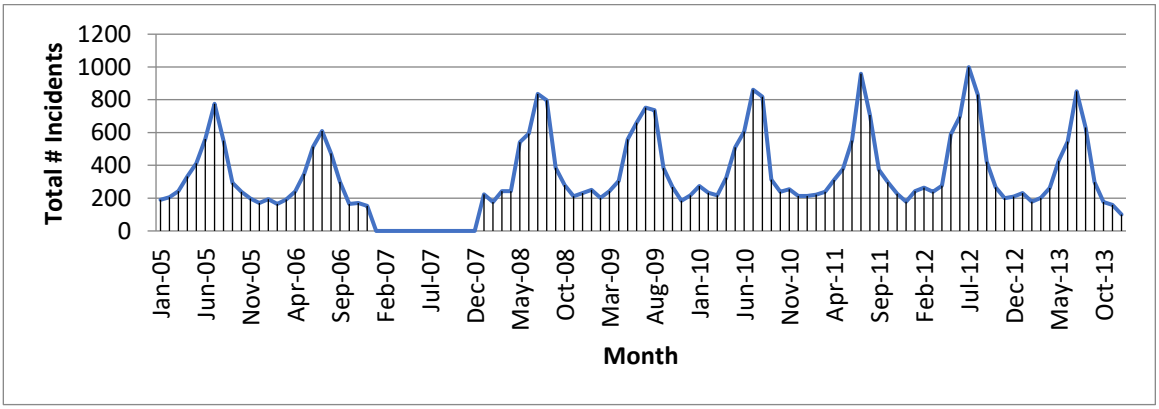

Fig 3.6: Multi-year time series line chart of monthly incident totals (2005–2013)

3.4.2.2. Multi-Year Monthly Incident Heat Map

A heat map can most simply be thought of as a two-dimensional representation of data, where colour is used to represent attribute value. The heat map value in this study is the total number of incidents, and the two dimensions are the month (y-axis) and the year (x-axis). The heat map is an alternative visualisation to those shown in section 0 above. Trends are identified by locating areas of common attribute value (colour) in both dimensions. In Figure 3.7, darker blue areas are associated with a larger number of total monthly incidents while the lighter areas represent a lower number of monthly incidents.

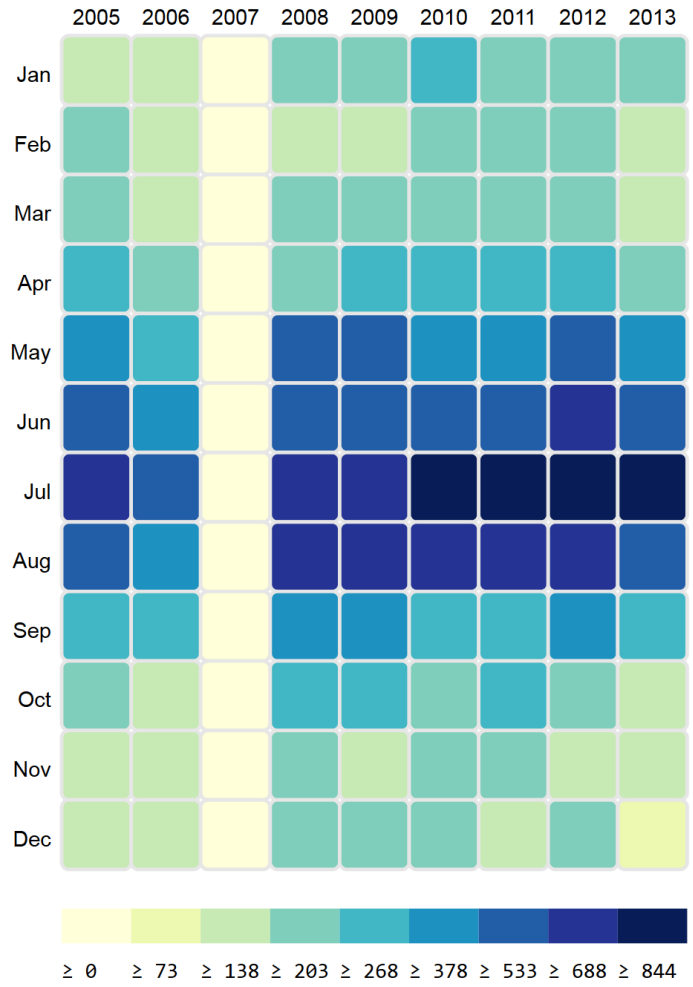

Fig 3.7 Multi-year monthly total incident heat map

3.4.3. Hourly Total Incident Heat Map

The hourly total incident heat map allows the user to visualise the 24-hour distribution of SAR incident alert time as a simple circular heat map. The heat map is broken up into 24 sectors, with each sector representing an hour of the day. The colour coding is used to represent the total number of SAR incident alerts that were received in a particular hour, where dark red represents the hour with the maximum number of incidents and dark blue represents the hour with the minimum number of incidents. This visualisation allows the user to quickly identify the hours of the day where the greatest numbers of SAR alerts are

expected to be received. Figure 3.8 shows the aggregate hourly distribution of SAR incident alerts from 2005 to 2013.

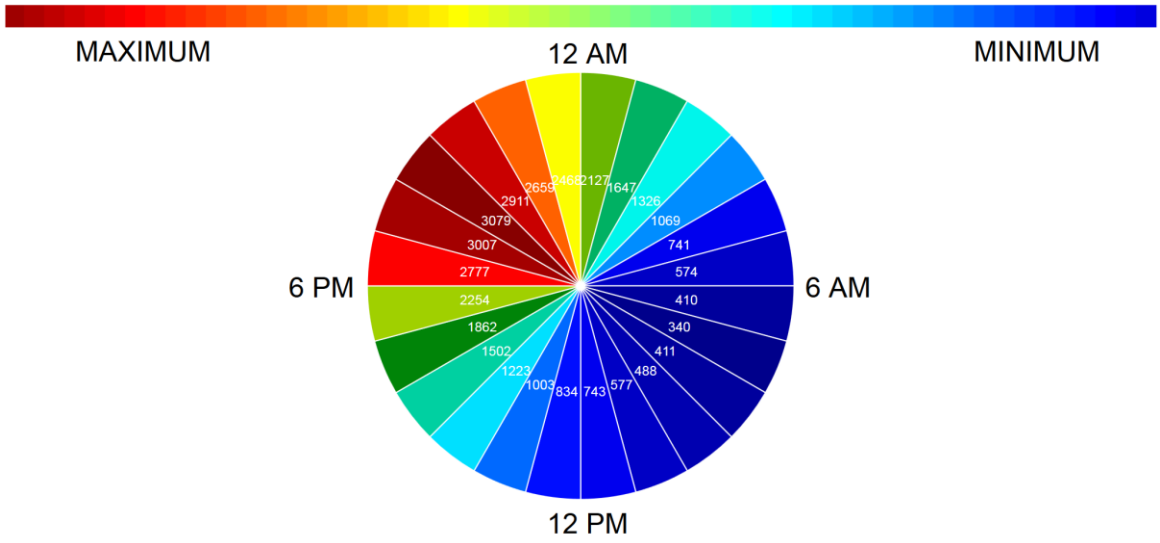

Fig 3.8 Aggregate hourly total incident heat map of SAR incident alerts from 2005 to 2013

3.4.4. Spatial Analysis Map

The spatial analysis map allows the user to visualise the location of SAR incidents on a map. In this visualisation the user can exploit the spatial proximity and similarity of events to extract meaning (Ware 2004). Figure 3.9 provides a coastline contour for an area of interest to allow the user to reference the incident location to a known geographic area. Two aspects of the spatial analysis map are discussed below, the analysis map itself, and the SISAR data layer.

The analysis map was constructed using a geoJSON of the Canadian coastline and the D3 default map projection library (Murray 2013). The size and shape of the country being mapped determines the most suitable projection. Since the SISAR data used in this study covers all of Canada, selecting a map projection that could be used to display the location of all incidents is challenging. Maps of very large countries like Canada often appear distorted due to the curvature of the earth. The distortion is minimal over small distances, but for maps of Canada that include the Canadian Arctic it can be extreme. Since the majority of the SISAR incident data is located below 60° North, we have chosen to use

a standard Albers map projection. The Albers projection is commonly used for land masses that extend in an east-to-west orientation, like Canada and the United States (ESRI n.d.). Figure 3.9 shows a zoomed in map view of Atlantic Canada.

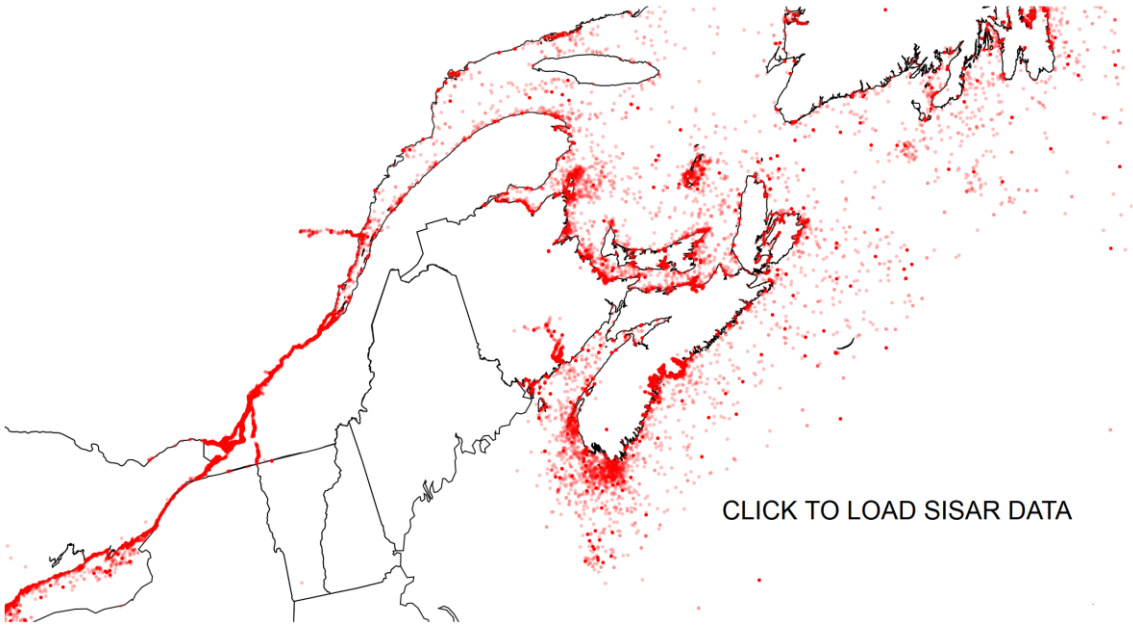

Fig 3.9 Geospatial analysis map with incident location shown as red point locations

The SISAR data used in this study covers all of Canada's coastal search and rescue area. The data set contains roughly 36,000 incidents, each with an associated geo-referenced position. By plotting the position of each incident on the analysis map we can visualise the spatial distribution of incidents. By looking at the spatial proximity among incidents we can identify areas of higher incident concentration. Shaharabi (2003) provided an excellent example of how this information, when combined with kernel density estimation and hierarchical clustering methods, can be used to identify areas of higher risk. The approach taken in this study was to try and use attribute data from the SISAR dataset to produce a visual analytic to help identify areas of higher risk.

The approach taken was to use the severity of the incident to determine the opacity of the plotted SISAR data. The visual effect is that more severe incidents appear as opaque bright red dots, while false alarms appear almost transparent (Figure 3.10). The use of this

visual analytic will be discussed in section 3.5 below. Equation 1 describes how opacity is derived using SAR incident severity data.

$$Opacity = \frac{1}{Incident\ Severity^2} \qquad \text{Equation 1}$$

Fig 3.10 Zoomed in map view showing the geo-reference position of incidents plotted as bright red circles with the opacity determined by Equation 1. Hovering the mouse pointer over each geo-referenced data point provides the detailed summary of the incident, as in the example reproduced here.

3.5. SISAR Data Analysis and Results

This section showcases a few potential use-cases for the visualisations presented in this chapter. Visualisations have been selected that allow an analyst to explore both temporal

and spatial trends in the SISAR data set using a standard web browser. Specifically, three questions are addressed:

1. What is the temporal (by hour, month, and day of week) distribution of the 2013 SAR incidents?
2. Based on the historical data for all SAR cases, what is the expected annual response case demand broken down by month?
3. Based on the historical data for all SAR cases, what regions show a high concentration of most severe incidents (spatial trends)?

3.5.1. What is the Temporal Distribution of the Response Case Load?

The interactive incident dashboard developed for this project allows the user to quickly identify monthly and weekday trends in the SISAR data. For any given calendar year, the user can quickly examine the total number of incidents responded to in a particular month or on a particular weekday. Fig 3. showed the 2013 monthly distribution of incidents. A distinct peak in the total number of incidents is easily observed during the summer months (June to August). The peak during the summer months is observed during every year in the SISAR data, and is best illustrated by the multi-year time series line chart of monthly incident totals shown in Fig 3.. This is likely due to the increase in pleasure boat activity associated with the summer months and was previously reported by Malik et al. (2011) and the Government of Canada (2019). In an attempt substantiate this claim, the available SISAR data was processed to produce a bar chart visualisation showing the monthly distribution of average vessel length involved in each SAR incident from 2005 to 2013. Figure 3.11 shows a significant decrease in average vessel length during the summer months, which is likely due to the increase in the number of smaller pleasure boats involved in incidents.

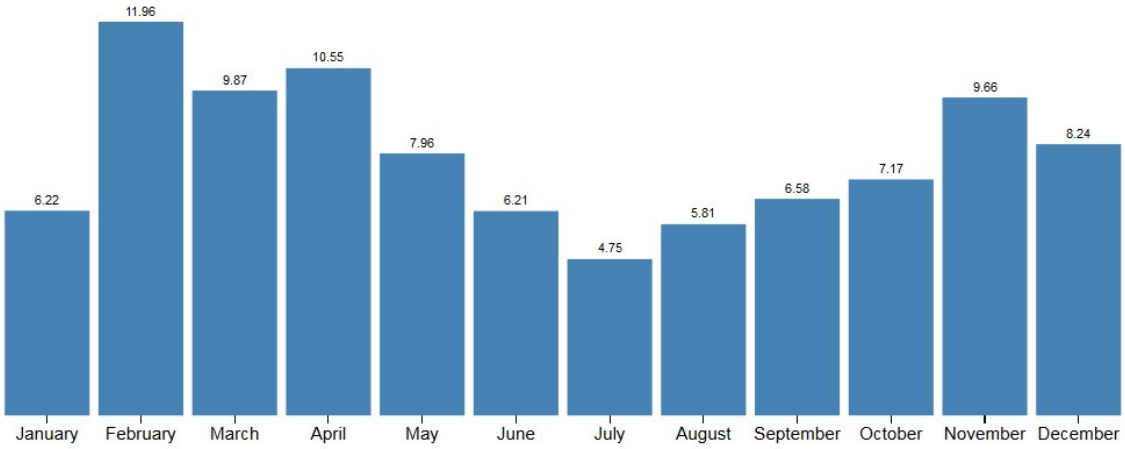

Fig 3.11 Average SAR incident vessel length (meters) by month (2005–2013)

In addition to the increase in the total number of incidents experienced during the summer months, it was also observed that during the summer months a greater proportion of incidents occurred on the weekend (Saturday and Sunday). For example, a user selecting July will see that the weekend accounted for 46% of the total number of incidents. Compare this with January where the weekend only accounted for 24% of the total number of incidents. For comparison, Figure 3.12 shows the weekday distribution of SAR incidents for July and January.

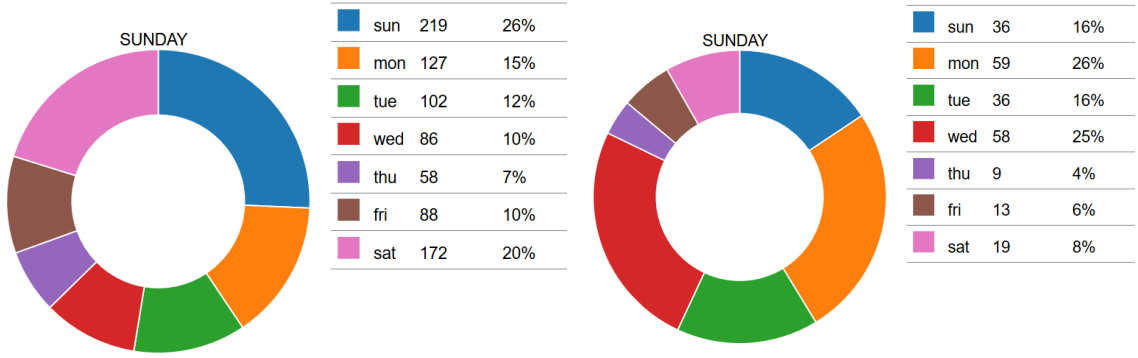

(a) Weekday distribution of July 2013 total SAR incidents

(b) Weekday distruition of January 2013 total SAR incendents

Fig 3.36 Comparison of weekday distribution of 2013 SAR incidents for July (a) and January (b)

Lastly, the hourly distribution of SAR incidents was examined. By aggregating all incidents found in the SISAR database we can generate the hourly total incident heatmap discussed in section 0 above. What is clear is that there are an elevated number of incidents between the hours of 6 pm and 11 pm. It can be reasoned that the CCG is notified of a vessel in distress when they fail to report back to their home destination by the evening. This reporting behaviour is associated with pleasure boat activity where a mariner is performing a day trip, where no overnight boating activity is expected. In this case, the SAR incident is triggered by a failure to arrive at the intended destination, return to port on time, or is generally considered overdue (Government of Canada 2003). Malik et al. (2012) also report a very similar hourly distribution of SAR incident case load for the USCG Great Lakes region. Figure 3.13 shows the hourly distribution of SAR incident alert time from 2005 to 2013.

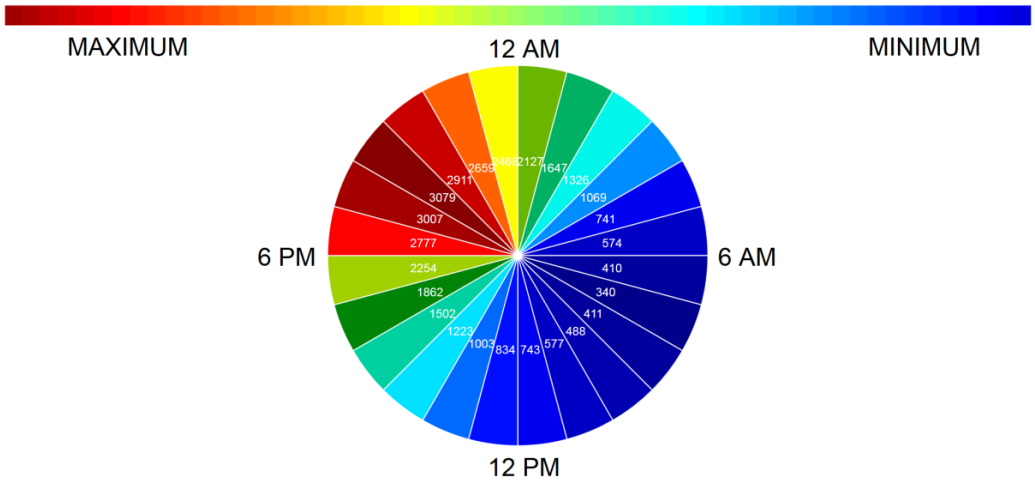

Fig 3.13 Hourly distribution of SAR incident case load

3.5.2. What is the Expected Annual Response Case Demand?

Response case demand exhibits a strong seasonal variation. As was previously discussed, summer months show a significant increase in the number of incidents, while the remainder of the year is relatively consistent. Fig 3. provided a multi-year heat map of SISAR incidents. What is clear is that over multiple years, incident levels increase significantly between May and September, and drop significantly outside of this time frame.

Specifically, the CCG experiences a peak in SAR incidents during the month of July (829 +- 121 incidents) and a low during the month of January (227 +- 29 incidents).

Understanding the spatial distribution of incidents is critical in planning emergency response operations and the allocation of resources (Marven, Canessa and Keller 2007; Akbari, Eiselt and Pelot 2017; Malik et al. 2011). Resources are often pre-positioned in areas with a higher concentration of SAR incidents to minimise response times and ultimately reduce the cost of providing lifesaving services. SISAR data provides a rich source of historical geo-referenced SAR incident data. The challenge is producing a visualisation that allows the user to understand the significance of areas of higher SAR incident concentration. In this study a visual analytic was created that uses the severity of incidents to aid in the interpretation of incident spatial location data. Figure 3.14 shows how using incident severity to control the opacity of incident location markers improves the definition of areas of severe incidents. This also improves the localisation of hot spots, where more severe incidents are tightly grouped.

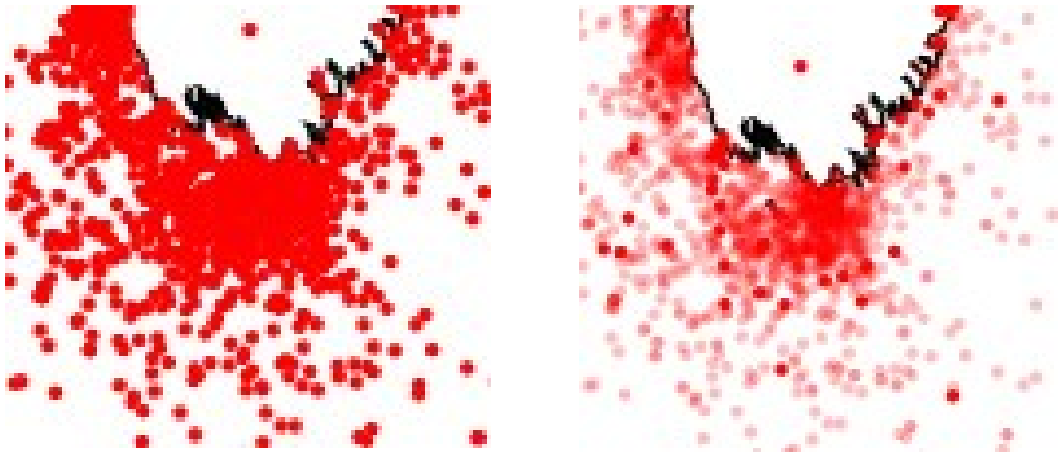

(a) Spatial distribution of SAR incidents

(b) Spacing distribution of SAR incidents with opacity determined using incident severity (Equation 1)

Fig 3.14 Spatial distribution of SAR incidents off the southern tip of Nova Scotia, Canada

3.6. Discussion

Under-reporting in historical SAR incident databases can significantly affect the outcome of quantitative analyses, potentially leading to poor decision outcomes (Psarros et al. 2010). Under-reporting in the SISAR database used for this study could have a significant impact on the results discussed in Sect. 3.5. Under-reporting in SISAR is known to the CCG and believed to be largely due to technical challenges and human errors in constructing the database (Government of Canada 2019a). The CCG has determined the total missing cases, by region from 2006 to 2010: Quebec 0.9%, Newfoundland and Labrador 2.9%, Central and Arctic 2.7%, Maritimes 4.6%, and Pacific 30.9%. Furthermore, to mitigate bias concerns related to the missing cases, a CCG evaluation team examined a sample of the missing cases and concluded that the missing cases are not biased (ibid). The fact that the total missing cases have been measured and that there was no bias in the missing cases helps to ensure that the SISAR database remains a primary data source supporting SAR incident data analysis in Canada.

Several times in this chapter we mentioned the USCG visual analytic tool cgSARVA (Malik et al. 2011), which focused on USCG historical response operation incident data in the Great Lakes region from 2002 to 2011. The Great Lakes region represents a major inland waterway where SAR is a shared responsibility between two nations. Canada and the United States have a long history of providing cross-border SAR in this region. It would seem reasonable that a complete assessment of maritime response, asset allocation, and risk assessment should reflect the cooperative nature of SAR in the Great Lakes region.

The inclusion of Canadian SAR stations and incident data in cgSARVA would undoubtedly influence the risk profiles generated by cgSARVA and reported in Malik et al. (2012). The generation of updated risk profiles that account for Canadian data could provide insight into the benefits of enhanced cross-border SAR coordination. Looking more broadly, maritime search and rescue in the Arctic also demands a high degree of international coordination and collaboration. The great importance of cooperation among Arctic nations in conducting SAR operations in the North is detailed in the Agreement on Cooperation on Aeronautical and Maritime Search and Rescue in the Arctic (Arctic Council 2011). The pooling of historical incident data and SAR resource locations and capabilities

from all the parties to the Agreement could enable a more comprehensive analysis of SAR capabilities in the region and
ultimately improve the delivery of SAR services.

Many researchers are also now starting to link environmental conditions and accident data to add context to historical SAR incidents. Wu, Pelot, and Hilliard (2009) have studied the influence of weather conditions on the relative incident rate of fishing vessels in Atlantic Canadian waters. Their analysis considered the following environmental factors: wave height, sea surface temperature, air temperature, ice concentration, fog presence, and precipitation. Ice concentration was shown to have the greatest influence on the magnitude of the relative incident rates for fishing vessels. In areas with low ice concentration, wave height was associated with higher incident rates. The presence of fog and precipitation was found to not be an important
influence on relative incident rate.

More recently, Rezaee, Pelot, and Ghasemi (2016) extended the analysis of Wu, Pelot, and Hilliard (2009) and determined that the influence of weather conditions on relative incident rates in Atlantic Canadian waters is also largely dependent on vessel length. Similar studies have been conducted in other maritime areas. Goerlandt et al. (2017) examined navigational shipping accidents in the northern Baltic Sea area, successfully integrating accident data and environmental conditions. Atmospheric and sea ice data were used to reconstruct the navigational conditions that existed at the time of the accident to contextualize the incident, aimed at improving wintertime maritime transportation risk analysis.

Lastly, SAR response time estimation is receiving increasing attention in the literature and is a key factor in determining optimal SAR station location and assignment of SAR units. Siljander, Venalainen, Goerlandt, and Pellikka (2015) applied GIS-based tools and methods to evaluate SAR response time, considering environmental conditions. Their analysis considered the capabilities of the SAR unit and prevailing wave conditions at the time of the incident to improve estimates of response time for use in strategic SAR planning. SAR response times can be significant in the remote areas of the northwest Atlantic and Arctic. Not only are these regions remote, the environmental conditions can be very harsh, further increasing SAR response times. New methods are required to

improve estimates of ship speeds in adverse environmental conditions, such as sea ice conditions, to improve the accuracy of response time estimation.

3.7. Conclusion

The CCG has collected data and information about SAR incidents involving CCG assets and personnel since the 1980s. This data provides CCG personnel with necessary information to support SAR planning, management, and operations. This rich SAR incident dataset provides researchers and analysts with a multivariate dataset that can be used to support a wide range of analysis and visualizations. In this chapter we discussed the use of SISAR incident data to explore temporal and spatial trends in the data using interactive web visualization techniques. The most prominent trends observed in the data included the increase in SAR incidents during the summer months, predominately on weekends and in the evening hours between 6 pm and 11 pm.

In addition to temporal trends, the spatial location of SAR incidents was also examined. By plotting the coordinates for each SAR event on top of a map projection of the Canadian eastern coastline, it was possible to identify areas of high concentration of incidents. In this chapter we highlight the high concentration of incidents off the southern tip of Nova Scotia (see Fig. 3.14). In addition to plotting the location of the incident, the severity of the incident was used to create a visual analytic to control the opacity of the incident location point symbol (red circle). The use of opacity was effective in refining regions of higher concentration of severe incidents.

These interactive visualizations were effective in identifying several temporal and spatial patterns in the SISAR data. These visualizations could be used by an analyst to support decisions regarding SAR station manning, SAR station location, and employee shift scheduling (monthly, daily, and hourly). The continued use of SISAR data to improve decision-making in the CCG will help to ensure the delivery of SAR services is cost-effective and that response times are minimized, ultimately saving more lives.

References

Akbari, A., H. Eiselt and R. Pelot. 2017. A maritime search and rescue location analysis considering multiple criteria, wtih simulated demand. *INFOR: Information Systems and Operational Research* 56(1): 92–114.

Akbari, A., R. Pelot and H. Eiselt. 2018. A modular capacitated multi-objective model for locating maritime search and rescue vessels. *Annuals of Operational Research* 267(1): 3–28.

Bostock, M. 2019). D3js data-driven documents. https://d3js.org/. Accesed 28 June 2019.

Bostock, M., V. Ogievetsky and J. Heer. 2011. D^3 Data-Driven Documents. *IEEE Transactions on Visualization and Computer Graphics* 17(12): 2301–2309.

David, A., and C. auro. 2015. Web 3D data visualization of spatio temporal data using data driven document (D3js). *International Journal of Computer Applications* 111(4): 42–46.

ESRI ArcGIS. n.d. Albers equal area conic projection (ArcMap 10.7). http://desktop.arcgis.com/en/arcmap/latest/map/projections/albers-equal-area-conic.htm. Accessed 2 July 2019.

Government of Canada. 2003. *Alerting, detection, and response: Dealing with accidents at sea.* St. John's, NL: Fisheries and Oceans Canada.

Government of Canada. (2019, June 25). *Canadian Coast Guard Search and Rescue and Canadian Coast Guard Auxiliary Evaluation Report*. Retrieved from Department of Fisheries and Oceans Canada: https://www.dfo-mpo.gc.ca/ae-ve/evaluations/11-12/SAR-CCGA-eng.htm#2.1

Government of Canada. (2019, July 3). *Department of National Defence Reports and Publications*. Retrieved from Search and Resuce Posture Review 2013: https://www.canada.ca/en/department-national-defence/corporate/reports-publications/search-and-rescue-posture-review-2013.html

Government of Canada. 2019*a*. Maritime search and rescue in Canada. http://www.ccg-gcc.gc.ca/eng/CCG/SAR_Maritime_Sar. Accessed 25 June 2019.

Malik, A., B. Maciejewski, B. Maule and S. Ebert. 2011. A visual analytics process for maritime resource allocation and risk assessment. In *2011 IEEE Conference on Visual Analytics Science and Technology (VAST)*, 221–230 (Providence, RI: Institute of Electrical and Electronics Engineers).

Malik, A., R. Maciejewski, Y. Jang, S. Oliveros, Y. Yang, B. Maule, ... D.S. Ebert. 2012. A visual analytic process for maritime response, resource allocation and risk assessment. *Information Visualization* 13(2): 93–110.

Marven, C.A., R.R. Canessa and P. Keller. 2007. Exploratory spatial data analysis to support maritime search and rescue planning. In *Geomatics soltuions for disaster management*, eds J. Li, S. Zlatanova and A.G. Fabbri, 271–288. Berlin/Heidelberg: Springer.

Murray, S. 2013. Interactive data visualization for the web: An introduction to designing with D3. Sebastopol, CA: O'Reilly Media Inc.

Pelot, R., and L. Plummer. 2008. Spatial analysis of traffic and risks in the coastal zone. *Journal of Coastal Conservation* 11: 201–207.

Purdue University. (2019, July 4). *Visual Analytics for Command, Control and Interoperability Environments (VACCINE)*. Retrieved from www.purdue.edu/discoverypark/vaccine

Razi, N., & M. Karatas. 2016. A multi-Objective Model for Locating Search and Rescue Boats. *European Journal of Operational Research, 254*, 279-293.

Shaharabi, J. 2003. Spatial and temporal analysis of maritime fishing and shipping traffic incidents. Halifax, NS: Dalhousie University.

United States Department of Homeland Security, Science and Technology. 2018. Snapshot: How Coast Guard response is benefitting from S&T's university partnerships. https://www.dhs.gov/science-and-technology/news/2018/01/30/snapshot-how-coast-guard-response-benefitting-st-s-university. Accessed 25 June 2019.

Van Wijk, J., and S. Selow. 1999. Cluster and calendar based visualizations of time series data. In *Proceedings of the 1999 IEEE Symposium on Information Visualization*, San Francisco, CA, USA, 1999, 4–9.

Ware, C. 2004. *Information visualization: Preception for design*. San Francisco, CA: Elsevier Inc.

Appendix 6: Making Sense of Marine-Based Search and Rescue Response Time using Network Analysis

Stoddard, M.A., Pelot, R., Etienne, L., and Goerlandt, F. (2024). Making Sense of Marine-Based Search and Rescue Response Time using Network Analysis. Book Chapter in A. Chircop et al. (eds.), Area-Based Management Approaches to Shipping Risk Mitigation: Canadian and Comparative Perspectives, Springer Cham, https://doi.org/10.1007/978-3-031-60053-1

Chapter 13

Making Sense of Marine-Based Search and Rescue Response Time using Network Analysis

Mark A. Stoddard, Ron Pelot, Floris Goerlandt, and Laurent Etienne

Abstract

Navigation in polar waters follows standard navigational practice, with special consideration for the presence of sea ice and its expected impact on safe ship operation. Experienced polar ship operators rely on timely access to authoritative sea ice analysis and knowledge of the safe operational limits of their ship to determine the navigability of polar waters. Several sea ice risk assessment frameworks exist to assist ship operators with onboard decision-making, most notably, the Polar Operational Limit Assessment Risk Indexing System (POLARIS). The result from POLARIS is referred to as the Risk Index Outcome (RIO). By adjusting ship speed in response to the RIO value, it is possible to account for sea ice risk in the estimation of ship transit time in polar waters. In this chapter we discuss the use of network analysis techniques to generate the fastest route between two locations in the Arctic and to compute surface ship incident response service areas (IRSA) and incident response isochrones (IRI) for different times of year and ship ice classes. The use of IRSA and IRI to support area-based management (ABM) tools that aim to formally incorporate historical observations of shipping activity into quantitative assessments is also discussed. Incorporating IRSA and IRI results into ABM tools would provide decision-makers with a useful tool to possibly help plan and coordinate incident response in polar waters and support ABM of commercial vessel operation and search and rescue provision.

Keywords: POLARIS, service area, isochrone, network analysis, optimization

13.1 Introduction

Reductions in sea ice due to climate change continue to affect navigability in the Canadian Arctic and other polar regions (Smith and Stephenson 2013; Melia, Haines and Hawkins 2016). Many of the maritime areas experiencing changes in sea ice conditions are becoming more accessible for longer periods, resulting in increased maritime activity and higher volumes of shipping traffic. As accessibility improves, global interest in Arctic maritime activity from various economic sectors will likely continue to increase (Arctic Council 2009). Increases in Arctic shipping will put new pressures on the limited infrastructure and services supporting Arctic shipping, especially the search and rescue (SAR) capabilities of many Arctic nations. While Arctic states continue to build infrastructure and response capacity, polar ship operators must continue to demonstrate a high degree of self-reliance and sound decision-making. The International Maritime Organization (IMO) International Code for Ships Operating in Polar Waters (Polar Code 2014/15) also provides mariners with guidance to reduce operational risks in polar waters via safety and environmental prevention measures (Fedi et al. 2018). Currently, the Polar Code requires that all vessels operating in polar waters be prepared to wait at least five days for SAR resources to arrive on-scene (World Maritime Organization, 2015). The combination of the remoteness of the Canadian Arctic and lack of SAR infrastructure has the potential to push maritime-based SAR response well beyond five days, and in some cases the incident location may be inaccessible by available maritime-based SAR assets.

Accessibility in the Arctic can be assessed using navigability and expected ship transit times as proxy indicators. Navigability is commonly determined using risk-based methods to identify go/no-go areas for a particular polar ship class, on the basis of the ice risk present in an area of operations (Mudryk et al. 2021). Ice risk is typically determined by ship bridge watch officers and/or qualified ice navigators using a variety of frameworks developed by transportation authorities and ship classification societies. The Polar Code currently recommends the use of the Polar Operational Limit Assessment Risk Indexing System (POLARIS). A ship operator can use POLARIS to assess the navigability of an area of operation by converting observed sea ice conditions into a Risk Index Outcome (RIO). The RIO result is specific to a ship's polar class (Fedi, Faury and Etienne 2020).

The more positive the RIO value, the more navigable the area of operation. POLARIS is already widely used by researchers to support a variety of analysis that involve Arctic navigation and navigability, such as trans-Arctic routing (Melia, Haines and Hawkins 2016; Aksenov et al. 2017), economic analysis of polar routes (Lloyds of London 2014; Smith and Stephenson 2013), and modelling and simulation of shipping activity (Wei et al. 2020; Wang et al. 2022).

In this chapter we examine how variable sea ice conditions in the Canadian Arctic affect the fastest route between two locations and expected transit time. The method to compute the fastest route between two points in the Arctic accounts for changes in the navigability along a route due to sea ice risk. The method to compute transit time integrates sea ice risk assessment and knowledge of expected ship speeds in different ice regimes. The result is a transit time estimate that accounts for changes in ship speed due to varying levels of sea ice risk encountered along the route. By combining these two methods we are now able to compute incident response service areas (IRSA) and incident response isochrones (IRI) for different times of year, different polar class vessels, and locations of interest. IRSA and IRI are analysis tools that are used to determine the reachable areas of a geographic area within a maximum response time cut-off (MRTC). All figures presented in this chapter were produced by the authors.

The use of IRSA and IRI simplifies the analysis of expected transit time from an arbitrary location in the Arctic to a point of interest, such as a SAR incident location, coastal community or area-based management (ABM) location of interest. This allows one to quickly assess and visualize many of the complex navigational challenges associated with maritime mobility in Arctic waters, supporting a variety of ABM applications. One focus of the discussion here is on the potential to apply IRSA and IRI concepts to a previous effort conducted by the National Research Council of Canada (NRC) that examined exposure time until recovery at fixed locations in the Arctic (Kennedy, Gallagher and Aylward 2013). The goals of the NRC study were to identify and assess key factors that influence exposure time and to use the results to strengthen policy and regulations relating to operational requirements and life-saving appliance testing conditions. The discussion

here demonstrates how IRSA and IRI concepts could be used to better quantify the potential contribution of vessels of opportunity (VOO) in the analysis marine-based SAR response.

13.2 Theoretical Background

13.2.1 Incident Response and Maritime SAR

In Canada, SAR is one of the primary responsibilities of the Canadian Coast Guard (CCG). Through the effective use of dedicated SAR resources, the CCG responds to approximately 6,000 maritime incidents per year (Government of Canada 2019). Following each response operation, incident reports and logs are entered in a database known as the Search and Rescue Program Information Management System (SISAR) (Stoddard and Pelot 2020). SISAR incident data is one of the primary data sources used to capture statistics relating to maritime SAR cases to inform demand for programme services and the achievement of outcomes (Government of Canada 2019a). SAR incident data provides a rich multivariate spatiotemporal dataset that can support a wide range of analysis. This chapter focusses only on the location of historical maritime incidents to provide a basic understanding of the spatial distribution of historical incident locations in the Canadian Arctic, broadly supporting the ABM objectives of the CCG. Figure 13.1 provides an overview of historical maritime incidents which occurred between 2001 and 2020. Much of the analysis in this chapter is focused on the Baffin Bay region. Baffin Bay was selected for discussion for two reasons: (1) it is an area of high incident occurrence, and (2) it presents a very challenging navigational environment throughout the year, especially during the yearly sea ice free-up and break-up.

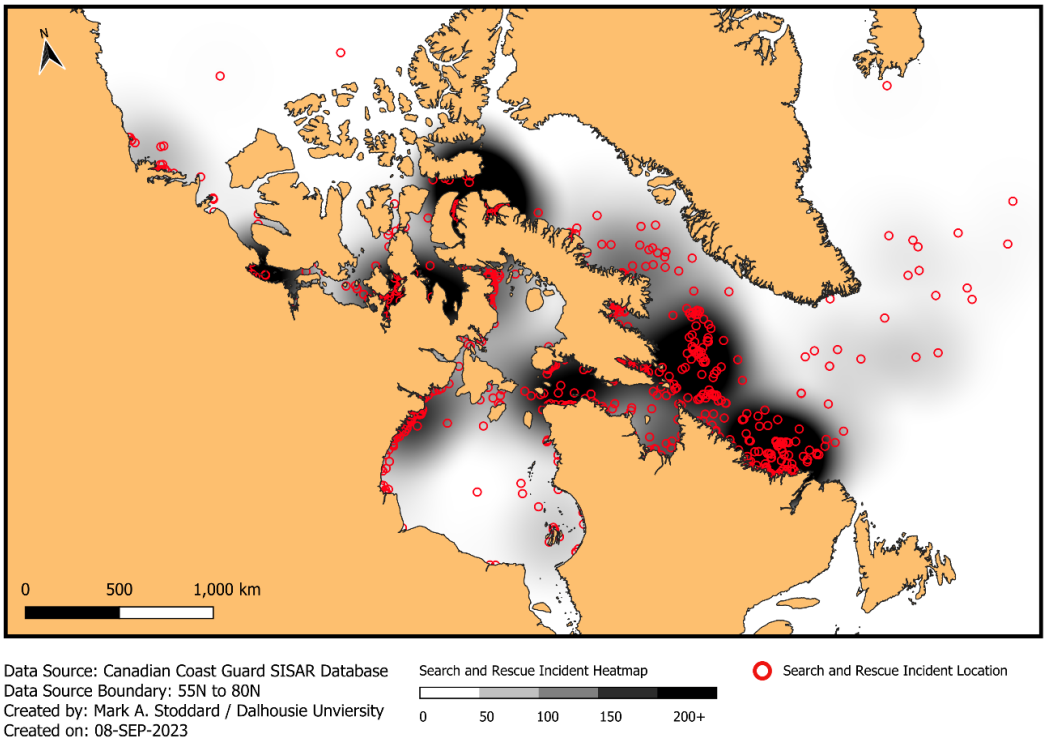

Fig. 13.1 Spatial distribution of SISAR incident data collected between 2001 and 2020.

13.2.2 Route planning and transit time estimation in variable sea ice conditions

Navigation risk assessment tools, such as POLARIS, are widely used to assess sea ice risk and determine its impact on safe ship operations (Fedi, et al., 2018). The POLARIS assessment can be applied over wide areas using national sea ice analysis charts from the United States National Ice Center (USNIC) and Canadian Ice Service (CIS) to determine the accessibility of maritime locations in the Arctic. Accessibility is a crucial element in incident response operations, especially when considering remote maritime locations that lack supporting infrastructure in the Canadian Arctic. POLARIS is a useful tool to determine the navigability in an intended area of operations, but it does not provide extensive guidance on the selection of safe ship speeds in different RIO categories. The current guidance is limited to recommended ship speeds for polar class ships operating on RIO values between 0 and -10 (Maritime Safety Committee 2014a). No speed recommendations are specified in the POLARIS framework outside of this RIO value range.

Due to the spatial variability of sea ice conditions and the navigational complexity of the Arctic archipelago, standard approaches to calculate travel distance and time, such as Euclidean and Manhattan distance, are not feasible or even practical. One approach is to determine transit distance and time using network analysis methods, relying on the computation of total network distance and travel time along predefined arcs in an undirected graph (Siljander et al. 2015). Several network analysis algorithms exist to compute the shortest/fastest path between a source node and destination node in a graph, such as Dijkstra's shortest path algorithm (Dijkstra 1959).

Smith and Stephenson (2013) demonstrated the use of network analysis methods to study new trans-Arctic shipping routes. Their method successfully combined the Transport Canada Arctic Ice Regime Shipping System (AIRSS) navigability assessment (similar to the POLARIS methodology) and sea ice data from different coupled atmosphere-ocean general circulation models (GCM) to compute trans-Arctic shipping routes and expected transit times using a terrain sensitive least-cost path algorithm. The optimal route was the route that accumulated the lowest possible travel time between origin and destination along the network arcs. The total transit time is the linear sum of the travel time of each arc in the graph that was traversed (Smith and Stephenson 2013). Wang, Zhang and Qian (2018) provide a complementary example of combining AIRSS with GCM outputs, to generate routes in the Arctic using a modified A* network optimization algorithm. More recently, Wei et al. (2020) generated Arctic shipping routes using a two-step process: (1) calculate the technical accessibility of a grid cell by an ice class ship, and (2) find the fastest route. Technical accessibility of a grid cell was determined using AIRSS with forecasted ice properties (thickness and concentration) from the output of a GCM. The cell-based least-cost path algorithm in a geographical information system was then used to determine the optimal path from origin to destination.

A good estimate of ship speed in different RIO categories is critical to improve the estimation of travel time and related metrics such as fuel consumption and emissions. Much research has been devoted to improving our understanding of the complex relationship between ice conditions, ship design and operating characteristics. McCallum (1996) provided an early approach to predict expected ship speed in ice using a polynomial fit

between minimum and maximum expected ship speeds for several Canadian Arctic Class (CAC) ships in different ice risk regimes. Ice risk was determined using AIRSS. Similarly, Somanathan, Flynn and Szymanski (2006) also discuss the use of AIRSS to create a relationship between the AIRSS ice numeral and ship ice class to calculate a speed through ice. Kotovirta et al. (2009) examined the use of a mathematical relationship between ship net thrust and ice thickness/resistance. Automatic information systems (AIS) data was used for statistical validation of the transit times calculated by their method. More recently, researchers have begun to directly associate AIS data collected in polar regions with daily sea ice analysis to gain new insight into expected ship speed. Loptien and Axell (2014) examined the relationship between AIS reported speed over ground and sea ice forecasts in the Baltic Sea to produce a mixed-effects model to predict vessel speed from forecasted ice properties, such as ice concentration, ice thickness and ridge density. Lensu and Goerlandt (2019) and Goerlandt et al. (2017) provide two more recent examples of combining AIS and sea ice data for the Baltic Sea area to obtain insights in their relationship with operational ship speeds in ice for different types of ship operations. Lastly, Tremblett, Garvin and Oldford (2021) used shore-based AIS data collected in the North American Great Lakes region between 2010 and 2019 to examine the distribution of observed vessel speeds in different RIO risk categories derived from CIS sea ice charts produced for the Great Lakes region. The authors do caution that POLARIS does not currently provide risk values (RV) for lake ice conditions or provide a mapping of sea ice equivalence, so great care must be taken when interpreting the results from this study.

13.2.3 Service Areas and Isochrones

An “isochrone” is defined as the line joining the equal travel time distances from any given location and have been used to understand the relationship between movement and time for more than 130 years (Dovey, Woodcock and Pike 2017). A service area is defined as all geographic points within the polygon created by the isochrone. In this chapter we introduce the use of service areas and isochrones to study the relationship between ship movement and transit time in the Arctic. Isochrones and service areas are an effective tool to examine accessibility and mobility simultaneously, which is highly desirable when studying Arctic transportation. Determining the accessibility of and mobility in polar waters is one of the

primary motivations for using the POLARIS assessment. POLARIS is used to determine if an area is accessible, meaning it is safely navigable, and to enable risk-based decisions related to safe ship speeds in ice.

The focus here is on the use of service areas and isochrones to better understand marine-based SAR response at different locations in the Arctic and response time cut-offs. Reference is made to service areas as IRSA and isochrones as IRI. IRSA and IRI have several potential uses in support of maritime ABM, but the focus here is on their use for marine-based SAR response in polar waters.

13.3 Methods

In this section we discuss data sources and analysis workflows used to produce the geospatial products presented and discussed throughout this chapter. Bi-weekly sea ice analysis data from the USNIC was used as the basis for the POLARIS calculations discussed here. POLARIS was used to compute and visualize navigational risk, and the expected transit time was determined by combining POLARIS RIO results with expected ship speeds in different RIO result categories as reported by Stoddard et al. (2023). Dijkstra's algorithm was used to perform network optimization and compute the fastest path between two points in an undirected transportation graph. Service area isochrones were produced by computing the concave hull of all nodes in the transportation graph from which an incident location can be reached by the fastest path within a given service level target, specified in hours. Figure 13.2 provides an overview of the geospatial data processing workflow for producing the fastest routes in ice, transit time and incident response service areas and isochrones.

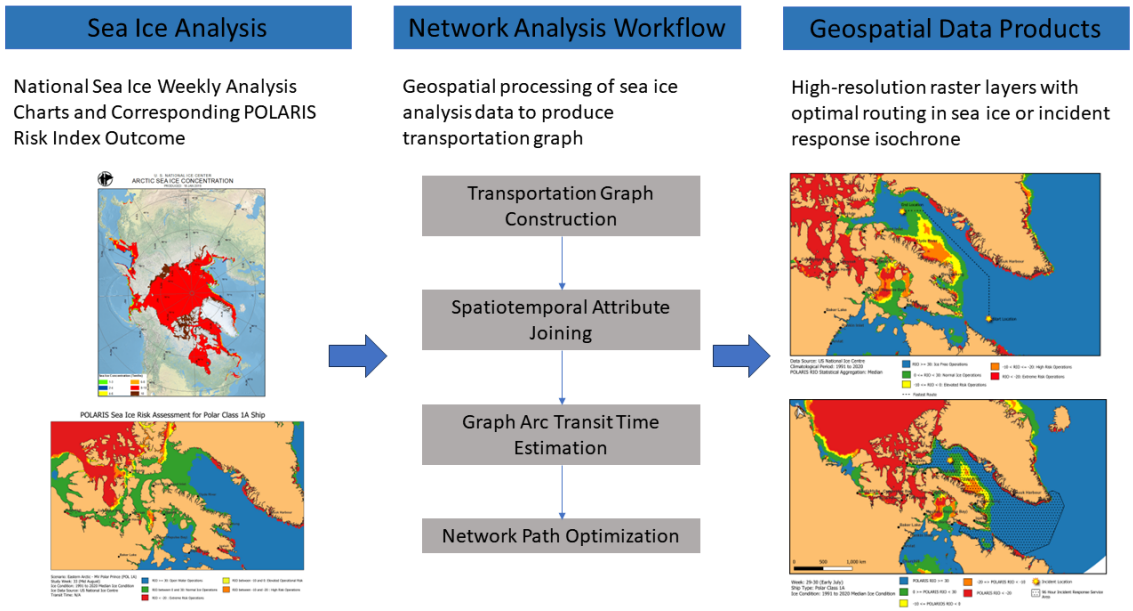

Fig. 13.237 Geospatial data processing workflow for producing optimal ship routes in ice and ISRA

13.3.1 Sea ice analysis

Several authoritative sources of sea ice analysis exist, including USNIC, CIS, Danish Meteorological Institute, Icelandic Meteorological Office, and the Norwegian Meteorological Institute. To promote interoperability and data exchange, all national ice centres publish sea ice charts in a standard World Meteorological Organization (WMO) ice chart archive vector format known as Sea Ice Grid (SIGRID-3) (USNIC 2022). Operational sea ice charts show ice regimes as distinct polygons within a mapped region. An ice regime is defined as an area with a relatively consistent distribution of any mix of ice types, including open water. Ice analysts working for national ice centres have access to a variety of high resolution data sources to estimate the partial ice concentrations of various ice types in an ice regime and encode the information according to a WMO standard (IOC/UNESCO 2004).

Bi-weekly sea ice charts for the Arctic from the USNIC were selected for this study because of their circumpolar coverage and historical date coverage range. USNIC sea ice charts are produced through a detailed analysis of available *in situ* remote sensing and model data sources. The USNIC digital ice analysis charts (hemispheric, regional and daily)

have two main components: the shapefile containing the ice analysis ice information (ice polygons and related attributes) and the metadata describing the ice analysis data (National Snow and Ice Data Center 2015). Both components of the USNIC sea ice charts were used in this study.

13.3.2 Navigational risk assessment in polar waters using POLARIS

POLARIS provides a quantitative framework to assess navigational risk in polar waters. Each polygon in a USNIC sea ice analysis chart is used to describe an area with a relatively consistent distribution of one or more ice types and may include open water. The concentration of each ice type (determined by observed stage of development and thickness) is reported in tenths. POLARIS specifies a RV for each ice type and polar class ship type. The output of the POLARIS assessment is referred to as RIO. The RIO is determined by calculating the linear sum of the RVs associated with each ice type present in a given ice polygon, multiplied by the respective ice type concentration (in tenths):

$$RIO = C_1RV_1 + C_2RV_2 + \cdots + C_nRV_n \qquad \text{Equation 1}$$

where $C_1, C_2, \ldots, C_n$ are the concentrations of the ice types present in an ice regime and $RV_1, RV_2, \ldots, RV_n$ are the risk values provided by POLARIS. The RIO value is then evaluated, and a series of decision rules are applied to determine an appropriate operational limitation due to the presence of sea ice in the area of operation (Maritime Safety Committee 2014b). The decision rules applied in this study are shown below in Table 13.1.

Table 13.1 POLARIS RIO results decision rules, and associated risk level descriptions used for this study

Decision Rule	**Risk Level**
RIO >= 30	Open Water Operations
0 <= RIO < 30	Normal Ice Operations
-10 <= RIO < 0	Elevated Operational Risk

-20 <= RIO <-10	High Risk Operations
RIO < -20	Extreme Risk Operations

It is possible to use POLARIS to compute and visualize the RIO for each polygon in the USNIC sea ice analysis chart for a chosen POLARIS scenario. The POLARIS scenario refers to the selection of ship polar class and the decision rule used to determine the different RIO result categories. The result is a new sea ice analysis product we refer to as the single chart POLARIS scenario risk map. A POLARIS scenario risk map is unique to each polar class ship type and selection of decision rule. Figure 13.3 provides an example of a POLARIS scenario map for a Polar Class 1A ship.

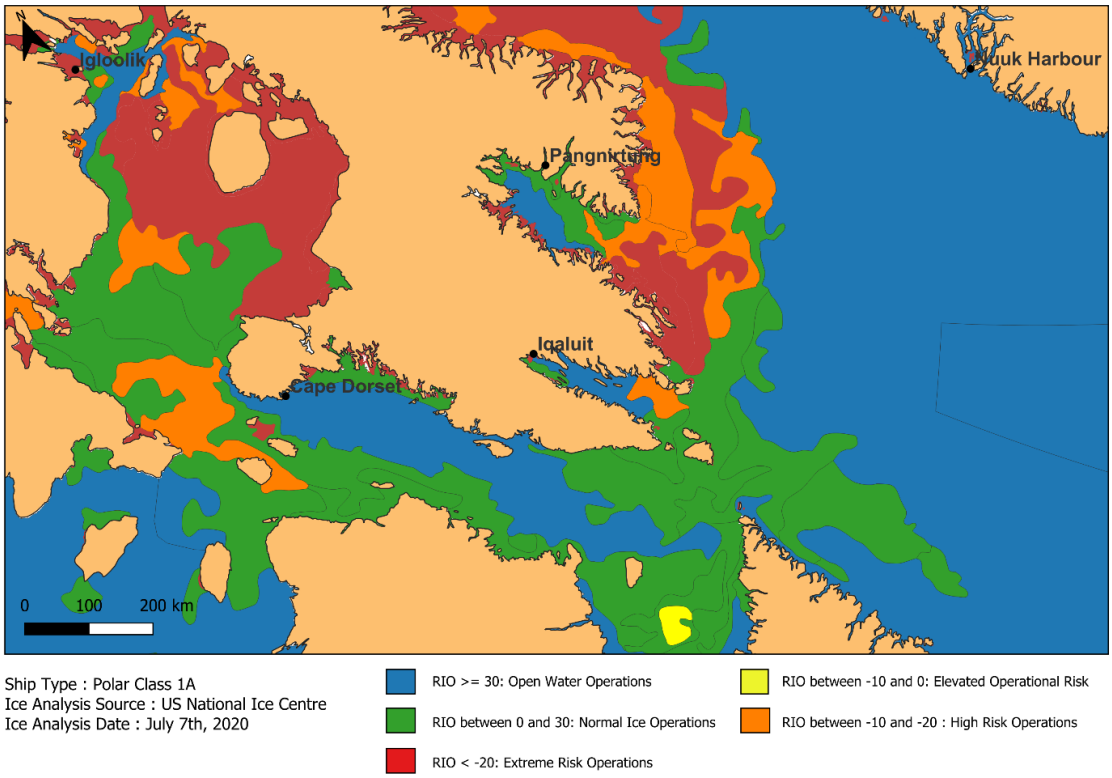

Fig. 13.3. Single chart POLARIS risk map for a Polar Class 1A ship operating in the eastern Arctic on 7 July 2020.

For strategic navigation planning it is often necessary to plan routes based on the ice conditions expected to be encountered during a future voyage. Stoddard et al. (2016) demonstrated how statistical aggregations of historical POLARIS RIO results can be used to support strategic navigation planning in polar waters. Using gridded CIS daily sea ice analysis charts from 2007 to 2014, the authors computed six statistical aggregations of historical RIO results throughout the Canadian Arctic including (1) minimum RIO, (2) 25th percentile RIO, (3) average RIO, (4) median RIO, (5) 75th percentile, and (6) maximum RIO.

This study focuses on the use of gridded USNIC bi-weekly sea ice analysis charts that cover the climatological period from 1991 to 2020 to compute the median POLARIS RIO value. In total, 1,295 USNIC bi-weekly sea ice analysis charts were first gridded, resulting in 4,212,296 georeferenced grid cells containing the sea ice analysis attributes from each chart. The median RIO value for each grid cell was then computed on a bi-weekly basis, resulting in a final output of 26 gridded bi-weekly POLARIS scenario risk maps. Figure 13.4 shows how the features of the bi-weekly POLARIS scenario risk map are spatially joined with the analysis grid to produce the gridded bi-weekly POLARIS scenario risk map. This process is repeated for all USNIC bi-weekly sea ice analysis charts produced within the climatological period, and then a median RIO value is computed for each grid cell.

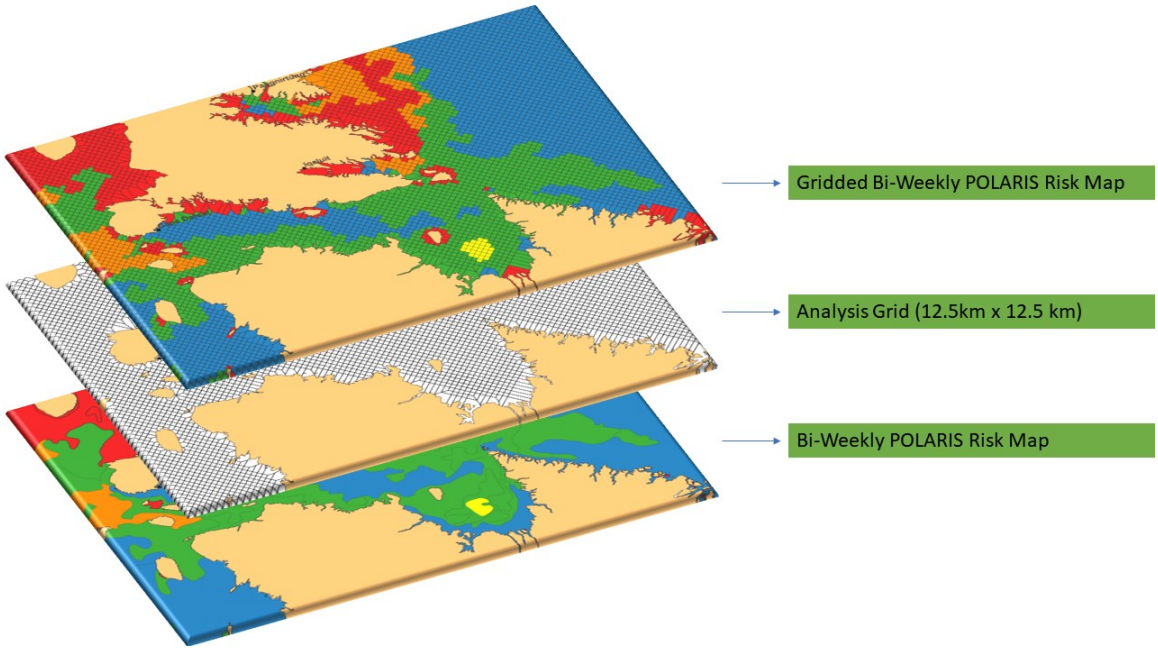

Fig. 13.4 Geospatial processing of map layers to generate the gridded bi-weekly POLARIS scenario risk map (top layer)

13.3.3 Transportation Graph and Transit Time Estimation

In order to utilize network optimization algorithms to compute the fastest route through an area of operations, we constructed an undirected graph for each bi-weekly analysis period, consisting of 137,494 nodes and 1,099,952 arcs. A node was created at the centroid of each grid cell in our analysis grid, with each node inheriting the sea ice analysis and POLARIS RIO attributes from the associated grid cell. Arcs were created by connecting adjacent nodes by straight line segments. The RIO value for each arc was computed by averaging the RIO value of the start and end node. The transit time for each arc was determined by dividing the arc length (km) by the expected ship speed in each RIO category (km/h). The ship speeds shown in Table 13.2 were first reported by Stoddard et al. (2023) and were derived from the visual inspection of a histogram of AIS reported vessel speed over ground in different RIO result categories observed over a two-year period. Since the speed is specified based on the RIO result category, it is not necessary to consider the polar class of vessel when determining the appropriate ship speed along an arc. This is because the polar class of the vessel is already considered when computing the RIO value for each polar ship

ice class. The fastest path is therefore the path from a start location to an end location that minimizes the total transportation cost (total transit time).

Table 13.2 Ship speed versus RIO category

RIO Category	Ship Speed (km/h)	Ship Speed (kts)
RIO >= 30	26	14
0 <= RIO < 30	16	8.5
-10 <= RIO < 0	9	5
-20 <= RIO < -10	5.5	3
RIO < -20	0	0

To compute the fastest path between two points in our network we utilized the QGIS software implementation of Dijkstra's algorithm (Dijkstra 1959). The fastest path is the selection of arcs in the graph that minimizes the total transit time, computed by summing the transit cost of all selected arcs that form the path from start to end location. Figure 13.5 shows a computer-generated fastest route through the Canadian Arctic Archipelago. This route represents the fastest route for a Polar Class 1A ship in Week 37–38 (mid-September) using the 1991–2020 median RIO value.

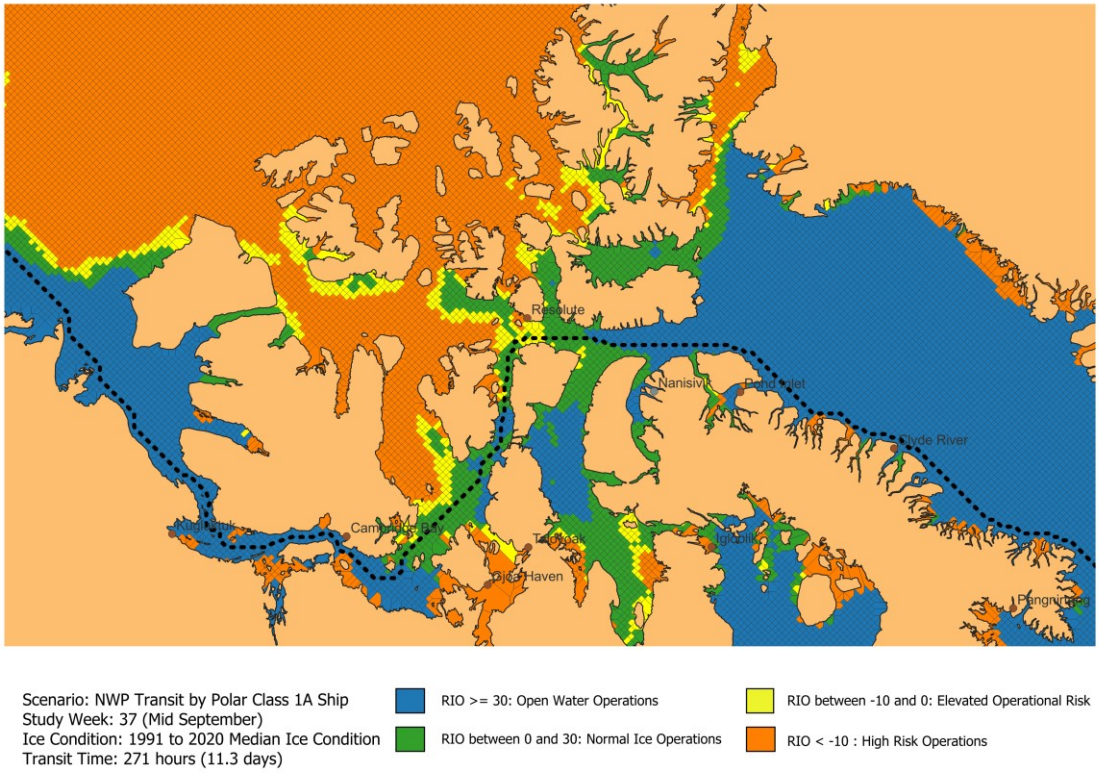

Fig.13.5 Segment of a computer-generated trans-Arctic route from South West Greenland to Chukchi Sea, Alaska, for a polar class 1A ship in week 37 using the expected ship speed in the median RIO value observed over the climatological period from 1991 to 2020

In addition to computing the fastest path, we are also interested in computing IRSA and IRI in the Canadian Arctic. To simplify the following discussion, we first introduce the concept of the service area analysis scenario (SAAS). The SAAS refers to the selection of (1) polar class ship type, (2) analysis time period, (3) RIO value statistic, (4) expected ship speed in each RIO result category, (5) MRTC and (6) a specified geographic location of interest. The IRSA contains all the nodes and arcs of the transportation network that can be reached for a given SAAS. The IRI is a curve of equal travel time (isochrone) formed at the furthest locations in the network that can be reached for given SAAS. Mathematically, the IRSA is the concave hull formed from all nodes in the transportation graph that can be reached within the specified time cut-off. Figure 13.6 illustrates the relationship between the transportation graph, incident response service area and incident response isochrone.

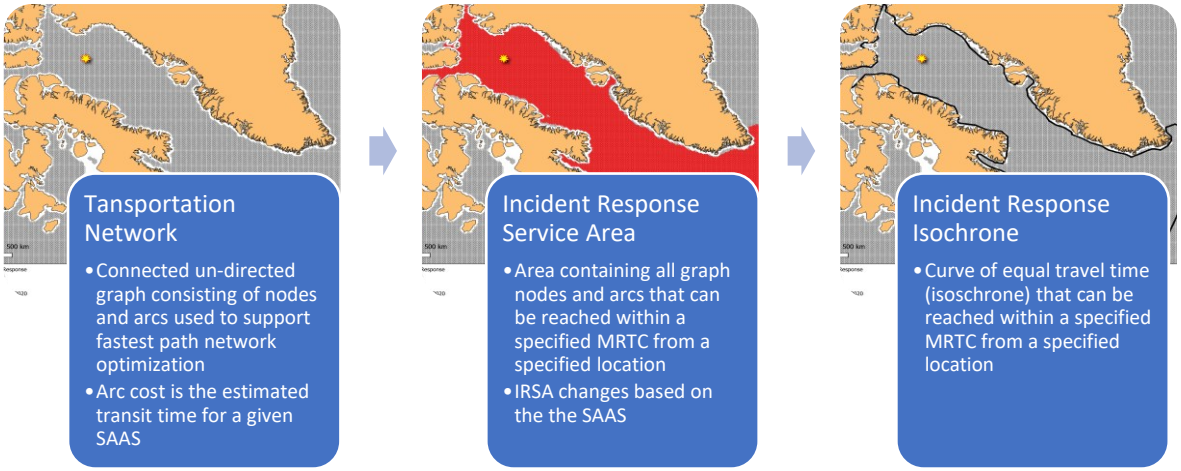

Fig. 13.6 Relationship between transportation network, incident response service area and incident response isochrone

The methods discussed here are applied below to examine several different aspects of incident response in the Baffin Bay region of the Eastern Arctic. The emphasis will be on generating results that can help guide discussion related to incident response in polar waters, as well as introducing the concept of ISRA and IRI to support SAR response operations and ABM more generally. While the results shown below are focused on a notional incident in Baffin Bay, the methods are applicable throughout the Arctic region. Computational results have been produced for a variety of polar class ships, bi-weekly analysis periods and MRTC to help draw attention to the factors that influence ISRA and IRI and their interpretation.

13.4 Results

In this section we apply the methods discussed above to examine incident response in the eastern Arctic. All results were produced using the same incident location (central Baffin Bay) to simplify the comparison of results and follow-on discussion. All POLARIS risk maps, ISRA and IRI have been computed for an International Association of Classification Societies (IACS) Polar Class 1A ship, with some exceptions for the comparison of modelling results for different ship classes. The 1A ship ice class was chosen because it is one of the most common ship ice classes found operating in the Canadian Arctic during the navigable summer season. In practice, the methods discussed in the previous section, and

shown in this section, can be produced for any incident location, time of year, ship ice class and selection of RIO value summary statistic. The three primary results presented and discussed in this section include:

1. Fastest route in polar waters
2. Incident response service areas
3. Incident response isochrones

13.4.1 Fastest Route in Polar Waters

The fastest path is the route that minimizes the total transit time from a start node to an end node in our Arctic transportation graph. Figure 13.7 provides an overview of the fastest route between a start and end location in the eastern Arctic for a Polar Class 1A ship during each bi-weekly analysis period. The 1991 to 2020 median RIO value was used to assess the navigational risk throughout the year. The figure shows how the route and the corresponding transit time changes throughout the year depending on the POLARIS RIO results at the time of operation. We also observe that for a significant portion of the year there is no feasible route for a polar class 1A ship between the start and end location due to the severity of the sea ice conditions. This would indicate that the severity of sea ice conditions exceeds the safe operating limits of a Polar Class 1A ship during that time.

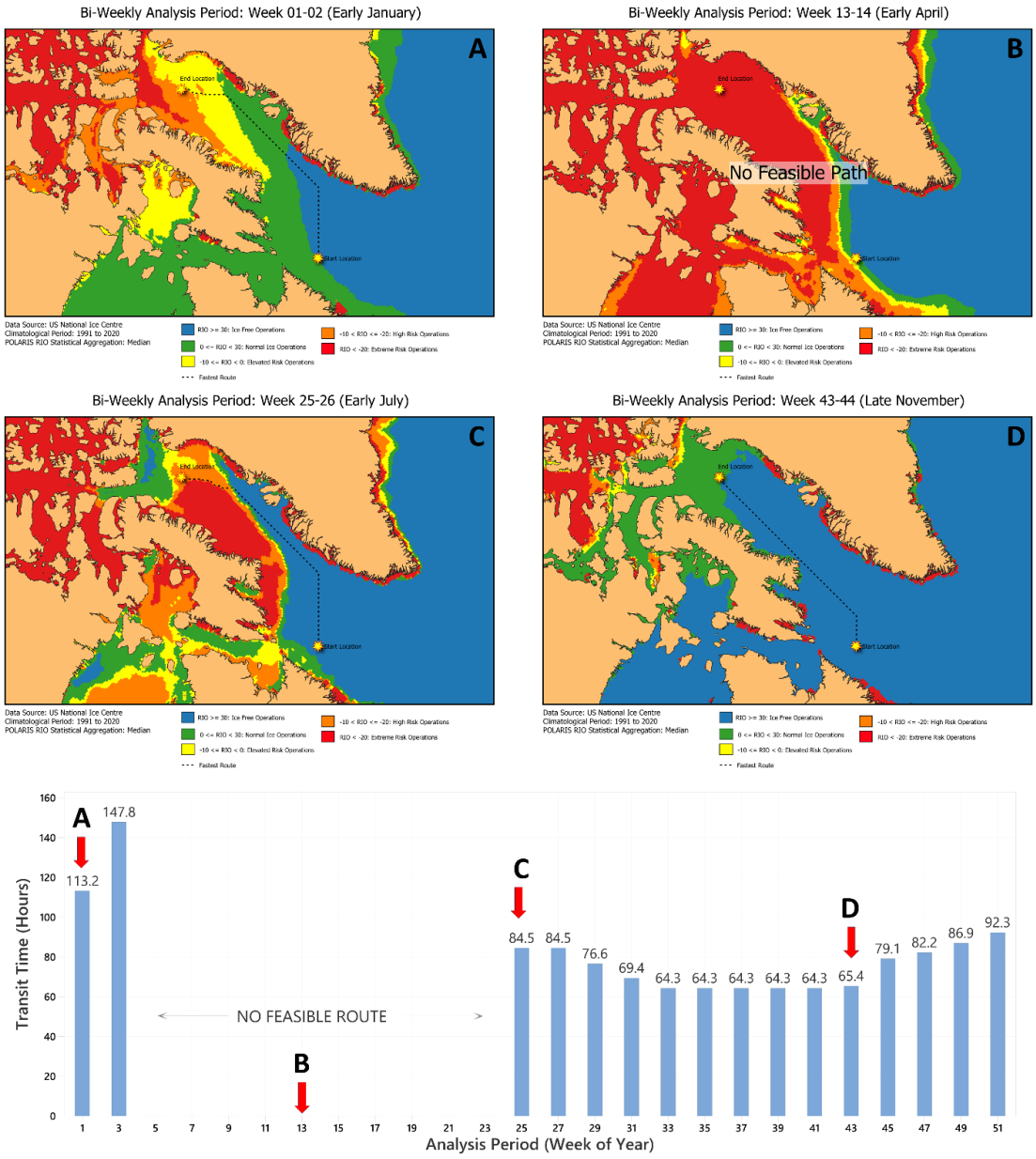

Fig. 13.7 Overview of the fastest route and expected transit time between two locations in the Arctic.

It is also possible to compare expected transit time results for different polar ship classes. In Figure 13.8 we compare the year-round estimated transit time for a Polar Class 1A and Polar Class PC5 ship using a multi-line plot. For awareness, a Polar Class 1A is capable of summer/autumn operation in thin first-year ice (ice thickness from 30 to 70cm),

while a Polar Class PC5 is capable of year-round operation in medium first-year ice (ice thickness from 70 to 120 cm). The enhanced ice operating capabilities of the PC5 vessel allow it to operate safely over a much wider range of sea ice conditions than a 1A vessel. The result is twofold: (1) a PC5 vessel can typically operate at higher speed when sea ice is present when compared to a 1A vessel, and (2) a PC5 vessel has a longer operating season when compared to a 1A vessel.

Using the start and end location from the eastern Arctic transit scenario shown in Figure 13.7, we computed the fastest route and expected transit for Polar Class 1A and PC5. Figure 13.8 shows the expected transit time results as a multi-line plot. For a large portion of the year there is no feasible route between the start and end location for the Polar Class 1A vessel, that is, starting in late January/early February (Week 5) and ending in late June (Week 25). Periods where no feasible route exists appear as areas of discontinuity in the line plot. Notable observations from the comparison of Polar Class 1A and PC5 vessels are summarized in Table 13.3.

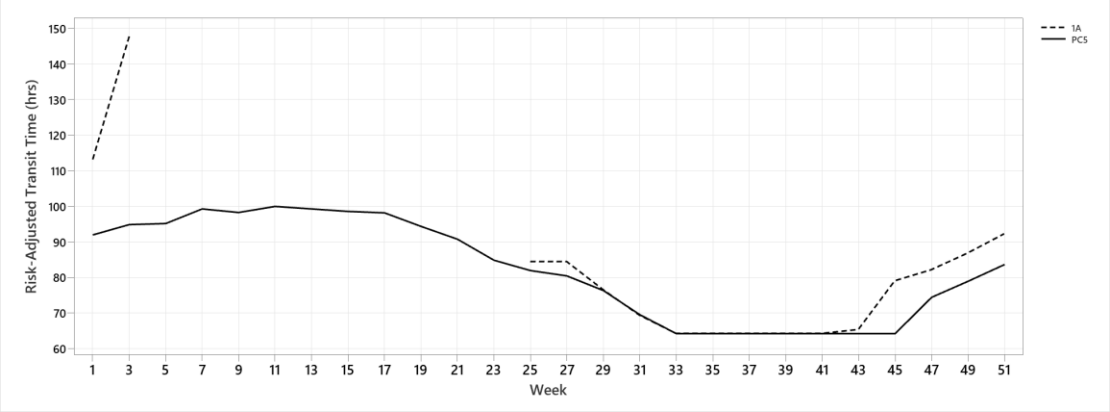

Fig. 13.9 Comparison of the year-round risk-adjusted transit time for a Polar Class 1A and PC5 ship between a start and end location in the eastern Arctic. Note: When no feasible route exists, the line is not drawn for that particular ship class.

Table 13.3 Summary of year-round risk-adjusted transit time results for Polar Class 1A and PC5

	Polar Class 1A	**Polar Class PC5**
No feasible route (weeks)	5 to 25	N/A
Maximum expected transit time (hours)	147.8	100.0
Maximum expected transit time (week(s) of occurrence)	3	11
Minimum expected transit time (hours)	64.3	64.3
Minimum expected transit time (week(s) of occurrence)	33 to 41	33 to 45

13.4.2 Incident response service area and POLARIS

Now that we can compute the fastest path between any start and end nodes in the Arctic transportation network, it is possible to compute the IRSA. The IRSA shown in Figure 13.9 was generated for a Polar Class 1A ship operating in the eastern Arctic during Week 29–30 using a 96-hour MRTC. The IRSA can be interpreted as containing all possible start nodes in the graph that can reach the incident location (end node) within the specified MRTC. The MRTC used for the analysis in this section is 96 hours. Figure 13.10 shows how the IRSA size changes throughout the year as the RIO changes due to varying sea ice conditions throughout the year. Other factors that influence service area size are the MRTC (see Figure 13.11) and ship ice class (see Figure 13.12).

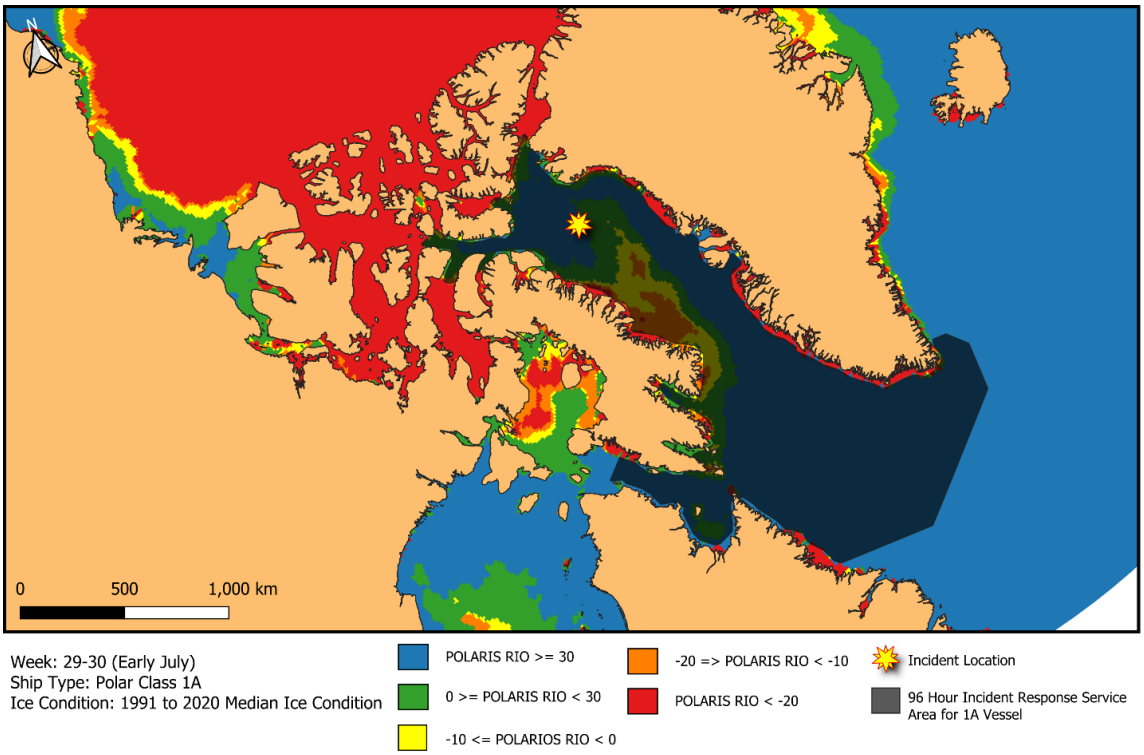

Fig. 13.9 Computed service area for a Polar Class 1A ship in Week 29–30.

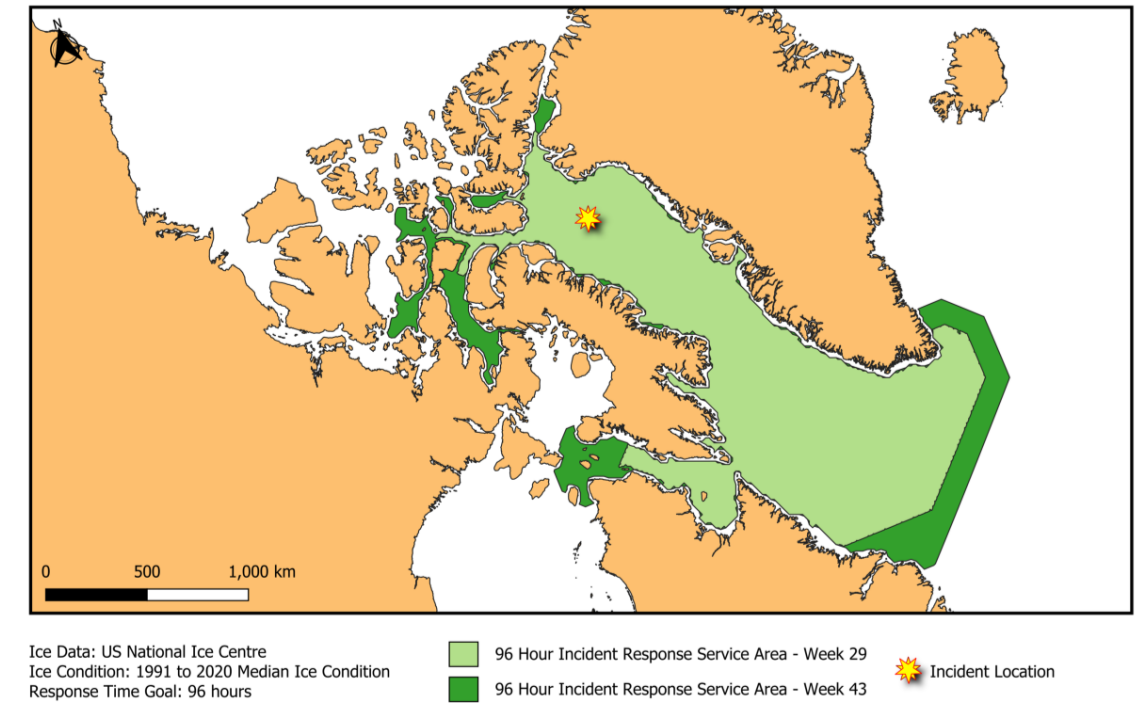

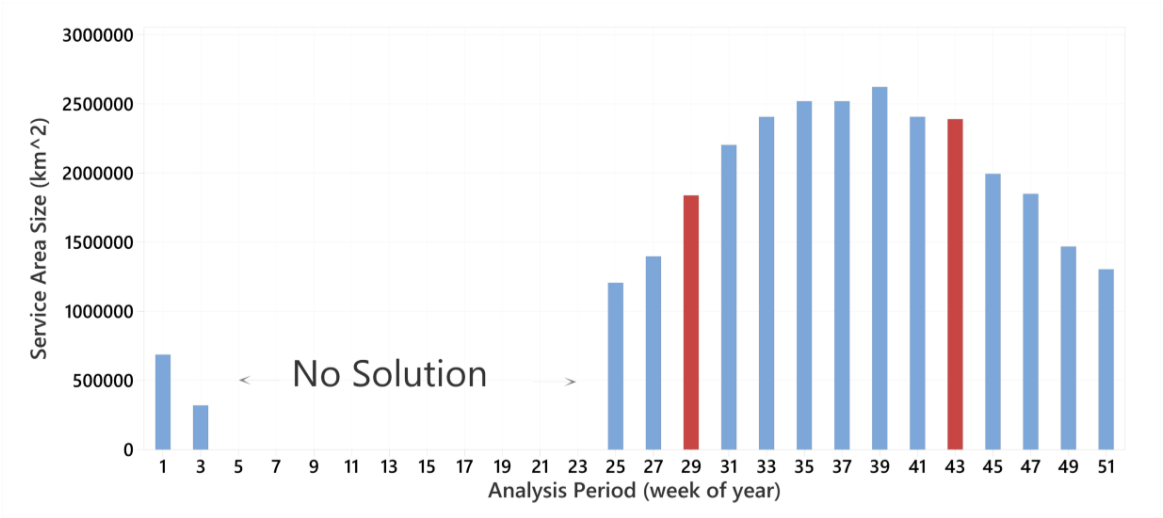

Fig. 13.10 Comparison of geographic size of the IRSA for a Polar Class 1A vessel throughout the year for a given SAAS.

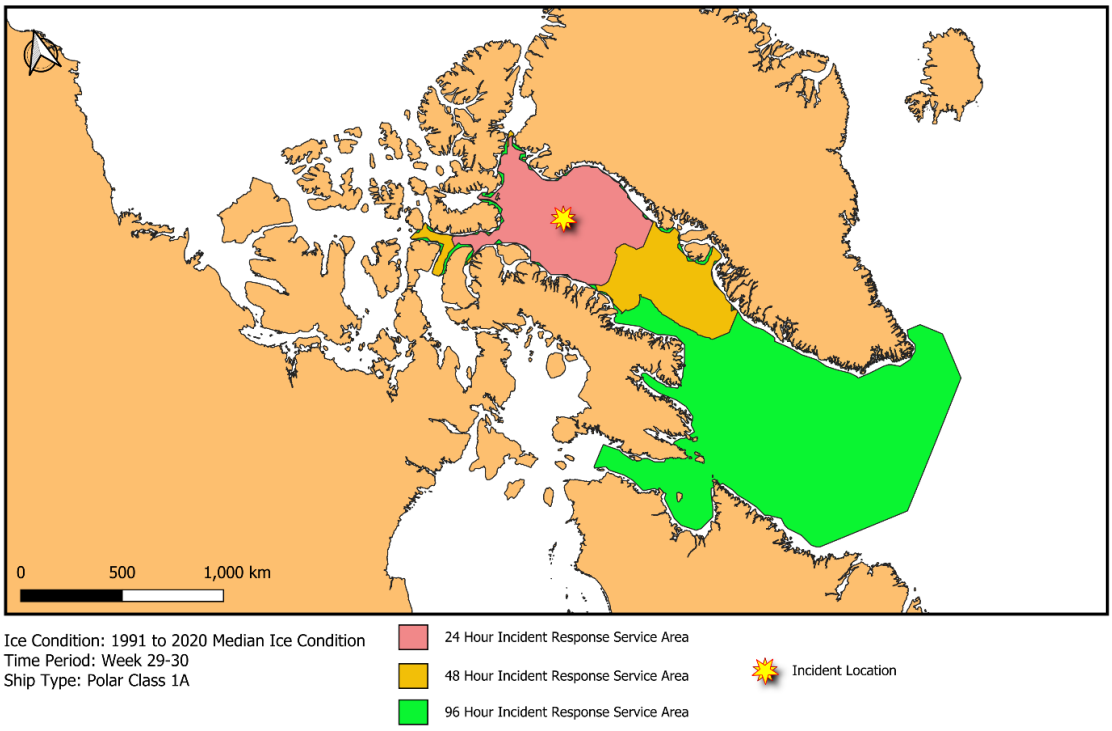

Fig. 13.11 Comparison of the IRSA size for a Polar Class 1A ship in Week 29-30 for 24 hr, 48 hr, and 96 hr MRTC.

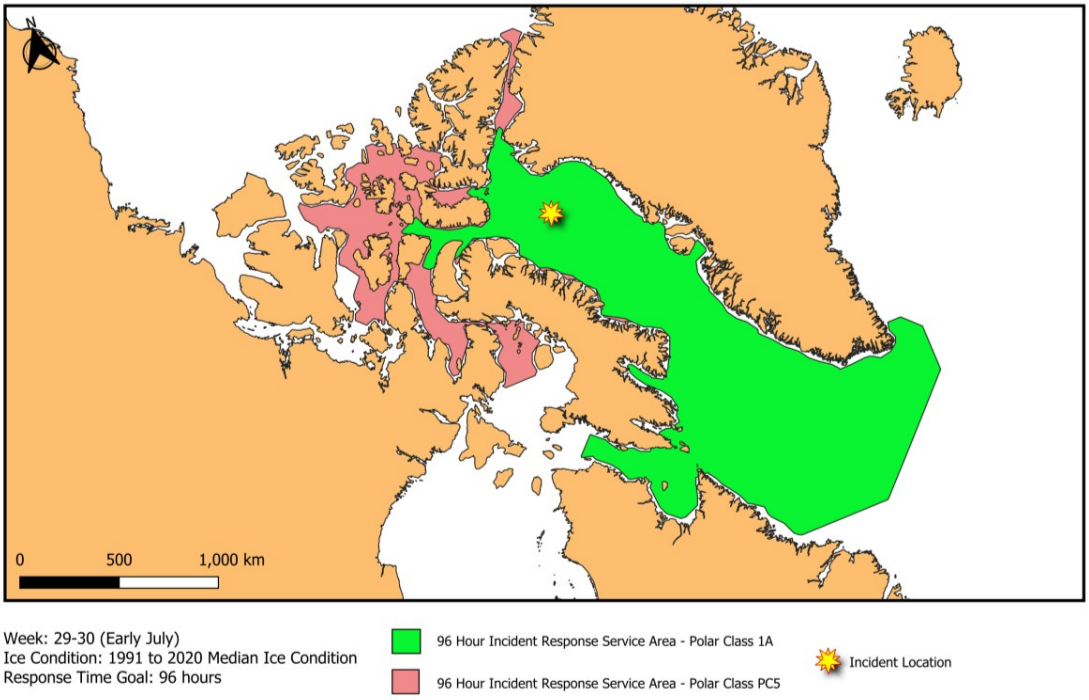

Fig. 13.12 Comparison of the IRSA for a Polar Class 1A and PC5 ship in Week 29–30.

Sometimes it might be more convenient to visualize the MRTC isoline, which is referred to in this study as the IRI. This is the isoline formed around the maximum extent of the service area. The travel time from any arbitrary point on the isochrone to the incident location is equal to the MRTC. Figure 13.13 compares the 96-hour incident response isochrone for a Polar Class 1A and PC5 ship in Week 29–30.

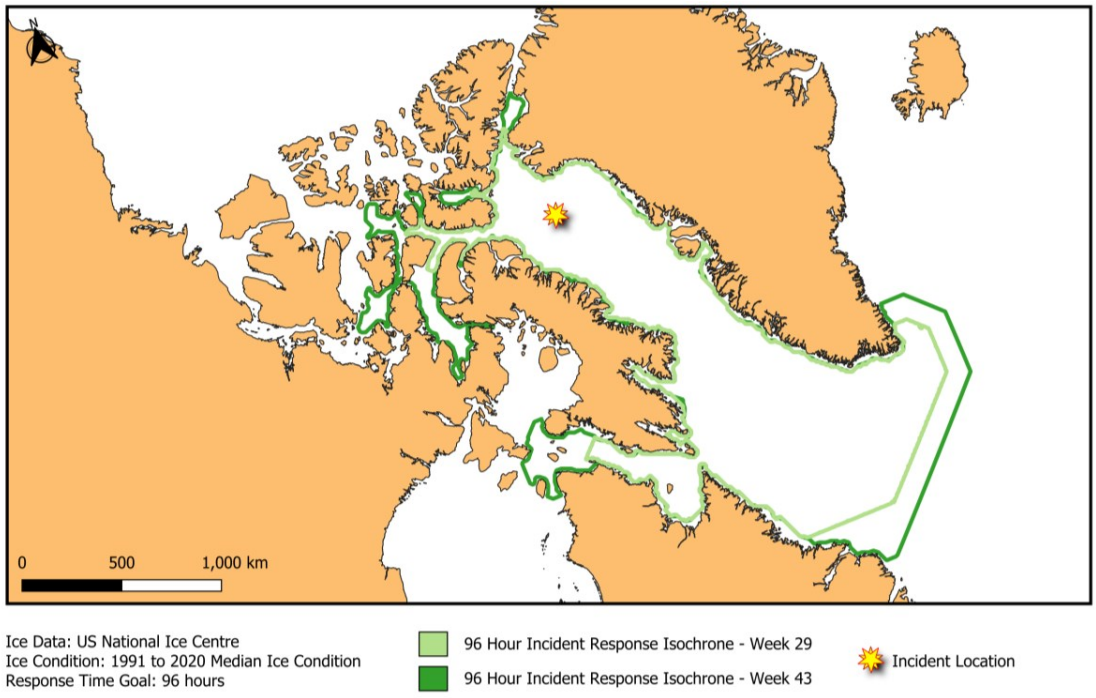

Fig. 13.13 Comparison of 96-hour IRI for a Polar Class 1A in Week 29 and Week 43.

13.5 Discussion

The application of traditional network analysis methods to compute optimal routes in polar waters has resulted in several useful analytics and metrics with potential to support quantitative studies related to incident response and ABM in the Canadian Arctic. Our approach integrates sea ice analysis, navigation risk assessment and network optimization to compute the expected transit time between two points in polar waters. Once computed, the expected transit time provides an objective measure to examine surface ship incident response in polar waters. The results indicate that incident response times are heavily influenced by the geographic location of the incident and responding vessel, time of year, sea ice conditions and the ship ice class of the vessel responding to the incident.

The complex geography and variable sea ice conditions found in the Canadian Arctic Archipelago are significant contributors to the spatiotemporal variability of emergency response time and overall maritime mobility. The remoteness of the Canadian Arctic and lack of infrastructure affects the timeliness of SAR response, especially maritime-based SAR response. Ships must be prepared to wait days before maritime-based

SAR resources arrive at the incident location. Currently, and as mentioned above, the Polar Code requires that all vessels operating in polar waters be prepared to wait at least five days for SAR resources to arrive on-scene (Polar Code 2014/15). The National Research Council of Canada (NRC) has previously evaluated the expected time until recovery for several geographic locations in the Arctic (Kennedy, Gallagher and Aylward 2013). The NRC study examined emergency response at eight locations dispersed throughout northern Canada, but was limited to two hypothetical emergency scenarios, namely, (1) mild August environmental conditions, and (2) severe August environmental conditions. Figure 13.14 shows the location of the NRC maximum exposure evaluation sites overlayed on the SISAR incident data discussed above. The geographical locations selected by NRC were based on a number of considerations. The first was to ensure that locations were selected throughout the Canadian Arctic in order to provide results that cover the vastness of the region. The second consideration involved the frequency of travel based on current shipping routes and maritime traffic and expected future shipping activity. The third consideration was to ensure the selected locations were positioned at varying distances from existing infrastructure, such as airports, communities and ports. A future examination of maximum exposure time could also consider using the location of historical SISAR incidents in the site selection process.

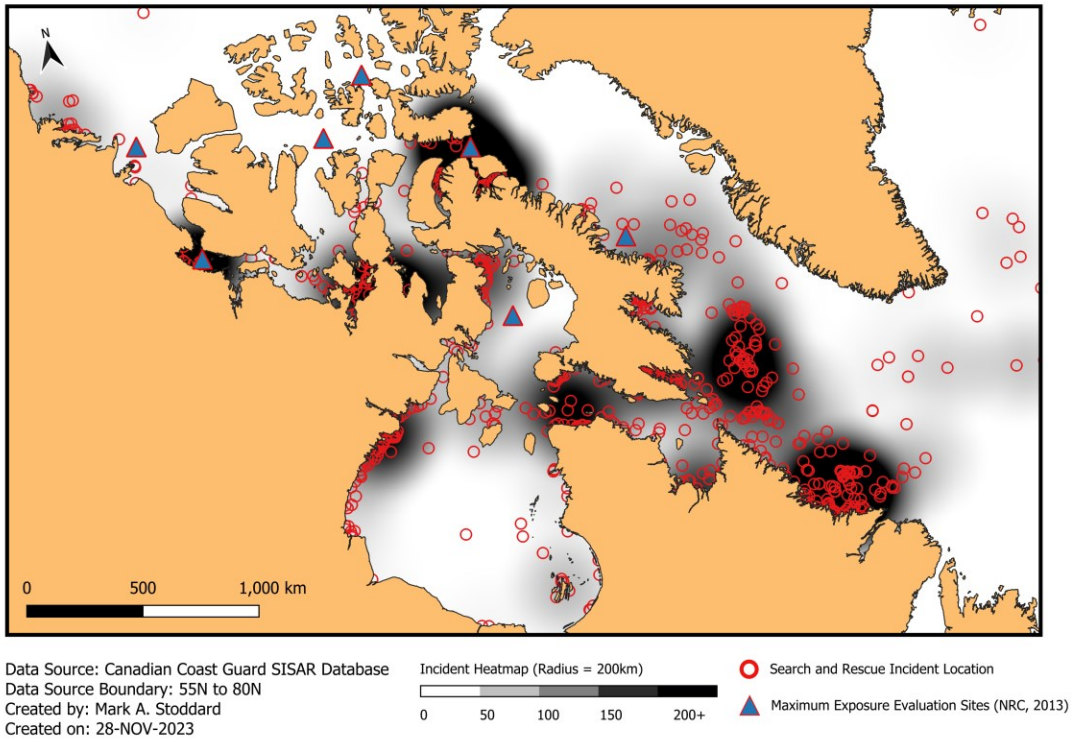

Fig. 13.14 SISAR incident data from 2001 to 2020 with an overlay of the NRC maximum exposure time evaluation sites.

The use of IRSA and IRI to quantify and visualize the expected transit time for marine-based assets would be another possible extension to the NRC study of maximum exposure time in the Arctic. This additional analysis would allow for a greater consideration of the spatiotemporal variability of expected response time for marine-based SAR assets throughout the year. The use of IRSA and IRI computed on a bi-weekly basis would allow for a more complete analysis of expected transit time for marine-based response assets throughout the year and its impact on expected exposure time. Figure 13.15 shows the Week 33 (mid-August) 12-hour, 24-hour and 48-hour IRSA for a selected NRC maximum exposure evaluation site. The results provide a convenient method to visualize the expected transit time for a Polar Class 1A vessel to reach the NRC evaluation site. A vessel located anywhere in a given IRSA polygon would be able to reach the location of interest within the associated time cut-off.

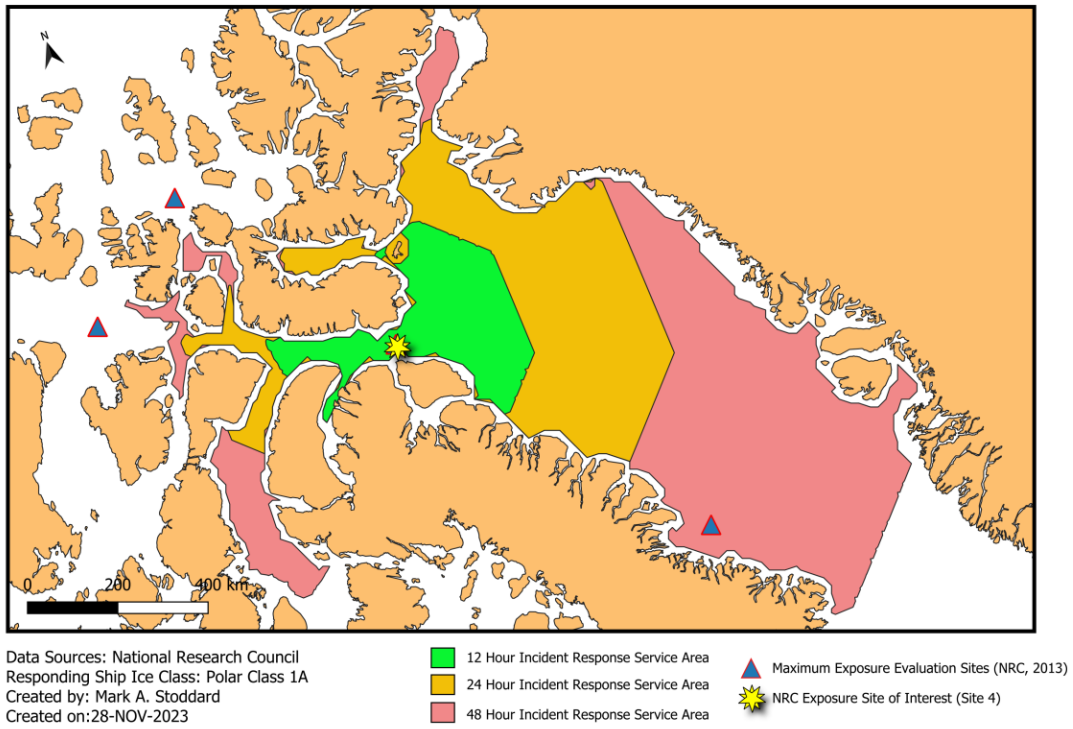

Fig. 13.15 12-hour, 24-hour, and 48-hour IRSA for a Polar Class 1A vessel operating in Week 33 assuming 1990 to 2021 median RIO value for Week 33–34.

More specifically, the IRSA and IRI concepts could be used to extend the study results for marine-based SAR response to more formally consider the contribution of VOO in their analysis. This additional analysis would not require a significant change in the study methodology. This could be achieved by combining the analysis of historical shipping activity data (polar class ship type, time and location) and IRSA results to determine the probability of a VOO being available and able to respond to an incident within the specified time cut-offs. This approach could also support a wide variety of ABM tools that aim to incorporate historical shipping activity into the overall assessment of marine-based SAR response for pre-selected evaluation sites in the Canadian Arctic. Figure 13.16 provides an example of how observations of shipping activity can be combined with IRSA to begin to quantify the expected contribution of VOO to incident response and maximum exposure time. In this case, we see that no VOO can reach the evaluation site within 12 hours, three VOO can reach the site within 12 to 24 hours, and 49 VOO can reach the site within 24 to 48 hours. The location and number of VOO shown in Figure 13.16 are representative of a

single instant in time. By analysing shipping traffic data over multiple years, it would be possible to statistically characterize VOO availability to support this form of analysis.

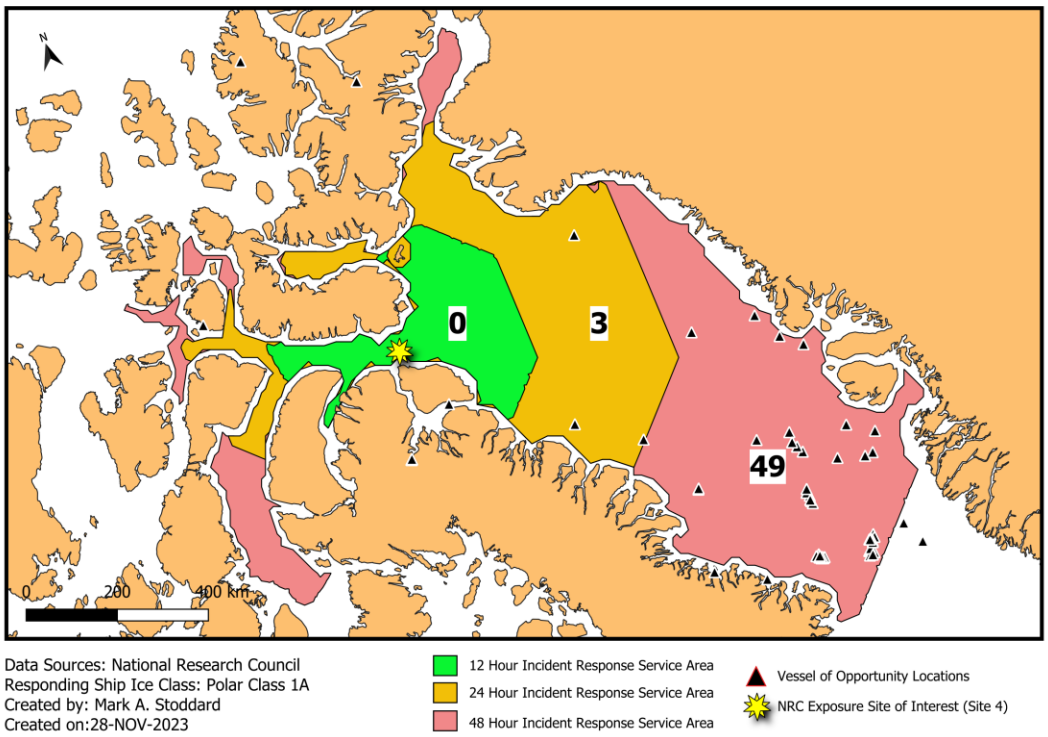

Fig. 13.16 12-hour, 24-hour, and 48-hour IRSA for a Polar Class 1A vessel operating in Week 33, with an example overlay of vessel of opportunity locations and total vessel counts in each IRSA.

Two major limitations of our approach to analysing incident response using IRSA and IRI are (1) the temporal resolution of sea ice analysis and (2) the use of bi-weekly median RIO values over the 1991 to 2020 climatological period for route generation and transit time estimation. Our method relies on the use of bi-weekly sea ice analysis from the USNIC to assess navigational risk. The consequence of relying on bi-weekly sea ice analysis is that all subsequent analysis products derived from this sea ice analysis must also be produced on a bi-weekly basis to avoid over-resolving the data. It also means that our network optimization model assumes that sea ice conditions do not change over a two-week period. For short voyages this should not create much concern, but when examining trans-Arctic routes that could exceed 10+ days it may seem unreasonable to assume sea ice condition will remain static during voyage execution. Special consideration should also be

given to voyages planned during the periods of seasonal break-up and freeze-up, when ice conditions can change dramatically over even a few weeks. This issue is less of a concern when conducting strategic planning, but is of greater concern at the tactical ship operations level. Secondly, the use of the climatological median RIO value in our analysis will limit the usefulness of our results for tactical applications.

13.5.1 Temporal Resolution of Sea Ice Analysis

Currently, the USNIC is the only authoritative source of detailed characterizations of sea ice that provide circumpolar coverage of the Arctic and Antarctic regions. The USNIC takes imagery and ancillary data from a variety of space-based and terrestrial sensor systems, such as synthetic aperture radar and passive microwave, to produce detailed characterizations of ice concentration, ice type and general ice thickness. Once the ice analysis is complete, numerous products are created and provided open access to a very broad user community. USNIC sea ice analysis products are grouped by region and produced for different time periods, depending on the nature of analysis contained in the product. The USNIC product relied on for this study is the Arctic Sea Ice GIS Shapefile, which is produced bi-weekly. This product has the desired coverage area and sea ice analysis attribute data to compute POLARIS RIO values throughout the Arctic.

While suitable for strategic navigation assessment, it may be more desirable to assess navigational risk using a daily product for tactical navigation assessment. The use of daily sea ice analysis products in our network analysis would make the fastest path optimization and transit time estimation results more applicable at the tactical level. Figure 13.17 compares the fastest path and transit time results using USNIC bi-weekly sea ice analysis and CIS daily sea ice analysis produced at the start and end of the bi-weekly analysis period. There is good agreement between the fastest route and transit time produced from the USNIC and CIS sea ice analysis products at the beginning of the bi-weekly analysis period. When we compare the results using the same USNIC bi-weekly chart and a CIS daily product issued toward the end of the USNIC bi-weekly period, we start to observe significant differences between the fastest route and transit time. It should be noted that ice conditions are known to change rapidly in the June/July timeframe, so we

would expect the greatest differences between the use of bi-weekly and daily products to be observed during the yearly sea ice break-up and freeze-up periods.

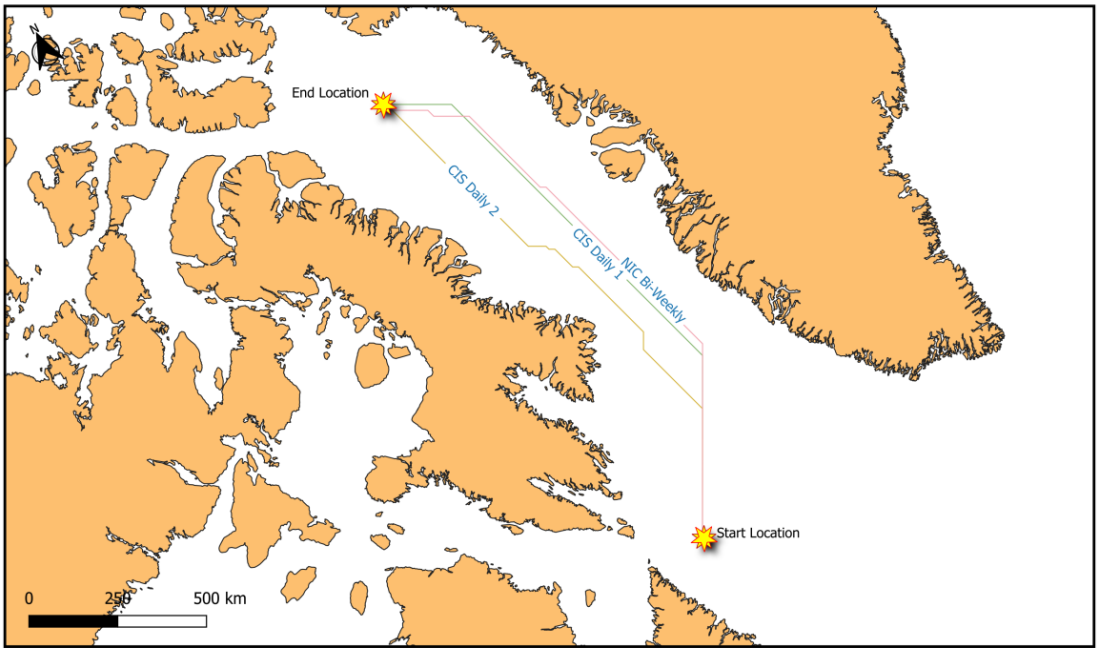

Data Source 1: US National Ice Centre
Data Source 2: Canadian Ice Service

POLARIS RIO Source	US NIC Bi-Weekly - 2020-07-09	CIS Daily 1 - 2020-07-09	CIS Daily 2 - 2020-07-23
Transit Time (hrs)	67.5	67.1	64.9

Fig. 13.17 Comparison of fastest route and transit time using the USNIC bi-weekly ice chart issued on 9 July 2020 and the CIS daily ice chart issued at the start and end of the USNIC bi-weekly analysis period (9 and 23 July 2020).

13.5.2 Use of Climatological Period Summary Statistics

For strategic planning, it is often necessary to plan voyages based on the ice conditions expected to be encountered during a planned voyage. The selection of the appropriate sea ice analysis to use for strategic planning is a difficult task and often relies on expert judgement and the selection of sea ice analysis from similar years. Our analysis has so far relied on the use of summary statistics of historical POLARIS RIO values over a given climatological period to support strategic planning. There are two commonly used 30-year climatology periods used for strategic sea ice analysis, namely, 1981 to 2010 and 1991 to 2020. The USNIC moved to a baseline period of 1981 to 2010 starting 1 July 2013 (National Snow and Ice Data Center 2013). The CIS have adopted a different approach,

updating their 30-year ice climate normal every 10 years, with the current period being 1991 to 2020.

In this study we have chosen to use the 1991 to 2020 climatological period when examining historical sea ice conditions and their expected impact on polar ship operations. The results focus on the 1991 to 2020 median RIO value when assessing sea ice risk and its impact on ship routing, transit time and incident response service areas. The other statistical aggregations that have been computed for our study area include (1) minimum RIO value, (2) first quartile RIO value, (3) mean RIO value, (4) third quartile RIO value and (5) maximum RIO value. Future studies could compare ship routing and transit time results using different statistical aggregations of POLARIS RIO values to better understand the impact this has on route generation and transit time.

The selection of RIO value affects both the fastest route optimization and expected transit time. When selecting the maximum RIO value (most positive) the resulting optimal route is expected to be the most direct route possible between the start and end location, achieving the minimum expected transit time. One would also expect this voyage to also have the highest average ship speed. Figure 13.18 shows the fastest route and transit time computed using different statistical aggregations of historical RIO values observed over the climatological period from 1991 to 2020. Figure 13.18 shows the spatial variability in the fastest route and transit time based on the selected RIO value statistic. The maximum RIO corresponds to the highest RIO value observed during the climatological period, representing the most favourable operating conditions observed.

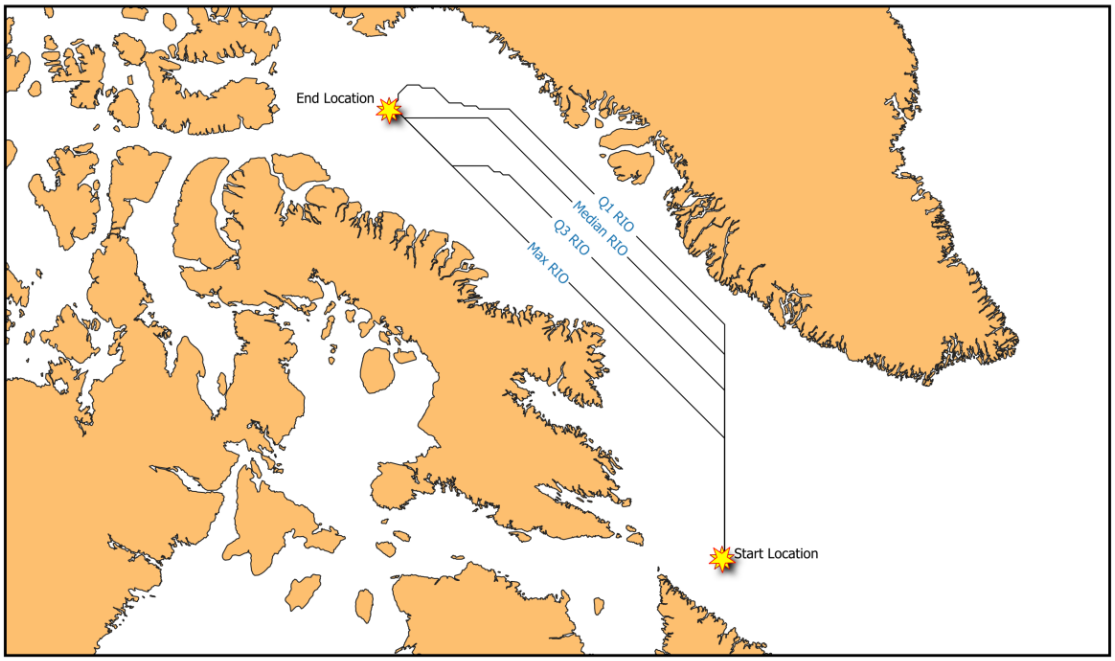

Data Source: US National Ice Centre
Climatological Analysis Period: 1991 to 2020
Bi-Weekly Analysis Period: Week 29-30 (Early July)

POLARIS RIO Summary Statistic	Min RIO	Q1 RIO	Median RIO	Q3 RIO	Max RIO
Transit Time (hrs)	No Solution	90.5	72.7	67.4	64.3

Fig. 13.18 Comparison of fastest route and transit time using different statistical aggregations of historical RIO values observed over the climatological period from 1991 to 2020

Figure 13.19 compares the fastest route between the same two points using (1) a single USNIC sea ice chart produced on 16 July 2020 and (2) the 1991 to 2020 median RIO value. In this case, we see that the fastest route and transit time using the sea ice chart from 16 July 2020 is faster, arriving at the end location 6.4 hours earlier. This would indicate that the RIO values derived from the sea ice chart from 16 July 2020 are more favourable than the 1991–2020 median RIO.

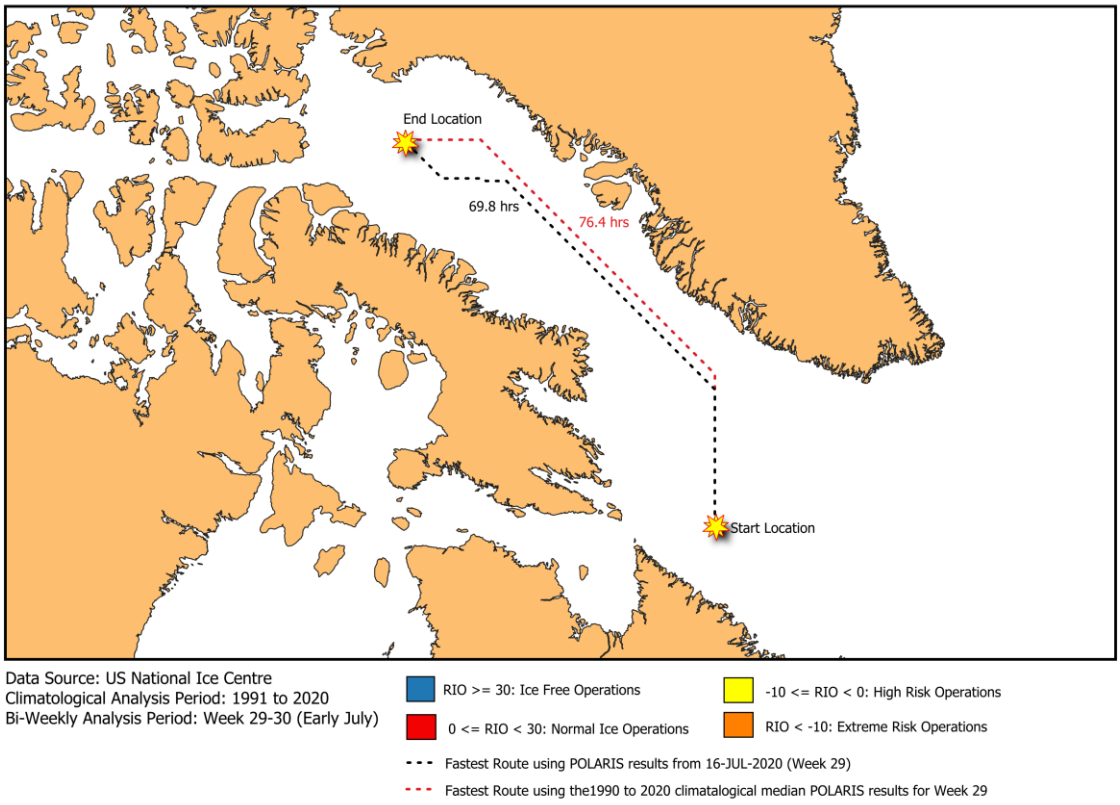

Fig. 13.19 Comparison of risk-adjusted transit time between two points in the eastern Arctic using the 1991 to 2020 climatological median POLARIS RIO and the POLARIS RIO from a single USNIC sea ice chart for the same bi-weekly period.

13.6 Conclusion

In this chapter, we have demonstrated how network analysis techniques can be used to determine the fastest route between two locations in the Arctic and to compute IRSA and IRI. The results provide several valuable insights into the spatiotemporal variability of marine-based transit time and ship routing in polar waters. The use of IRSA and IRI to determine the expected response time for marine-based SAR assets was discussed as a possible extension to a 2013 study of maximum exposure time in the Canadian Arctic completed by the NRC. The use of IRSA and IRI to support ABM tools that aim to formally incorporate historical observations of shipping activity into quantitative assessments was also discussed. Incorporating IRSA and IRI results into area-based management tools would provide decision-makers with a useful tool to possibly help plan and coordinate

incident response in polar waters, and support ABM of commercial vessel operation and SAR provision.

Future technical work should concentrate on examining the use of different sources of sea ice analysis to better understand how change to the source data can impact the fastest route and expected transit time results. The use of modelled sea ice data from ice forecasting and GCM systems also offers a particularly interesting opportunity to compare expected RIO values derived from the statistical analysis of historical observations and from the model results. Computing IRSA and IRI using the RIO values derived from forecasted and/or modelled sea ice conditions may give decision-makers a better understanding of the future navigability of the Canadian Arctic and its impact on ship routing and expected transit times. These insights could be used to update policies, industry practices and regulations that aim to improve shipping safety and SAR response, or even assist the rationalization of SAR service delivery and also indicate where infrastructure development would be most beneficial.

The presented methodology and results in this chapter are not intended to provide a ready solution to the challenge of marine-based SAR response in polar waters. It is, however, hoped that the results, especially the data analysis and visualizations throughout this chapter, will stimulate new discussions and insights on the quantitative performance aspects of maritime SAR and Arctic navigation more generally. It is also hoped that these discussions can assist in improving ABM of shipping risks in the Canadian Arctic and beyond.

References

Aksenov, Y., Popova, E. E., Yool, A., Nurser, G., Williams, T. D., Bertino, L., & Bergh, J. (2017). On the future navigability of Arctic sea routes: High-resolution projections of the Arctic Ocean and sea ice. *Marine Policy, 75*, 300-317.

Aksenov, Y., Popova, E. E., Yool, A., Nurser, G., Williams, T. D., Bertino, L., & Bergh, J. (2017). On the future navigability of Arctic sea routes: High-resolution projections of the Arctic Ocean and sea ice. *Marine Policy, 75*, 300-317.

Alasia, A., Bedard, F., Belanger, J., Guimond, E., & Penny, C. (2017). *Measuring remoteness and accessibility: A set of indicies for Canadian Communities.* Statistics Canada. Retrieved from www.publications.gc.ca/pub?id=9.835126&sl=0

Andersson, M., & Johansson, R. (2010). Multiple Sensor Fusion for Effection Abnormal Behavior Detection in Counter Piracy Operations. *Proceedings of International Waterside Security Conference.*

ARCDEV. (1998). *Final Public report of the ARCDEV Project.* Retrieved from https://trimis.ec.europa.eu/sites/default/files/project/documents/arcdev.pdf

Arctic Council. (2009). *Arctic Marine Shipping Assessment 2009 Report.* Arctic Council.

Bilge, T. A., Fournier, N., Mignac, D., Hume-Wright, L., Bertino, L., Williams, T., & Teitsche, S. (2022). An Evaluation of the Performance of Sea Ice Thickness Forecasts to Support Arctic Marine Transport. *Journal of Marine Science and Engineering*(10), 265.

Boylan, B. (2021, September). Increased maritime traffic in the Arctic: Implications for governance of Arctic sea routes. *Marine Policy, 131*.

Cairns, W. (2005). AIS and Long Range Identification and Tracking. *Journal of Navigation*, 58:181-189.

Canadian Ice Service. (2009). *Canadian Ice Service Arctic Regional Sea Ice Charts in SIGRID-3 Format.* Boulder, CO: Natinoal Snow and Ice Data Centre.

Canadian Ice Service. (2021). *Ice climate normals for the northern Canadian waters 1991 to 2020.* Governement of Canada.

Cau, Y., Liang, S., Sun, L., Liu, J., Cheng, X., Wang, D., . . . Feng, K. (2022). Trans-Arctic shipping routes expanding faster than the model projections. *Global Evironmental Change, 73*.

Chamberlain, J., Yue, B., Parsons, G., & Mulvie, J. (2008). Advanced Remote Sensing for Better Bottom-Fast Ice Identification. *RADARSAT-2 Workshop.*

Chircop, A., Goerlandt, F., Pelot, R., & Aporta, C. (2024). *Area-Based Management of Shipping: Canadian and Comparative Perspectives.* Springer Cham. doi:https://doi.org/10.1007/978-3-031-60053-1

Collard, F., Mouche, A., Danilo, C., Chapron, B., Isern-Fontanet, J., Johannessen, J., & Backberg, B. (2008). *Routine High Resolution Observation of Selected Major Surface Currents from Space.* SEASAR.

Crawford, A., Stroeve, J., Smith, A., & Jahn, A. (2021). Arctic open-water periods are projected to lengthen dramatically by 2100. *Communications Earth & Environment, 2*(109). doi:https://doi.org/10.1038/s43247-021-00183-x

Crisp, D. (2004). *The State-of-the-Art in Ship Detection in Syntehtic Aperature Radar Imagery.* Adelaide, AS: Defence Science and Technology Organization.

Dahlbom, A., & Niklasson, L. (2007). Tragectory Clustering for Coastal Surveillance. *10th Conference of the International Soceity for Information Fusion.*

Department of Health and Aged Care. (2001). *Measuring remoteness: Accessibility/Remoteness Index of Australia (ARIA).* Government of Australia. Retrieved April 10, 2024, from https://www.nintione.com.au/?p=5335

Dijkstra, E. (1959). A note on two problems in connxion with graphs. *Numerische Mathematik, 1*(1), 269-271.

DNV-GL. (2014). *The Arctic - The nex frontier.*

Dolny, J. (2018). *Methodology for Defining Technical Safe Speeds for Light Ice-Strengthened Government Vessels Operating in Ice.* Ship Structure Committee. United States Coast Guard.

Dovey, K., Woodcock, I., & Pike, L. (2017). Isochrone Mapping of Urban Transport: Car-dependency, Mode-choice, and Design Research. *Planning Practice & Research, 32*(4), 402 - 416.

Eriksen, T., Hoye, G., Narheim, B., & Jenslokken, M. (2006). Maritime Traffic Monitoring using space-based AIS Recevier. *Acta Astronautica*, 58(10): 537-549.

Etienne, L., & Pelot, R. (2013). Simulation of maritime paths taking into account ice conditions in the Arctic. *Symposium for GIS and Computer Cartography for Coastal Zone Management (CoastGIS)*, (pp. 116-119).

European Commission. (2014). *Defining Proxy Indicators for Rural Development Programs.* Journal of the European Union.

Fedi, L., Etienne, L., Haury, O., Rigot-Muller, P., Stephenson, S., & Cheaitou, A. (2018). POLARIS in the Arctic. *Journal of Ocean Technology, 13*(4), 58-71.

Fedi, L., Faury, O., & Etienne, L. (2020). Mapping and analysis of maritime accidents in the Russian Arctic through the lens of the Polar Code and POLARIS system. *Marine Policy*(118), 1-9.

Finnish Transport Safety Agency. (2017). *Finnish ice classes equivalent to class notations of recognized classification societies and the determination of the ice classes of ships.* Helsinki, Finland: Trafi.

Fraser, D. (2020). A Change in the Ice Regime: Polar Code Implementation in Canada. In A. Chircop, F. Goerlandt, C. Aporta, & R. Pelot, *Governance of Arctic Shipping.* Springer Polar Sciences.

Fu, S., Zhang, D., Montewka, J., Yan, X., & Zio, E. (2016). Towards a probabilistic model for predicting ship besetting in ice in Arctic waters. *Reliability Engineering & System Safety*, 124-136.

Georlandt, F., Montewka, J., Zhang, W., & Kujala, P. (2017). An analysis of ship escort and convoy operations in ice conditions. *Safety Science, 95*, 198-209.

Goerlandt, F., & Pelot, R. (2020). An Exploratory Application of the International Risk Governance Council's Risk Governance Framework to Shipping Risks in the Canadian Arcitc. In A. Chircop, *Governance in Arctic Shipping.* Springer Polar Sciences.

Goerlandt, F., Montewka, J., Zhang, W., & Kujala, P. (2017). An analysis of ship escort and convoy operations in ice conditions. *Safety Science, 95*, 198-209.

Goerlandt, F., Montewka, J., Zhang, W., & Kujala, P. (2017). An analysis of ship escort and convoy operations in ice conditions. *Safety Science, 95*, 198-209.

Goerlandt, F., Montewka, J., Zhang, W., & Kujala, P. (2017). An Analysis of Ship Escort and Convoy Operations in ice Conditions. *Safety Science*, 198-209.

Government of Canada. (2019, June 25). *Canadian Coast Guard Search and Rescue and Canadian Coast Guard Auxiliary Evaluation Report*. Retrieved from Department of Fisheries and Oceans Canada: https://www.dfo-mpo.gc.ca/ae-ve/evaluations/11-12/SAR-CCGA-eng.htm#2.1

Greidanus, H., & Kourti, N. (2006). Findings of the CELIMS Project - Detection and Classification of Marine Traffic from Space. *Proceedings of SEASAR 2006.* Frascati, Italy.

Headland, R. (2022). *Transits of the Northwest Passage to End of the 2022 Navigation Season: Atlantic Ocean to Arctic Ocean to Pacific Ocean.* Scott Polar Research Institute. Cambridge University.

Heiberg, H. B., Reistad, M., & A., B. (2006). *Use of ASAR wave spectra in operational wave analysis and forcasting: report from the EnviWave project.* Oslo: Norweigian Meteorological Institute.

Higginbotham, J., & Grosu, M. (2014). The Northwest Territories and Arctic Maritime Development in the Beaufort Regimes. *CIGI Policy Brief*, 40:1-12.

Hirose, T., Kapfer, M., Bennett, J., Cott, P., Manson, G., & Solomon, S. (2008). Bottomfast Ice Mapping and the Measurement of Ice Thickness on Tundra Lakes using C-Band SAR Remote Sensing. *Journal of the American Water Resources Association*, 44(2): 285-292.

Howell, S., & Yackel, J. (2004). A Vessel Transit Assessment of Sea Ice Variability in the Western Arctic, 1969-2002: Implications for ship navigation. *Canadian Journal of Remote Sensing*, 30(2):205-215.

IACS. (2009). *International Association of Classification Societies Charter.* International Association of Classificaiton Socieities.

IACS. (2023). *Requires Concerning POLAR CLASS.* International Association of Classification Socieities.

Intergovernmental Oceanographic Commission of UNESCO. (2004). *SIGRID-3: A Vector archive formate for sea ice charts.* JCOMM Technical Report.

International Maritime Organization. (2004). *Regulation 19 - Carriage requirements for shipborne navigational systems and equipment.* London: International Maritime Organization.

International Maritime Organization. (2016). *International Code for Ships Operating in Polar Waters (POLAR CODE).* International Maritime Organization.

International Telecommunication Union. (2014). *Technical characteristics for an automatic identification system using time division multiple access in the VHF maritime mobile frequency band.* Geneva: International Telecommunication Union.

Kang, M., Lee, H., Yang, C., & Yoon, W. (2008). Estimation of Ocean Current Velocity in Coastal Area using RADARSAT-1 SAR Images and HF-Radar Data. IGRASS 2008.

Kazemi, S., Abhari, S., Lavesson, N., Johnson, H., & Ryman, P. (2013). Open Data for Anomaly Detection in Maritime Surveillance. *Expert Systems with Applications*, 40: 5719 - 5729.

Kennedy, A., Gallagher, J., & Aylward, K. (2013). *Evaluating Exposure Time Until Recovery by Location.* Ottawa, Ontario: National Research Council Canada.

Khan, B., Khan, F., Veitch, B., & Yang, M. (2018). An operational risk analysis tool to analyze marine transportation in Arctic waters. *Reliability Engineering & System Safety, 169*, 485-502. doi:https://doi.org/10.1016/j.ress.2017.09.014.

Kim, H., Jeong, S.-Y., Woo, S.-H., & Han, D. (2018). Study on the procedure to obtain an attainable speed in pack ice. *International Journal of Naval Architecture and Ocean Engineering*(10), 491-498. doi:https://doi.org/10.1016/j.ijnaoe.2017.09.004

Kotovirta, V., Jalonen, R., Axell, L., Riska, K., & Berglund, R. (2009). A system for Route Optimization in Ice-Covered Waters. *Cold Regions Science and Technology*(55), 52-62.

Kubat, I., & Timco, G. (2003). *Vessel Damage in the Canadian Arctic.* National Research Council of Canada.

Lack, D. A., & Corbett, J. J. (2012). Black carbon from ships: a review of the effects of ship speed, fuel. *Atmostpheric Chemistry and Physics*(12), 3985-4000.

Laxhammer, R. (2008). Anomaly Detection for Sea Surveillance. *11th International Conference on Information Fusion* (pp. 47-54). Fusion 2008.

Lee, H.-W., Roh, M.-I., & Kim, K.-S. (2021). Ship Route Planning in Arctic Ocean based on POLARIS. *Ocean Engineering*(234), 1-14.

Lehtola, V., Montewka, J., Goerlandt, F., Guinness, R., & Lensu, M. (2019). Finding safe and efficient shipping routes in ice-covered waters: A framework and a model. *Cold Regions Science and Technology*(165), 1-14. doi:https://doi.org/10.1016/j.coldregions.2019.102795

Lensu, M., & Goerlandt, F. (2019). Big Maritime Data for the Baltic Sea with a Focus on the Winter navigation System. *Marine Policy*, 53-65.

Li, F., Goerlandt, F., Kujala, P., Lehtiranta, J., & Lensu, M. (2018). Evaluation of selected state-of-the-art methods for ship transit simulation in various ice conditions based on full-scale measurement. *Cold Regions Science and Technology, 151*, 94-108. doi:10.1016/j.coldregions.2018.03.008

Liu, C., Musharraf, M., Li, F., & Kujala, P. (2022). A data mining method for automatic identification and analysis of. *Ocean Engineering*(266).

Liu, C., Musharraf, M., Li, F., & kujala, P. (2022). A data mining method for automatic identification and analysis of icebreaker assistance operation in ice-covered waters. *Ocean Engineering, 266*. doi:https://doi.org/10.1016/j.oceaneng.2022.112914

Lloyds of London. (2014). *Arctic Opening: Opportunity and risk inthe high north.* London.

Loptien, U., & Axell, L. (2014). Ice and AIS: ship speed data and sea ice forecasts in the Baltic Sea. *The Cryosphere*(8), 2409-2418.

Marchenko, N. A., Aandreassen, N., Kuznetsova, S. Y., Ingimundarson, V., & Jakobsen, U. (2018, March). TransNav. *Arctic Shipping and Risks: Emergency Categories and Response Capacities*.

Marchenko, N., Borch, O., Markov, S., & Andreassen, N. (2015). Maritime activity in the high north - The range of unwanted incidents and risk patterns. *International Conference on Port and Ocean Engineering under Arctic Conditions 2015.* POAC. Retrieved from http://hdl.handle.net/11250/2392588

Maritime Safety Committee. (2014a). *POLARIS – proposed system for determining operational limitations in ice.* IACS.

Maritime Safety Committee. (2014b). *Technical background to POLARIS.* IACS.

McCallum, J. (1996). *Safe Speed in Ice - An analysis of transit speed and ice decision numerals.* Ottawa, ON: Transport Canada.

Melia, N., Haines, K., & Hawkins, E. (2015). Improved Arctic sea ice thickness projections using bias-corrected CMIP5 simulations. *The Cryoshpere*, 2237-2251.

Melia, N., Haines, K., & Hawkins, E. (2016). Sea ice decline and 21st century trans-Arctic shipping routes. *Geophyscial Research Letters*(43), 9720-9728.

Monroe, K. R., & Maher, K. H. (1995). Psychology and Rational Actor Theory. *Political Psychology, 16*(1), 1-21. doi:https://doi.org/10.2307/3791447

Montewka, J., Goerlandt, F., Kujala, P., & Lensu, M. (2015). Towards probabilistic models for the prediction of a ship performance in dynamic ice. *Cold Regions Science and Technology*(112), 14-28.

Montewka, J., Goerlandt, F., Kujala, P., & Lensu, M. (2015). Towards Probabilitic Models for the Prediction of a Ship Performance in Dynamic Ice. *Cold Regions Science and Technology*(112), 14-28.

Montewka, J., Goerlandt, F., Lensu, M., & Guinness, R. (2019). Towards a hybrid model of ship performance in ice suitable for route planning purpose. *Proceedings of the Instituation of Mechanical Engineers, Part O: Journal of Risk and Reliability, 233*(1), 18-34. doi:10.1177/1748006X18764511

Mudryk, L. R., Dawson, J., Howell, S. E., Derksen, C., Zagon, T. A., & Brady, M. (2021, August). Impact of 1, 2, and 4 Degrees Celcius of Global Climate Wharing on Ship Navigation in the Canadian Arctic. *Nature Climate Change, 11*, 673 to 679.

Muller, M., Knol-Kauffman, M., Jeuring, J., & Palerme, C. (2023). Arctic shipping trends during hazardous weather and sea-ice conditions and the Polar Code's effectiveness. *npj Ocean Sustainability, 2*(12). doi:https://doi.org/10.1038/s44183-023-00021-x

National Snow and Ice Data Center. (2013, July 13). *Frequently Asked Questions on Arctic Sea Ice*. Retrieved April 19, 2023, from Arctic Sea Ice News and Analysis: https://nsidc.org/arcticseaicenews/faq/#1979average

National Snow and Ice Data Centre. (2015a). *Format for gridded sea ice information (SIGRID).* Boulder, CO: National Snow and Ice Data Centre.

Olsen, R., & Wahl, T. (2000). The Role of Wide Swath SAR in High-Latitude Coastal Management. *John Hopkins APL Technical Digest*, 20(1) 136-140.

Piercey, C., Kennedy, A., & Power, J. (2019). *Methodology for Estimating Exposure Time in Polar Regions.* National Research Council. doi:https://doi.org/10.4224/40002043

QGIS. (2023). *QGIS: A free and open source geographic information system*. Retrieved from https://qgis.org/en/site/

Renn, O., & Sellke, P. (2011). Risk, Society and Policy Making: Risk governance in a complex world. *International Journal of Performability engineering, 7*(4), 349-366.

Renn, O., Jaeger, C. C., Rosa, E. A., & Webler, T. (2000). The Rational Actor Paradigm in Risk Theories: Analysis and Critique. In M. Cohen, *RIsk in the Modern Age.* London: Palgrave Macmillan. doi:https://doi.org/10.1007/978-1-349-62201-6_2

Rhodes, B., Bomberger, N., Seibert, M., & Waxman, A. (2005). Maritime Situation Monitoring and Awareness using Learning Mechanisms. *Proceedings of IEEE Military Communications Conference.*

Roy, J. (2010). Rule-Based Expert Systems for Maritime Anomaly Detection. *SPIE 7666, Sensors and Command, Control, Communications, and Intelligence (C3I) Technologies for Homeland Security and Homeland Defense.*

Runge, H., Breit, H., Eineder, M., Schulz-Stellenfleth, J., Bard, J., & Romeiser, R. (2004). Mapping of Tidal Currents with SAR Along Track Interferometry. *IGARSS '04*.

Schrijver, A. (1998). *Theory of Linear and Interger Programming.* John Wiley $ Sons.

Siljander, M., Venalainen, E., Goerlandt, F., & Pellikka, P. (2015). GIS-based cost distance modelling to support strategic maritime search and rescue planning: A feasibility study. *Applied Geography, 57*, 54-70.

Simila, M., & Lensu, M. (2018). Estimated the Speed of Ice-Going Ships by Integrating SAR Imagery and Ship Data from an Automatic Identification System. *Remote Sensing*(10), 1-23.

Smith, C., & Stephenson, S. (2013). New tans-arctic shipping routes navigable by mid-century. *Proceedings of the National Academy of Sciences of the United States of America (PNAS)*, 110:E1191.

Smith, L., & Stephenson, S. (2013). New Trans-Arctic Shipping Routes Navigable by Midcentury. *Proceedings of the National Academy of Sciences - PNAS*, 1191-1195.

Snider, D. (2012). *Polar Ship Operations - A practical guide.* London: The Nautical Institute.

Somanathan, S., Flynn, P. C., & Szymanski, J. (2006). The Northwest Passage: A Simulation. *Proceedings of the 2006 Winter Simulation Conference*, (p. 7).

Spire Maritime. (2023). *Historical AIS Data*. Retrieved from Spire: https://spire.com/maritime/solutions/historical-ais-data/

Statistics Canada. (2016). *Data Products, 2016 Census*. Retrieved from Statistics Canada Census Program: https://www12.statcan.gc.ca/census-recensement/2016/dp-pd/index-eng.cfm

Stephenson, S. R., Smith, L. C., & Agnew, J. A. (2011). Divergent long-term tranjectories of human access to the Arctic. *Nature Climate Change*, 156-160.

Stoddard, M. A., & Pelot, R. (2020). Historical Maritime Search and Rescue Incident Data Analysis. In *Governance of Arctic Shipping.* Springer Polar Sciences.

Stoddard, M. A., Etienne, L., Pelot, R., Fournier, M., & Beveridge, L. (2018). From Sensing to Sense-making: Assessing and Visualizing Ship Operational Limitations in the Canadian Arctic Using Open-Access Ice Data. In L. P. Hidlebrand, L. W. Brigham, & T. M. Johansson, *Sustainable Shipping in a Changing Arctic* (pp. 99-113). Springer.

Stoddard, M. A., Pelot, R., Etienne, L., & Goerlandt, F. (2023). Determining Ship Speeds in Ice using the Polar Operational Limitation Assessment Risk Indexing System (POLARIS). *TBD*, 1-18.

Stoddard, M. A., Pelot, R., Etienne, L., & Goerlandt, F. (2023). Polar Class Ship Speeds in Ice: Obersvation and Analysis. *TBD*, 1-7.

Stoddard, M., Etienne, L., Fournier, M., Pelot, R., & Beveridge, L. (2016). Making sense of Arctic maritime traffic using the Polar Operational Limits Assessment Risk Indexing System (POLARIS). *Earth and Environmental Science*, 1-8.

Stoddard, M., Pelot, R., Goerlandt, F., & Etienne, L. (2023). Making Sense of Marine-Based Search and Rescue Response Time using Network Analysis. *TBD*, 1-29.

Tan, X., Su, B., Riska, K., & Moan, T. (2013). A six-degree-of-freedom numerical model for level ice-ship interaction. *Cold Regions Science and Technology, 92*, 1-16.

Tran, T., Browne, T., Musharraf, M., & Veitch, B. (2023). Pathfinding and Optimization for Vessels in Ice: a literature review. *Cold Regions Science and Technology*(211), 1-8.

Transport Canada. (1998). *Arctic Ice Regime Shipping System (AIRSS) Standards, TP 12259E.* Ottawa: Government of Canada.

Tremblett, A. J., Garvin, M. J., & Oldford, D. (2021). Preliminary Study on the Applicability of the POLARIS Methodology for Ships Operating in Lake Ice. *Proceedsings of the 26th International Conference on Port and Ocean Engineering under Arctic Conditions*, (p. 12). Moscow.

U.S. National Ice Center. (2022). *U.S. National Ice Center Arctic and Antarctic Sea Ice Charts in SIGRID-3 Format, Version 1.* Boulder, Colorado.

U.S. National Ice Centre. (2023). *Arctic Ice Products*. Retrieved from https://usicecenter.gov/Products/ArcticHome

Vachon, P. (2006). Ship Detection in SAR Imagery. *Proceedings of OceanSAR 2006 - Third Workshop on Coastal and Marine Applications of SAR.* St. John's, NL.

Wang, C., Ding, C., Yang, Y., & Dou, T. (2022). Risk Assessment of Ship Navigation in the Northwest Passage: Historical and Projection. *Sustainability*(14). doi:https://doi.org/10.3390/su14095591

Wang, F., & Xu, Y. (2011). Estimating O–D travel time matrix by Google Maps API: implementation, advantages, and implications. *Annals of GIS, 17*(4), 199-209.

Wang, Y., Zhang, R., & Qian, L. (2018). An Improved A* Algorithm Based on Hesitant Fuzzy Set Theory for Multi-Criteria Arctic Route Planning. *Symmetry*(10), 1-20.

Wei, T., Yan, Q., Qi, W., Ding, M., & Wang, C. (2020). Projections of Arctic sea ice conditions and shipping routes in the twenty-first century using CMIP6 forcing scenarios. *Evironmental Research Letters*(15), 1-10.

Weick, K. E., & Sutcliffe, K. M. (2005). Organizing and the Process of Sensemaking. *Organization Science, 16*(4), 409-421.

Wilbrink, J. G. (2017). *Remoteness as a proxy for social vulnerability in Malawian Traditional Authorities: An open data and open-source approach.* The Hague - Netherlands: Delft University.

Williams, T., Korosov, A., Rampal, P., & Olason, E. (2021). Presentation and Evaluation of the Arctic Sea Ice Forecasting System neXtSIM-F. *The Cryoshpere*(15), 3207-3227.

Wilson, K. (2004). Shipping in the Canadian Arctic: Other possible climate change scenarios. *Proceedings of IGARSS'04: Geoscience and Remote Sensing*, 3: 1853.

Wilson, K., Falkingham, H., Melling, H., & De Abreu, R. (2004). Shipping in the Canadian Arctic: Other possible climate change scenarios. *Proceedings of IEEE International Symposium on Geoscience and Remote Sensing*, 3: 1853-1856.

World Maritime Organization. (2016). *International Code for Ships Operating in Polar Waters (POLAR CODE).* World Maritime Oganization.

Wright, C. (2016). *Arctic Cargo: A history of marine transportation in Canada's North.* Marquis Book Printing.

Xi, Y., Miller, E. J., & Saxe, S. (2018). Exploring the Impact of Different Cut-Off Times on Isochrone Measurements of Accessibility. *Transportation Research Record, 2672*(49), 113-124.

Dijkstra, E. (1959). A note on two problems in connxion with graphs. *Numerische Mathematik, 1*(1), 269-271.

Fedi, L., Etienne, L., Haury, O., Rigot-Muller, P., Stephenson, S., & Cheaitou, A. (2018). POLARIS in the Arctic. *Journal of Ocean Technology, 13*(4), 58-71.

Fedi, L., Faury, O., & Etienne, L. (2020). Mapping and analysis of maritime accidents in the Russian Arctic through the lens of the Polar Code and POLARIS system. *Marine Policy*(118), 1-9.

Goerlandt, F., Montewka, J., Zhang, W., & Kujala, P. (2017). An Analysis of Ship Escort and Convoy Operations in ice Conditions. *Safety Science*, 198-209.

Government of Canada. 2019. Canadian Coast Guard Search and Rescue and Canadian Coast Guard Auxiliary Evaluation Report - 2019. https://www.dfo-mpo.gc.ca/ae-ve/evaluations-eng.htm

IOC/UNESCO. 2004. Intergovernmental Oceanographic Commission of UNESCO. (2004). *SIGRID-3: A Vector archive formate for sea ice charts.* JCOMM Technical Report.

Kennedy, A., Gallagher, J., & Aylward, K. (2013). *Evaluating Exposure Time Until Recovery by Location.* Ottawa, Ontario: National Research Council Canada.

Kotovirta, V., Jalonen, R., Axell, L., Riska, K., & Berglund, R. (2009). A system for Route Optimization in Ice-Covered Waters. *Cold Regions Science and Technology*(55), 52-62.

Lensu, M., & Goerlandt, F. (2019). Big Maritime Data for the Baltic Sea with a Focus on the Winter navigation System. *Marine Policy*, 53-65.

Lloyds of London. (2014). *Arctic Opening: Opportunity and risk inthe high north.* London.

Loptien, U., & Axell, L. (2014). Ice and AIS: ship speed data and sea ice forecasts in the Baltic Sea. *The Cryosphere*(8), 2409-2418.

Maritime Safety Committee. (2014a). *POLARIS – proposed system for determining operational limitations in ice.* IACS.

Maritime Safety Committee. (2014b). *Technical background to POLARIS.* IACS.

McCallum, J. (1996). *Safe Speed in Ice - An analysis of transit speed and ice decision numerals.* Ottawa, ON: Transport Canada.

Melia, N., Haines, K., & Hawkins, E. (2016). Sea ice decline and 21st century trans-Arctic shipping routes. *Geophyscial Research Letters*(43), 9720-9728.

Mudryk, L. R., Dawson, J., Howell, S. E., Derksen, C., Zagon, T. A., & Brady, M. (2021, August). Impact of 1, 2, and 4 Degrees Celcius of Global Climate Wharing on Ship Navigation in the Canadian Arctic. *Nature Climate Change, 11*, 673 to 679.

National Snow and Ice Data Center. (2013, July 13). *Frequently Asked Questions on Arctic Sea Ice*. Retrieved April 19, 2023, from Arctic Sea Ice News and Analysis: https://nsidc.org/arcticseaicenews/faq/#1979average

National Snow and Ice Data Centre. (2015). *Format for gridded sea ice information (SIGRID).* Boulder, CO: National Snow and Ice Data Centre.

Siljander, M., Venalainen, E., Goerlandt, F., & Pellikka, P. (2015). GIS-based cost distance modelling to support strategic maritime search and rescue planning: A feasibility study. *Applied Geography, 57*, 54-70.

Smith, C., & Stephenson, S. (2013). New tans-arctic shipping routes navigable by mid-century. *Proceedings of the National Academy of Sciences of the United States of America (PNAS)*, 110:E1191.

Somanathan, S., Flynn, P. C., & Szymanski, J. (2006). The Northwest Passage: A Simulation. *Proceedings of the 2006 Winter Simulation Conference*, (p. 7).

Stoddard, M. A., & Pelot, R. (2020). Historical Maritime Search and Rescue Incident Data Analysis. In *Governance of Arctic Shipping.* Springer Polar Sciences.

Stoddard, M. A., Pelot, R., Etienne, L., & Goerlandt, F. (2023). Polar Class Ship Speeds in Ice: Obersvation and Analysis. *In Publication*, 1-7.

Stoddard, M., Etienne, L., Fournier, M., Pelot, R., & Beveridge, L. (2016). Making sense of Arctic maritime traffic using the Polar Operational Limits Assessment Risk Indexing System (POLARIS). *Earth and Environmental Science*, 1-8.

Tremblett, A. J., Garvin, M. J., & Oldford, D. (2021). Preliminary Study on the Applicability of the POLARIS Methodology for Ships Operating in Lake Ice. *Proceedsings of the 26th International Conference on Port and Ocean Engineering under Arctic Conditions*, (p. 12). Moscow.

USNIC. U.S. National Ice Center. (2022). *U.S. National Ice Center Arctic and Antarctic Sea Ice Charts in SIGRID-3 Format, Version 1.* Boulder, Colorado.

Wang, C., Ding, C., Yang, Y., & Dou, T. (2022). Risk Assessment of Ship Navigation in the Northwest Passage: Historical and Projection. *Sustainability*(14). doi:https://doi.org/10.3390/su14095591.

Wang, Y., Zhang, R., & Qian, L. (2018). An Improved A* Algorithm Based on Hesitant Fuzzy Set Theory for Multi-Criteria Arctic Route Planning. *Symmetry*(10), 1-20.

Wei, T., Yan, Q., Qi, W., Ding, M., & Wang, C. (2020). Projections of Arctic sea ice conditions and shipping routes in the twenty-first century using CMIP6 forcing scenarios. *Evironmental Research Letters*(15), 1-10.

World Maritime Organization. (2014). International Code for Ships Operating in Polar Waters (Polar Code), Resolution MSC.385(94) adopted 21 November 2014 (effective 1 January 2017); Amendments to the International Convention for the Safety of Life at Sea 1974, Resolution MSC.386(94) adopted on 21 November 2014 (effective 1 January 2017); International Code for Ships Operating in Polar Waters (Polar Code), Resolution MEPC.265(68) adopted on 15 May 2015 (effective 1 January 2017); Amendments to MARPOL Annexes I, II, IV and V, Resolution MEPC.266(68) adopted on 15 May 2015 (effective 1 January 2017). Consolidated version at http://www.imo.org/en/MediaCentre/HotTopics/polar/Documents/POLAR%20CODE%20TEXT%20AS%20ADOPTED.pdf.

Appendix 7: Copyright Releases

05-MAY-2024

Springer International Publishing

Reprints@springernature.com

I am preparing my PhD thesis for submission to the Faculty of Graduate Studies at Dalhousie University, Halifax, Nova Scotia, Canada. I am seeking your permission to include a manuscript version of the following paper(s) as a chapter in the thesis:

Stoddard, M.A., Etienne, L., Pelot, R., Fournier, M., Beveridge, L. (2018). From Sensing to Sense-Making: Assessing and Visualizing Ship Operational Limitations in the Canadian Arctic Using Open-Access Ice Data. In: Hildebrand, L., Brigham, L., Johansson, T. (eds) Sustainable Shipping in a Changing Arctic. WMU Studies in Maritime Affairs, vol 7. Springer, Cham. https://doi.org/10.1007/978-3-319-78425-0_6

Dalhousie graduate theses are collected and stored online by Dalhousie University and Library and Archives of Canada. I am seeking your permission for the material described above to be stored online in Dalhousie University's institutional repository and in Library and Archives of Canada (LAC)'s Theses Canada Collection.

Full publication details and a copy of this permission letter will be included in the thesis.

Yours sincerely,

Mark A. Stoddard

Permission is granted for:

a) the inclusion of the material described above in your thesis.
b) for the material described above to be included in the copy of your thesis that is sent to the Library and Archives of Canada inclusion in Theses Canada.
c) For the material described above to be included in the copy of your thesis that is sent to Dalhousie University's institutional repository.

Name:	Springer Nature - Copyright Clearance House - License # 5783001224551	Title:	N/A
Signature:	N/A	Date:	06 May 2024

05-MAY-2024

IOP Publishing Limited

ees@ioppublishing.org

I am preparing my PhD thesis for submission to the Faculty of Graduate Studies at Dalhousie University, Halifax, Nova Scotia, Canada. I am seeking your permission to include a manuscript version of the following paper(s) as a chapter in the thesis:

Stoddard, M.A., Etienne, L., Pelot, R., Fournier, M., Beveridge, L. (2016). Making sense of Arctic maritime traffic using the Polar Operational Limits Assessment Risk Indexing System (POLARIS). IOP Conference Series: Earth and Environmental Science. Issue 34. https://doi.org/10.1088/1755-1315/34/1/012034

Dalhousie graduate theses are collected and stored online by Dalhousie University and Library and Archives of Canada. I am seeking your permission for the material described above to be stored online in Dalhousie University's institutional repository and in Library and Archives of Canada (LAC)'s Theses Canada Collection.

Full publication details and a copy of this permission letter will be included in the thesis.

Yours sincerely,

Mark A. Stoddard

Permission is granted for:

d) the inclusion of the material described above in your thesis.

e) for the material described above to be included in the copy of your thesis that is sent to the Library and Archives of Canada inclusion in Theses Canada.

f) For the material described above to be included in the copy of your thesis that is sent to Dalhousie University's institutional repository.

Name: IOP Publishing - CC BY Licensing Title: _____

Signature: _____ Date: 13 – MAY - 2024

05-MAY-2024

Springer Nature

Bookpermissions@springernature.com

I am preparing my PhD thesis for submission to the Faculty of Graduate Studies at Dalhousie University, Halifax, Nova Scotia, Canada. I am seeking your permission to include a manuscript version of the following paper(s) as a chapter in the thesis:

Stoddard, M.A., Pelot, R. (2020). Historical Maritime Search and Rescue Incident Data Analysis. In: Chircop, A., Goerlandt, F., Aporta, C., Pelot, R. (eds) Governance of Arctic Shipping. Springer Polar Sciences. Springer, Cham. https://doi.org/10.1007/978-3-030-44975-9_3

Dalhousie graduate theses are collected and stored online by Dalhousie University and Library and Archives of Canada. I am seeking your permission for the material described above to be stored online in Dalhousie University's institutional repository and in Library and Archives of Canada (LAC)'s Theses Canada Collection.

Full publication details and a copy of this permission letter will be included in the thesis.

Yours sincerely,

Mark A. Stoddard

Permission is granted for:

g) the inclusion of the material described above in your thesis.
h) for the material described above to be included in the copy of your thesis that is sent to the Library and Archives of Canada inclusion in Theses Canada.
i) For the material described above to be included in the copy of your thesis that is sent to Dalhousie University's institutional repository.

Name: Springer Nature – Copyright Clearance Center – Open Access - BY Title: _____

Signature: N/A Date: 05 May 2024

05-JUL-2024

Springer Nature

Bookpermissions@springernature.com

I am preparing my PhD thesis for submission to the Faculty of Graduate Studies at Dalhousie University, Halifax, Nova Scotia, Canada. I am seeking your permission to include a manuscript version of the following paper(s) as a chapter in the thesis:

Stoddard, M.A., Pelot, R., Etienne, L., and Goerlandt, F. (2024). Making Sense of Marine-Based Search and Rescue Response Time using Network Analysis. Book Chapter in A. Chircop et al. (eds.), Area-Based Management Approaches to Shipping Risk Mitigation: Canadian and Comparative Perspectives, Springer Cham, https://doi.org/10.1007/978-3-031-60053-1

Dalhousie graduate theses are collected and stored online by Dalhousie University and Library and Archives of Canada. I am seeking your permission for the material described above to be stored online in Dalhousie University's institutional repository and in Library and Archives of Canada (LAC)'s Theses Canada Collection.

Full publication details and a copy of this permission letter will be included in the thesis.

Yours sincerely,

Mark A. Stoddard

Permission is granted for:

j) the inclusion of the material described above in your thesis.

k) for the material described above to be included in the copy of your thesis that is sent to the Library and Archives of Canada inclusion in Theses Canada.

l) For the material described above to be included in the copy of your thesis that is sent to Dalhousie University's institutional repository.

Name: Springer Nature – Copyright Clearance Center – Open Access - BY Title: _____

Signature: N/A Date: 05 JUL 2024

Appendix 8: List of Publications

This thesis gives an overview of the following published and unpublished manuscripts, referred to in the text by their Roman numerals. The author contributions to each manuscript are described in the following section. The copyright releases for all published manuscripts are provided in Appendix 7 - Copyright Release Request Letter.

PI. Stoddard, M.A., Etienne, L., Pelot, R., Fournier, M., Beveridge, L. (2018). From Sensing to Sense-Making: Assessing and Visualizing Ship Operational Limitations in the Canadian Arctic Using Open-Access Ice Data. In: Hildebrand, L., Brigham, L., Johansson, T. (eds) Sustainable Shipping in a Changing Arctic. WMU Studies in Maritime Affairs, vol 7. Springer, Cham. https://doi.org/10.1007/978-3-319-78425-0_6

PII. Stoddard, M.A., Etienne, L., Pelot, R., Fournier, M., Beveridge, L. (2016). Making sense of Arctic maritime traffic using the Polar Operational Limits Assessment Risk Indexing System (POLARIS). IOP Conference Series: Earth and Environmental Science. Issue 34. https://doi.org/10.1088/1755-1315/34/1/012034

PIII. Stoddard, M.A., Pelot, R., Etienne, L., and Goerlandt, F. (2024). Determining Ship Speeds in Ice using the Polar Operational Limitation Assessment Risk Indexing System (POLARIS). **Drafted for submission.**

PIV. Stoddard, M.A., Pelot, R., Etienne, L., and Goerlandt, F. (2024). An approach to Support Strategic Route Analysis in ice-covered waters using the Ice Risk-Adjusted Estimated Time of Arrival (I-ETA). **Drafted for submission.**

PV. Stoddard, M.A. and Pelot, R. (2020). Historical Maritime Search and Rescue Incident Data Analysis. Book Chapter in A. Chircop et al. (eds.), Governance of Arctic Shipping, Springer Polar Sciences, https://doi.org/10.1007/978-3-030-44975-9_3

PVI. Stoddard, M.A., Pelot, R., Etienne, L., and Goerlandt, F. (2024). Making Sense of Marine-Based Search and Rescue Response Time using Network Analysis. Book Chapter in A. Chircop et al. (eds.), Area-Based Management Approaches to Shipping Risk Mitigation: Canadian and Comparative Perspectives, Springer Cham, https://doi.org/10.1007/978-3-031-60053-1

Appendix 9: Original Features of Thesis

The research presented in this thesis has been conducted over a 10-year period and has already made several contributions to the academic literature on arctic navigation risk assessment (PI&PII), and marine-based search and rescue (SAR) incident analysis (PV&PVI). The focus of this research has been on integrating existing arctic navigation risk concepts, open data sources, and spatial data analysis techniques to enable the strategic assessment of ship operations in ice-covered waters. Use cases of interest included strategic route assessment and marine-based SAR response time estimation.

Relevant sources of publicly available data have been identified, processed, and catalogued to enable the computational methods presented in this thesis. Results were prepared using various information visualization tools and techniques to aid in analysis and interpretation of marine-based SAR response time and maritime accessibility. The results have led to several new insights on strategic routing and transit time estimation in ice-covered waters, and an improved understanding of the spatiotemporal variability of marine-based SAR response time in the Canadian Arctic.

The following features presented in this thesis are believed to be novel contributions to the literature made during the conduct of this PhD research (2013 to Present):

- The combined use of POLARIS and a historical archive of open-access sea ice analysis to statistically assess and visualize ship operational limitations throughout the Canadian Arctic. Existing methods to assess sea ice risk typically rely on individual sea ice analysis charts, in-situ ice observations, or modeled sea ice data. These methods do not allow for the statistical assessment of navigability in ice-covered waters. The sea ice risk assessment method presented in this thesis overcomes this limitation by computing different statistical aggregations of historical POLARIS results to support strategic navigation planning. This analysis was aided by the introduction of the POLARIS risk map, which enabled the visualization of a variety of different strategic decision attributes, such as time of year, ship ice class, and statistical aggregation of POLARIS RIO results. [PI]

- The use of POLARIS and open-access sea ice analysis to make sense of observed vessel kinematic behavior in ice-covered waters. This analysis combined timely knowledge of the maritime environment (sea ice condition) and shipping activity, providing new insights into the analysis of observed kinematic behavior of a vessel operating in ice-covered waters and the detection of vessel kinematic anomalies. Standard navigational practice forms the basis of most rules used for kinematic anomaly detection; widely employed to identify vessels exhibiting unusual or unexpected behavior. Kinematic anomalies in vessel behavior relate to the location, course, speed, and maneuver (rate of turn, etc.) of the vessel. Detection of these behaviors in most modern vessel monitoring systems is accomplished using defined rules within the system that generate an indication and/or warning when a vessel violates a rule, such as entering a defined exclusion area, or violating an upper or lower bound on vessel speed. The expectation of the presence of sea ice challenges the use of conventional rules for kinematic anomaly detection in the Canadian Arctic because of the complexity of the navigating environment due to the presence of sea ice. The methods and results presented in this thesis provide the necessary information to make sense of vessel kinematic behavior in ice-covered waters, and to help determine if it is expected or anomalous. [PII]

- The combination of historical satellite-AIS data, USNIC sea ice analysis, and POLARIS to determine expected ship speed in different POLARIS Risk Index Outcome (RIO) result categories. This analysis was novel in its scope and scale, requiring the geospatial processing of 22 million AIS messages transmitted in the Canadian Arctic over a two-year period, and 101 bi-weekly circumpolar sea ice analysis charts over the same two-year period. This analysis allowed for the detailed observation of 184 ice-classed ships operating over the full range of POLARIS RIO values, enabling the statistical analysis of ship speeds in different POLARIS RIO categories. [PIII]

- The use of POLARIS and USNIC sea ice analysis to compute the Expected Transit Time (ETT) in ice-covered waters. This analysis integrates concepts of POLARIS

risk assessment, sea ice analysis, and expected ship speed in different POLAIRS RIO result categories to determine the ETT. The ETT is a transit time estimate intended for use in polar waters that accounts for expected changes in ship speed along a planned or executed route due to varying sea ice conditions. [PIII]

- An original approach to strategic route analysis in ice-covered waters, referred to as the Ice Risk-Adjusted Estimated Time of Arrival (I-ETA). I-ETA is a special case of the ETT calculation, combining the ETT calculation and network optimization techniques to compute the fastest path between two points (the I-ETA). This analysis combined POLARIS sea ice risk assessment, historical sea ice analysis, and network optimization to compute the I-ETA. The I-ETA was designed to help overcome the challenge of computer generating strategic routes over wide areas in complex polar navigating environments. [PIV]

- The application of contemporary interactive data visualization techniques on Canadian Search and Rescue (SAR) historical incident data. This analysis applied several data visualization techniques, both static and dynamic, to produce new analytical insights from historical SAR incident data. Several spatial and temporal analysis techniques were demonstrated, and trends in Canadian SAR incident data were identified and reported. [PV]

- An original approach to determining marine-based SAR response time in ice-covered waters using network analysis techniques. This analysis introduced two novel concepts, (1) the Incident Response Service Area (IRSA) and (2) the Incident Response Isochrone (IRI). The computation of the IRSA and IRI requires the use of the I-ETA method previously discussed [PIV]. The IRSA is a polygon containing all polar class ship locations that can reach a SAR incident location within a specified maximum response time. The IRI is a curve of equal travel time formed at the furthest ship locations that can reach the SAR incident location within the service target. IRSA and IRI provide new tools to support Area-Based Management (ABM) of commercial vessel operation, and SAR service provision [PVI].